Charles University in Prague
First Faculty of Medicine

Study program: Biochemistry and Pathobiochemistry

Ing. Roman Vozdek

The metabolism and signaling of hydrogen sulfide: the role of CBS-related proteins in *Caenorhabditis elegans*

Metabolismus a signalizace sirovodíku: úloha proteinů příbuzných k CBS u *Caenorhabditis elegans*

Ph.D. Thesis

Supervisor: Prof. MUDr. Viktor Kožich, CSc.

Prague, 2013

Prohlašuji, že jsem závěrečnou práci vypracoval samostatně a že jsem řádně uvedl a citoval všechny použité prameny a literaturu. Současně prohlašuji, že práce nebyla využita k získání jiného nebo stejného titulu.

Souhlasím s trvalým uložením elektronické verze mé práce v databázi systému meziuniverzitního projektu Theses.cz za účelem soustavné kontroly podobnosti kvalifikačních prací.

V Praze, 15.10.2013 ROMAN VOZDEK

Identifikační záznam:

VOZDEK, Roman. *Metabolismus a signalizace sirovodíku: úloha proteinů příbuzných k CBS u Caenorhabditis elegans* [*The metabolism and signaling of hydrogen sulfide: the role of CBS-related proteins in Caenorhabditis elegans*]. Praha, 2013, 150 s., Disertační práce (Ph.D.). Universita Karlova v Praze, 1. lékařská fakulta, Ústav dědičných metabolických poruch. Vedoucí práce Kožich, Viktor.

Key words:

Hydrogen sulfide, cystathionine beta-synthase, *C. elegans*, hypoxia, metabolism, signaling

Klíčová slova:

Sirovodík, cystathionin-beta-synthasa, *C. elegans*, hypoxie, metabolismus, signalizace

ACKNOWLEDGEMENT

First, I would like to express my gratitude to Prof. Viktor Kožich, my research supervisor, for his patient guidance, useful critique of this research, and excellent supervision in the beginning of my scientific career. I would like to express my great appreciation to Dr. Aleš Hnízda for his cooperation, advices and support which was a great help at important stages of the study.

My special thanks are extended to Dr. Jakub Krijt, Ms. Alena Dutá, Ms. Katka Raková, Dr. Vojtěch Spiwok and Ms. Hana Prouzová for their helpful comments and excellent technical assistance. The assistance provided by Dr. Kostrouchová is also greatly appreciated. I would also like to extend my thanks to the staff of the laboratory of the Institute of Inherited Metabolic Disorders, especially our research team, for their help and camaraderie, and our former leader Prof. Elleder for his brilliant advice and enthusiasm for research.

I am particularly grateful for the opportunity to collaborate with the Horvitz lab at MIT in Cambridge, USA. Special thanks are due, particularly to Dr. Dengke Ma and Prof. H. Robert Horvitz who shared their ideas and scientific enthusiasm with me. I also wish to thank Prof. Csaba Szabo for giving me the opportunity to join his team at the University of Texas in Galveston, USA, and for his kind care during my visit.

Finally, I wish to thank my family for their support and encouragement throughout my study. Without them I would not have been able to finish my project.

I would also like to thank the Ministry of Education of the Czech Republic, the Wellcome Trust, the Grant Agency of Charles University, and the research program of the Charles University in Prague for their financial support.

ABSTRACT

Hydrogen sulfide (H_2S) is a toxic gas that causes respiratory failure and death at high concentrations, but at low concentrations, it functions as a signaling molecule in vasodilation and neuromodulation, and it protects cells and tissues from reperfusion injury, hypoxia, hyperglycemia and endothelial dysfunction. Several model organisms have been used to study the physiological roles and signaling pathways of H_2S. The roundworm *Caenorhabditis elegan*s is a remarkable model for studying the physiology, developmental biology and signaling of H_2S; however, the metabolism of H_2S in this animal is largely unknown. Cystathionine beta-synthase (CBS) is one of three H_2S-producing enzymes in mammals. Notably, *C. elegans* possesses 6 genes that encode proteins homologous to CBS, namely *cbs-1*, *cbs-2*, *cysl-1*, *cysl-2*, *cysl-3* and *cysl-4*. In this thesis we studied the roles of these genes in H_2S metabolism and signaling. First, we identified *cbs-1* as the gene encoding CBS in *C. elegans*; the recombinant purified CBS-1 protein exhibited canonical CBS activity, and RNA interference-mediated silencing of *cbs-1* resulted in decreased CBS activity and increased homocysteine levels in worm extracts, recapitulating the phenotypes of CBS deficiency in mammals. Notably, the nematode and human enzymes differ in their domain architecture and in their allosteric regulation. Next, we determined that in *C. elegans*, the remaining CBS-related proteins have other roles that are not present in mammals. Whereas *cbs-2* and *cysl-4* are pseudogenes, *cysl-1*, *cysl-2* and *cysl-3* encode proteins that are homologous to the plant and bacterial *O*-acetylserine(thiol)lyases. CYSL-1 is involved in the activation of hypoxia-inducible factor-1 (HIF-1). The increased levels of H_2S during hypoxia promote the interaction of CYSL-1 with a proline hydroxylase EGL-9, leading to the sequestration of EGL-9 and the activation of HIF-1. Therefore, CYSL-1 transduces the H_2S signal as a response to hypoxia and protects cells from various toxic agents and stressors. CYSL-2 functions as a cyanoalanine synthase (CAS) in the cyanide detoxification pathway, the activity of which releases H_2S. Thus, in contrast to mammals, *C. elegans* possesses four different enzymes that produce H_2S *de novo*. The role of CYSL-3 remains unclear, nevertheless, our data suggest that via its sulfhydrylase activity, CYSL-3 might maintain cellular H_2S homeostasis. In summary, these studies revealed that the CBS-related proteins have distinct and specific roles in *C. elegans*, demonstrated novel aspects of H_2S metabolism and signaling in animals, and presented *C. elegans* as a novel and unique model for CBS deficiency.

ABSTRAKT

Sirovodík (H_2S) je toxický plyn, který ve vysokých koncentracích způsobuje respirační selhání a smrt organismu, zatímco v nízkých koncentracích hraje roli jako vasodilatátor, neuromodulátor, a chrání buňky a tkáně před reperfuzním poškozením, hypoxií, hyperglykémií či dysfunkcí endotelu. Ke studiu fyziologie a signalizace H_2S je využíváno hned několik modelových organismů. Hlístice *Caenorhabditis elegans* je pozoruhodným modelem ke studiu fyziologie, vývojové biologie, a v neposlední řadě i signalizace H_2S, nicméně metabolismus sirovodíku v tomto organismu není známý. Cystathionin-beta-synthasa (CBS) je jedním ze tří enzymů produkujících H_2S u živočichů. Zajímavé je, že u *C. elegans* je postulováno hned šest genů kódující homologní proteiny k CBS (*cbs-1*, *cbs-2*, *cysl-1*, *cysl -2*, *cysl -3* a *cysl -4*). Cílem této práce bylo zjistit funkci těchto genů v metabolismu a signalizaci H_2S u *C. elegans*. Nejprve jsme identifikovali *cbs-1* jako gen kódující CBS; rekombinantní purifikovaný protein CBS-1 vykázal CBS aktivitu a RNA interference *cbs-1* vedla ke snížené CBS aktivitě a zvýšené hladině homocysteinu v červích homogenátech, což rekapituluje deficit CBS u savců. Je zajímavé, že hlístí a savčí CBS mají odlišnou doménovou architekturu a tedy i posttranslační regulaci. Dále jsme zjistili, že ostatní proteiny příbuzné k CBS mají u *C. elegans* jiné úlohy, které u savců chybí. Zatímco *cbs-2* a *cysl-4* jsou pseudogeny, *cysl-1*, *cysl-2* a *cysl-3* kódují proteiny homologní k rostlinným a bakteriálním *O*-acetylserin(thiol)lyasám. CYSL-1 hraje roli v signalizační dráze transkripčního faktoru HIF-1 (hypoxia-inducible factor 1). Zvýšená hladina H_2S během hypoxie vede k interakci CYSL-1 s prolinovou hydroxylasou EGL-9, což způsobuje inhibici EGL-9 a následnou aktivaci HIF-1. CYSL-1 tedy transmituje signály sirovodíku jako odpověď na hypoxii, a brání tak buňky proti nejrůznějším toxickým a stresovým jevům. CYSL-2 je kyanoalanin synthasa (CAS) působící v detoxifikační cestě kyanidů, jejíž aktivita produkuje H_2S. *C. elegans* má tedy na rozdíl od savců čtyři různé enzymy, které intracelulárně produkují *de novo* H_2S. Role CYSL-3 u *C. elegans* není doposud jasná, nicméně naše data naznačují, že CYSL-3 pomocí sulfhydrylásové aktivity může udržovat homeostázu H_2S v buňkách. Tyto studie dohromady zjistily, že proteiny příbuzné k CBS mají odlišné a vysoce specifické funkce u *C. elegans*, ukazují nové aspekty signalizace a metabolismu H_2S u živočichů a představují *C. elegans* jako nový unikátní model ke studiu deficitu CBS.

CONTENT

1. INTRODUCTION

Hydrogen sulfide (H_2S) is a toxic gas with a rotten-egg odor, and its beneficial effects have long been known. The ancient Greeks experienced its benefits by bathing in sulfur-containing springs (Moss G. A., 2010), and there is evidence that the consumption of a diet rich in foods containing organosulfur compounds that release H_2S, such as garlic or onion, is associated with longevity (Mulrow C. et al., 2000). Over the last two decades it was demonstrated that H_2S is naturally produced in cells, and its essential biological roles have been postulated (Wang R., 2012). Moreover, recent studies have shown that the administration of exogenous H_2S has therapeutic potential in cardiovascular diseases such as atherosclerosis, in wound healing and in preventing reperfusion injury (Szabo C., 2007). Both the beneficial and toxic effects of H_2S are noteworthy and similar to those of the other gaseous signaling molecules, carbon monoxide (CO) and nitric oxide (NO). Many studies have reported that CO and NO play important roles in animal physiology and the pathology of many diseases; on the basis of these studies, several new drugs have been developed (Wu L. and Wang R., 2005). H_2S is the third gasotransmitter that has been discovered, and it is involved in many physiological and pathological processes; however, its metabolism and signaling are only partially understood.

1.1 H_2S metabolism

Most of the sulfide in the body is provided by the metabolic activity of microflora in the intestine (Macfarlane G. T. et al., 1992) or by non-enzymatic processes using H_2S donors such as diallyl trisulfide (in garlic), which are present in sulfur-rich diets (Benavides G. A. et al., 2007). In the last two decades, it was determined that H_2S is extensively generated in cells by non-enzymatic and enzymatic mechanisms (Kimura H., 2011). Studies have also reported that the sequestration of H_2S is mediated by many mechanisms, including the enzymatic and non-enzymatic degradation of H_2S (Wang R., 2012). These findings suggest the complexity of the mechanisms by which H_2S homeostasis is maintained in the body.

1.1.1 Non-enzymatic intracellular production of H_2S

Large amounts of sulfide can be stored in cells, termed “bound sulfane sulfur” (Table 1) or acid-labile sulfur (iron sulfur clusters) (Ogasawara Y. et al., 1994). H_2S can be released from bound sulfane sulfur as a response to elevated reducing conditions in the cells;

reduced glutathione or thioredoxin may participate in this process. These findings suggest that the H_2S generated from the bound sulfur sulfane pool regulates the cellular redox environment and protects cells from oxidative stress. In contrast, the release of H_2S from the acid-labile sulfur pool occurs in response to acidic conditions below the critical pH of 5.4 (Ishigami M. et al., 2009). However, the physiological relevance of these phenomena is not yet clear.

1.1.2 *De novo* biosynthesis of H_2S

In mammals, there are 3 enzymes that can biosynthesize H_2S *de novo*, namely, cystathionine *β*-synthase (CBS), cystathionine *γ*-lyase (CGL) and 3-mercaptopyruvate sulfurtransferase (3MST) (Kimura H., 2011).

CBS is a pyridoxal 5-phosphate (PLP)-dependent enzyme that catalyzes various reactions by replacing the functional group at the *β*-position of amino acids (Braunstein A. E. and Goryachenkova E. V., 1984). By this mechanism, CBS produces α-aminoacrylate, which is an external aldimine in the enzyme active site (Jhee K. H. et al., 2000). CBS can utilize serine or cysteine as the primary substrate, leading to the release of water or sulfide, respectively. Recovery of the enzyme is mediated by the binding of the secondary substrate to replace PLP. Subsequently, PLP covalently binds to a lysine residue in the enzyme active site, forming an internal aldimine. The secondary substrate can be water or sulfide, releasing serine or cysteine, respectively. However, the preferred secondary substrate for CBS is homocysteine, which leads to the formation of cystathionine. Consistent with this process, CBS deficiency leads to homocysteinemia, which demonstrates the essential role of CBS in the maintenance of homocysteine homeostasis (Kraus J. P. and Kožich V., 2001). Cysteine can also be utilized as a secondary substrate by CBS, leading to the production of lanthionine, but this activity is catalytically inefficient (Singh S. et al., 2009).

Table 1. Bound sulfane sulfur

thiosulfate	$S_2O_3^{2-}$
persulfide	Cys-S-SH (thiocysteine)
protein persulfide	Prot-S-SH (*S*-sufhydration)
glutathion persulfide	Glut-S-SH (thioglutathion)
thiosulfonate	R-SO_2SH (thiotaurin)
polysulfide	Cys-S-S_n-S-Cys (thiocystine)
polythionate	SO^{3-}-S-S-S-SO^{3-} (tetrathionate)
elementar sulfur	protein-(S^0 (protein associated sulfur)

CGL is a PLP-dependent enzyme that catalyzes gamma replacement reactions (Aitken S. M. and Kirsch J. F., 2005). CGL can catalyze the degradation of cystathionine into cysteine, α-ketobutyrate and ammonia in the transsulfuration pathway (Stipanuk M.

H., 1986). *In vitro*, CGL can also produce homolanthionine and cystathionine, along with H_2S. In these reactions, the thiol group of homocysteine is replaced by the addition of homocysteine or cysteine, thus releasing sulfide. Under normal intracellular concentrations of homocysteine, the most effective manner in which CGL produces H_2S is the catabolism of cysteine into H_2S, ammonia and pyruvate (Chiku T. et al., 2009). For this reaction, CGL utilizes cystine (the oxidized form of cysteine) to form cysteine persulfide, from which H_2S can be released in the form of S^0 (oxidized H_2S) by a non-enzymatic process (Yamanishi T. and Tuboi S., 1981).

The third known H_2S-producing enzyme is 3MST, which functions with the PLP-dependent cysteine aminotransferase (CAT). CAT utilizes cysteine to produce mercaptopyruvate, which is then utilized by 3MST to produce H_2S (Shibuya N. et al., 2009). 3MST requires a reducing agent such as thioredoxin or dihydrolipoic acid to complete the decomposition of mercaptopyruvate into H_2S (Mikami Y. et al., 2011).

Although the three H_2S-producing enzymes are expressed in various tissues and cells, it is unclear how each enzyme contributes to the overall homeostasis of H_2S in the body or in specific tissues. CBS and CGL are enzymes of the transsulfuration pathway that converts homocysteine into cysteine, and they are expressed in the liver, pancreas and kidney. CBS is also expressed in the brain, where it acts as a H_2S-producing enzyme (Abe K. and Kimura H., 1996), whereas CGL is expressed in the vascular and respiratory systems and produces

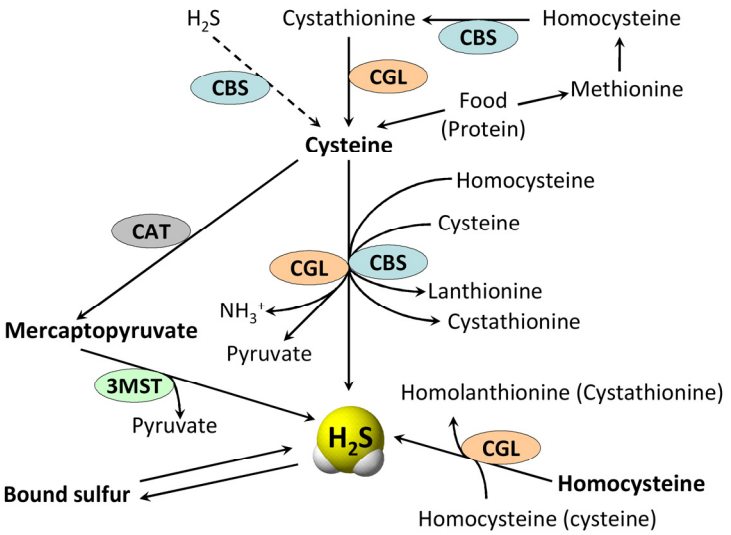

Figure 1. Intracellular H_2S production in mammals. Hydrogen sulfide (H_2S) is enzymatically biosynthesized *de novo* by various reactions. The primary source of H_2S can be i) cysteine, which is absorbed from food, biosynthesized from methionine via the transsulfuration pathway, or produced from H_2S by CBS activity, ii) homocysteine, which is formed in the transsulfuration pathway, or iii) mercaptopyruvate, which is produced by CAT from cysteine. CBS and CGL produce H_2S by the catalyzing the β-replacement of cysteine or the γ-replacement of homocysteine and cystine, respectively. 3MST produces H_2S from mercaptopyruvate in the presence of a reducing agent. In addition, H_2S can be produced in cells from the bound sulfur pools (bound sulfane sulfur and acid labile sulfur). CBS, cystathionine β-synthase; CGL, cystathionine γ-lyase; 3MST, 3-mercaptopyruvate sulfurtransferase; CAT, cysteine aminotransferase.

H_2S in these tissues (Yang G. et al., 2008). 3MST is expressed in many of these tissues, but its contribution to H_2S production is not well understood. Nevertheless, there is growing evidence that 3MST acts as a H_2S-producing enzyme that regulates mitochondrial function (Modis K. et al., 2012).

1.1.3 Catabolism of H_2S

High concentrations of H_2S are toxic for cells because they inhibit the activity of cytochrome c oxidase (COX). The catabolism of H_2S can be mediated by its exhalation, excretion in the urine or degradation into non-toxic compounds (Wang R., 2012). The most common catabolic pathway of H_2S is its oxidation to sulfite (SO_3^{2-}) and, subsequently, to sulfate (SO_4^{2-}), which is then excreted in the urine. The oxidation pathway that occurs in the mitochondria is a complex process requiring several enzymes (Figure 2). First, H_2S binds to the membrane-bound sulfide:quinone oxidoreductase (SQR) to form persulfide (SQR-S-SH). Sulfur dioxygenase (ETHE1) ensures the efficient oxidation of persulfide into SO_3^{2-}, which is further oxidized by sulfite oxidase (SOD) into SO_4^{2-} (Hildebrandt T. M. and Grieshaber M. K., 2008). Alternatively, the SQR-bound persulfide can be converted into SO_3^{2-} and then, reversibly, to thiosulfate ($S_2O_3^{2-}$) by an isoform of the rhodanase-family protein, thiosulfate sulfurtransferase (TST). Thiosulfate can be utilized by rhodanase during cyanide detoxification to form thiocyanate (SCN^-) or reduced back into sulfide. 3MST, a homolog of the rhodanase-like protein family, does not produce thiosulfate (Ramasamy S. et al., 2006), suggesting that 3MST functions exclusively in H_2S production and/or cysteine detoxification. Notably, once H_2S binds to SQR, ubiquinone accepts electrons from H_2S and transfers the

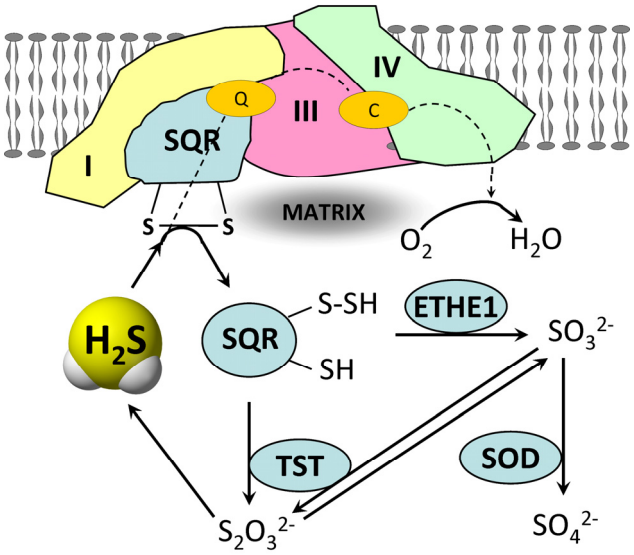

Figure 2. Oxidation of H_2S in the mitochondria. H_2S forms persulfide with SQR. Persulfide is then either oxidized to sulfite by ETHE1 or to thiosulfate and sulfite by TST. Thiosulfate can be either reduced back into sulfide in the presence of a reducing agent such as glutathione or thioredoxin, or oxidized back to sulfite and then, to sulfate, by SOD. The electrons from H_2S (dashed line) are utilized by the respiratory chain super-complexes (I, II, III, IV) for oxidative phosphorylation. SQR, sulfide:quinone oxidoreductase; ETHE1, sulfur dioxygenase; SOD, sulfite oxidase; TST; thiosulfate sulfur transferase

electrons to the complex III of the mitochondrial respiration pathway (Marcia M. et al., 2010). Thus, the mitochondrial oxidation of H_2S mediated by SQR pathway has an impact on cellular bioenergetics (see below).

Another possible H_2S-catabolic pathway is its methylation, which is catalyzed by the enzyme thiol *S*-methyltransferase (TSMT). This process occurs in the cytosol and produces methanethiol (CH_3-SH). TSMT can further methylate methanethiol to dimethylsulfide (CH_3-S-CH_3), which is considerably less toxic. TSMT exhibits its highest activity in the colonic and cecal mucosa (Weisiger R. A. et al., 1980), and it displays lower activities in the liver, lungs, and kidneys. The importance of the methylation process in the catabolism of H_2S is unclear because sulfide methylation is 10,000 times slower than sulfide oxidation, at least in the colonic mucosa (Levitt M. D. et al., 1999). Thus, the methylation of H_2S might not occur in cells due to its detoxification, but methanethiol might be biosynthesized to serve as a signaling molecule. H_2S can also react non-enzymatically with oxidants, which drastically decreases the H_2S levels in cells, especially during oxidative stress (Carballal S. et al., 2011). These reactions that scavenge various radical species represent another possible mechanism by which H_2S modulates various physiological responses in cells (see below). The involvement of each H_2S-detoxification pathway and its contribution to the regulation of specific H_2S-signaling pathways is largely unknown and requires additional studies.

1.2 Molecular mechanisms of H_2S signaling

The physical properties of gaseous H_2S allow its transportation across membranes by diffusion without the need for transporters; thus, H_2S is widely distributed in the body. There is growing evidence that H_2S derived from exogenous and endogenous sources serves as a signaling molecule, but the contribution of sulfide from each source to the pool is unknown. The steady-state sulfide concentrations in the intracellular and extracellular space are unclear because prior studies have reported a 10^5-fold concentration range. The concentration of exogenous H_2S that is necessary to initiate a physiological response is 10-1000 µmol/l, but recent studies suggest that the H_2S concentrations in blood and tissues are 10-100 times lower (Furne J. et al., 2008; Olson K. R., 2009; Whitfield N. L. et al., 2008). The chemical properties of sulfide indicate that under physiological conditions (37 °C, pH 7.4), approximately 80% of the free sulfide pool is present in the form of HS^-, whereas 20% is present in the state as H_2S (Wang R., 2012).

Table 2. Selected examples of H_2S signaling

Mechanism	Target	Regulation	Effect
metal binding	hemoglobin	reduces oxygen transport	hypoxia
	myoglobin	reduces oxygen transport	hypoxia
	cytochrome c	diminishes electron transport	impaired bioenergetics
	cytochrome c oxidase	diminishes electron transport	impaired bioenergetics
	cytochrome c oxidase	activates K_{ATP} channel	muscle relaxation
S-sulfhydration	PTP1B	inactivates PTP1B	ER stress resistance
	p65	inhances NF-κB/RPS3 interaction	anti-inflammatory effect
	GAPDH	increases GAPDH activity	increased rate of glycolysis
	KEAP1	activates Nrf2	stress resistance
	Kir6.1, SUR	opens KATP channel	vasodilatation
	SQR	Increased electron transport	improved bioenergetics
radical scavenging	$NO^{\cdot}$	sequestration of NO	impaired NO signaling
	H_2O_2, $OH^{\cdot}$, $ONOO^{-}$	decreased ROS	oxidative stress resistance

The H_2S signaling is mediated by at least 3 different direct molecular mechanisms that exert a wide array of physiological and pathological effects (Table 2). H_2S is a strong nucleophile that targets metalloproteins such as cytochrome c oxidase and carbonic anhydrase, and it interacts with the heme moiety and other metal ions (Cu, Fe). These interactions usually result in the inhibition of protein function, as determined for COX (Hill B. C. et al., 1984). The binding of H_2S to COX results in the impairment of electron transport in the inner mitochondrial membrane, leading to the inability of cells to produce ATP. In addition, the binding of H_2S to hemoglobin or myoglobin results in the formation of sulfhemoglobin or sulfmyoglobin, respectively, which have decreased affinities for oxygen (O_2), diminishing inter-organ and intracellular oxygen transport (Pietri R. et al., 2011).

Another mode of H_2S action is the covalent modification of thiols, especially the cysteine residues in various proteins. This process, termed "*S*-sulfhydration" occurs at cysteine residues that are accessible for modification (at the protein surface or active site), and their thiol group is oxidized by the formation of disulfide bonds (proteinCys-S-S-R) (Nagy P. and Winterbourn C. C., 2010), sulfenic acid (proteinCys-S-OH) (Finkel T., 2012), or the cyclic sulfenamide conformation (Krishnan N. et al., 2012). Several proteins are sulfhydrated, including the p65 subunit of the nuclear factor NF-κB (Sen N. et al., 2012) and KEAP1, which regulates the Nrf2 transcription factor (Hourihan J. M. et al., 2013). Notably, *S*-sulfhydration (Cys-S-SH) is more common than *S*-nitrosylation (Cys-S-NO), which is a mechanism of another signaling molecule and gasotransmitter, NO.

Whereas *S*-sulfhydration is considered to increase and stabilize protein activity, *S*-nitrosylation leads to the inhibition of protein function, as determined for glyceraldehyde 3-phosphate dehydrogenase (GAPDH) (Mustafa A. K. et al., 2009) and the transcription factor NF-κB (Sen N. et al., 2012). H_2S and NO may act sequentially during the post-translational modification of proteins and thus activate and subsequently inactivate proteins, respectively. However, a recent study showed that *S*-sulfhydration and *S*-nitrosylation may act in the same manner, i.e., to inactivate enzymatic activity, as determined for the protein tyrosine phosphatase PTP1B (Krishnan N. et al., 2012). Furthermore, *S*-sulfhydration of SQR, which serves as the primary catabolic pathway for H_2S (see above), does not regulate SQR function but transfers electrons from H_2S to the inner mitochondrial membrane, thus improving the production of ATP and O_2 consumption. This positive effect of H_2S on cellular bioenergetics is mediated by low H_2S concentrations, while the inhibitory effect occurs at higher concentrations (above 20 μM) (Bouillaud F. and Blachier F., 2011; Lagoutte E. et al., 2010). Therefore, the concentration of H_2S in mitochondria is a critical factor that dictates the regulation of mitochondrial function, which reveals the dual mode of H_2S signaling in mitochondria.

H_2S is also a strong reducing agent that participates in the regulation of the redox balance by directly reacting with various reactive oxygen species (ROS) (Li Q. and Lancaster J. R., Jr., 2013). The resulting scavenging of free radicals modulates the redox balance in cells and protects them against oxidative stress (Carballal S. et al., 2011). Although these reactions appear to have low catalytic rates, the direct antioxidant properties of H_2S depend on its concentration; thus, the significance of these reactions may increase at higher levels of H_2S (Nagy P. and Winterbourn C. C., 2010). As noted above, H_2S might also maintain the cellular redox balance by reducing disulfide bonds. The role of H_2S in the maintenance of the redox environment is more complex.

Another possible mechanism of H_2S action is its role as a substrate for enzymatic reactions. CBS can utilize serine and sulfide to form cysteine at a low catalytic rate (see above, Figure 1) (Braunstein A. E. et al., 1971; Nozaki T. et al., 2001). This enzymatic activity has evolved from the plant and bacterial sulfur assimilation pathways (Kredich N. M. and Tomkins G. M., 1966), in which *O*-acetylserine(thiol)lyases (OAS-TL) utilize *O*-acetylserine and sulfide to form cysteine; this reaction serves as a regulatory mechanism for plant H_2S signaling (Hell R. and Wirtz M., 2011). Future studies will address the role of the serine sulfhydrylase activity mediated by CBS in H_2S signaling in animals.

1.3 Role of H_2S in hypoxia

Various human disorders, such as ischemic heart disease and stroke, share common mechanisms relating to hypoxia. Mammals and other vertebrates respond to hypoxic conditions by the vasodilation of the peripheral arteries and the vasoconstriction of the pulmonary vessels, thus improving oxygen delivery to critical tissues. The change in oxygen concentration is monitored by O_2-sensing tissues, which transduce the signal to elicit a physiological response. There are several hypotheses on how O_2 sensing works (Sylvester J. T. et al., 2012). A decrease or an increase in the concentration of ROS during hypoxia leads to the depolarization of voltage-gated calcium channels and causes vasoconstriction/vasodilation. It is also hypothesized that the impairment of oxidative phosphorylation during hypoxia activates the AMP kinase, leading to the opening of the voltage-gated calcium channels. There is evidence that the decreased activity of heme oxygenase, which produces carbon monoxide, or nitric oxide synthase, which produces nitric oxide, is involved in acute O_2-sensing and signaling.

Notably, recent studies have proposed that H_2S serves as an O_2 sensor/transducer (Olson K. R. et al., 2006). This hypothesis is based on several observations: exposure to H_2S mimics hypoxia, degradation of H_2S is an O_2-dependent process (the H_2S concentration dramatically increases during anoxia), H_2S production depends on O_2 availability (carbon monoxide produced by the O_2-dependent heme oxygenase inhibits CBS activity (Morikawa T. et al., 2012)), and increased H_2S production and hypoxia trigger identical responses (Olson K. R., 2013). However, it is not clear whether hypoxia and H_2S function via the same pathway or whether these two factors operate in parallel or even sequentially to promote the hypoxia-mediated responses. For example, it is known that K_{ATP} channels that regulate the vasodilation of smooth muscle cells are modulated by both hypoxia and H_2S, but the mechanism is unclear (Weir E. K. and Archer S. L., 1995; Zhao W. et al., 2001). Future studies on H_2S signaling during hypoxic conditions will address this issue.

Notably, the tissue damage caused by oxygen deprivation can be partially alleviated by repeated short-term hypoxia, suggesting that cells possess adaptation mechanisms that permit survival. The mechanisms responsible for these physiological responses are not well understood; nevertheless, the observed beneficial effects of H_2S during hypoxia led to the hypothesis that H_2S is important for the long-term protection against hypoxia. In rodents, exogenous H_2S leads to a hibernation-like state (suspended animation) with decreased

metabolic rate and core body temperature (Blackstone E. et al., 2005), and it reduces oxygen demand; 20 minutes after exposure to H_2S, the animals can survive many hours in a 5% oxygen atmosphere compared to animals that were not treated with H_2S, which were able to survive only briefly. This effect protects animals from hypoxia and hemorrhage and diminishes ischemia-reperfusion injury (Blackstone E. and Roth M. B., 2007; Ganster F. et al., 2010). The proposed mechanism for the H_2S-dependent decrease in oxygen demand is the H_2S-mediated inhibition of COX, which decreases the generation of ROS in the mitochondria. In cultured rat cells and in the animal model organism *C. elegans*, H_2S activates the hypoxia-inducible factor-1 (HIF-1) (Budde M. W. and Roth M. B., 2010; Liu X. et al., 2010), which is a crucial transcription factor for the adaptation to hypoxic conditions (Semenza G. L., 2000). However, the mechanism of this activation is unknown and requires further studies (see below).

The role of H_2S during hypoxia in mammals has a likely evolutionary basis. H_2S played an important role during the evolution of life because it was the main energy source for lithotrophic organisms (Olson K. R., 2012). It appears that the ancient mechanism of utilizing H_2S for electrons in bioenergetics was retained in higher animals for O_2-dependent H_2S detoxification, signaling, and for the H_2S-mediated regulation of mitochondrial function.

1.4 Studies on H_2S signaling in *C. elegans*

Several studies have demonstrated that the exposure to H_2S and the modulation of H_2S metabolism increase the viability and survival of animals in otherwise lethal conditions, such as hypoxia, and oxidative and toxic stresses. H_2S-induced changes in animal physiology have also been studied in invertebrate model organisms. For example, exposure to H_2S increases the desiccation tolerance of fruit flies (Zhong J. F. et al., 2010). Studies have shown that the exposure of the nematode *Caenorhabditis elegans* to non-lethal concentrations of H_2S increases its thermotolerance and prolongs its longevity (Miller D. L. and Roth M. B., 2007). The roundworm *C. elegans* is a popular model organism for studying animal physiology, developmental biology and signaling pathways due to its easy cultivation, low cost of maintenance, short generation time and genetic tractability. Consequently, in the past 5 years, *C. elegans* has been used as a model for studying H_2S signaling and its physiological responses.

It was proposed that SIR-2.1, a homolog of the NAD^+-dependent deacetylases, plays a role in prolonging the lifespan of *C. elegans* in response to H_2S. Unlike the wild type strain, *sir2.1* mutants do not have a prolonged lifespan during exposure to 50 ppm H_2S (Miller D. L. and Roth M. B., 2007). H_2S activates two transcription factors, namely, hypoxia-inducible factor 1 (HIF-1, the worm ortholog of the mammalian HIF-1α subunit) and skinhead 1 (SKN-1, the worm ortholog of the mammalian NRF2) (Miller D. L. et al., 2011). HIF-1 and SKN-1 are responsible for alleviating hypoxic and other oxidative or xenobiotic stresses (An J. H. and Blackwell T. K., 2003). Because *hif-1* or *skn-1* mutant nematodes have significantly decreased lifespans (Hwang A. B. and Lee S. J., 2011; Kell A. et al., 2007; Tullet J. M. et al., 2008), it is tempting to speculate that H_2S prolongs the longevity of *C. elegans* via the activation of HIF-1 and/or SKN-1. Consistent with this hypothesis is the finding that a component of garlic, diallyl trisulfide (a H_2S donor) increases the lifespan of worms via *skn-1* activation (Powolny A. A. et al., 2011). While the mechanism by which the H_2S signals are transduced in the cells to activate SKN-1 is unknown, the mechanism of HIF-1-activation has been partially described. Nevertheless, the relationships between H_2S and SIR2.1, HIF-1 and SKN-1, as well as the mechanisms by which they prolong the lifespan in *C. elegans*, remain to be determined.

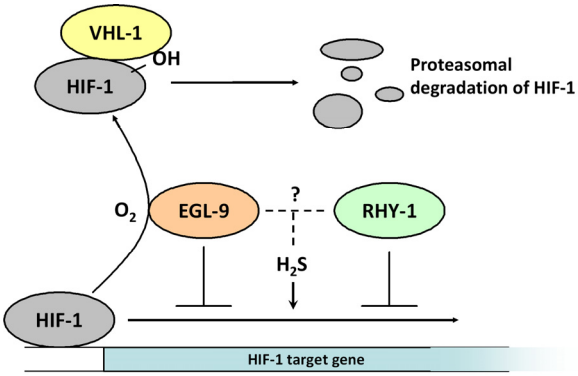

Figure 3. Hypoxia-mediated activation of HIF-1. In normoxic conditions, EGL-9 hydroxylates the proline residue of HIF-1, which permits the binding of the ubiquitin ligase VHL-1 to HIF-1, leading to the degradation of HIF-1. Hypoxia leads to sequestration of EGL-9 activity. EGL-9 also inhibits the transcriptional activity of HIF-1 via an unknown, VHL-1-independent pathway. H_2S activates HIF-1 independently of VHL-1. RHY-1, another regulator of HIF-1 activity, operates independently of VHL-1 and H_2S.

1.4.1 The role of H_2S in HIF-1 signaling in *C. elegans*

HIF-1 is a conserved transcription factor that is activated in cells during hypoxia. The depletion of oxygen impairs the activity of EGL-9, which is a conserved dioxygenase that is homologous to the mammalian EGLN protein family (Taylor M. S., 2001). EGL-9 directly hydroxylates a proline residue of HIF-1, which permits the binding of the von Hippel-Lindau 1 (VHL-1) ubiquitin ligase that targets HIF-1 for proteasomal degradation

(Epstein A. C. et al., 2001) (Figure 3). Notably, hypoxia diminishes the hydroxylation of HIF-1 by *vhl-1*-dependent HIF-1 inhibition and inhibits HIF-1 transcriptional activity by a *vhl-1*-independent mechanism. There are two known regulators of this pathway in *C. elegans*- EGL-9 and RHY-1, which is a conserved transmembrane acyltransferase (Shao Z. et al., 2009; Shen C. et al., 2006). Intriguingly, the experiments with *vhl-1* and *egl-9* mutants showed that the effect of H_2S on HIF-1 is mediated by *vhl-1*-independent signaling (Budde M. W. and Roth M. B., 2010) (Figure 3). Exogenous H_2S leads to the translocation of HIF-1 to the nucleus and promotes HIF-1 transcriptional activity in the hypodermis (Budde M. W. and Roth M. B., 2010). Notably, H_2S and hypoxia result in different tissue-specific patterns of HIF-1 activation; hypoxia results in HIF-1 activation in the gut. The mutually exclusive roles of hypoxia and H_2S and the relationship between EGL-9 and RHY-1 in HIF-1-regulation are not yet established. It is also unclear whether H_2S-metabolizing enzymes can modulate the activation of HIF-1.

1.4.2 H_2S metabolism in *C. elegans*

Although H_2S metabolism in *C. elegans* has not been studied, knowledge of the *C. elegans* genome sequence and expression studies has allowed the identification of genes encoding putative H_2S-metabolizing enzymes in *C. elegans*. Intriguingly, a large number of genes encoding homologs of H_2S-producing enzymes have been identified in the *C. elegans* genome (Mathew N. D. et al., 2011), namely, 10 genes encoding proteins homologous to CBS, 3 genes encoding homologs of CGL, and 7 genes encoding homologs of 3MST (Table 3). However, there are fewer genes that encode homologs of H_2S-catabolizing enzymes; 2 genes encode proteins homologous to SQR (*sqrd-1* and *sqrd-2*), 1 gene encodes a homolog of ETHE1 (*ethe-1*), and 1 gene encodes a homolog of SOD (*suox-1*). Studies that investigated the genes responsible for the survival of *C. elegans* in otherwise lethal H_2S

Table 3. Genes encoding putative H_2S-producing enzymes in *C. elegans*

Enzyme	Gene name	Sequence
CBS	*cbs-1*	ZC373.1
	cbs-2	F54A3.4
	cysl-1	C17G1.7
	cysl-2	K10H10.2
	cysl-3	R08E5.2
	cysl-4	F59A7.9
	NA	F01D4.8
	NA	T25D3.3
	NA	T01H8.2
	NA	F13B12.4
CGL	*cth-1*	F22B8.6
	cth-2	ZK1127.10
	cbl-1	C12C8.2
3MST	*mpst-1*	D2023.5
	mpst-2	H12D21.4
	mpst-3	H12D21.7
	mpst-4	F11G11.9
	mpst-5	Y59H11AM.2
	mpst-6	Y59H11AM.3
	mpst-7	R186.6

CBS, cystathionine beta-synthase;
CGL, cystathionine gamma-lyase;
3MST, 3-mercaptopyruvate sulfurtransferase

concentrations have identified *sqrd-1*, a HIF-1 target gene, as an essential factor for the survival of *C. elegans* (Budde M. W. and Roth M. B., 2010; Budde M. W. and Roth M. B., 2011). Moreover, mutations in *ethe-1* also decrease the resistance of *C. elegans* to H_2S. These findings suggest that *C. elegans* cells have an oxidative pathway for the catabolism of H_2S. However, it is not clear whether HIF-1 also triggers the expression of SQR in mammalian cells. While the catabolism of H_2S appears to be conserved in *C. elegans*, the large number of genes encoding H_2S-producing enzymes suggests that the metabolism of H_2S is more complex; it is also not clear whether these paralogs have overlapping (H_2S-producing activity) or distinct roles in *C. elegans* biology. Thus, studying the roles of these genes might reveal novel aspects of H_2S metabolism and signaling in animals and other evolutionarily distant organisms.

2. AIMS OF THE STUDY

In contrast to other animals, the roundworm *Caenorhabditis elegans* possesses a large number of genes encoding putative H_2S-producing enzymes, however, the role of these genes in *C. elegans* is unknown. In this Ph.D. project we aimed to study the genes that encode CBS-related proteins in *C. elegans*. Specifically, we aimed to determine the roles of these proteins in *C. elegans* and to understand our results in the context of the present knowledge on H_2S signaling and metabolism.

Specific aims:

A) Characterization of the cystathionine beta-synthase in *C. elegans*

- To determine which gene encodes CBS in *C. elegans* using phylogenetic analysis of the amino acid sequences, to determine the catalytic activity of the recombinant purified CBS proteins and study the biochemical and phenotypic consequences of inactivation of the CBS-encoding genes.
- To determine the conserved structural features in the nematode and human CBS enzymes using *in silico*, biochemical and biophysical analyses and to discuss the potential use of *C. elegans* as a model for human CBS deficiency.

B) Roles of the CBS-related proteins in *C. elegans*

- To determine the biochemical properties of the CBS-related recombinant purified proteins, specifically, their catalytic activities, substrate binding affinities, and quaternary structures and conformations.
- To propose the roles of the CBS-related proteins in *C. elegans*

C) Novel aspects of H_2S metabolism and signaling in the model system *C. elegans*

- To discuss the role of CBS-related proteins in H_2S metabolism and signaling, and propose future directions.

3. RESULTS AND DISCUSSION

3.1 Characterization of cystathionine beta-synthase in *C. elegans*

One goal of our project was to use the roundworm *C. elegans* to develop a novel CBS-deficient model system that could be utilized for studying the pathogenetic mechanisms of CBS deficiency and/or the physiological actions of endogenously produced H_2S. To accomplish our goal, we first identified the gene encoding the cystathionine beta-synthase in the *C. elegans* genome and examined its expression pattern. Next, we characterized the recombinant nematode CBS-1 enzyme by biophysical methods and determined its catalytic properties and conformation. Finally, we examined the effect of CBS deficiency by RNA interference in *C. elegans*. These data and a description of the materials and methods used in the study were published in the Biochemical Journal (Supplement 6.1.1).

3.1.1 The *cbs-1* gene encodes cystathionine beta-synthase in *C. elegans*

We used several approaches to determine which gene encodes CBS in *C. elegans*. Our *in silico*, biochemical and genetic data showed that the *cbs-1* gene encodes CBS in *C. elegans.*

C. elegans possesses 6 candidate CBS-encoding genes

BLASTp searches revealed that the *C. elegans* genome contains at least 10 genes encoding hypothetical proteins that are homologous to CBS. Analysis of the level of homology and a phylogenetic study showed that 2 of these proteins (CBS-1 and CBS-2) are the most homologous to CBS. Four other proteins, CYSL-1 - CYSL-4, were determined to be the most homologous to the plant OAS-TL enzymes, which are considered to be the ancestors of CBS. In the *C. elegans* database WormBase, 4 other hypothetical proteins are listed as CBS-related proteins; however an *in silico* alignment revealed that they have very low homology to CBS, and phylogenetic analysis revealed that these proteins constitute a novel class of proteins belonging to the *β*-family of PLP-dependent proteins. Therefore, we focused on the characterization of the genes encoding the CBS and OAS-TL proteins, while the remaining 4 genes, which are unlikely to encode CBS proteins in *C. elegans*, were excluded from further studies. Nevertheless, it would be interesting to elucidate the roles of these 4 proteins in *C. elegans* to expand the functional divergence of proteins belonging to the family of CBS-related proteins.

cbs-2 and cysl-4 are pseudogenes

We analyzed the transcriptional activities of all 6 putative CBS-encoding genes in *C. elegans*, namely, *cbs-1*, *cbs*-2, *cysl-1*, *cysl-2*, *cysl-3* and *cysl-4*. First, we used various *C. elegans* cDNA molecules as templates to amplify the transcripts by PCR. Four mRNAs (*cbs-1*, *cysl-1*, *cysl-2* and *cysl-3*) were successfully amplified and sequenced to confirm their identity with the sequences deposited in the *C. elegans* database, WormBase. On the other hand, we were unable to amplify the *cbs-2* and *cysl-4* mRNAs. Next, we searched the online databases GenBank and PeptideAtlas for evidence that these genes are expressed. Consistent with our PCR data, we found ESTs and peptide data for the *cbs-1*, *cysl-1*, *cysl-2* and *cysl-3* genes, but not for *cbs-2* and *cysl-4*. These data suggest that *cbs-2* and *cysl-4* are not expressed in *C. elegans*, and these genes were excluded from further studies.

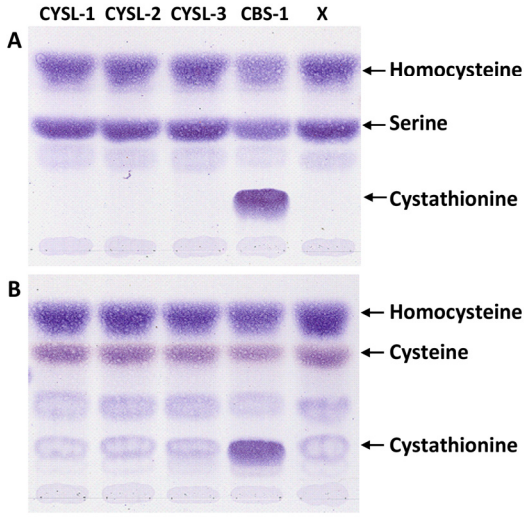

Figure 4. Analysis of the cystathionine-synthesizing activities of the worm CBS-related proteins. A) TLC analysis of canonical CBS activity condensing serine and homocysteine into cystathionine. B) TLC analysis of the H_2S-producing activity of CBS, which condenses cysteine and homocysteine into cystathionine. Only CBS-1 condenses serine or cysteine with homocysteine to form cystathionine and water or sulfide, respectively. Amino acids were detected by ninhydrin. Lane X represents reaction mixture without enzyme.

Only CBS-1 exhibits CBS activity

Next, we studied the catalytic activities of the 4 CBS-related proteins that are expressed in *C. elegans*, namely, CBS-1, CYSL-1, CYSL-2 and CYSL-3. We used a bacterial system to express and purify the recombinant proteins. We purified 1-3 mg of each protein to greater than 90% homogeneity, from 1 liter of bacterial culture. All 4 CBS-related proteins possess the cofactor pyridoxal-5'-phosphate (PLP), as determined by UV-visible absorption spectroscopy. We determined that only CBS-1 exhibits typical CBS activity and that it condenses either serine or cysteine with homocysteine to form cystathionine and water or sulfide, respectively (Figure 4). These data strongly suggested that CBS-1 is the only

protein that exhibits CBS activity in *C. elegans* and that the other CBS-related proteins, namely, CYSL-1, CYSL-2 and CYSL-3 have other roles in *C. elegans* biology.

CBS-1 maintains homocysteine homeostasis in C. elegans

To examine the phenotypic and biochemical effects of *cbs-1* deficiency in nematodes, we performed RNA interference to silence the *cbs-1* gene. The *cbs-1* knockdown animals had approximately 10% CBS activity and exhibited elevated homocysteine levels, which is a typical feature of CBS deficiency in mammals (Kraus J. P. and Kožich V., 2001). Moreover, we observed severe developmental and morphological effects that might, in part, recapitulate the pathogenesis of human CBS deficiency (see below). These data support our previous findings that cystathionine beta-synthase is encoded by the *cbs-1* gene in *C. elegans*.

3.1.2 *C. elegans* as a model for CBS deficiency

The use of *C. elegans* as a model for CBS deficiency requires the knowledge of the regulation of the nematode CBS enzyme. In animals, CBS is a modular protein with catalytic and regulatory domains. The structural arrangement of these domains, which is crucial for the allosteric regulation of CBS activity, differs in various species. To study whether the structure of the worm protein is conserved with the human enzyme, we used *in silico* analysis and studied the enzymatic, biochemical and biophysical properties of specific CBS-1 domains. Our data revealed the completely novel arrangement of the CBS enzyme domains, which has not been observed for CBS proteins in any other species. These data suggest that the regulation of the CBS enzyme is altered in *C. elegans* in comparison with mammals. The use of *C. elegans* as a model for CBS deficiency might elucidate the roles of the catalytic and regulatory domains of the CBS enzyme in the pathogenic mechanisms of the nematode and mammalian CBS deficiency.

C. elegans lacks the canonical animal mechanisms that regulate the CBS enzyme activity

The alignment of the amino acid sequences of CBS proteins across phyla revealed the unique structural arrangement of the nematode enzyme (Figure 5). We observed that CBS-1 possesses 2 regions that are homologous to the catalytic domain in other CBS proteins. Notably, the critical lysine residue responsible for the covalent binding of PLP to the protein is conserved only in the C-terminal region, whereas, in the N-terminal region this residue is replaced by glutamic acid. This observation suggested that the catalytic domain

is encoded in the C-terminal region. The N- and C-terminal domains were expressed separately, and the N-terminal domain was successfully purified and found to exhibit neither CBS activity nor PLP-binding. However, the C-terminal domain was not soluble after expression in *E. coli*, suggesting that the N-terminal domain is essential for the correct CBS-1 conformation and/or folding. Moreover, the experiments evaluating the quaternary protein structure suggested that CBS-1 is a monomeric protein, while its orthologs form homodimeric and higher oligomeric structures (Jhee K. H. et al., 2000; Meier M. et al., 2001). Thus, we concluded that the two domains of monomeric CBS-1 might recapitulate the dimeric conformation of CBS enzymes in other phyla, with the N-terminal domain stabilizing the CBS-1 protein. Nevertheless, the exact role of the N-terminal domain of CBS-1 remains to be determined.

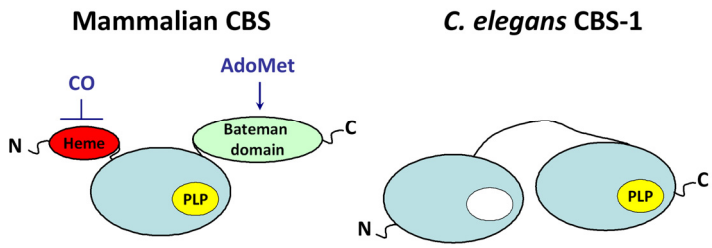

Figure 5. Structural arrangement of the CBS subunits in mammals and nematodes. The mammalian enzyme contains a heme-binding domain and a Bateman domain. Carbon monoxide (CO) or *S*-adenosylmethionine (AdoMet) can bind to the heme and Bateman domains to inhibit or activate CBS, respectively. The nematode ortholog lacks both of these domains but contains two regions homologous to the catalytic domain of the mammalian enzyme. The N-terminal domain does not bind PLP and is catalytically inactive.

We showed that CBS-1 does not possess the heme-binding and Bateman domains that are essential for the regulation of CBS activity in other animals (Figure 5). Heme can bind carbon monoxide, which inhibits CBS activity (Shintani T. et al., 2009; Singh S. et al., 2007) while the Bateman domain binds *S*-adenosylmethionine (Kery V. et al., 1998) which is a known activator of CBS. Thus, we conclude that the nematode protein is not regulated in the same manner as the mammalian enzyme.

The use of C. elegans to study the pathogenic mechanisms in CBS deficiency

We showed that the RNA interference-mediated silencing of *cbs-1* leads to several phenotypic changes. We observed a developmental delay in the knockdown animals, which is consistent with previous reports that the exposure to homocysteine leads to a developmental delay in *C. elegans* (Khare S. et al., 2009). These data suggest that the elevated homocysteine level in *cbs-1* knockdown animals is the major cause of this phenotype. We also observed the abnormal morphology of several tissues, such as the intestine and pharyngeal muscle cells. Consistent with this observation, the *cbs-1* gene is

expressed mostly in these tissues, as determined using a GFP reporter. Therefore, we concluded that studies of such phenotypic changes might lead to the discovery of novel pathogenic mechanisms in human CBS deficiency.

Unlike the human CBS protein, the nematode enzyme lacks the regulatory domains for binding to carbon monoxide or *S*-adenosylmethionine. Thus, the common pathological processes resulting from CBS deficiency in *C. elegans* and mammals might be associated with the impairment of the canonical catalytic activity of the CBS enzyme and not the decreased ability of the CBS enzyme to bind either carbon monoxide or *S*-adenosylmethionine. In addition, the role of decreased H_2S production in the pathogenic mechanisms of CBS deficiency can also be studied using *C. elegans* as a model system (see below).

3.2 Roles of the *C. elegans* CBS-related proteins (OAS-TL)

Because the 3 CBS-related proteins did not exhibit CBS activity, we used phylogenetic analysis to explore their evolutionary counterparts in other phyla and to predict their *in vivo* functions. This analysis revealed that the *C. elegans* paralogs constitute a novel class of *O*-acetylserine(thiol)lyases (OAS-TL) with the highest homology to their plant orthologs. These data suggest that the genes encoding the worm and plant orthologs evolved from a common ancestor that was duplicated in the nematode genome. Consequently, all purified proteins were analyzed for the structural and catalytic properties that were observed previously in plant OAS-TL enzymes. Together with previous studies, our data show that these proteins have distinct roles in *C. elegans*. These data were published in the journal BBA- Proteins and Proteomics (Supplement 6.1.2). In addition, a paper on the specific role of CYSL-1 was published in the journal Neuron (Supplement 6.1.3). Both publications contain descriptions of all materials and methods used in these studies.

3.2.1 All the nematode OAS-TL proteins can bind and metabolize *O*-acetylserine

We determined that all the nematode OAS-TL proteins bind the canonical substrate, *O*-acetylserine, and convert it to α-aminoacrylate by a β-replacement reaction. All 3 proteins subsequently utilize sulfide or cyanide as a secondary substrate to produce cysteine or β-cyanoalanine, respectively. The production of cysteine from *O*-acetylserine occurs in the sulfur assimilation pathway, exclusively in plants and bacteria (Hell R. and Wirtz M.,

2011; Kredich N. M. and Tomkins G. M., 1966). In contrast, *C. elegans* lacks serine *O*-acetyltransferase (SAT), the enzyme that produces *O*-acetylserine. Therefore, it is unlikely that the nematode OAS-TL proteins utilize *O*-acetylserine for sulfur assimilation to biosynthesize cysteine parallel to the transsulfuration pathway. We propose that these proteins have different roles in *C. elegans* (see below). Nevertheless, there is a possibility that *C. elegans* may obtain traces of *O*-acetylserine from food (bacteria), and we hypothesize that *O*-acetylserine might regulate the *in vivo* function of these proteins by binding to their active sites.

3.2.2 The *C. elegans* OAS-TL paralogs exhibit different conformations

In contrast to CBS-1, the 3 nematode CBS-related proteins possess only one region conserved with the catalytic domain of other CBS enzymes. We determined that all 3 *C. elegans* OAS-TL enzymes exist predominantly as dimers and thus have the same structural arrangement and oligomeric status as their plant or bacterial orthologs (Becker M. A. et al., 1969; Bonner E. R. et al., 2005). However, we observed that these paralogs exhibit different kinetic behaviors and conformations relative to each other, as revealed by different retention times during electrophoretic and gel filtration procedures under non-denaturing conditions. Furthermore, molecular dynamic simulations suggested that the nematode OAS-TL paralogs differ in their conformations during catalysis. These findings suggested that the *C. elegans* OAS-TL paralogs have distinct functions in cells.

3.2.3 The *C. elegans* OAS-TL paralogs have distinct roles in *C. elegans*

Combined with data from other studies, our i*n silico*, genetic, biochemical and physiological data revealed that the nematode OAS-TL paralogs have distinct roles in the nematodes.

CYSL-1 transduces H_2S signals to activate HIF-1 in response to hypoxia

We determined that the recombinant CYSL-1 protein exhibits *O*-acetylserine sulfhydrylase activity, and previous studies have suggested that this activity can be crucial for alleviating sulfide toxicity in nematodes, as determined by the screening of *C. elegans* mutants (Budde M. W. and Roth M. B., 2011). However, genetic screens to identify novel regulators of the EGL-9/HIF-1 pathway identified the *cysl-1* gene as a suppressor of *egl-9*. These screens showed that RHY-1 inhibits CYSL-1, which then inhibits EGL-9. Thus, CYSL-1 activates HIF-1, which modulates animal behavior and alleviates sulfide and

cyanide toxicity in *C. elegans*. Notably, the enzymatic activity of CYSL-1 does not play a role in the inhibition of EGL-9. In fact, we determined that the nematode CYSL-1 protein interacts (via its active site) with the C-terminus of EGL-9, leading to the sequestration of EGL-9 and the subsequent activation of HIF-1. Furthermore, the CYSL-1/EGL-9 association is enhanced by exposure to H_2S. However, the exact mechanism by which H_2S activates CYSL-1 remains to be determined.

Intriguingly, this mechanism of interaction evolved from the ancient regulation of cysteine biosynthesis in bacteria and plants (Figure 6). The OAS-TL enzymes in these species interact with the C-terminus of serine acetyltransferase (SAT), which leads to the inhibition of OAS-TL activity (Hell R. and Wirtz M., 2011). H_2S activates the formation of this plant cysteine synthase complex and the nematode CYSL-1/EGL-9 complex. Previous studies have shown that *O*-acetylserine, the canonical substrate of the OAS-TL enzymes, may dissociate the cysteine synthase complex, demonstrating its regulatory role in plants (Wirtz M. et al., 2004). Because we observed that the affinity of CYSL-1 for *O*-acetylserine is very high compared to its paralogs, we hypothesized that *O*-acetylserine might compete with the EGL-9 C-terminus for binding to the active site of CYSL-1 and thus might regulate HIF-1 signaling. Consistent with this hypothesis is the observation that the HIF-1 activation is dependent on food availability (which is proposed source of *O*-acetylserine in *C. elegans*) (Chen D. et al., 2009). Further studies will be needed to understand this complex regulatory network.

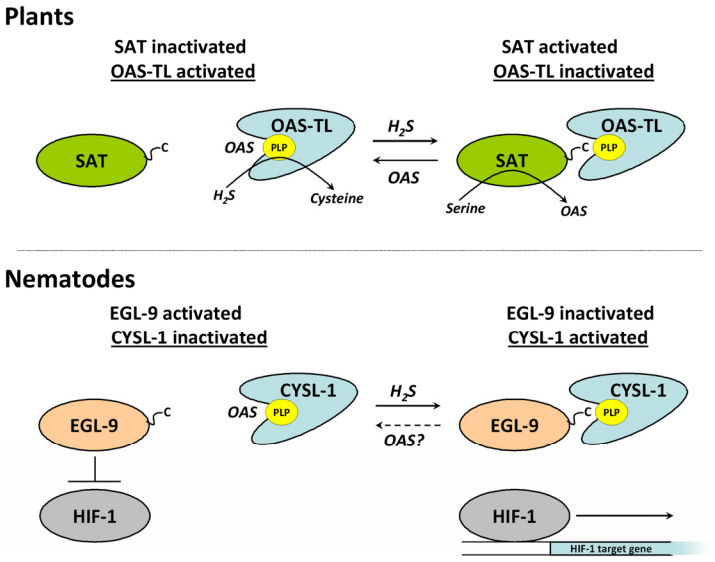

Figure 6. The role of the nematode CYSL-1 evolved from an interacting mode of cysteine synthase complexes in plants (microorganisms). The plant OAS-TL and serine *O*-acetyltransferase (SAT) interact to regulate cysteine biosynthesis in the sulfur assimilation pathway. The nematode CYSL-1 and EGL-9 interact to regulate HIF-1 activity. Both protein interactions are enhanced by H_2S. *O*-acetylserine (OAS) dissociates the protein complex in plants and possibly in nematodes.

CYSL-2 functions as a cyanoalanine synthase in the cyanide detoxification pathway

We determined that the recombinant CYSL-2 protein catalyzes various *β*-replacement reactions. It can utilize *O*-acetylserine, *S*-sulfocysteine and cysteine as primary substrates and condense them with sulfide or cyanide to form cysteine or beta-cyanoalanine, respectively. CYSL-2 is the sole CBS-related protein in *C. elegans* that can utilize cysteine to detoxify cyanide, using its cyanoalanine synthase (CAS) activity (Figure 7). This activity of CYSL-2, which is utilized for cyanide detoxification in plants and bacteria (Hell R. and Wirtz M., 2011), is consistent with studies showing that *cysl-2* mutants exhibit a decreased ability to survive exposure to cyanide and cyanide-producing bacteria, while the mutants with up-regulated *cysl-2* exhibit increased survival compared to the wild-type strain (Budde M. W. and Roth M. B., 2011; Saldanha J. N. et al., 2013). Furthermore, *cysl-2* is a HIF-1 target gene that can be upregulated via HIF-1 activation during exposure to cyanide or cyanide-producing bacteria (Budde M. W. and Roth M. B., 2011; Shao Z. et al., 2010). Thus, it is likely that CYSL-2 serves as the cyanoalanine synthase in the cyanide detoxification pathway.

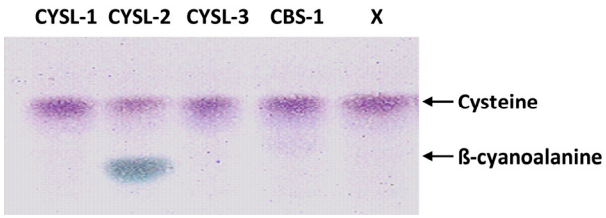

Figure 7. CYSL-2 exhibits cyanoalanine synthase activity. The cyanoalanine synthase activities of the nematode CBS-related proteins were analyzed. TLC analysis showed that only CYSL-2 utilizes cysteine and cyanide to form β-cyanoalanine. Amino acids were detected by ninhydrin. Lane X represents reaction mixture without enzyme.

The role of CYSL-3 is unclear

Although our data show that CYSL-3 exhibits canonical *β*-replacement activities, its function in *C. elegans* is unclear and remains to be explored. Because CYSL-3 does not exhibit CBS or CAS activity and does not interact with the EGL-9 C-terminus, the role of CYSL-3 is distinct from its paralogs in *C. elegans*. Kinetic analysis revealed that CYSL-3 has a high affinity for sulfide. We determined that apart from *O*-acetylserine, CYSL-3 also binds to *S*-sulfocysteine and converts it to thiosulfate. These data suggest a role for CYSL-3 in maintaining the homeostasis of sulfide or *S*-sulfocysteine. Notably, *in silico* analysis revealed that in comparison with the CYSL-3 paralogs and orthologs, the CYSL-3 active site possesses a novel amino acid in the conserved substrate-binding motif. Thus, we hypothesize that in *C. elegans*, CYSL-3 possesses a different catalytic activity and utilizes a novel primary substrate other than *O*-acetylserine or *S*-sulfocysteine. We cannot exclude

the possibility that CYSL-3 functions as an interacting partner similar to CYSL-1. Additional functional studies are necessary to address the role of CYSL-3 in *C. elegans*.

3.3 Novel aspects of H_2S signaling and metabolism in *C. elegans*

We determined that the CBS-related proteins play distinct roles in H_2S metabolism and/or signaling (Figure 8). The contribution of our findings to the understanding of H_2S metabolism and signaling in *C. elegans* was summarized and published as a review in the journal General Physiology and Biophysics (Supplement 6.1.4).

The nematode model of CBS deficiency

We determined that the nematode protein CBS-1 and its human ortholog produce H_2S from cysteine. We concluded that *cbs-1* knockdown in worms would be a promising model to study the roles of H_2S in the pathogenesis of CBS deficiency. However, there is no currently available *C. elegans* strain with a deletion of the CBS gene, and RNA interference of the *cbs-1* gene is not convenient and reproducible. However, there are 10 currently available *C. elegans* strains that carry various missense mutations (www.cgc.cbs.umn.edu), and the CBS activities in these strains are being analyzed. We expect that further studies utilizing *cbs-1* knockdown worms will elucidate the conserved aspects of H_2S signaling and its role in various physiological and pathological processes.

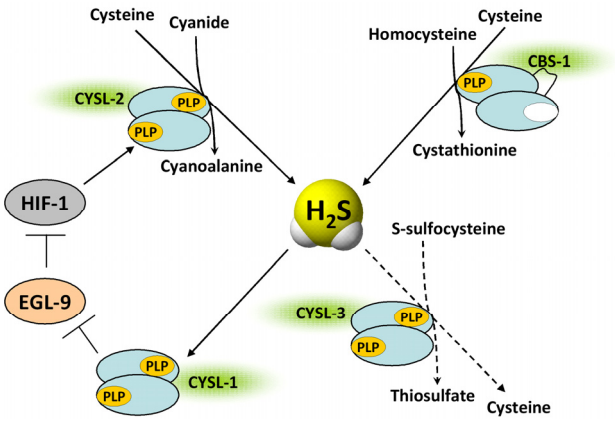

Figure 8. The proposed role of the nematode CBS-related proteins in H_2S metabolism and signaling. CBS-1 serves as a cystathionine beta-synthase that produces hydrogen sulfide (H_2S), CYSL-1 serves as a regulator of EGL-9 upon increase in the level of H_2S, CYSL-2 serves as a cyanoalanine synthase to produce H_2S, and CYSL-3 exhibits sulfhydrylase activity *in vitro* but its role in *C. elegans* remains to be determined.

The roles of H_2S and hypoxia in HIF-1 signaling in C. elegans

The incubation of nematodes in environments with nonlethal concentrations of H_2S is associated with *C. elegans* longevity (Miller D. L. and Roth M. B., 2007). H_2S is a known activator of HIF-1, which is crucial for the prolonged lifespan of *C. elegans* (Zhang Y. et

al., 2009). In our study we clarified the mechanism by which H_2S activates HIF-1 in *C. elegans*, and we described the combinatorial effect of H_2S and HIF-1 on the nematode lifespan. We showed that CYSL-1, which is the specific regulator of EGL-9, transduces H_2S signals in the cells to activate HIF-1, which is a typical animal transcription factor (Semenza G. L., 2000). Previous studies have shown that exogenous sources of H_2S, such as NaSH, can also activate HIF-1 in cultured rat cells (Liu X. et al., 2010). However, there is no evidence that the CYSL-1/EGL-9 mechanism that promotes HIF-1 activity is conserved in other evolutionarily distant animals; the EGL-9 orthologs lack the C-terminus that is essential for the interaction with CYSL-1, and OAS-TL enzymes have not been found in other animals. Nevertheless, all known components of the HIF-1 pathway are conserved, and we hypothesize that human CBS may play a role in HIF-1 signaling similar to its homolog CYSL-1 but by a different mechanism; for example, CBS in mammals (the CYSL-1 ortholog) can inhibit EGLN (the EGL-9 ortholog) via H_2S production or via utilization of H_2S for serine sulfhydrylase activity (see above).

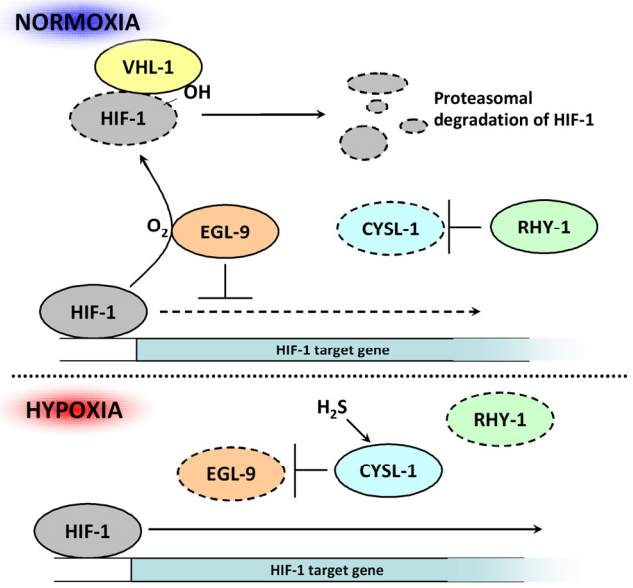

Figure 9. CYSL-1 transduces H_2S signals during hypoxia to activate HIF-1. RHY-1, an ortholog of the human acyltransferase, inhibits CYSL-1 by an unknown mechanism. Upon receiving the H_2S signal, CYSL-1 interacts via its active site with the C-terminus of EGL-9. This interaction sequesters EGL-9, and thus during hypoxia, EGL-9 cannot inhibit HIF-1 by vhl-1-dependent or vhl-1-independent pathways.

Hypoxia and H_2S are responsible for the activation of HIF-1 (Jiang H. et al., 2001). Because we observed that CYSL-1 operates during hypoxia and during exposure to hydrogen sulfide, we concluded that CYSL-1 acts as a sensor of hypoxia through the transmission of the H_2S signal, which increases during hypoxia (see above). We propose that hypoxia works in parallel with H_2S to activate HIF-1 via VHL-1-dependent and VHL-1-independent mechanisms (Figure 9). Notably, there are contradictory reports on the H_2S-mediated effects on HIF-1 activity during hypoxic conditions. There is evidence that the exogenous H_2S leads to HIF-1 accumulation and expression of the HIF-1 target gene VEGF in hypoxic cells, which is an effect that can be mimicked by $CoCl_2$ (Liu X. et al.,

2010). On the other hand, it was reported that H_2S inhibits the mammalian HIF-1 production and increases the VHL-1-dependent HIF-1 degradation in hypoxic cultured human and rat cells (Kai S. et al., 2012; Wu B. et al., 2012). Thus, H_2S inhibits the expression of VEGF, leading to the impaired angiogenic activity of vascular endothelial cells during hypoxia (Wu B. et al., 2012). These apparent contradictions in the H_2S-mediated HIF-1 signaling during hypoxia must be explained in future studies.

The cyanoalanine synthase CYSL-2 is a novel H_2S-metabolizing enzyme in animals

In *C. elegans*, HIF-1 activation is associated with strong upregulation of the *cysl-2* gene (Shen C. et al., 2005). We showed that CYSL-2 functions as a cyanoalanine synthase to detoxify cyanides and releases H_2S in *C. elegans*. Cyanoalanine synthases have previously been found only in bacteria and plants (Hatzfeld Y. et al., 2000). Our data clearly demonstrates that unlike mammals, *C. elegans* possesses 4 different enzymes that produce H_2S *de novo* – cystathionine beta-synthase, cystathionine gamma-lyase, 3-mercaptopyruvate sulfurtransferase and cyanoalanine synthase. These data also demonstrate that some roundworms may possess metabolic enzymes that are typical of plants and bacteria. There is no evidence that the OAS-TL proteins are conserved in other animals, but previous studies suggest that some insects also utilize a CAS activity to detoxify cyanide (Ogunlabi O. O. and Agboola F. K., 2007; Stauber E. J. et al., 2012). These findings strongly suggest that the OAS-TL enzymes might be conserved in animals that are evolutionarily distant from nematodes.

Previous data showed that *cysl-2* is also strongly upregulated during hypoxia and upon exposure to H_2S (Miller D. L. et al., 2011; Shen C. et al., 2005). Our data show that CYSL-2 can produce H_2S and utilize H_2S as a substrate in enzymatic reactions similar to the CBS enzymes (see above). Therefore, we hypothesize that when the H_2S concentration increases (for instance, during hypoxia), CYSL-2 maintains the H_2S homeostasis in *C. elegans* and is directly involved in the H_2S signaling. These hypothetical functions of CYSL-2 require further investigation.

Final remarks

Our data show that the metabolism of H_2S in *C. elegans* is much more complex than in mammals; *C. elegans* possesses the novel H_2S-producing enzyme cyanoalanine synthase, many copies of genes that encode the conserved H_2S-producing enzymes, and genes that encode the OAS-TL proteins with sulfhydrylase activities. Although we hypothesize that

the OAS-TL genes do not function in the sulfur assimilation pathway, unlike their plant or microbial orthologs, the OAS-TL genes may play a role in catabolizing H_2S. We hypothesize that the nematode OAS-TL genes evolved during the Permian-Triassic extinction event, approximately 250 million years ago for adaptation to the increased H_2S levels in the environment (Grice K. et al., 2005). Our findings also suggest that the interaction mechanism of CYSL-1 has been co-opted from the ancient metabolic functions of OAS-TL enzymes to utilize high levels of H_2S for the protection of nematodes from hypoxic conditions. We also hypothesize that the additional duplication of these genes in nematodes increased their resistance to the omnipresent cyanogenic species. It will be interesting to see if future studies will discover similar or identical functions of the CBS-related proteins in other evolutionarily distant animals or if these functions are unique to nematodes.

4. CONCLUSIONS

We have determined that the *Caenorhabditis elegans* CBS-related proteins have distinct roles. We discovered the gene that encodes the CBS enzyme in *C. elegans*. We show that the nematode protein CBS-1 exhibits a canonical activity that is mediated by a conserved catalytic domain, but it has a unique structural arrangement and lacks the typical regulatory domains present in its animal orthologs. We observed several biochemical and morphological changes in *C. elegans* due to CBS deficiency. Our data show that *C. elegans* can be used as a novel model organism to study the pathological mechanisms of CBS deficiency.

We identified a phylogenetically novel family of *O*-acetylserine(thiol)lyases (OAS-TL), which are newly characterized animal orthologs of the corresponding plant and bacterial enzymes, and we studied their specific functions in *C. elegans*. We showed that *C. elegans* possesses a cyanide detoxification pathway that is mediated by the activity of CYSL-2, which had previously been observed only in plants and bacteria. We determined that, in contrast to other animals, *C. elegans* possesses 4 enzymes that produce H_2S, and we proposed that *S*-sulfocysteine might be a novel endogenous substrate for these proteins in other species. We hypothesized that the roundworm *C. elegans* does not utilize *O*-acetylserine from the sulfur assimilation pathway to produce cysteine, but it may utilize *O*-acetylserine in low concentrations from food to regulate OAS-TL functions.

We elucidated one of the H_2S-signaling pathways in *C. elegans*. We characterized that the specific role of CYSL-1 in this pathway is the regulation of HIF-1 activity. CYSL-1 utilizes an evolved mechanism from the ancient regulation of the sulfur assimilation pathway in plants and bacteria. We also described the connection between high concentration of H_2S and low concentration of O_2 in the increased resistance of nematodes to toxic agents and stressors.

We reported the differences between the CBS-related proteins in *C. elegans* and showed that the OAS-TL genes in the nematode genome did not arise from the duplication of the CBS gene in nematodes but from a common ancestor shared with the plant OAS-TL genes. These data are consistent with the hypothesis that the OAS-TL genes evolved to protect animals from hypoxia and increasing H_2S concentrations in the environment. Our data show that the metabolism of H_2S is much more complex in roundworms than in mammals and suggest that the roundworms use their own signaling mechanisms for protection against hypoxic conditions.

5. ABBREVIATIONS

3MST	3-Mercaptopyruvate SulfurTransferase
ATP	Adenosin TriPhosphate
CAS	CyanoAlanine Synthase
CAT	Cysteine AminoTransferase
CBS	Cystathionine Beta-Synthase
CGL	Cystathionine Gamma-Lyase
CO	Carbon monOxide
COX	Cytochrom c OXidase
CYSL	CYsteine Synthase-Like
EGL	EGg Laying defective (Prolin hydroxylase)
ETHE1	ETHylmalonic Encephalopathy 1 (Sulfur dioxygenase)
GAPDH	GglycerAldehyde 3-Phosphate DeHydrogenase
H_2S	Hydrogen Sulfide
HIF	Hypoxia-Inducible Factor
NO	Nitric Oxide
OAS-TL	*O*-AcetylSerine(Thiol)Lyase
PCR	Polymerase Chain Reaction
PLP	PyridoxaL 5-Phosphate
RHY	Regulator of HYpoxia-inducible factor
ROS	Reactive Oxygen Species
SAT	Serine AcetylTransferase
SIR-2.1	Yeast SIR related
SQR	Sulfide:Quinone oxidoReductase
SOD	Sulfite OxiDase
TSMT	Thiol S-MethylTransferase
TST	Thiosulfate SulfurTransferase
VEGF	Vascular Endothelial Growth Factor
VHL	Von Hippel-Lindau (Ubiquitin ligase)

6. LIST OF AUTHOR'S SCIENTIFIC ACTIVITY DURING THE Ph.D. STUDY

6.1. Publications

6.1.1 **Vozdek R.**, Hnizda A., Krijt J., Kostrouchova M., Kozich V. *Novel Structural Arrangement of Nematode Cystathionine beta-Synthases: Characterization of Caenorhabditis elegans CBS-1*. Biochem J. (2012)443, 535-547; IF = 4.654

6.1.2 **Vozdek R.**, Hnizda A., Krijt J., Sera L., Kozich V. *Biochemical Properties of Nematode O-acetylserine(thiol)lyase Paralogs Imply Their Distinct Roles in Hydrogen Sulfide Homeostasis*. BBA-Proteins Proteomics. In press; IF = 3.733

6.1.3 Ma D. K., **Vozdek R.**, Bhatla N., Horvitz H. R. *CYSL-1 Interacts with the O_2-Sensing Hydroxylase EGL-9 to Promote H_2S-Modulated Hypoxia-Induced Behavioral Plasticity in C. elegans*. Neuron. (2012)73, 925-940; IF = 15.766

6.1.4 Modis K., Wolanska K., **Vozdek R.** *Hydrogen Sulfide in Cell Signaling: Signal Transduction, Cellular Bioenergetics and Physiology in C. elegans.* Gen Physiol Biophys. (2013)32, 1-22; IF = 0.852

6.2. Presentations

6.2.1 **Vozdek R.**, et al. *Characterization of recombinant cysteine synthase in Caenorhabditis elegans*. Poster. 7th Discussions in Structural Molecular Biology, Nove Hrady, 12 - 14 March 2009

6.2.2 **Vozdek R.**, et al. *Characterization of recombinant cysteine synthase in Caenorhabditis elegans*. Poster. 24. pracovní dny – Dědičné metabolické poruchy, Jeseník, 13. - 15. května 2009

6.2.3 **Vozdek R.**, et al. *Charakterizace cystathionin-β-synthasy u Caenorhabditis elegans*. Oral presentation. 10. studentská vědecká konference 1. lékařské fakulty 27. května 2009

6.2.4 **Vozdek R.**, et al. *Characterization of recombinant cysteine synthase in Caenorhabditis elegans*. Poster. 7th International Conference on Homocysteine Metabolism, Prague, 21 - 25 June 2009

6.2.5 **Vozdek R.**, et al. *Characterization of recombinant cysteine synthase in Caenorhabditis elegans*. Poster. 17th International *C. elegans* Meeting, Los Angeles, 24 - 28 June 2009

6.2.6 **Vozdek R.**, et al. *Characterization of recombinant cysteine synthase in Caenorhabditis elegans*. Poster. 34th FEBS Congress, Prague, 4 - 9 July 2009

6.2.7 **Vozdek R.**, et al. *Characterization of Caenorhabditis elegans gene C17G1.7 – an ortholog of human cystathionine β-synthase*. Poster. 59th Annual Meeting ASHG, Honolulu 20 – 25 October 2010

6.2.8 **Vozdek R.**, et al. *Caenorhabditis elegans possesses three genes encoding cysteine synthase with different tissue-specific localization*. Oral presentation. 11. studentská vědecká konference 1. lékařské fakulty 19. května 2010

6.2.9 **Vozdek R.**, et al. *Caenorhabditis elegans possesses three genes encoding cysteine synthase with different tissue-specific localization*. Poster. 25. pracovní dny – Dědičné metabolické poruchy, Trenčianské Teplice, 5. - 7. května 2010

6.2.10 **Vozdek R.**, et al. *Caenorhabditis elegans as a model of homocystinuria: characterization of nematode cystathionine beta-synthase*. Poster. FASEB Summer Research Conferences "Folic Acid, Vitamin B12, and one carbon metabolism", Carefree, 1 – 6 August 2010

6.2.11 **Vozdek R.**, et al. *Caenorhabditis elegans as a model of homocystinuria: characterization of nematode cystathionine beta-synthase*. Poster. 26. pracovní dny – Dědičné metabolické poruchy, Mikulov, 11. - 13. května 2011

6.2.12 **Vozdek R.**, et al. *Caenorhabditis elegans as a model of homocystinuria: characterization of nematode cystathionine beta-synthase*. Poster. European *C. elegans* Neurobiology Meeting, Fodele, Greece, 9 - 11 October 2011

6.2.13 **Vozdek R.**, et al. *Unusual structural arrangement of nematode cystathionine beta-synthases suggests evolutionary divergent regulation of their catalytic activity*. Poster. 8th International Conference on Homocysteine Metabolism, Lisbon, 18 – 24 June, 2011

6.2.14 **Vozdek R.**, et al. *Unusual structural arrangement of nematode cystathionine beta-synthases suggests evolutionary divergent regulation of their catalytic activity*. Poster. 25th Anniversary Symposium of the Protein Society 21 July – 2 August, 2011

6.2.15 **Vozdek R.**, et al. *Caenorhabditis elegans possesses four genes encoding cystathionine beta-synthase-related proteins with distinct role in H_2S biology*. Oral presentation. 1st European conference on the biology of the hydrogen sulfide 15 June – 18 June, 2012

6.2.16 **Vozdek R.**, et al. *A roundworm Caenorhabditis elegans possesses a large number of H_2S producing enzymes*. Poster. 2nd European conference on the biology of the hydrogen sulfide 8 -11 September, 2013

6.3. Grants

2009-2011 - Grant Agency of Charles University: *Characterization of cysteine biosynthetic pathways in Caenorhabditis elegans.* (Principal investigator)

6.4. Awards

2008 - Award in undergraduated section of Congress of Medical Sciences for students, First Faculty of Medicine, Charles University in Prague

2012 - Award in graduated section of Congress of Medical Sciences for students, First Faculty of Medicine, Charles University in Prague

2012 - Young Investigator Award among Ph. D. students and postdoctoral researchers at the First European Conference on the Biology of Hydrogen Sulfide, Smolenice, Slovakia

6.5 Educational activity

2012 - Consultant of the Bachelor Thesis: Poláchová M. A. *Characterization of mutant cystathionine beta-synthase in C. elegans*. Institute of Chemical Technology, Prague

2013 - Consultant of the Master Thesis: Poláchová M. A. *Role of cystathionine beta-synthase in H_2S signaling in C. elegans*. Institute of Chemical Technology, Prague

6.6 Participation on peer-review system

2013 - Ad hoc reviewer for the journal "Physiological research"

7. REFERENCES

Abe K. and Kimura H., 1996, *The possible role of hydrogen sulfide as an endogenous neuromodulator.* J Neurosci. **16**(3): p. 1066-1071.

Aitken S. M. and Kirsch J. F., 2005, *The enzymology of cystathionine biosynthesis: strategies for the control of substrate and reaction specificity.* Arch Biochem Biophys. **433**(1): p. 166-175.

An J. H. and Blackwell T. K., 2003, *SKN-1 links C. elegans mesendodermal specification to a conserved oxidative stress response.* Genes Dev. **17**(15): p. 1882-1893.

Becker M. A., Kredich N. M., and Tomkins G. M., 1969, *The purification and characterization of O-acetylserine sulfhydrylase-A from Salmonella typhimurium.* J Biol Chem. **244**(9): p. 2418-2427.

Benavides G. A., Squadrito G. L., Mills R. W., et al., 2007, *Hydrogen sulfide mediates the vasoactivity of garlic.* Proc Natl Acad Sci U S A. **104**(46): p. 17977-17982.

Blackstone E., Morrison M., and Roth M. B., 2005, *H2S induces a suspended animation-like state in mice.* Science. **308**(5721): p. 518.

Blackstone E. and Roth M. B., 2007, *Suspended animation-like state protects mice from lethal hypoxia.* Shock. **27**(4): p. 370-372.

Bonner E. R., Cahoon R. E., Knapke S. M., et al., 2005, *Molecular basis of cysteine biosynthesis in plants: structural and functional analysis of O-acetylserine sulfhydrylase from Arabidopsis thaliana.* J Biol Chem. **280**(46): p. 38803-38813.

Bouillaud F. and Blachier F., 2011, *Mitochondria and sulfide: a very old story of poisoning, feeding, and signaling?* Antioxid Redox Signal. **15**(2): p. 379-391.

Braunstein A. E., Goryachenkova E. V., Tolosa E. A., et al., 1971, *Specificity and some other properties of liver serine sulphhydrase: evidence for its identity with cystathionine -synthase.* Biochim Biophys Acta. **242**(1): p. 247-260.

Braunstein A. E. and Goryachenkova E. V., 1984, *The beta-replacement-specific pyridoxal-P-dependent lyases.* Adv Enzymol Relat Areas Mol Biol. **56**: p. 1-89.

Budde M. W. and Roth M. B., 2010, *Hydrogen sulfide increases hypoxia-inducible factor-1 activity independently of von Hippel-Lindau tumor suppressor-1 in C. elegans.* Mol Biol Cell. **21**(1): p. 212-217.

Budde M. W. and Roth M. B., 2011, *The Response of Caenorhabditis elegans to Hydrogen Sulfide and Hydrogen Cyanide.* Genetics. **189**(2): p. 521-532.

Carballal S., Trujillo M., Cuevasanta E., et al., 2011, *Reactivity of hydrogen sulfide with peroxynitrite and other oxidants of biological interest.* Free Radic Biol Med. **50**(1): p. 196-205.

Epstein A. C., Gleadle J. M., McNeill L. A., et al., 2001, *C. elegans EGL-9 and mammalian homologs define a family of dioxygenases that regulate HIF by prolyl hydroxylation.* Cell. **107**(1): p. 43-54.

Finkel T., 2012, *From sulfenylation to sulfhydration: what a thiolate needs to tolerate.* Sci Signal. **5**(215): p. pe10.

Furne J., Saeed A., and Levitt M. D., 2008, *Whole tissue hydrogen sulfide concentrations are orders of magnitude lower than presently accepted values.* Am J Physiol Regul Integr Comp Physiol. **295**(5): p. R1479-1485.

Ganster F., Burban M., de la Bourdonnaye M., et al., 2010, *Effects of hydrogen sulfide on hemodynamics, inflammatory response and oxidative stress during resuscitated hemorrhagic shock in rats.* Crit Care. **14**(5): p. R165.

Grice K., Cao C., Love G. D., et al., 2005, *Photic zone euxinia during the Permian-triassic superanoxic event.* Science. **307**(5710): p. 706-709.

Hatzfeld Y., Maruyama A., Schmidt A., et al., 2000, *beta-Cyanoalanine synthase is a mitochondrial cysteine synthase-like protein in spinach and Arabidopsis.* Plant Physiol. **123**(3): p. 1163-1171.

Hell R. and Wirtz M., 2011, *Molecular Biology, Biochemistry and Cellular Physiology of Cysteine Metabolism in Arabidopsis thaliana.* Arabidopsis Book. **9**: p. e0154.

Hildebrandt T. M. and Grieshaber M. K., 2008, *Three enzymatic activities catalyze the oxidation of sulfide to thiosulfate in mammalian and invertebrate mitochondria.* Febs J. **275**(13): p. 3352-3361.

Hill B. C., Woon T. C., Nicholls P., et al., 1984, *Interactions of sulphide and other ligands with cytochrome c oxidase. An electron-paramagnetic-resonance study.* Biochem J. **224**(2): p. 591-600.

Hourihan J. M., Kenna J. G., and Hayes J. D., 2013, *The gasotransmitter hydrogen sulfide induces nrf2-target genes by inactivating the keap1 ubiquitin ligase substrate adaptor through formation of a disulfide bond between cys-226 and cys-613.* Antioxid Redox Signal. **19**(5): p. 465-481.

Hwang A. B. and Lee S. J., 2011, *Regulation of life span by mitochondrial respiration: the HIF-1 and ROS connection.* Aging (Albany NY). **3**(3): p. 304-310.

Chen D., Thomas E. L., and Kapahi P., 2009, *HIF-1 modulates dietary restriction-mediated lifespan extension via IRE-1 in Caenorhabditis elegans.* PLoS Genet. **5**(5): p. e1000486.

Chiku T., Padovani D., Zhu W., et al., 2009, *H2S biogenesis by human cystathionine gamma-lyase leads to the novel sulfur metabolites lanthionine and homolanthionine and is responsive to the grade of hyperhomocysteinemia.* J Biol Chem. **284**(17): p. 11601-11612.

Ishigami M., Hiraki K., Umemura K., et al., 2009, *A source of hydrogen sulfide and a mechanism of its release in the brain.* Antioxid Redox Signal. **11**(2): p. 205-214.

Jhee K. H., McPhie P., and Miles E. W., 2000, *Domain architecture of the heme-independent yeast cystathionine beta-synthase provides insights into mechanisms of catalysis and regulation.* Biochemistry. **39**(34): p. 10548-10556.

Jiang H., Guo R., and Powell-Coffman J. A., 2001, *The Caenorhabditis elegans hif-1 gene encodes a bHLH-PAS protein that is required for adaptation to hypoxia.* Proc Natl Acad Sci U S A. **98**(14): p. 7916-7921.

Kai S., Tanaka T., Daijo H., et al., 2012, *Hydrogen sulfide inhibits hypoxia- but not anoxia-induced hypoxia-inducible factor 1 activation in a von hippel-lindau- and mitochondria-dependent manner.* Antioxid Redox Signal. **16**(3): p. 203-216.

Kell A., Ventura N., Kahn N., et al., 2007, *Activation of SKN-1 by novel kinases in Caenorhabditis elegans.* Free Radic Biol Med. **43**(11): p. 1560-1566.

Kery V., Poneleit L., and Kraus J. P., 1998, *Trypsin cleavage of human cystathionine beta-synthase into an evolutionarily conserved active core: structural and functional consequences.* Arch Biochem Biophys. **355**(2): p. 222-232.

Khare S., Gomez T., Linster C. L., et al., 2009, *Defective responses to oxidative stress in protein l-isoaspartyl repair-deficient Caenorhabditis elegans.* Mech Ageing Dev. **130**(10): p. 670-680.

Kimura H., 2011, *Hydrogen sulfide: its production, release and functions.* Amino Acids. **41**(1): p. 113-121.

Kraus J. P. and Kožich V., 2001, *Cystathionine-β-synthase and its deficiency*, in *Homocysteine in Health and Disease*, Carmel and Jacobsen, Editors., Cambridge University Press, Cambridge, U.K. p. 223-243.

Kredich N. M. and Tomkins G. M., 1966, *The enzymic synthesis of L-cysteine in Escherichia coli and Salmonella typhimurium.* J Biol Chem. **241**(21): p. 4955-4965.

Krishnan N., Fu C., Pappin D. J., et al., 2012, *H2S-Induced sulfhydration of the phosphatase PTP1B and its role in the endoplasmic reticulum stress response.* Sci Signal. **4**(203): p. ra86.

Lagoutte E., Mimoun S., Andriamihaja M., et al., 2010, *Oxidation of hydrogen sulfide remains a priority in mammalian cells and causes reverse electron transfer in colonocytes.* Biochim Biophys Acta. **1797**(8): p. 1500-1511.

Levitt M. D., Furne J., Springfield J., et al., 1999, *Detoxification of hydrogen sulfide and methanethiol in the cecal mucosa.* J Clin Invest. **104**(8): p. 1107-1114.

Li Q. and Lancaster J. R., Jr., 2013, *Chemical foundations of hydrogen sulfide biology.* Nitric Oxide. **35C**: p. 21-34.

Liu X., Pan L., Zhuo Y., et al., 2010, *Hypoxia-inducible factor-1alpha is involved in the pro-angiogenic effect of hydrogen sulfide under hypoxic stress.* Biol Pharm Bull. **33**(9): p. 1550-1554.

Macfarlane G. T., Gibson G. R., and Cummings J. H., 1992, *Comparison of fermentation reactions in different regions of the human colon.* J Appl Bacteriol. **72**(1): p. 57-64.

Marcia M., Ermler U., Peng G., et al., 2010, *A new structure-based classification of sulfide:quinone oxidoreductases.* Proteins. **78**(5): p. 1073-1083.

Mathew N. D., Schlipalius D. I., and Ebert P. R., 2011, *Sulfurous gases as biological messengers and toxins: comparative genetics of their metabolism in model organisms.* J Toxicol. **2011**: p. 394970.

Meier M., Janosik M., Kery V., et al., 2001, *Structure of human cystathionine beta-synthase: a unique pyridoxal 5'-phosphate-dependent heme protein.* Embo J. **20**(15): p. 3910-3916.

Mikami Y., Shibuya N., Kimura Y., et al., 2011, *Thioredoxin and dihydrolipoic acid are required for 3-mercaptopyruvate sulfurtransferase to produce hydrogen sulfide.* Biochem J. **439**(3): p. 479-485.

Miller D. L. and Roth M. B., 2007, *Hydrogen sulfide increases thermotolerance and lifespan in Caenorhabditis elegans.* Proc Natl Acad Sci U S A. **104**(51): p. 20618-20622.

Miller D. L., Budde M. W., and Roth M. B., 2011, *HIF-1 and SKN-1 coordinate the transcriptional response to hydrogen sulfide in Caenorhabditis elegans.* PLoS One. **6**(9): p. e25476.

Modis K., Coletta C., Erdelyi K., et al., 2012, *Intramitochondrial hydrogen sulfide production by 3-mercaptopyruvate sulfurtransferase maintains mitochondrial electron flow and supports cellular bioenergetics.* Faseb J. **27**(2): p. 601-611.

Morikawa T., Kajimura M., Nakamura T., et al., 2012, *Hypoxic regulation of the cerebral microcirculation is mediated by a carbon monoxide-sensitive hydrogen sulfide pathway.* Proc Natl Acad Sci U S A. **109**(4): p. 1293-1298.

Moss G. A., 2010, *Water and health: a forgotten connection?* Perspect Public Health. **130**(5): p. 227-232.

Mulrow C., Lawrence V., Ackermann R., et al., 2000, *Garlic: effects on cardiovascular risks and disease, protective effects against cancer, and clinical adverse effects.* Evid Rep Technol Assess (Summ),(20): p. 1-4.

Mustafa A. K., Gadalla M. M., Sen N., et al., 2009, *H2S signals through protein S-sulfhydration.* Sci Signal. **2**(96): p. ra72.

Nagy P. and Winterbourn C. C., 2010, *Rapid Reaction of Hydrogen Sulfide with the Neutrophil Oxidant Hypochlorous Acid to Generate Polysulfides.* Chem Res Toxicol. **23**: p. 1541-1543.

Nozaki T., Shigeta Y., Saito-Nakano Y., et al., 2001, *Characterization of transsulfuration and cysteine biosynthetic pathways in the protozoan hemoflagellate, Trypanosoma cruzi. Isolation and molecular characterization of cystathionine beta-synthase and serine acetyltransferase from Trypanosoma.* J Biol Chem. **276**(9): p. 6516-6523.

Ogasawara Y., Isoda S., and Tanabe S., 1994, *Tissue and subcellular distribution of bound and acid-labile sulfur, and the enzymic capacity for sulfide production in the rat.* Biol Pharm Bull. **17**(12): p. 1535-1542.

Ogunlabi O. O. and Agboola F. K., 2007, *A soluble beta-cyanoalanine synthase from the gut of the variegated grasshopper Zonocerus variegatus (L.).* Insect Biochem Mol Biol. **37**(1): p. 72-79.

Olson K. R., Dombkowski R. A., Russell M. J., et al., 2006, *Hydrogen sulfide as an oxygen sensor/transducer in vertebrate hypoxic vasoconstriction and hypoxic vasodilation.* J Exp Biol. **209**(Pt 20): p. 4011-4023.

Olson K. R., 2009, *Is hydrogen sulfide a circulating "gasotransmitter" in vertebrate blood?* Biochim Biophys Acta. **1787**(7): p. 856-863.

Olson K. R., 2012, *Mitochondrial adaptations to utilize hydrogen sulfide for energy and signaling.* J Comp Physiol B. **182**(7): p. 881-897.

Olson K. R., 2013, *Hydrogen sulfide as an oxygen sensor.* Clin Chem Lab Med. **51**(3): p. 623-632.

Pietri R., Roman-Morales E., and Lopez-Garriga J., 2011, *Hydrogen sulfide and hemeproteins: knowledge and mysteries.* Antioxid Redox Signal. **15**(2): p. 393-404.

Powolny A. A., Singh S. V., Melov S., et al., 2011, *The garlic constituent diallyl trisulfide increases the lifespan of C. elegans via skn-1 activation.* Exp Gerontol. **46**(6): p. 441-452.

Ramasamy S., Singh S., Taniere P., et al., 2006, *Sulfide-detoxifying enzymes in the human colon are decreased in cancer and upregulated in differentiation.* Am J Physiol Gastrointest Liver Physiol. **291**(2): p. G288-296.

Saldanha J. N., Parashar A., Pandey S., et al., 2013, *Multiparameter Behavioral Analyses Provide Insights to Mechanisms of Cyanide Resistance in Caenorhabditis elegans.* Toxicol Sci.

Semenza G. L., 2000, *HIF-1: mediator of physiological and pathophysiological responses to hypoxia.* J Appl Physiol. **88**(4): p. 1474-1480.

Sen N., Paul B. D., Gadalla M. M., et al., 2012, *Hydrogen sulfide-linked sulfhydration of NF-kappaB mediates its antiapoptotic actions.* Mol Cell. **45**(1): p. 13-24.

Shao Z., Zhang Y., and Powell-Coffman J. A., 2009, *Two distinct roles for EGL-9 in the regulation of HIF-1-mediated gene expression in Caenorhabditis elegans.* Genetics. **183**(3): p. 821-829.

Shao Z., Zhang Y., Ye Q., et al., 2010, *C. elegans SWAN-1 Binds to EGL-9 and regulates HIF-1-mediated resistance to the bacterial pathogen Pseudomonas aeruginosa PAO1.* PLoS Pathog. **6**(8): p. e1001075.

Shen C., Nettleton D., Jiang M., et al., 2005, *Roles of the HIF-1 hypoxia-inducible factor during hypoxia response in Caenorhabditis elegans.* J Biol Chem. **280**(21): p. 20580-20588.

Shen C., Shao Z., and Powell-Coffman J. A., 2006, *The Caenorhabditis elegans rhy-1 gene inhibits HIF-1 hypoxia-inducible factor activity in a negative feedback loop that does not include vhl-1.* Genetics. **174**(3): p. 1205-1214.

Shibuya N., Tanaka M., Yoshida M., et al., 2009, *3-Mercaptopyruvate sulfurtransferase produces hydrogen sulfide and bound sulfane sulfur in the brain.* Antioxid Redox Signal. **11**(4): p. 703-714.

Shintani T., Iwabuchi T., Soga T., et al., 2009, *Cystathionine beta-synthase as a carbon monoxide-sensitive regulator of bile excretion.* Hepatology. **49**(1): p. 141-150.

Singh S., Madzelan P., and Banerjee R., 2007, *Properties of an unusual heme cofactor in PLP-dependent cystathionine beta-synthase.* Nat Prod Rep. **24**(3): p. 631-639.

Singh S., Padovani D., Leslie R. A., et al., 2009, *Relative contributions of cystathionine beta-synthase and gamma-cystathionase to H2S biogenesis via alternative trans-sulfuration reactions.* J Biol Chem. **284**(33): p. 22457-22466.

Stauber E. J., Kuczka P., van Ohlen M., et al., 2012, *Turning the 'mustard oil bomb' into a 'cyanide bomb': aromatic glucosinolate metabolism in a specialist insect herbivore.* PLoS One. **7**(4): p. e35545.

Stipanuk M. H., 1986, *Metabolism of sulfur-containing amino acids.* Annu Rev Nutr. **6**: p. 179-209.

Sylvester J. T., Shimoda L. A., Aaronson P. I., et al., 2012, *Hypoxic pulmonary vasoconstriction.* Physiol Rev. **92**(1): p. 367-520.

Szabo C., 2007, *Hydrogen sulphide and its therapeutic potential.* Nat Rev Drug Discov. **6**(11): p. 917-935.

Taylor M. S., 2001, *Characterization and comparative analysis of the EGLN gene family.* Gene. **275**(1): p. 125-132.

Tullet J. M., Hertweck M., An J. H., et al., 2008, *Direct inhibition of the longevity-promoting factor SKN-1 by insulin-like signaling in C. elegans.* Cell. **132**(6): p. 1025-1038.

Wang R., 2012, *Physiological implications of hydrogen sulfide: a whiff exploration that blossomed.* Physiol Rev. **92**(2): p. 791-896.

Weir E. K. and Archer S. L., 1995, *The mechanism of acute hypoxic pulmonary vasoconstriction: the tale of two channels.* Faseb J. **9**(2): p. 183-189.

Weisiger R. A., Pinkus L. M., and Jakoby W. B., 1980, *Thiol S-methyltransferase: suggested role in detoxication of intestinal hydrogen sulfide.* Biochem Pharmacol. **29**(20): p. 2885-2887.

Whitfield N. L., Kreimier E. L., Verdial F. C., et al., 2008, *Reappraisal of H2S/sulfide concentration in vertebrate blood and its potential significance in ischemic preconditioning and vascular signaling.* Am J Physiol Regul Integr Comp Physiol. **294**(6): p. R1930-1937.

Wirtz M., Droux M., and Hell R., 2004, *O-acetylserine (thiol) lyase: an enigmatic enzyme of plant cysteine biosynthesis revisited in Arabidopsis thaliana.* J Exp Bot. **55**(404): p. 1785-1798.

Wu B., Teng H., Yang G., et al., 2012, *Hydrogen sulfide inhibits the translational expression of hypoxia-inducible factor-1alpha.* Br J Pharmacol. **167**(7): p. 1492-1505.

Wu L. and Wang R., 2005, *Carbon monoxide: endogenous production, physiological functions, and pharmacological applications.* Pharmacol Rev. **57**(4): p. 585-630.

Yamanishi T. and Tuboi S., 1981, *The mechanism of the L-cystine cleavage reaction catalyzed by rat liver gamma-cystathionase.* J Biochem. **89**(6): p. 1913-1921.

Yang G., Wu L., Jiang B., et al., 2008, *H2S as a physiologic vasorelaxant: hypertension in mice with deletion of cystathionine gamma-lyase.* Science. **322**(5901): p. 587-590.

Zhang Y., Shao Z., Zhai Z., et al., 2009, *The HIF-1 hypoxia-inducible factor modulates lifespan in C. elegans.* PLoS One. **4**(7): p. e6348.

Zhao W., Zhang J., Lu Y., et al., 2001, *The vasorelaxant effect of H(2)S as a novel endogenous gaseous K(ATP) channel opener.* Embo J. **20**(21): p. 6008-6016.

Zhong J. F., Wang S. P., Shi X. Q., et al., 2010, *Hydrogen sulfide exposure increases desiccation tolerance in Drosophila melanogaster.* J Insect Physiol. **56**(12): p. 1777-1782.

SUPPLEMENT

Supplement contains reprints of publications (6.1.1 - 6.1.4)

Publication 6.1.1

Novel Structural Arrangement of Nematode Cystathionine beta-Synthases: Characterization of *Caenorhabditis elegans* CBS-1

Biochemical Journal (2012)

BJ www.biochemj.org

Biochem. J. (2012) **443**, 535–547 (Printed in Great Britain) doi:10.1042/BJ20111478

Novel structural arrangement of nematode cystathionine β-synthases: characterization of *Caenorhabditis elegans* CBS-1

Roman VOZDEK, Aleš HNÍZDA, Jakub KRIJT, Marta KOSTROUCHOVÁ and Viktor KOŽICH[1]

Institute of Inherited Metabolic Disorders, Charles University in Prague, First Faculty of Medicine and General University Hospital, Ke Karlovu 2, 128 08, Praha 2, Czech Republic

CBSs (cystathionine β-synthases) are eukaryotic PLP (pyridoxal 5 *-phosphate)-dependent proteins that maintain cellular homocysteine homoeostasis and produce cystathionine and hydrogen sulfide. In the present study, we describe a novel structural arrangement of the CBS enzyme encoded by the *cbs-1* gene of the nematode *Caenorhabditis elegans*. The CBS-1 protein contains a unique tandem repeat of two evolutionarily conserved catalytic regions in a single polypeptide chain. These repeats include a catalytically active C-terminal module containing a PLP-binding site and a less conserved N-terminal module that is unable to bind the PLP cofactor and cannot catalyse CBS reactions, as demonstrated by analysis of truncated variants and active-site mutant proteins. In contrast with other metazoan enzymes, CBS-1 lacks the haem and regulatory Bateman domain essential for activation by AdoMet (*S*-adenosylmethionine) and only forms monomers. We determined the tissue and subcellular distribution of CBS-1 and showed that *cbs-1* knockdown by RNA interference leads to delayed development and to an approximately 10-fold elevation of homocysteine concentrations in nematode extracts. The present study provides the first insight into the metabolism of sulfur amino acids and hydrogen sulfide in *C. elegans* and shows that nematode CBSs possess a structural feature that is unique among CBS proteins.

Key words: cystathionine β-synthase (CBS), *Caenorhabditis elegans*, domain architecture, homocysteine, hydrogen sulfide, knockdown.

INTRODUCTION

Methionine and cysteine are sulfur amino acids that play important roles in many biochemical reactions. Methionine, an essential amino acid, can be irreversibly converted into cysteine in a series of reactions. Methionine is first converted into AdoMet (*S*-adenosylmethionine), which serves as a methyl donor in various transmethylation reactions. A product of these transmethylations, *S*-adenosylhomocysteine, is further converted into homocysteine, which is a key intermediate in the metabolism of sulfur amino acids. In animal tissues, homocysteine is universally remethylated to methionine by methionine synthase using methyltetrahydrofolate as the methyl donor. In addition, a number of tissues can convert homocysteine into cystathionine and further to cysteine via the transsulfuration pathway through two PLP (pyridoxal 5*-phosphate)-dependent enzymes, CBS (cystathionine β-synthase) and CGL (cystathionine γ-lyase) [1].

CBS is a cytosolic enzyme that catalyses the formation of cystathionine with the release of water or hydrogen sulfide, depending on whether homocysteine is condensed with serine or cysteine. The human and rodent CBSs that have been characterized are tetrameric enzymes and each of their ~63 kDa polypeptide chains contains three different domains. The N-terminal domain binds haem, the presence of which has been suggested to increase CBS activity during the oxidation of the intracellular environment [1a,2]. Other studies suggest that haem may play a structural role that is necessary for the correct folding of the CBS protein [3,4]. The middle portion of the polypeptide chain forms the catalytic domain and is well conserved among the fold-type II PLP-dependent proteins [5]. The C-terminal domain possesses two defined CBS domains, a hydrophobic domain, CBS1, and a less conserved domain, CBS2, that are together referred to as the Bateman domain. Together, these two CBS domains bind AdoMet, an allosteric activator of mammalian CBS [6]. The C-terminal domain of mammalian CBS is also thought to be responsible for multimerization of the enzyme into homotetramers and higher oligomeric forms [6,7]. The C-terminal autoinhibitory domain of mammalian CBS can be removed by *in vitro* or *in vivo* proteolytic processing, yielding a ~45 kDa truncated form (45CBS) that forms dimers and is more active than the full-length enzyme [6,8,9].

The canonical domain architecture of mammalian CBSs is not conserved across phyla. The CBS enzymes of *Saccharomyces cerevisiae*, *Trypanosoma cruzi* and *Drosophila melanogaster* have been experimentally characterized; the N-terminal haem-binding domain is absent in yeast and protozoan CBS, in contrast with its presence in *Drosophila* [10–12], whereas the catalytic domain is conserved in the CBS enzymes of all three of these species. The C-terminal portion exhibits the highest degree of variability. The yeast and *Drosophila* CBS proteins contain the Bateman domain, but lack a response to AdoMet. Interestingly, although the C-terminal portion of the yeast CBS inhibits the activity of the enzyme and supports the formation of tetramers and octamers [13], *Drosophila* CBS forms only dimers [12]. In contrast, the protozoan CBS does not contain the Bateman domain and is not activated by AdoMet. Although its C-terminus is shortened, the protozoan CBS is still able to form tetramers [11]. The phylogenetic variability in the domain architecture of CBSs suggests that the activity of these enzymes is regulated differently in evolutionarily distant organisms.

In the present study, we characterized the structural and functional properties of the CBS in *Caenorhabditis elegans*, a

Abbreviations used: AdoMet, *S*-adenosylmethionine; BN, blue native; BS[3], bis(sulfosuccinimidyl) suberate; CBS, cystathionine β-synthase; CGL, cystathionine γ-lyase; DTT, dithiothreitol; EST, expressed sequence tag; GFP, green fluorescent protein; LC–MS/MS, liquid chromatography–tandem MS; PLP, pyridoxal 5*-phosphate; RNAi, RNA interference; RT, reverse transcription; SEC, size-exclusion chromatography; UTR, untranslated region; WT, wild-type.

[1] To whom correspondence should be addressed (email Viktor.Kozich@LF1.cuni.cz).

well-established model organism used to study human diseases. We first identified a transcriptionally active gene encoding CBS in *C. elegans*, we then determined its pattern of expression and characterized the enzymatic and structural properties of the encoded protein. Finally, we determined the phenotypic effects of *cbs-1* inhibition using RNA-mediated interference. These data describe novel structural features that are unique among CBS enzymes and provide the first insight into the metabolism of sulfur amino acids and hydrogen sulfide in *C. elegans*.

EXPERIMENTAL

C. elegans strains

The WT (wild-type) *C. elegans* Bristol strain N2 was obtained from the *C. elegans* Stock Center (University of Minnesota, Minneapolis, MN, U.S.A.), and the RB839 strain carrying the *F54A3.4* (*ok666*) allele was provided by the *C. elegans* Gene Knockout Consortium (Oklahoma Medical Research Foundation, Oklahoma City, OK, U.S.A.). Worm cultures were maintained as described previously [14].

Bioinformatics

BLASTp searches were performed by online BLAST software using the *C. elegans* protein database (release WS215). Protein domain modelling was performed by Swiss-model (automatic modelling mode) using the crystal structure of human 45CBS (PDB code 1JBQ, chain A) as a template [15]. PDB structures were subsequently evaluated in the Prosa program [16] and visualized in Swiss-PDBViewer 4.0.4 [17]. Phylogenetic trees were constructed in the online portal system Mobyle [18]. Multiple alignments of amino acid sequences were performed using ClustalW2 online software with default parameters [19]. Conserved regions were also separated for further analysis by ClustalW2. For phylogenetic analysis, alignment was bootstrapped 100 times and analysed by the maximal likelihood method using the PHYML 3.0 program [20]. Bootstrap output trees were analysed by the PHYLIP 3.67 CONSENSE program; the final tree shape was visualized in the Dendroscope program [21].

PCR amplification and DNA sequencing

Nematode cDNA was prepared by RT (reverse transcription) using isolated total RNA from mixed stages of N2 worms and a RT kit with an oligo(dT) primer (Promega). Open reading frames of *ZC373.1* and *F54A3.4* were amplified by PCR using either cDNA prepared by RT–PCR or a *C. elegans* cDNA library (Invitrogen) as the template (a list of the primers is given in Supplementary Table S1 at http://www.BiochemJ.org/bj/443/bj4430535add.htm). PCR products were cloned into the pCR4-TOPO vector (Invitrogen), and the authenticity of the DNA sequence was verified by dideoxy sequencing using an ABI PRISM 3100-Avant sequencer (Applied Biosystems).

GFP (green fluorescent protein) reporter assay

To determine the expression pattern of *cbs-1*, we generated a translational fusion vector using the PCR fusion technique described previously [22]. The 1.8 kb of 5′ upstream sequence and the entire coding region of *ZC373.1* were amplified by PCR using primers A and B (Supplementary Table S1), and genomic *C. elegans* DNA as a template. The vector pPD95.75 was used as a template for amplification of the GFP-coding sequence using primers C and D (Supplementary Table S1). The two PCR products were mixed and used as a template for PCR fusion using nested primers E and F (Supplementary Table S1). The 6.8-kb PCR product was injected into *C. elegans* hermaphrodite gonads together with the plasmid pRF4 as a phenotypic marker for injection. Transgenic animals were separated, and the F2 progeny were screened for the GFP signal. An Olympus BX60 microscope and a Nikon Eclipse E800 with C1 confocal module and 488 nm laser and differential interference contrast optics were used for specimen examination.

Bacterial expression and protein purification

Initially, recombinant CBS-1 was expressed as a fusion protein with an N-terminal GST tag and further purified by affinity chromatography to 75 % purity (see Supplementary Figure S4, lane 6) according to a previously described procedure for human CBS [23]. The contaminating polypeptide with the highest abundance, a 40-kDa fragment that represented approximately 20 % of the total protein, was identified as the N-terminal portion of CBS-1 (residues 1–375) by peptide mass fingerprinting using MS detection (results not shown). This N-terminal fragment was observed with similar abundance even when the purification procedure was modified to limit proteolytic cleavage of the recombinant protein (the modification involved performing affinity chromatography at 4 °C and increasing the concentration of protease inhibitors in the bacterial crude extract). To overcome this obstacle that was not previously reported for other CBS orthologues, we constructed a new vector that produced double-tagged CBS-1 with a cleavable N-terminal GST tag and a C-terminal His tag. The open reading frame of the *ZC373.1* gene encoding CBS-1 was amplified by PCR using a *C. elegans* cDNA library as the template. PCR was performed with Taq polymerase using primers P and R (Supplementary Table S1). The 2.1-kb DNA fragment obtained by digestion of the PCR product with BamHI and XhoI was cloned into the BamHI- and XhoI-digested pGEX-6p-1 vector. Express Competent *Escherichia coli* cells (New England Biolabs) were transformed with the plasmid that encodes double-tagged CBS-1 (GST–CBS–1–His_6) and cultured in the presence of 100 μM IPTG (isopropyl β-D-thiogalactopyranoside) at 18 °C for 24 h. The GST–CBS-1 fusion protein was purified according to the purification protocol for human CBS described previously [24] with the following modifications: after cleavage by the PreScission protease (GE Healthcare), recombinant CBS-1 was loaded on to a Ni-Sepharose column that had been equilibrated with IMAC buffer [20 mM phosphate (pH 7.5), containing 0.5 M NaCl, 20 mM imidazole and 1 mM DTT (dithiothreitol)]. The column was washed with IMAC buffer containing 50 mM imidazole. CBS-1 was then eluted with IMAC buffer containing 75 mM imidazole. The protein enrichment procedure yielded approximately 1 mg of CBS-1 per litre of bacterial culture. The purity of isolated CBS-1 was analysed by SDS/PAGE [pre-cast 3–8 % gradient gel (Invitrogen)] with Coomassie Brilliant Blue staining. The protein concentration was determined using Bradford reagent (Sigma–Aldrich) with BSA as the standard. The absorption spectrum of CBS-1 was recorded using a UV–visible spectrophotometer (Shimadzu UV-2550) at room temperature (25 °C).

SEC (size-exclusion chromatography)

SEC was performed on an HPLC platform (Shimadzu LC-10A system). Recombinant purified CBS-1 was loaded on to a Bio-Sil SEC HPLC column (catalogue number 125-0060, Bio-Rad

Laboratories) that had been previously equilibrated with buffer containing 50 mM Tris/HCl (pH 8.0), 1 mM DTT and 100 mM NaCl. The analysis was performed at a flow rate of 1.0 ml/min at 25 °C; the elution profile was obtained by measurement of the absorbance at 280 nm. Calibration was performed using ferritin, aldolase, conalbumin (GE Healthcare), BSA (Thermo Fisher Scientific) and human 45CBS produced in *E. coli* and purified as described previously [24].

Native PAGE, BN (blue native)-PAGE and chemical cross-linking

Native electrophoresis was performed on 8 % polyacrylamide gels using the Laemmli buffer system without SDS [25]. Per lane, 5 μg of CBS-1 and of the standards (BSA and human 45CBS) were loaded. BN electrophoresis was performed as described previously [26] with the High Molecular Weight Calibration kit for electrophoresis (GE Healthcare) and rabbit aldolase as the protein marker. Chemical cross-linking was performed using three different concentrations of BS^3 [bis(sulfosuccinimidyl) suberate]; the molar ratios of CBS-1 (0.5 mg/ml) to the cross-linker were 1:10, 1:50 and 1:100. Cross-linked proteins were analysed using precast 3–8 % gradient polyacrylamide gels. As a positive control for efficient cross-linking, we used dimeric human 45CBS reacted with BS^3 at a protein/cross-linker molar ratio of 1:10. All of the proteins analysed by electrophoretic techniques were stained with EZ Blue Gel reagent (Sigma–Aldrich).

Pulse proteolysis

Pulse proteolysis of CBS-1 in a urea gradient was performed with thermolysin as described previously for human CBS [27].

Fluorescence-based thermal-shift assay

Protein samples (0.5 mg/ml) were dissolved in 20 mM Tris/HCl (pH 8.0), and 5×Sypro Orange dye (Bio-Rad Laboratories). Using the real-time PCR Detection System CFX96 Touch (Bio-Rad Laboratories), the proteins were incubated in a thermal gradient from 25 °C to 70 °C at increments of 0.5 °C and with 1-min-hold intervals. The degree of protein unfolding was monitored by a FRET (fluorescence resonance energy transfer) channel that captured the spectral properties of Sypro Orange unfolded protein complexes (excitation wavelength ≈ 470 nm and emission wavelength ≈ 570 nm). The data were analysed by CFX Manager software, and the melting temperatures were determined using the first derivative spectra.

CD and fluorescence spectroscopy

The CD spectra of CBS-1 protein variants [0.5 mg/ml in 50 mM phosphate buffer (pH 7.5)] were recorded using a Jasco J-810 chiroptic spectrometer. The intrinsic fluorescence of CBS proteins in 50 mM Tris/HCl (pH 8.0), was measured in the same buffer using a PerkinElmer LS55 fluorescence spectrometer. The excitation wavelength for tryptophan was 298 nm (slit width of 5 nm) with an emission signal scanned from 300 to 700 nm (slit width of 5 nm).

Determination of substrate specificity

All enzyme assays were performed at 25 °C with an incubation time of 10 min to ensure a linear increase in cystathionine or cysteine production. The reaction mixtures (50 μl) contained 1 μg/ml purified recombinant CBS-1, 10 mM tested substrates in the combinations shown in the Results section, 1 mM PLP, 1 mM DTT, 1 mg/ml BSA and 150 mM Tris/HCl (pH 7.0). The reactions were stopped by the addition of 25 μl of 1 M trichloracetic acid, and the reaction products were determined by HPLC [28] or LC–MS/MS (liquid chromatography–tandem MS) analysis [29] with the modifications described below.

Temperature and pH optima and kinetic analysis

We measured cystathionine production using LC–MS/MS analysis [29] with the following modifications: assays were performed in 100 mM Bis/Tris buffer with 2 μg/ml purified recombinant CBS-1 and unlabelled serine as the substrate. The temperature optimum for CBS-1 activity was determined in 5 °C temperature intervals from 5 °C to 80 °C at pH 8.0, and the pH optimum of CBS-1 was determined at 25 °C in 0.5 pH unit intervals using 100 mM Bis/Tris buffer at pH 6–10. Kinetic analyses at different concentrations of serine or homocysteine were performed at 25 °C and pH 8.0, and the data were evaluated by non-linear data fitting using software Origin 8 (OriginLab). All measurements were repeated four times and the results are shown as means ± S.D.

Site-directed mutagenesis and preparation of CBS-1 protein variants

We prepared and analysed a series of mutant CBS-1 enzymes that included two missense variants of full-length CBS-1 (E62K and K421A) and six truncated CBS-1 variants (CBS-1b, Δ1–372, Δ1–322, Δ1–299, b/360 and b/375) (Figure 4A). All CBS-1 variants were cloned into the pGEX vector, which produces GST-tagged proteins. The sequences of primers used for cloning and site-directed mutagenesis are shown in Supplementary Table S1. Proteins were expressed and purified according to the procedure developed for CBS-1. The yields of purified mutant proteins were slightly lower, typically approximately 0.5 mg per litre of bacterial culture. The mutant proteins were analysed by UV–visible spectroscopy, CD and fluorescence spectroscopy and by BN-PAGE as described above for CBS-1. The catalytic activities for the reaction of serine with homocysteine were assessed in 100 mM Tris/HCl (pH 8.5) at 25 °C.

RNA-mediated interference

The *cbs-1*-specific sequence (~ 350 bp in length) was prepared by PCR amplification of a *C. elegans* cDNA library primers G and H (Supplementary Table S1) and cloned into the pCR4-TOPO vector. Single-stranded RNAs were prepared from linearized DNA by *in vitro* transcription using T3 DNA-dependent RNA polymerase (construct DNA digested by NotI) and T7 DNA-dependent RNA polymerase (construct DNA digested by SalI). The sense and antisense single-stranded RNAs were mixed and incubated at 68 °C for 10 min, followed by incubation at 37 °C for 30 min. The double-stranded RNA was further purified by phenol/chloroform extraction and precipitated by ethanol; the RNA pellet was diluted in water to an approximate concentration of 2 μg of RNA/μl. The double-stranded RNA was injected into the gonads of young adult hermaphrodite worms as described previously [30]. The embryos of microinjected animals were synchronized in 9–12 h intervals. Nematodes were grown at 16 °C on nematode growth medium plates and fed with *E. coli* strain OP50. After RNAi (RNA interference), the nematodes were seeded in 1× PBS buffer on 2 % agarose and screened by their phenotype.

Determination of CBS-1 antigen levels and measurement of enzymatic activity in *C. elegans* extracts

Worms were grown at 16 °C as described above and collected 7 days after embryo microinjection as a mixed population of all larval stages. Worm lysates were prepared by sonication of worm pellets resuspended in 1 vol. of 100 mM PBS containing protease

inhibitor cocktails for prokaryotic (P8465, Sigma–Aldrich) and eukaryotic (P8340, Sigma–Aldrich) cells. Crude extracts were centrifuged for 1 h at 4 °C and 20000 *g* and the supernatants were used for the determination of CBS-1 levels and CBS activity. Western blotting was used to examine CBS-1 antigen levels after RNAi. The samples were submitted to SDS/PAGE (pre-cast 3–8 % gradient gel), and protein immunodetection was performed by Western blot analysis using custom-made rabbit polyclonal anti-CBS-1 antibody prepared against purified recombinant CBS-1 (Exbio Praha). Actin, which was detected using a rabbit anti-actin antibody (Abcam), was used for the normalization of protein loading. The signal levels of CBS-1 and actin were determined by chemiluminescence (Pierce) by employing the ChemiGenius station and Gene Tools software for semi-quantification [31]. The enzyme assay was performed according to a previously described protocol [29] with the modification that the reaction mixture was incubated at 16 °C for 30 min.

Measurement of metabolites in *C. elegans* extracts

Worm lysates were prepared by sonication of worm pellets that had been resuspended in 1 vol. of 100 mM PBS without protease inhibitors (Cole-Parmer GE130 Ultrasonic processor, amplitude 20 for 2 min with 1 s on/off pulses). The crude extracts were centrifuged at 20000 *g* for 1 h at 4 °C, and the supernatants were used for HPLC aminothiol determination as described previously [28]. The cystathionine concentration was determined by LC–MS/MS using the EZ:faast kit for amino acid analysis (Phenomenex) [29]. The concentrations of all metabolites measured were normalized to the amount of protein present in the sample.

RESULTS

CBS in *C. elegans* is encoded by *ZC373.1*

We used a BLASTp search as an *in silico* approach to identify genes that encode a CBS in *C. elegans*. Using the query sequences of three enzymes of the CBS family (human CBS, trypanosomal CBS and bacterial cysteine synthases), we identified ten genes with predicted amino acid sequences that are homologous with the catalytic domains of the known CBSs; these genes are annotated in WormBase (http://www.wormbase.org/) as 'CBS and related proteins'. Alignment of the predicted amino acid sequences of the *C. elegans* genes *ZC373.1* and *F54A3.4* revealed the highest homology with human CBS (UniProt entry P35520). These predicted proteins exhibited 54 % sequence identity with the human protein, whereas the other eight predicted proteins showed lower homology, with 21–44 % sequence identity (Supplementary Table S2 at http://www.BiochemJ.org/bj/443/bj4430535add.htm). The BLASTp searches using all ten nematode CBS homologues as the query sequences against the UniProt database, together with phylogenetic analysis, indicated that only ZC373.1 and F54A3.4 are homologous with CBS, whereas the remaining eight amino acid sequences are homologous with other proteins within the family of fold-type II PLP-dependent enzymes (Supplementary Figure S1 at http://www.BiochemJ.org/bj/443/bj4430535add.htm).

An annotation in the WormBase database shows that the *ZC373.1* gene is trans-spliced to SL1 and contains ten exons, including 23 bp of the 5′-UTR (untranslated region) and 149 bp of the 3′-UTR followed by a polyadenylation sequence. The *F54A3.4* gene is predicted to contain either eight exons without any 5′- or 3′-UTRs (http://www.wormbase.org/) or only seven exons terminated by a 77 bp 3′-UTR sequence (http://www.ncbi.nlm.nih.gov/IEB/Research/Acembly/). To determine whether the *ZC373.1* and *F54A3.4* genes are transcribed and spliced into the predicted full-length mRNAs, we analysed their coding regions by RT–PCR and by sequencing of PCR products. We found two differently spliced variants of the *ZC373.1*; one sequence is identical with the WormBase annotation (*cbs-1*), and the other is a new *ZC373.1* splice variant (*cbs-1b*) containing a 5-bp shortening of exon 7 in its 5′-terminus that leads to a frame-shift with a premature stop codon at amino acid residue 377 (Figure 1A and Supplementary Figure S2 at http://www.BiochemJ.org/bj/443/bj4430535add.htm). In contrast, we were unable to amplify either of the two hypothetical full-length *F54A3.4* mRNAs using several PCR conditions, various primers and various cDNA templates.

Because we did not succeed in detecting the *F54A3.4* mRNA by RT–PCR, we used additional approaches to examine the possible role of this gene in *C. elegans*. *In silico* analysis of the GenBank® database revealed three ESTs (expressed sequence tags) of *F54A3.4*: CK587466.1, CB389123.1 and FN902238.1; however, only FN902238.1 has been mapped to the sense strand of the *F54A3.4* region (http://www.ncbi.nlm.nih.gov/nucleotide/). Furthermore, the proteomic database PeptideAtlas did not contain any peptide matches to the hypothetical protein F54A3.4 (http://www.peptideatlas.org/) [32]. Moreover, expression analysis using translational fusion proteins F54A3.4–GFP and ZC373.1–GFP (cbs-1–GFP) (see below) showed that the GFP signals reflecting the expression pattern of the appropriate genes were observed only in worms carrying ZC373.1–GFP, in contrast with the expression patterns observed in several worms carrying F54A3.4–GFP. Finally, *F54A3.4* does not appear to have functional significance in *C. elegans* because the mutant strain RB839, which carries a deletion of *F54A3.4*, showed CBS activity and homocysteine concentrations indistinguishable from those of the WT strain (results not shown), and did not exhibit abnormal behavioural or a developmental phenotype (results not shown).

On the basis of the findings listed above, *F54A3.4* appears to be a pseudogene and was not further examined in the present study. All of the data above strongly indicate that the *C. elegans* genome contains only one expressed orthologue of the human CBS gene, i.e. *ZC373.1*. In accordance with the recommended nomenclature, this gene was named *cbs-1*.

CBS-1 is a cytoplasmic enzyme that is expressed in the hypodermis and intestine, and in muscle cells

To determine the expression pattern and subcellular localization of *cbs-1*, we constructed the translational vector cbs-1–GFP, which contains the promoter and the entire CBS-1 sequence tagged at the C-terminus with GFP (Figure 1A). In worms expressing cbs-1–GFP, the GFP signal was observed in the hypodermis, intestine, body-wall muscle cells and pharyngeal muscles pm3, pm4, pm5, pm6, pm7 and pm8 in all larval stages as well as in adults (Figure 2). Our data using a translational reporter showed a similar expression pattern, as did previous transcriptional screens, and a novel expression of *cbs-1* in pharyngeal muscles. We did not observe a GFP signal in embryos, although previous transcriptional screens and peptide mapping studies have reported expression of *cbs-1* in this developmental stage [32,33]. The observed GFP signal was distributed diffusely within cells and spared the nucleus, suggesting that CBS-1 is localized in the cytoplasm. These data provide the first reported insight into the tissue and subcellular localization of nematode CBS-1 at the protein level and indicate which nematode tissues can metabolize homocysteine to cystathionine and/or cysteine to hydrogen sulfide.

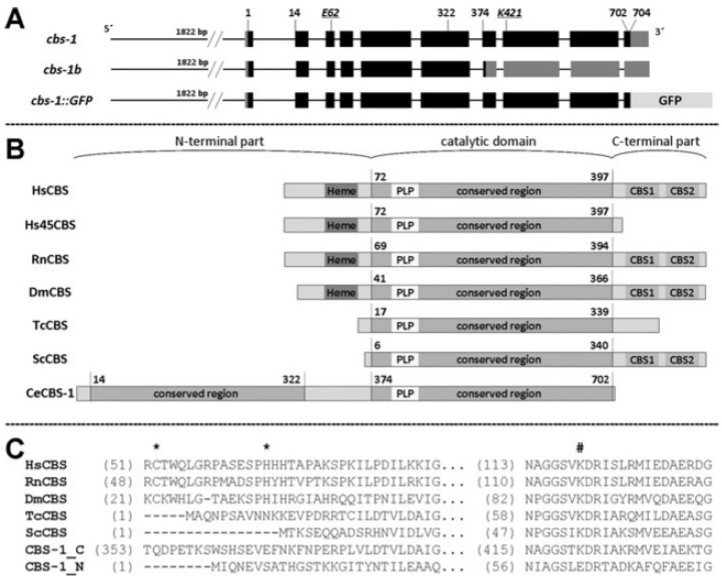

Figure 1 Organization of the *cbs-1* gene and domain architecture of CBS in various organisms

(**A**) Gene organization. The top diagram shows the organization of gene *ZC373.1* (*cbs-1*) encoding CBS-1. The numbers indicate the codon position encoding the appropriate amino acid. Exons are indicated as black boxes, and the 5′- and 3′-UTR sequences are indicated as grey boxes. The middle diagram shows the novel splice *ZC373.1* variant *cbs-1b*. The bottom diagram shows the translational fusion construct used in the GFP reporter assay. The length of the entire promoter used in the cbs-1–GFP construct is indicated by the number of base pairs of the 5′-upstream sequence. (**B**) Domain organization of various CBSs. The published structures of different CBSs were analysed for the presence of a haem-binding site (marked Heme), conserved catalytic regions with a PLP-binding site (marked PLP) and Bateman domain composed of two CBS domains (CBS1 and CBS2). The primary structures are aligned by the PLP-binding lysine residue; the numbers indicate the first and the last amino acid residues of conserved domains in the protein sequence. The aligned proteins are HsCBS (*Homo sapiens* CBS, UniProt entry P35520), Hs45CBS (truncated human CBS with 1–413 residues), RnCBS (*Rattus norvegicus* CBS, UniProt entry P32232), DmCBS (*D. melanogaster* CBS, UniProt entry Q9VRD9), TcCBS (*T. cruzi* CBS, UniProt entry Q9BH24), ScCBS (*S. cerevisiae* CBS, UniProt entry P32582) and CBS-1 (*C. elegans* CBS, UniProt entry Q23264). (**C**) Amino acid alignment of haem- and PLP-binding sites in various CBSs with separated N- and C-terminal conserved regions of CBS-1. The N-terminal region of CBS-1 does not contain the lysine residue that binds PLP. The cysteine and histidine residues that bind haem are indicated by asterisks, and the PLP-binding lysine residues are indicated by #.

CBS-1 is a haem-independent protein that lacks activation by AdoMet

To experimentally characterize the structural and enzymatic properties of CBS-1, *cbs*-1 cDNA was expressed in *E. coli*. Recombinant CBS-1 (704 residues of native CBS-1 with five additional amino acids at the N-terminus, six additional histidine residues at the C-terminus and a size of ~78 kDa) was purified to greater than 95% purity (Supplementary Figure S4 at http://www.BiochemJ.org/bj/443/bj4430535add.htm). The UV–visible absorption spectrophotometry of the purified recombinant CBS-1 showed a peak at 412 nm, confirming the presence of covalently bound PLP that forms an internal aldimine, but it did not reveal a Soret band associated with a haem moiety (Figure 4F). This analysis confirmed that, in contrast with other characterized metazoan CBS enzymes, the nematode enzyme is a haem-independent CBS.

We next tested four reactions that have been described for previously characterized CBSs: (i) cystathionine-synthesizing activity that produces cystathionine and water from homocysteine and serine; (ii) formation of cystathionine and hydrogen sulfide from homocysteine and cysteine; (iii) cysteine synthase activity that produces cysteine from *O*-acetylserine and hydrogen sulfide; and (iv) serine sulfhydrylase activity in which cysteine is synthesized from serine and hydrogen sulfide. CBS-1 exhibited high enzymatic activity for synthesis of cystathionine from homocysteine utilizing either serine or cysteine and considerably lower cysteine synthase and serine sulfhydrase activities for synthesis of cysteine. The specific activities of CBS for the production of cystathionine from serine and cysteine were ~1500 μmol · h^{-1} · mg^{-1} and ~300 μmol · h^{-1} · mg^{-1} respectively, and its specific cysteine synthase and serine sulfhydrase activities were ~5 μmol · h^{-1} · mg^{-1} and ~30 μmol · h^{-1} · mg^{-1} respectively. None of these activities were stimulated by 1 mM AdoMet (results not shown), which is consistent with the absence of a Bateman domain in CBS-1 (see below). These data show that the nematode CBS-1 enzyme exhibits typical CBS activity and that it is not activated by AdoMet.

CBS-1 has a unique structural arrangement

Alignment of the predicted amino acid sequence of CBS-1 with the sequences of previously characterized human, rat, *Drosophila*, trypanosome and yeast CBS enzymes revealed that the *C. elegans* enzyme possesses unique and novel domain architecture. In contrast with other CBSs, *C. elegans* CBS-1 lacks both the haem-binding N-terminus and the entire C-terminus found in other species (Figures 1B and 1C). Moreover, amino acid alignment together with protein modelling revealed that a single polypeptide chain of CBS-1 contains a unique tandem arrangement of two conserved CBS cores that belong to a family of fold-type II PLP-dependent proteins (Figure 1B and 3). Phylogenetic analysis of these two CBS-1 modules revealed that, in contrast with the C-terminal module, the N-terminal module has a lower homology with other CBS enzymes and does not belong to any of the fold-type II PLP-dependent protein families tested (Supplementary Figure S3 at http://www.BiochemJ.org/bj/443/bj4430535add.htm).

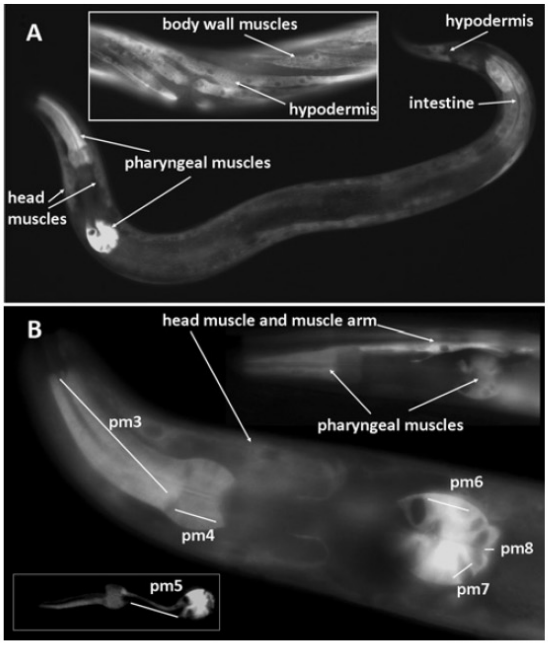

Figure 2 Expression pattern of *cbs-1* in worms

The images show transgenic worms that carry the translational fusion vector cbs-1–GFP. (**A**) L4 larval stage showing the distribution of the GFP signal in the pharyngeal muscles, intestine, hypodermis and muscle cells. The middle part of the adult body (inset) shows the GFP signal in the body wall muscles and hypodermis. (**B**) Head of the worm showing GFP signal in pharyngeal muscles and a head muscle cell with its muscle arm; the GFP signal is distributed in the pharyngeal muscles pm3, pm4, pm6, pm7 and pm8. Some worms also exhibited a GFP signal in pm5 (inset).

Furthermore, the critical PLP-binding lysine residue in the N-terminal module is replaced by a glutamic acid residue (Figures 1C and 3). Analysis of the PLP-binding site using homology modelling with the structure of 45CBS as the template revealed that the fully conserved glycine residue (Gly^{256} in human 45CBS) in the N-terminal module is replaced by a bulky asparagine residue (Asn^{197}) that may sterically affect PLP binding (Figure 3). Thus the *in silico* data strongly suggest that the N-terminal module of nematode CBS-1 cannot bind the PLP essential for the catalytic activity of the enzyme.

The catalytic activity of CBS-1 is mediated only by the C-terminal module

To confirm the hypothesis that the catalytic function of CBS-1 is mediated only by its C-terminal module, we generated individual CBS-1 modules in *E. coli*. While the CBS-1b variant, which lacks the C-terminal module of CBS-1, was highly soluble after expression in *E. coli*, all of the cloned CBS-1 variants without the N-terminal module showed substantially decreased solubility (Figure 4B) that prevented successful purification of proteins containing only the C-terminal module. However, we purified and characterized the CBS-1b and used UV–visible and fluorescence spectrometry to determine that it does not bind PLP; we also found that CBS-1b had virtually undetectable catalytic activity (Figures 4D, 4F and 4G and Table 1). These observations demonstrate that the PLP-binding site essential for catalytic activity is not located in the N-terminal module of the CBS-1 protein. Although CD spectrometry showed that the CBS-1b has a helical secondary structure similar to that of the WT CBS-1 protein (Figure 4E), BN-PAGE revealed that purified CBS-1b precipitates and may form higher-order oligomers (Figure 4C). These data indicate that the presence of both CBS-1 modules in one subunit is necessary for the maintenance of the global structural stability of CBS-1 and/or for proper folding of the recombinant protein.

Because analysis of the isolated N-terminal module indicated possible disruption of its native structure, we also generated and purified the CBS-1 mutants K421A, which abolishes a canonical PLP-binding site in the C-terminal module, and E62K, which creates a putative PLP-binding site in the N-terminal module. We observed altered fluorescence-based tryptophan spectra of the mutant proteins; their relative fluorescence showed different quenching of the tryptophan emission, and the existence of a wavelength maximum shift from ~340 to ~350 nm indicates higher accessibility of the tryptophan residues to the polar solvent in the K421A mutant (Figure 4G and Table 1). In contrast, both mutants retained oligomeric status identical with the WT as determined by BN-PAGE (Figure 4C), and CD measurements showed that the protein's secondary structure is not affected by either the K421A or E62K mutation (Figure 4E). The catalytic activity, PLP saturation and fluorescent properties of the E62K mutant were similar to those of WT (Figures 4D, 4F and 4G), supporting the idea that the structural properties of the N-terminal module do not permit PLP binding even if the canonical lysine residue is present. In contrast, the K421A mutant binds significantly less of the PLP cofactor, as determined by UV–visible absorption spectroscopy. The mutant enzyme's residual affinity for PLP probably results from the formation of an external aldimine; this affinity is manifested in its UV–visible spectrum by the presence of two bands with maxima at 403 and 418 nm and by the lack of the sharp maximum at 412 nm that is typical for internal aldimines (Figure 4F). The formation of an external aldimine in K421A was confirmed by fluorescence spectroscopy and, when excited at 298 nm, the emission spectrum of the mutant protein revealed a significantly higher extent of delayed fluorescence of Schiff bases for K421A in comparison with WT, E62K and CBS-1b (Figure 4G). Enhanced delayed fluorescence due to formation of external aldimines in the active site of the mutant enzyme has also been reported for the bacterial *O*-acetylsulfhydrylase mutant K42A [34]. Taken together, these experiments provide additional evidence that the catalytic activity of *C. elegans* CBS-1 is mediated only by the C-terminal module and that its N-terminal module cannot bind PLP cofactor either as an internal or as an external aldimine.

Analysis of the quaternary structure of nematode CBS-1 suggests a monomeric status of CBS-1

We analysed the quaternary structure of recombinant nematode CBS-1 to determine whether CBS-1 exists as a monomer with a structural arrangement similar to human 45CBS (the C-terminally truncated human CBS that lacks a Bateman domain and forms dimers of 90 kDa [15]), or whether CBS-1 forms dimers or higher-order oligomers. We first performed SEC using the standard proteins ferritin (440 kDa), aldolase (158 kDa), conalbumin (75 kDa) and BSA (66 kDa). To control for possible differences in the Stokes radii of the standard proteins and the CBS-related proteins that may influence their retention on the column, we analysed human 45CBS in parallel. Nematode CBS-1 exhibited a tailing peak with a retention time of 5.776 min (Figure 5A); on the basis of the calibration curve, the apparent native molecular mass of the protein was determined to be ~170 kDa. However, SEC of human 45CBS indicated a native molecular mass of

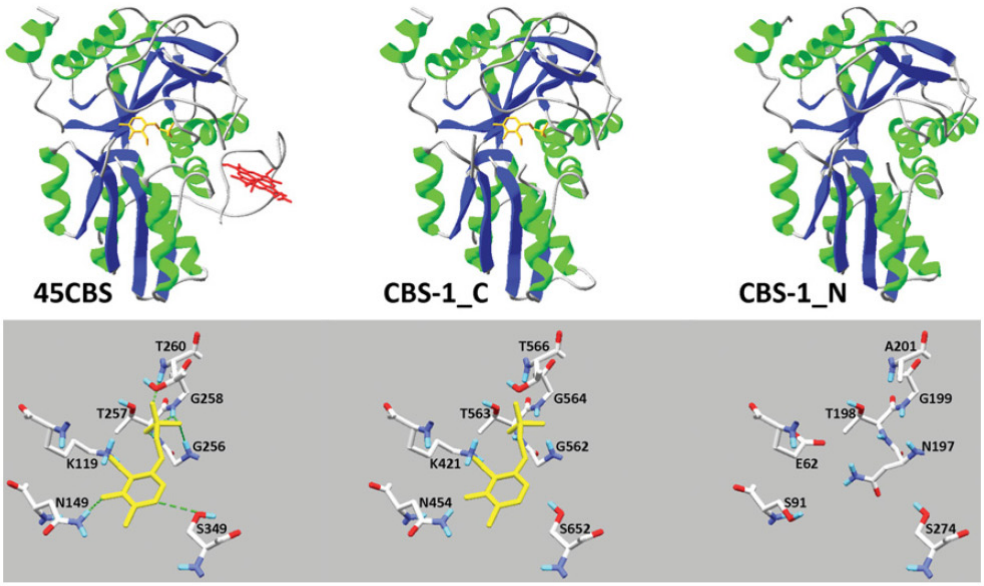

Figure 3 Computationally modelled CBS-1 domains

The images show the fold and PLP-binding site of human 45CBS, C-terminal module of CBS-1 (CBS-1_C) and N-terminal module of CBS-1 (CBS-1_N). The crystal structure of the human enzyme shows hydrogen bonds between amino acid residues and PLP, as indicated by broken green lines. Computational modelling of the individual CBS-1 modules revealed that both modules belong to the family of fold-type II PLP-dependent proteins and that the N-terminal module cannot bind PLP due to the absence of lysine and glycine residues in the consensus PLP-binding pocket.

approximately 150 kDa, suggesting that calibration with standard proteins may result in overestimation of the molecular mass of CBS proteins. According to the molecular mass markers used, SEC yielded ambiguous results compatible with both a monomeric and dimeric structure of CBS-1.

We next used additional techniques including native electrophoresis, BN electrophoresis and chemical cross-linking followed by SDS/PAGE to determine the most likely quaternary structure of CBS-1. These three techniques congruently showed that the 78 kDa nematode CBS-1 exists predominantly as a monomer. The evidence, which is shown in Figures 5(B)–5(D), is as follows: (i) in native PAGE, nematode CBS-1 migrates similarly to the 90 kDa marker of dimeric human 45CBS and between fractions containing monomeric and dimeric BSA respectively (66 kDa and 132 kDa); (ii) on BN electrophoresis, CBS-1 migrates between molecular mass markers of 66 and 140 kDa; and (ii) chemical cross-linking of CBS-1 did not result in changes in protein migration, suggesting modification of amino acid side chains within a single polypeptide chain, whereas human 45CBS readily formed a cross-linked dimeric product with a molecular mass of ~100 kDa. On the basis of these results, we propose that, in contrast with CBS enzymes from other species, recombinant nematode CBS-1 does not form oligomeric structures *in vitro*. Because the conserved catalytic regions of CBS-1 are homologous with each other, we hypothesize that they form an internal interface similar to that formed by subunit dimerization of human 45CBS (Figure 5E).

CBS-1 is more sensitive to denaturation and is more active than human 45CBS

We hypothesized that the above-described differences in the oligomeric assembly of nematode CBS-1 and human 45CBS might result in differences in the energetics of the two proteins. To explore this hypothesis, we used a fluorescence-based thermal-shift assay and pulse proteolysis in a urea gradient. Both approaches revealed significantly lower stability of CBS-1 compared with the human 45CBS; the melting point of CBS-1 was 10 °C lower than that of human 45CBS, and the resistance of CBS-1 to urea-induced unfolding decreased by ~2.8 M (Table 2 and Supplementary Figure S5 at http://www.BiochemJ.org/bj/443/bj4430535add.htm). These data show that the nematode CBS-1 is less energetically stable than the human 45CBS; this finding may be due to a lower energy of the interdomain interface or a higher structural flexibility of the worm CBS-1.

We considered the possibility that the observed structural and energetic differences between the nematode CBS-1 and human 45CBS result in different catalytic properties. We determined the temperature and pH optima and the kinetic parameters for the major CBS reaction, which produces cystathionine from serine and homocysteine. The CBS-1 protein exhibited the highest activity at pH 8.5 and 30 °C (Supplementary Figure S6 at http://www.BiochemJ.org/bj/443/bj4430535add.htm). These conditions are in accordance with the results of the thermal stability assay (see above). We speculate that the lower temperature optimum of CBS-1 compared with the human enzymes (37 °C) may reflect the lower body temperature of nematodes living in the soil. We also found that the affinity of CBS-1 for homocysteine is lower than that of 45CBS (Table 2); however, we observed inhibition of CBS activity at 7.5 and 10 mM homocysteine and this inhibition prevented the activity from increasing to more than ~1500 $\mu mol \cdot h^{-1} \cdot mg^{-1}$ (Supplementary Figure S6). Inhibition by high concentrations of homocysteine has been previously reported for yeast and human CBS enzymes [13,35]. Taken together, these data show that the nematode CBS-1 subunit is approximately 4-fold more active compared with the human 45CBS subunit as expressed by the turnover number (Table 2).

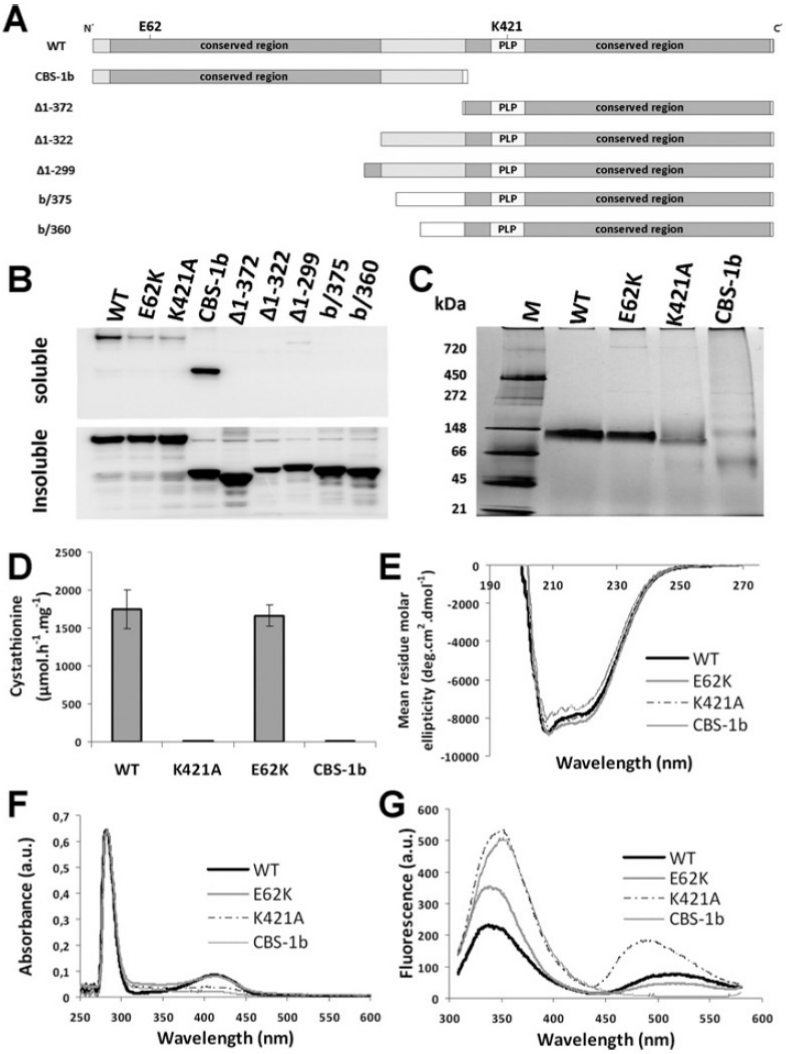

Figure 4 Structural and enzymatic analysis of recombinant CBS-1 variants

(**A**) Illustration of the CBS-1 variants expressed in *E. coli*. (**B**) Detection of CBS-1 variants in *E. coli* lysate after expression using soluble and insoluble fractions separated by centrifugation. (**C**) BN-PAGE of purified recombinant CBS-1 variants shows the monomeric status of the WT, K421A and E62K proteins. The N-terminal domain exhibits monomeric and oligomeric forms. Molecular mass markers are shown in kDa on the left-hand side. (**D**) CBS activity of the purified CBS-1 variants; K421A and CBS-1b have no CBS activity. Results are means ± S.D. (**E**) CD spectra at far-UV show a helical secondary structure for all of the purified CBS-1 variants. (**F**) The UV–visible spectrum of purified recombinant CBS-1 variants of equal concentration shows peaks in the 280 and 412 nm region, indicating light absorption by aromatic amino acids and PLP respectively. Soret peaks typical for haem are not present. (**G**) Emission spectrum after excitation of the tryptophan residues at 298 nm of purified recombinant CBS-1 variants of equal concentration.

CBS-1 mediates nematode development and maintains homocysteine homoeostasis

To explore the functional significance of *cbs-1* in *C. elegans*, we silenced the *cbs-1* gene by RNA-mediated interference and determined the phenotypic consequences of such silencing. To confirm the efficacy of *cbs-1* RNAi, we measured the amounts of CBS-1 antigen and CBS activity in worm extracts of CBS-1-inactivated and WT worms. Western blot analysis using an anti-CBS-1 antibody showed that after RNAi treatment worms exhibited a CBS-1 level that was approximately 10% that of the control strain (Supplementary Figure S7A at http://www.BiochemJ.org/bj/443/bj4430535add.htm). Although the mean CBS activity of normal worms was 36.0 $nmol \cdot h^{-1} \cdot mg^{-1}$, *cbs-1* RNAi animals exhibited a mean activity of only 5.4 $nmol \cdot h^{-1} \cdot mg^{-1}$, approximately ~15% of the control level (Supplementary Figure S7B). The results from both Western blot analysis and CBS activity measurement consistently confirmed that the RNAi experiments efficiently reduced the amount and activity of CBS-1.

RNAi resulted in a developmental delay phenotype in 97% of the worms (515 out of 530 individuals tested). These animals reached the egg-laying adult stage no earlier than the 9th day after embryo hatching, in contrast with control worms, which reached

Table 1 Enzymatic and structural properties of purified CBS-1 variants

ND, not detected, Trp, tryptophan.

Protein	WT	K421A	E62K	CBS-1b
Catalytic activity (μmol · h^{-1} · mg^{-1})	1742 ± 259	0.41 ± 0.03	1663 ± 144	0.27 ± 0.05
Absorption ratio 280/412 nm	7.6	16.1	7.9	29.2
PLP absorption maximum (nm)	412	403 and 418	412	ND
Trp relative fluorescence	233	534	354	505
Trp fluorescence wavelength maximum (nm)	338	350	339	352
Relative delayed fluorescence	76	181	48	ND

the same stage on the 5th day of development. The affected larvae had a shorter body length than the controls (Supplementary Figure S8 at http://www.BiochemJ.org/bj/443/bj4430535add.htm). After RNAi of larvae, the most severe abnormalities were observed in the tissues that express the highest amount of CBS-1 (i.e. gut and pharynx; see the data above on the translational cbs-1–GFP vector). The gut cells of these animals showed reduced pigment granule birefringence under Nomarski optical microscopy (Supplementary Figure 8), and the anterior bulb of the pharynx exhibited abnormal morphology, with a balloon-like appearance and enlarged diameter (Supplementary Figure 8). These data show that CBS-1 is essential for normal development in nematodes.

We determined metabolic flux through the trans-sulfuration pathway by measuring homocysteine, cystathionine and cysteine concentrations in worm homogenates. To eliminate possible differences in metabolic fluxes in worms at various stages of development, the worms were collected at the latest larval developmental stage (L4). The homocysteine and cystathionine levels in *C. elegans* extracts were ~10× and ~1.6× higher in the knockdown strain than in the controls, whereas cysteine concentrations did not differ between the two strains (Figure 6). The observation of elevated homocysteine levels in CBS-1-knockdown worms

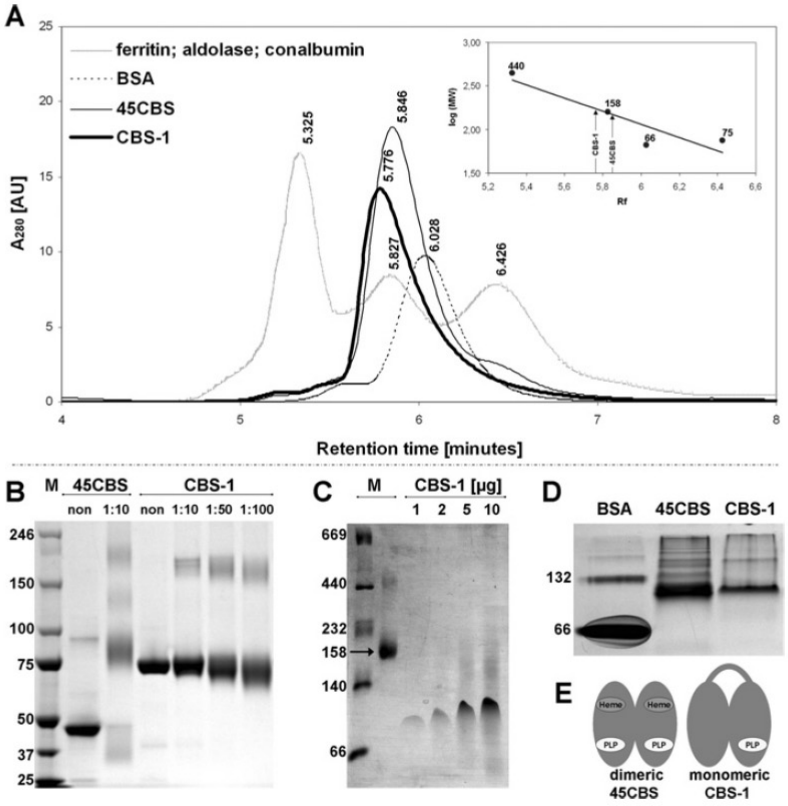

Figure 5 Determination of the quaternary structure of CBS-1

(**A**) SEC. The bold solid curve represents the elution profile of purified recombinant CBS-1, which has a retention time of 5.776 min and an estimated molecular mass of 168 kDa. The thin solid curve represents human 45CBS, which has a retention time of 5.846 min and an estimated molecular mass of 148 kDa. The dashed curve represents BSA with a retention time of 6.028. The grey (dotted) curve represents molecular standards eluted at the following retention times: ferritin (440 kDa), 5.325 min; aldolase (158 kDa), 5.827 min; and conalbumin (70 kDa), 6.426 min. AU, absorbance unit. (**B**) Cross-linking. Purified CBS-1 and human 45CBS were cross-linked with BS^3 in appropriate molar ratios of protein/modifier, as indicated in the Figure, and subjected to SDS/PAGE. In contrast with human 45CBS, which forms dimers, the mobility of CBS-1 does not change after cross-linking. (**C**) BN-PAGE. CBS-1, with a molecular mass of 78 kDa (four different amounts of loaded protein), migrates between molecular mass markers of 66 kDa and 140 kDa. The molecular protein mass markers include thyroglobulin (669 kDa), ferritin (440 kDa), catalase (232 kDa), lactate dehydrogenase (140 kDa), BSA (66 kDa) and aldolase (158 kDa). (**D**) Native PAGE. CBS-1, with a molecular mass of 78 kDa, migrates between molecular mass markers of 66 kDa and 132 kDa, similar to a ~90 kDa dimer of human 45CBS. In (**B**–**D**) the molecular mass is given in kDa on the left-hand side. M, marker. (**E**) Schematic diagram of the hypothetical quaternary structure of CBS-1 and comparison of its structure with that of human 45CBS.

Table 2 Stability and enzymatic properties of CBS-1 compared with human 45CBS

c_m, concentration of urea at which a fraction of folded proteins comprises 50 % of the entire protein population.

Protein	Nematode CBS-1	Human 45CBS
Oligomeric status	Monomer	Dimer
Michaelis constant K_m (mM)		
Serine	5.57 ± 0.68	2.20 ± 0.46†
Homocysteine	4.29 ± 0.97	0.33 ± 0.07†
Turnover number k_{cat} (s^{-1})		
Serine	48.12 ± 2.95	13.81 ± 0.88†
Homocysteine	43.31 ± 4.33	10.88 ± 0.72†
Catalytic efficiency k_{cat}/K_m ($mM^{-1} \cdot s^{-1}$)		
Serine	~8.5	~6
Homocysteine	~10	26.97 ± 5.87†
Characteristics of protein denaturation		
Midpoint of urea concentration c_m (M)	1.21 ± 0.02	4.08 ± 0.07*
Melting point T_m (°C)	41	51

*Value from Hnizda et al. [27].
†Value from Frank et al. [23].

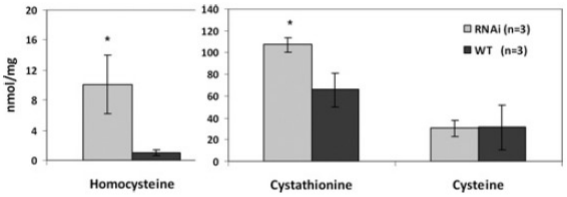

Figure 6 Metabolite levels in crude extracts of CBS-1-knockdown animals

The concentration of metabolites (in nanomoles per mg of protein) from RNAi and control experiments respectively. Homocysteine and cystathionine concentrations in CBS-1-deficient worms are significantly higher (10.1 and 107.1 nmol/mg of protein respectively) than in control worms (1.0 and 65.6 nmol/mg of protein respectively). Results are means ± S.D. from three independent experiments. *$P < 0.05$, as determined by Student's t test.

strongly supports an important role of this enzyme in maintaining homocysteine homoeostasis in *C. elegans*.

DISCUSSION

Evidence that CBS in *C. elegans* is encoded by *cbs-1*

In the present paper, we identified the *cbs-1* gene in *C. elegans*, which encodes an enzyme with cystathionine-synthesizing activity and is important for normal development of the nematode. Using a BLASTp search against a *C. elegans* protein database, we identified two nematode genes, *ZC373.1* and *F54A3.4*, that are highly homologous with CBS genes in other species. However, several lines of evidence demonstrate that only *ZC373.1* encodes a CBS, whereas *F54A3.4* is probably a pseudogene. The gene denoted *F54A3.4* has not been detected by RT–PCR, was not found by *in silico* searches in the appropriate EST and proteomic databases, and its partial deletion did not elicit biochemical or morphological phenotypic abnormalities. In contrast, *ZC373.1* mRNA has been detected by RT–PCR, its ESTs and peptides were annotated in appropriate databases, the enzyme was shown to be expressed endogenously in its entire length, and its knockdown resulted in severe biochemical and phenotypic consequences. Most importantly, the purified CBS-1 enzyme exhibited enzymatic properties consistent with previously characterized CBS enzymes from other species.

The unique domain architecture of nematode CBS enzymes

In silico analysis of the CBS-1 protein sequence showed that the CBS-1 of *C. elegans* possesses a unique multi-domain architecture that has not been reported previously for any other CBS. The unusual structure of CBS-1 includes the lack of a haem-binding region, the lack of a Bateman domain and the tandem arrangement of two conserved catalytic regions of which only the C-terminal region is catalytically active. Such a domain arrangement of predicted CBS enzymes in fully sequenced organisms has been found only in organisms from the nematode phylum, showing an evolutionarily divergent arrangement of the CBS protein in this phylum. Interestingly, the nematode *Loa loa* possesses a PLP-binding site in both CBS modules (Supplementary Figure S9 at http://www.BiochemJ.org/bj/443/bj4430535add.htm), suggesting that the unusual and unique structure of CBS enzymes in nematodes probably originates from a duplication of the conserved catalytic region in a common ancestor followed by mutations abolishing PLP binding in the N-terminal module.

To our knowledge there is no evidence, except of nematode CBS proteins, regarding fold-type II PLP-dependent proteins lacking a PLP-binding site. Thus the function, if any, of the N-terminal module in the nematode CBS-1 protein remains unclear. Several pieces of experimental evidence obtained in the present study clearly show that this module does not have canonical catalytic function. We speculate that mutations in this portion of the nematode CBS enzyme may have permitted the acquisition of novel structural and functional properties, such as changes in protein stability and folding, protein–protein interactions, or regulation of enzyme activity. Studies of truncated variants suggest that the N-terminal module may be important for proper folding and subsequent stability of CBS-1 (see above). Because CBS-1 forms a monomer, it is probable that its N-terminal and C-terminal modules interact to form a structure similar to that of the human 45CBS dimer. However, the proposed interdomain interaction cannot be sufficiently supported by the computational modelling procedures using previously solved crystal structures of CBS proteins, and thus it requires further study of the three-dimensional spatial arrangement of CBS-1 at atomic resolution. The N-terminal module of CBS-1 may also have a regulatory role. The existence of tandem duplicated conserved modules of which only one is catalytically active in a single polypeptide is similar to the well-known case of tyrosine protein kinases [JAKs (Janus kinases)]. In tandem with a catalytically active kinase domain, these kinases have a catalytically inactive pseudo-kinase domain that has been implicated in the regulation of their activity [36]. Alternatively, the N-terminal module of CBS-1 may also play a role in protein–protein interactions, such as the interactions with the SUMOylation enzyme apparatus or huntingtin that have been described for human and rodent CBS-1 orthologues respectively [37,38].

More intriguingly, expression of the spliced variant *cbs-1b* shows that the N-terminal module of CBS-1 can be produced *in vivo* without the catalytic C-terminal module. This finding suggests that the non-catalytic module may play a role in additional biological processes independent of the catalytic module. However, it should be noted that misspliced variants with premature stop codons are commonly targeted by a cellular RNA nonsense-mediated decay mechanism [39]; therefore, the existence of a separate nematode N-terminal domain *in vivo* should be investigated in future studies.

Possible biological roles of CBS-1 enzymatic activity in *C. elegans*

Because *cbs-1* is expressed in a limited number of tissues, it is tempting to speculate on the role of this enzyme in the organs

in which it is expressed. High expression of *cbs-1* was observed throughout post-embryonic development in the intestine, which is characterized by secretion of digestive enzymes and high metabolic activity in *C. elegans*, such as the synthesis and storage of macromolecules and detoxification of xenobiotics [40]. Thus the expression of *cbs-1* in *C. elegans* intestine may mirror the high expression of CBS in the mammalian liver, pancreas and small intestine, in which CBS plays an important role in homocysteine homoeostasis and/or in the provision of cysteine for glutathione production [41]. We hypothesize that the intestinal expression of *cbs-1* in worms may serve similar purposes, namely removal of homocysteine or cysteine biosynthesis.

Expression of *cbs-1* has also been observed in pharyngeal muscles and hypodermis. Because neither of these tissues shows high metabolic activity compared with the intestine, there are other possible explanations for CBS-1 activity in these tissues. Because both hypodermal cells and pharyngeal muscle cells secrete cuticle (http://www.wormatlas.org/), we propose that CBS-1 may provide cysteine, which is important for cuticle formation and its stabilization by disulfide bonds [42]. Another possible role for CBS-1 in muscle and hypodermis is the production of the neuromodulator and smooth muscle relaxant hydrogen sulfide [43]. The endogenous biosynthesis of H_2S via CBS might serve for smooth muscle relaxation in the strongly innervated nematode pharynx or in regulating the expression of HIF-1 (hypoxia-inducible factor 1) target genes in the hypodermis [44]. Interestingly, although CBS is thought to be the main enzyme that produces hydrogen sulfide in the mammalian brain [45], we did not observe a GFP signal in neurons. This finding suggests that the endogenous production of hydrogen sulfide in *C. elegans* neurons is mediated by different enzymes than in other species or that the role of hydrogen sulfide in *C. elegans* neurons is negligible.

C. elegans as a model of CBS deficiency

Because many genes implicated in human diseases are well-conserved across phyla [46], *C. elegans* is considered by many investigators to be a suitable model for studying cellular and metabolic mechanisms in selected genetic disorders [47–49]. In addition to its low cost of maintenance and short generation time, other advantages of the *C. elegans* model include the possibility of observing cellular processes *in vivo* and of easily screening for the effects of novel therapies [50,51]. In the present study, we examined the morphological and biochemical effects of nematode CBS-1 deficiency. These effects may in part recapitulate the human disease homocystinuria, which results from CBS deficiency. Homocystinuria is characterized by increased tissue, plasma and urinary concentrations of homocysteine, and by decreased concentrations of cystathionine and cysteine [52,53]. Its clinical features include liver steatosis, connective tissue disorder, thromboembolism and various degrees of central nervous system involvement [53]. In our CBS-1–GFP localization study, CBS-1-knockdown worms exhibited abnormal morphology of several tissues that express the *cbs-1* gene. Using light microscopy, we observed a reduced birefringent signal from pigment gut granules, which are considered to be lysosome-related organelles [54]. Although the function and composition of these granules has not been fully elucidated, the abnormal pattern of gut granules in CBS-1-knockdown animals may in part correspond to the liver steatosis observed in murine and human CBS deficiency. Furthermore, the observed abnormal pharyngeal morphology of CBS-1-deficient worms may possibly correspond to some of the neurological sequelae of human CBS deficiency. It appears that the CBS-knockdown nematodes produced in the present study may in part recapitulate some of the features of human homocystinuria due to CBS deficiency.

In the CBS-1-deficient nematodes produced in the present study, the amounts of CBS-1 antigen and enzyme activity decreased to ~10–15% those of WT worms. This degree of enzyme deficiency resulted in an approximately 10-fold increase in homocysteine concentrations in worm extracts compared with the WT strain, demonstrating an essential role for CBS-1 in maintaining homocysteine homoeostasis in *C. elegans*. Because exposure of worms to homocysteine in medium [55] leads to a similar developmental delay as the *cbs-1* RNAi in the present study, it is conceivable that high tissue levels of homocysteine may be directly responsible for the developmental delay phenotype that we observed. Surprisingly, and in contrast with human patients with CBS deficiency [53], cystathionine levels in CBS-1-deficient worms were only slightly increased. However, a similar elevation in plasma cystathionine was reported for one murine model of CBS deficiency [56]. We hypothesize that elevated cystathionine in CBS-1-deficient worms may be caused by three possible mechanisms: (i) elevated homocysteine may inactivate CGL, as proposed previously for a murine model of CBS deficiency [56]; (ii) elevated homocysteine may lead to formation of cystathionine via condensation of cysteine and homocysteine by CGL [57]; and (iii) cystathionine may be synthesized by a hypothetical cystathionine γ-synthase in the reverse trans-sulfuration pathway using cysteine and *O*-succinylhomoserine. Moreover, the CBS-1-deficient worms observed in the present study did not exhibit cysteine depletion, which is a common feature of human CBS deficiency. We hypothesize that cysteine levels in deficient worms are maintained by sufficient cysteine intake from *E. coli* or by biosynthesis of cysteine via a hypothetical sulfur assimilation pathway because *C. elegans* possesses several bacterial and plant cysteine synthase homologues (see above, [58]).

AUTHOR CONTRIBUTION

Roman Vozdek designed and performed most of the experiments and wrote the first draft of the paper; Aleš Hnízda purified and further characterized recombinant CBS-1; Jakub Krijt measured aminothiols and cystathionine by HPLC and LC–MS/MS in the appropriate studies; Marta Kostrouchová co-ordinated the experiments with *C. elegans*; and Viktor Kožich co-ordinated the whole project. All authors have extensively revised various versions of the paper and approved its final version prior to submission.

ACKNOWLEDGEMENTS

We thank Dr A. Fire for vector pPD95.75, and Eva Zouharová, Mrs Kateřina Raková, Hana Prouzová, Jitka Honzíková and Professor Milan Kodíček for technical assistance and advice.

FUNDING

This work was supported by a Wellcome Trust International Senior Research Fellowship in Biomedical Science in Central Europe [number 070255/Z/03/Z], the Grant Agency of the Charles University in Prague [grant numbers 21709 and SVV262502], the Ministry of Education of the Czech Republic [grant number MSM0021620806] and the Czech Science Foundation [grant number 304/08/0970].

REFERENCES

1 Finkelstein, J. D. (1998) The metabolism of homocysteine: pathways and regulation. Eur. J. Pediatr. **157**, S40–S44

1a Taoka, S., Ohja, S., Shan, X., Kruger, W. D. and Banerjee, R. (1998) Evidence for heme-mediated redox regulation of human cystathionine beta-synthase activity. J. Biol. Chem. **273**, 25179–25184

2 Banerjee, R. and Zou, C. G. (2005) Redox regulation and reaction mechanism of human cystathionine-beta-synthase: a PLP-dependent hemesensor protein. Arch. Biochem. Biophys. **433**, 144–156

3 Cherney, M. M., Pazicni, S., Frank, N., Marvin, K. A., Kraus, J. P. and Burstyn, J. N. (2007) Ferrous human cystathionine beta-synthase loses activity during enzyme assay due to a ligand switch process. Biochemistry **46**, 13199–13210
4 Smith, A. T., Majtan, T., Freeman, K. M., Su, Y., Kraus, J. P. and Burstyn, J. N. (2011) Cobalt cystathionine beta-synthase: a cobalt-substituted heme protein with a unique thiolate ligation motif. Inorg. Chem. **50**, 4417–4427
5 Mehta, P. K. and Christen, P. (2000) The molecular evolution of pyridoxal-5′-phosphate-dependent enzymes. Adv. Enzymol. Relat. Areas Mol. Biol. **74**, 129–184
6 Kery, V., Poneleit, L. and Kraus, J. P. (1998) Trypsin cleavage of human cystathionine beta-synthase into an evolutionarily conserved active core: structural and functional consequences. Arch. Biochem. Biophys. **355**, 222–232
7 Taoka, S., Widjaja, L. and Banerjee, R. (1999) Assignment of enzymatic functions to specific regions of the PLP-dependent heme protein cystathionine beta-synthase. Biochemistry **38**, 13155–13161
8 Skovby, F., Kraus, J. P. and Rosenberg, L. E. (1984) Biosynthesis and proteolytic activation of cystathionine beta-synthase in rat liver. J. Biol. Chem. **259**, 588–593
9 Zou, C. G. and Banerjee, R. (2003) Tumor necrosis factor-α-induced targeted proteolysis of cystathionine beta-synthase modulates redox homeostasis. J. Biol. Chem. **278**, 16802–16808
10 Jhee, K. H., McPhie, P. and Miles, E. W. (2000) Yeast cystathionine beta-synthase is a pyridoxal phosphate enzyme but, unlike the human enzyme, is not a heme protein. J. Biol. Chem. **275**, 11541–11544
11 Nozaki, T., Shigeta, Y., Saito-Nakano, Y., Imada, M. and Kruger, W. D. (2001) Characterization of transsulfuration and cysteine biosynthetic pathways in the protozoan hemoflagellate, *Trypanosoma cruzi*. Isolation and molecular characterization of cystathionine beta-synthase and serine acetyltransferase from Trypanosoma. J. Biol. Chem. **276**, 6516–6523
12 Koutmos, M., Kabil, O., Smith, J. L. and Banerjee, R. (2010) Structural basis for substrate activation and regulation by cystathionine beta-synthase (CBS) domains in cystathionine beta-synthase. Proc. Natl. Acad. Sci. U.S.A. **107**, 20958–20963
13 Jhee, K. H., McPhie, P. and Miles, E. W. (2000) Domain architecture of the heme-independent yeast cystathionine beta-synthase provides insights into mechanisms of catalysis and regulation. Biochemistry **39**, 10548–10556
14 Brenner, S. (1974) The genetics of *Caenorhabditis elegans*. Genetics **77**, 71–94
15 Meier, M., Janosik, M., Kery, V., Kraus, J. P. and Burkhard, P. (2001) Structure of human cystathionine beta-synthase: a unique pyridoxal 5′-phosphate-dependent heme protein. EMBO J. **20**, 3910–3916
16 Wiederstein, M. and Sippl, M. J. (2007) ProSA-web: interactive web service for the recognition of errors in three-dimensional structures of proteins. Nucleic Acids Res. **35**, W407–W410
17 Guex, N. and Peitsch, M. C. (1997) SWISS-MODEL and the Swiss-PdbViewer: an environment for comparative protein modeling. Electrophoresis **18**, 2714–2723
18 Neron, B., Menager, H., Maufrais, C., Joly, N., Maupetit, J., Letort, S., Carrere, S., Tuffery, P. and Letondal, C. (2009) Mobyle: a new full web bioinformatics framework. Bioinformatics **25**, 3005–3011
19 Chenna, R., Sugawara, H., Koike, T., Lopez, R., Gibson, T. J., Higgins, D. G. and Thompson, J. D. (2003) Multiple sequence alignment with the Clustal series of programs. Nucleic Acids Res. **31**, 3497–3500
20 Guindon, S. and Gascuel, O. (2003) A simple, fast, and accurate algorithm to estimate large phylogenies by maximum likelihood. Syst. Biol. **52**, 696–704
21 Huson, D. H., Richter, D. C., Rausch, C., Dezulian, T., Franz, M. and Rupp, R. (2007) Dendroscope: an interactive viewer for large phylogenetic trees. BMC Bioinf. **8**, 460
22 Boulin, T., Etchberger, J. F. and Hobert, O. (2006) Reporter gene fusions. In WormBook (The *C. elegans* Research Community, ed.), pp. 1–23, doi/10.1895/wormbook.1.106.1
23 Frank, N., Kent, J. O., Meier, M. and Kraus, J. P. (2008) Purification and characterization of the wild type and truncated human cystathionine beta-synthase enzymes expressed in *E. coli*. Arch. Biochem. Biophys. **470**, 64–72
24 Janosik, M., Meier, M., Kery, V., Oliveriusova, J., Burkhard, P. and Kraus, J. P. (2001) Crystallization and preliminary X-ray diffraction analysis of the active core of human recombinant cystathionine beta-synthase: an enzyme involved in vascular disease. Acta Crystallogr. Sect. D Biol. Crystallogr. **57**, 289–291
25 Laemmli, U. K. (1970) Cleavage of structural proteins during the assembly of the head of bacteriophage T4. Nature **227**, 680–685
26 Wittig, I., Braun, H. P. and Schagger, H. (2006) Blue native PAGE. Nat. Protoc. **1**, 418–428
27 Hnizda, A., Spiwok, V., Jurga, V., Kozich, V., Kodicek, M. and Kraus, J. P. (2010) Cross-talk between the catalytic core and the regulatory domain in cystathionine beta-synthase: study by differential covalent labeling and computational modeling. Biochemistry **49**, 10526–10534
28 Maclean, K. N., Sikora, J., Kozich, V., Jiang, H., Greiner, L. S., Kraus, E., Krijt, J., Crnic, L. S., Allen, R. H., Stabler, S. P. et al. (2010) Cystathionine beta-synthase null homocystinuric mice fail to exhibit altered hemostasis or lowering of plasma homocysteine in response to betaine treatment. Mol. Genet. Metab. **101**, 163–171
29 Krijt, J., Kopecka, J., Hnizda, A., Moat, S., Kluijtmans, L. A., Mayne, P. and Kozich, V. (2011) Determination of cystathionine beta-synthase activity in human plasma by LC–MS/MS: potential use in diagnosis of CBS deficiency. J. Inherited Metab. Dis. **34**, 49–55
30 Mello, C. and Fire, A. (1995) DNA transformation. Methods Cell Biol. **48**, 451–482
31 Janosik, M., Oliveriusova, J., Janosikova, B., Sokolova, J., Kraus, E., Kraus, J. P. and Kozich, V. (2001) Impaired heme binding and aggregation of mutant cystathionine beta-synthase subunits in homocystinuria. Am. J. Hum. Genet. **68**, 1506–1513
32 Schrimpf, S. P., Weiss, M., Reiter, L., Ahrens, C. H., Jovanovic, M., Malmstrom, J., Brunner, E., Mohanty, S., Lercher, M. J., Hunziker, P. E. et al. (2009) Comparative functional analysis of the *Caenorhabditis elegans* and *Drosophila melanogaster* proteomes. PLoS Biol. **7**, e48
33 McKay, S. J., Johnsen, R., Khattra, J., Asano, J., Baillie, D. L., Chan, S., Dube, N., Fang, L., Goszczynski, B., Ha, E. et al. (2003) Gene expression profiling of cells, tissues, and developmental stages of the nematode *C. elegans*. Cold Spring Harb. Symp. Quant. Biol. **68**, 159–169
34 Rege, V. D., Kredich, N. M., Tai, C. H., Karsten, W. E., Schnackerz, K. D. and Cook, P. F. (1996) A change in the internal aldimine lysine (K42) in *O*-acetylserine sulfhydrylase to alanine indicates its importance in transimination and as a general base catalyst. Biochemistry **35**, 13485–13493
35 Belew, M. S., Quazi, F. I., Willmore, W. G. and Aitken, S. M. (2009) Kinetic characterization of recombinant human cystathionine beta-synthase purified from *E. coli*. Protein Expression Purif. **64**, 139–145
36 Aringer, M., Cheng, A., Nelson, J. W., Chen, M., Sudarshan, C., Zhou, Y. J. and O'Shea, J. J. (1999) Janus kinases and their role in growth and disease. Life Sci. **64**, 2173–2186
37 Kabil, O., Zhou, Y. and Banerjee, R. (2006) Human cystathionine beta-synthase is a target for sumoylation. Biochemistry **45**, 13528–13536
38 Boutell, J. M., Wood, J. D., Harper, P. S. and Jones, A. L. (1998) Huntingtin interacts with cystathionine beta-synthase. Hum. Mol. Genet. **7**, 371–378
39 Zahler, A. M. (2005) Alternative splicing in *C. elegans*. In WormBook (The *C. elegans* Research Community, ed.), pp. 1–13, doi/10.1895/wormbook.1.31.1
40 McGhee, J. D. (2007) The *C. elegans* intestine. In WormBook (The *C. elegans* Research Community, ed.). pp. 1–36, doi/10.1895/wormbook.1.133.1
41 Finkelstein, J. D. (2000) Pathways and regulation of homocysteine metabolism in mammals. Semin. Thromb. Hemostasis **26**, 219–225
42 Page, A. P. and Johnstone, I. L. (2007) The cuticle. In WormBook (The *C. elegans* Research Community, ed.). pp. 1–15, doi/10.1895/wormbook.1.138.1
43 Kimura, H. (2011) Hydrogen sulfide: its production, release and functions. Amino Acids **41**, 113–121
44 Budde, M. W. and Roth, M. B. (2010) Hydrogen sulfide increases hypoxia-inducible factor-1 activity independently of von Hippel–Lindau tumor suppressor-1 in *C. elegans*. Mol. Biol. Cell **21**, 212–217
45 Abe, K. and Kimura, H. (1996) The possible role of hydrogen sulfide as an endogenous neuromodulator. J. Neurosci. **16**, 1066–1071
46 Kuwabara, P. E. and O'Neil, N. (2001) The use of functional genomics in *C. elegans* for studying human development and disease. J. Inherited Metab. Dis. **24**, 127–138
47 Chandler, R. J., Aswani, V., Tsai, M. S., Falk, M., Wehrli, N., Stabler, S., Allen, R., Sedensky, M., Kazazian, H. H. and Venditti, C. P. (2006) Propionyl-CoA and adenosylcobalamin metabolism in *Caenorhabditis elegans*: evidence for a role of methylmalonyl-CoA epimerase in intermediary metabolism. Mol. Genet. Metab. **89**, 64–73
48 Calvo, A. C., Pey, A. L., Ying, M., Loer, C. M. and Martinez, A. (2008) Anabolic function of phenylalanine hydroxylase in *Caenorhabditis elegans*. FASEB J. **22**, 3046–3058
49 Fisher, A. L., Page, K. E., Lithgow, G. J. and Nash, L. (2008) The *Caenorhabditis elegans K10C2.4* gene encodes a member of the fumarylacetoacetate hydrolase family: a *Caenorhabditis elegans* model of type I tyrosinemia. J. Biol. Chem. **283**, 9127–9135
50 Link, E. M., Hardiman, G., Sluder, A. E., Johnson, C. D. and Liu, L. X. (2000) Therapeutic target discovery using *Caenorhabditis elegans*. Pharmacogenomics **1**, 203–217
51 Kaletta, T. and Hengartner, M. O. (2006) Finding function in novel targets: *C. elegans* as a model organism. Nat. Rev. **5**, 387–398
52 Kraus, J. P., Janosik, M., Kozich, V., Mandell, R., Shih, V., Sperandeo, M. P., Sebastio, G., de Franchis, R., Andria, G., Kluijtmans, L. A. et al. (1999) Cystathionine beta-synthase mutations in homocystinuria. Hum. Mutat. **13**, 362–375
53 Kraus, J. P. and Kozich, V. (2001) Cystathionine-β-synthase and its deficiency. In Homocysteine in Health and Disease (Carmel, R. and Jacobsen, D. W., eds), pp. 223–243, Cambridge University Press, Cambridge
54 Hermann, G. J., Schroeder, L. K., Hieb, C. A., Kershner, A. M., Rabbitts, B. M., Fonarev, P., Grant, B. D. and Priess, J. R. (2005) Genetic analysis of lysosomal trafficking in *Caenorhabditis elegans*. Mol. Biol. Cell **16**, 3273–3288
55 Khare, S., Gomez, T., Linster, C. L. and Clarke, S. G. (2009) Defective responses to oxidative stress in protein l-isoaspartyl repair-deficient *Caenorhabditis elegans*. Mech. Ageing Dev. **130**, 670–680

56 Maclean, K. N., Sikora, J., Kozich, V., Jiang, H., Greiner, L. S., Kraus, E., Krijt, J., Overdier, K. H., Collard, R., Brodsky, G. L. et al. (2010) A novel transgenic mouse model of CBS-deficient homocystinuria does not incur hepatic steatosis or fibrosis and exhibits a hypercoagulative phenotype that is ameliorated by betaine treatment. Mol. Genet. Metab. **101**, 153–162

57 Singh, S., Padovani, D., Leslie, R. A., Chiku, T. and Banerjee, R. (2009) Relative contributions of cystathionine beta-synthase and gamma-cystathionase to H2S biogenesis via alternative trans-sulfuration reactions. J. Biol. Chem. **284**, 22457–22466

58 Budde, M. W. and Roth, M. B. (2011) The response of *Caenorhabditis elegans* to hydrogen sulfide and hydrogen cyanide. Genetics **189**, 521–532

Received 15 August 2011/13 December 2011; accepted 13 January 2012
Published as BJ Immediate Publication 13 January 2012, doi:10.1042/BJ20111478

Biochem. J. (2012) **443**, 535–547 (Printed in Great Britain) doi:10.1042/BJ20111478

online data

SUPPLEMENTARY ONLINE DATA

Novel structural arrangement of nematode cystathionine β-synthases: characterization of *Caenorhabditis elegans* CBS-1

Roman VOZDEK, Aleš HNÍZDA, Jakub KRIJT, Marta KOSTROUCHOVÁ and Viktor KOŽICH[1]

Institute of Inherited Metabolic Disorders, Charles University in Prague, First Faculty of Medicine and General University Hospital, Ke Karlovu 2, 128 08, Praha 2, Czech Republic

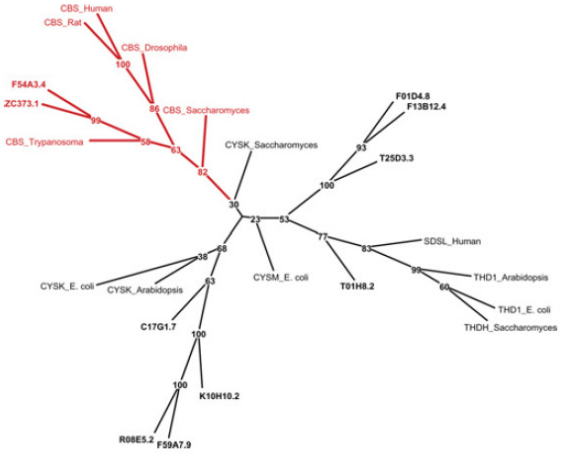

Figure S1 Unrooted tree of fold-type II PLP-dependent proteins with ten CBS homologues in *C. elegans*

For phylogenetic analysis, we used various proteins from the family of fold-type II PLP-dependent proteins: CBS_Human (UniProt entry P35520), CBS_Rat (UniProt entry P32232), CBS_Drosophila (UniProt entry Q9VRD9), CBS_Trypanosoma (UniProt entry Q9BH24), CBS_Saccharomyces (UniProt entry P32582), CYSK_Saccharomyces (UniProt entry P53206) CYSK_Arabidopsis (UniProt entry P47998), CYSM_E. coli (UniProt entry P16703), CYSK_E. coli (UniProt entry P0ABK5), SDSL_Human (UniProt entry Q96GA7), THDH_Saccharomyces (UniProt entry P00927), THD1_E. coli (UniProt entry P04968) and THD1_Arabidopsis (UniProt entry Q9ZSS6). Ten CBS homologues (bold font) are presented in Table S1. The numbers at the internal nodes represent bootstrapped values (maximum 100). The upper left-hand edge in red denotes the CBS branch. The tree topology demonstrates three separated groups for ten CBS homologues in *C. elegans*: ZC373.1 and F54A3.4 belong to the CBS branch, C17G1.7, R08E5.2, F59A7.9 and K10H10.2 belong to the cysteine synthase A branch, and the remaining homologues belong to other fold-type II PLP-dependent protein families. CYSK, cysteine synthase A; CYSM, cysteine synthase B; SDSL/THD, serine/threonine dehydratase family.

[1] To whom correspondence should be addressed (email Viktor.Kozich@LF1.cuni.cz).

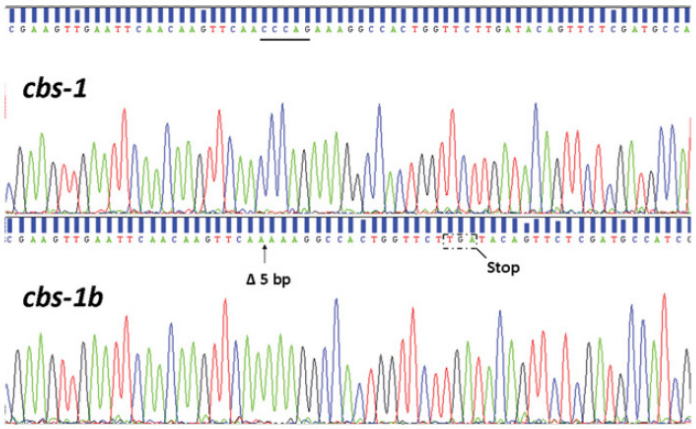

Figure S2 Sequences of *cbs*-1 RT–PCR products covering the exon 6 and 7 junction

Two splice variants of *cbs-1* were found. The novel *cbs-1b* transcript leads to a frameshift and a subsequent stop codon that allows for translation of the separated N-terminal module of CBS-1.

Figure S3 Unrooted tree of separated conserved regions from CBS-1 with various fold-type II PLP-dependent proteins

This tree is taken from the same phylogenetic study as that presented in Figure S1, with the exception that the two conserved regions from CBS orthologues ZC373.1 and F54A3.4, were separated for the analysis. The topology of the unrooted tree demonstrates that the N-terminal regions of CBS homologues (ZC373.1_N and F54A3.4_N) do not belong to any branch containing the analysed proteins, whereas the C-terminal regions (ZC373.1_C and F54A3.4_C) belong to the CBS branch. Alignment of the N-terminal module of *C. elegans* CBS-1 (the first of the two tandemly arranged regions, i.e. residues 14–322) revealed 29 % identity and an e-value of 5e – 27 compared with the catalytic core of human CBS (residues 72–397), whereas the C-terminal module (i.e. residues 374–702 of CBS-1) revealed much higher 54 % identity and an e-value of 2e – 99.

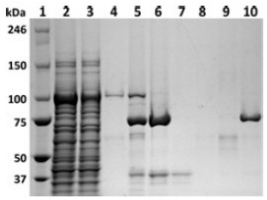

Figure S4 CBS-1 purification procedure

The purification procedure for CBS-1 is illustrated by a 3–8 % SDS-containing polyacrylamide gel stained with Coomassie EZ Blue. Lane 1, molecular mass markers; lane 2, bacterial extract after centrifugation; lane 3, flow-through fraction from glutathione–Sepharose column; 4, wash fraction of glutathione–Sepharose column; lane 5, fusion protein that was cleaved by PreScission protease; lane 6, elution of CBS-1 after on-column cleavage; lane 7, flow-through fraction from the Ni-Sepharose column; lanes 8 and 9, wash fractions of the Ni-Sepharose column by IMAC buffer containing 20 mM and 50 mM imidazole respectively; lane 10, elution of CBS-1 by IMAC buffer containing 75 mM imidazole. The molecular mass is given in kDa on the left-hand side.

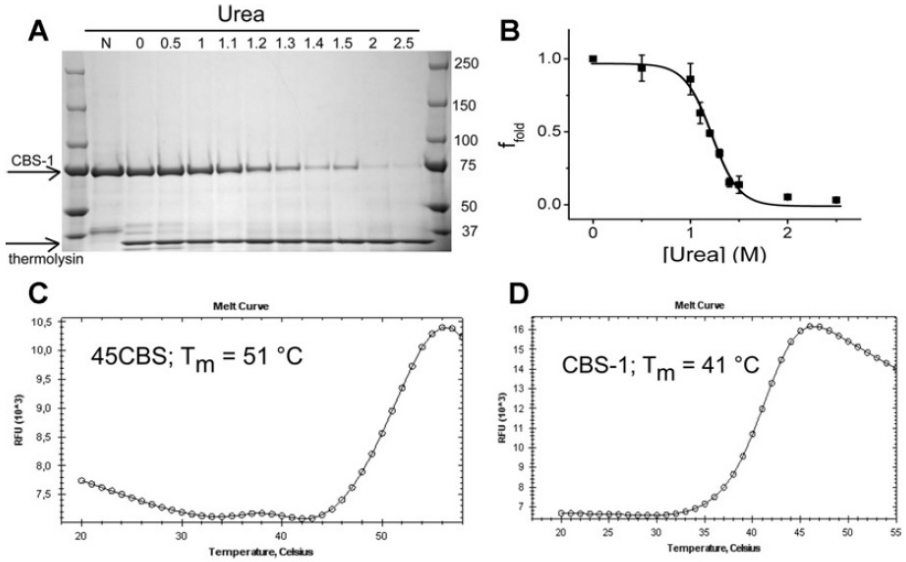

Figure S5 Pulse proteolysis and fluorescence-based thermal-shift assay

Pulse proteolysis in a urea gradient employing thermolysin and thermal-based assays were used to determine possible differences in enzyme stability between CBS-1 and human 45CBS. (**A**) Representative SDS/PAGE gel. The molar concentration of urea for the proteolytic pulse is indicated at the top of each lane and the molecular mass is given in kDa on the right-hand side. (**B**) F-fold values, which represent the fraction of the remaining intact protein after the proteolytic pulse, are plotted against the urea concentration. Results are means ± S.D. from three measurements and the curves were fitted by non-linear regression. (**C** and **D**) Melting curves in fluorescence-based thermal shift assays reveal melting points (T_m) of 51 °C and 41 °C for human 45CBS and CBS-1 respectively.

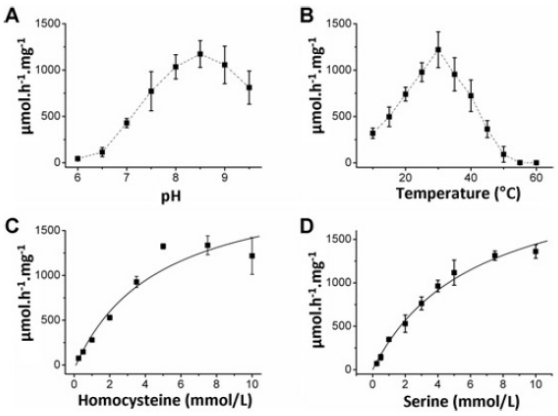

Figure S6 Enzymatic properties of recombinant CBS-1

(**A** and **B**) The dependence of CBS activity on pH and temperature respectively. The kinetic properties of CBS-1 for 1–10 mM homocysteine in a mixture with 10 mM serine are shown in (**C**), whereas the properties for 1–10 mM serine in a mixture with 10 mM homocysteine are shown in (**D**). Results are means ± S.D. from four measurements.

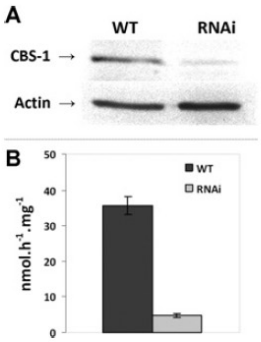

Figure S7 Western blot analysis and CBS assay of crude nematode extracts

(**A**) Western blot analysis showing a decreased level of CBS-1 protein in nematodes after RNAi. Actin was used as a reference protein. (**B**) CBS activity is significantly decreased in nematodes after RNAi. Results are means ± S.D. from two independent measurements.

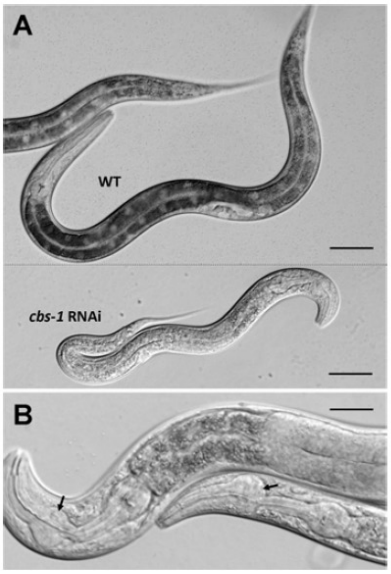

Figure S8 Inhibition of *cbs-1* by RNAi

Images show the body morphologies of worms in Nomarski optics. (**A**) L4 stage of *cbs-1* RNAi and WT worms. The affected worms exhibit decreased body mass and partial lack of pigment granules in the intestine. Scale bars, 50 μm. (**B**) Higher magnification of an affected adult nematode pharynx. The pharynx shows abnormal morphogenesis of the metacorpus with a balloon-like appearance indicated by an arrow. Scale bar, 25 μm.

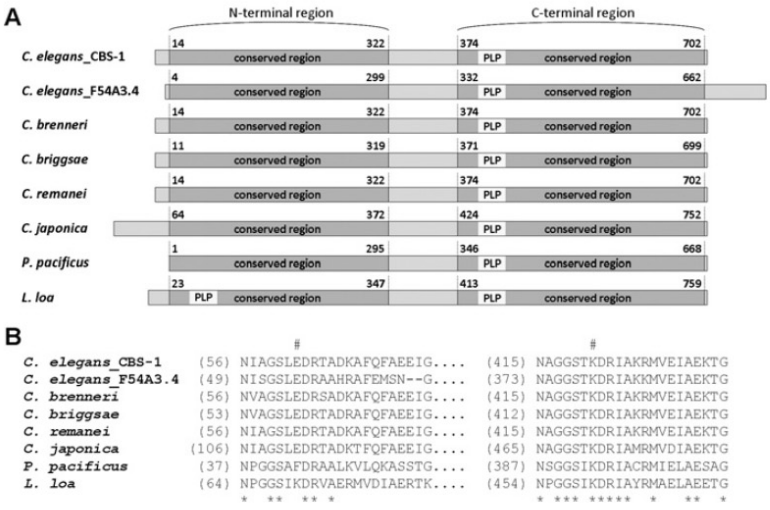

Figure S9 Domain architecture of CBS enzymes in nematodes

(**A**) Domain organization of nematode CBSs. The predicted amino acid sequences of hypothetical nematode CBSs were aligned with the sequence of *C. elegans* CBS-1, and the domain architecture of the proteins was inferred from the degree of homology. Primary structures are aligned by the PLP-binding lysine residue. The numbers indicate the first and the last amino acid residues in each of the conserved domains. Hypothetical proteins included in the alignment are as follows: *C. elegans*_ZC373.1 (CBS-1, UniProt entry Q23264); *C. brenneri* (WormBase accession number CN28558); *C. briggsae* (UniProt entry A8WRM3); *C. remanei* (UniProt entry E3MMP8); *C. japonica* (WormBase accession number JA15528); *C. elegans* F54A3.4 (UniProt entry Q9N4K2); *Pristionchus pacificus* (WormBase accession number PP12619); *Loa loa* (UniProt entry E1FTU4). (**B**) Amino acid alignment of hypothetical PLP-binding site of separated N-terminal and C-terminal conserved regions of various nematode CBSs. #, site of the putative PLP-binding lysine residues. ∗, conserved residue. Only *Loa loa* CBS contains a lysine residue in both PLP-binding sites.

Table S1 Primer sequences

Primers A–F were used to generate the cbs-1–GFP vector (see the GFP reporter assay section of the main text), G and H were used for the amplification of the shortened *cbs-1* coding sequence (see the RNA-mediated interference section of the main text), I–K (sense) and L–O (antisense) were used in combination to amplify the *F54A3.4* open reading frame (see the PCR amplification and sequencing section of the main text), P–U (sense) and V (antisense) were used for the amplification of the *cbs-1* coding sequence with specific cloning overhangs (see the Bacterial expression and purification section of the main text). Primers W–Z were used for site-directed mutagenesis.

Primer	Sequence
A, cbs-1_S	5′-ACTTGACGGAAAAGCTGGCAGA-3′
B, cbs-1_A	5′-AGTCGACCTGCAGGCATGCAAGCTGGCGTCTAGGAAATGACGCTCATTC-3′
C, GFP_S	5′-AGCTTGCATGCCTGCAGGTCG-3′
D, GFP_AS	5′-AAGGGCCCGTACGGCCGACTA-3′
E, cbs-1_S*	5′-GAGGAATGACCATCAATTTGA-3′
F, GFP_AS*	5′-GGAAACAGTTATGTTTGGTATA-3′
G , RNAi_S	5′-GACCCTCATGGATCTATTC-3′
H, RNAi_AS	5′-GACGCTCATTCATCCAATC-3′
I, F54_S1	5′-GACGAATTCATGTGCCTGCCTACCATTAAA-3′
J, F54_S2	5′-GGCAAGACGCCACTGGTGAA-3′
K, F54_S3	5′-AGAAGACAACAGTGGTCGGAGTGAGAT-3′
L, F54_AS1	5′-CAAGCGGCCGCTCAATAGAAAATGCGAGAGCG-3′
M, F54_AS2	5′-AGAGATTCCGGTGATGGTAC-3′
N, F54_AS3	5′-CAACGGCACCAGTTGAGTTG-3′
O, F54_AS4	5′-TGGCTTCCAGCACTGCCGC-3′
P, CBS-1_S	5′-CCTGGGATCCATGATCCAAAACGAAGTTTCC-3′
Q, Δ1–372	5′-CCTGGGATCCCCAGAAAGGCCACTGGTTCTT-3′
R, Δ1–322	5′-CCTGGGATCCGTGGTGACCAGAAAAGATGGA-3′
S, Δ1–299	5′-CCTGGGATCCATGGAATTAGAAATTATC-3′
T, b/375	5′-CCTGGGATCCATGGACCACAACCAAACAGCA-3′
U, b/360	5′-CCTGGGATCCATGATCCAACTAAACTTGCTG-3′
V, CBS-1_AS	5′-GCCGCTCGAGTTAGTGGTGATGGTGATGATGGGCGTCTAGGAAATGACG-3′
W, K421A_S	5′-TGAACGCTGGGGGATCAACAGCGGATCGTATTG-3′
X, K421A_AS	5′-CATTCTTTTGGCAATACGATCCGCTGTTGATCCC-3′
Y, E62K_S	5′-TCAATATTGCGGGATCTTTGAAAGACCGTACCG-3′
Z, E62K_AS	5′-GCTTTGTCAGCGGTACGGTCTTTCAAAGATCCC-3′

Table S2 Homologous level of CBS-related proteins in *C. elegans*

C. elegans genes are arranged by the level of homology with human CBS. The query sequences are as follows: human CBS (UniProt entry P35520), trypanosomal CBS (UniProt entry Q9BH24) and bacterial CS (UniProt entry P0ABK5). In each group of comparisons, the left-hand column lists the e-value, and the middle and right-hand column list identical and positive matches in percentages respectively. The Table shows three groups of ten CBS homologues in *C. elegans*: ZC373.1 and F54A3.4 have the highest homology with CBS; C17G1.7, R08E5.2, F59A7.9 and K10H10.2 are the most homologous with cysteine synthase; and the remaining homologues belong to other unspecified fold-type II PLP-dependent protein families. AA, number of amino acids in the hypothetical protein; COG, clusters of orthologous groups of proteins; CBS RE, CBS and related enzymes; NA, not assigned; SR, serine racemase.

			Homology [e-value, identities (%), positives (%)]								
Name	AA	COG	human CBS (551 AA)			*T. cruzi* CBS (384 AA)			*E. coli* CS (323 AA)		
ZC373.1	704	CBS RE	8e – 94	54	71	2e – 84	50	66	2e – 30	30	44
F54A3.4	755	CBS RE	4e – 92	54	68	8e – 87	51	66	6e – 27	32	46
C17G1.7	341	NA	2e – 54	44	60	4e – 41	36	51	5e – 62	44	59
K10H10.2	337	CBS RE	4e – 54	38	60	9e – 43	35	56	1e – 60	45	58
R08E5.2	337	CBS RE	1e – 51	37	58	2e – 42	36	55	1e – 57	41	57
F59A7.9	337	CBS RE	7e – 42	36	58	3e – 38	35	54	4e – 56	41	55
F01D4.8	430	CBS RE	2e – 10	24	43	0.012	25	49	0.043	26	46
T25D3.3	427	CBS RE	2e – 09	25	40	0.003	24	44	0.001	28	56
T01H8.2	317	SR	1e – 07	28	43	2e – 04	23	39	0.015	29	48
F13B12.4	435	CBS mRE	5e – 07	21	40	0.037 23	47	5e-04	26	45	

Received 15 August 2011/13 December 2011; accepted 13 January 2012
Published as BJ Immediate Publication 13 January 2012, doi:10.1042/BJ20111478

Publication 6.1.2

Biochemical Properties of Nematode *O*-acetylserine(thiol)lyase Paralogs Imply Their Distinct Roles in Hydrogen Sulfide Homeostasis

Biochimica et Biophysica Acta - Proteins and Proteomics (In Press)

Biochimica et Biophysica Acta xxx (2013) xxx–xxx

Contents lists available at ScienceDirect

Biochimica et Biophysica Acta

journal homepage: www.elsevier.com/locate/bbapap

Biochemical properties of nematode *O*-acetylserine(thiol)lyase paralogs imply their distinct roles in hydrogen sulfide homeostasis

Roman Vozdek [a], Aleš Hnízda [a,1], Jakub Krijt [a], Leona Šerá [b], Viktor Kožich [a,*]

[a] Institute of Inherited Metabolic Disorders, First Faculty of Medicine, Charles University in Prague and General University Hospital in Prague, Ke Karlovu 2, Prague 2, 128 08, Czech Republic
[b] Department of Biochemistry and Microbiology, Institute of Chemical Technology in Prague, Technická 5, Prague 6, 166 28, Czech Republic

ARTICLE INFO

Article history:
Received 14 August 2013
Received in revised form 23 September 2013
Accepted 25 September 2013
Available online xxxx

Keywords:
Hydrogen sulfide
Cyanide
S-Sulfocysteine
O-Acetylserine sulfhydrylase
Cysteine synthase
C. elegans

ABSTRACT

O-Acetylserine(thiol)lyases (OAS-TLs) play a pivotal role in a sulfur assimilation pathway incorporating sulfide into amino acids in microorganisms and plants, however, these enzymes have not been found in the animal kingdom. Interestingly, the genome of the roundworm *Caenorhabditis elegans* contains three expressed genes predicted to encode OAS-TL orthologs (*cysl-1–cysl-3*), and a related pseudogene (*cysl-4*); these genes play different roles in resistance to hypoxia, hydrogen sulfide and cyanide. To get an insight into the underlying molecular mechanisms we purified the three recombinant worm OAS-TL proteins, and we determined their enzymatic activities, substrate binding affinities, quaternary structures and the conformations of their active site shapes. We show that the nematode OAS-TL orthologs can bind *O*-acetylserine and catalyze the canonical reaction although this ligand may more likely serve as a competitive inhibitor to natural substrates instead of being a substrate for sulfur assimilation. In addition, we propose that *S*-sulfocysteine may be a novel endogenous substrate for these proteins. However, we observed that the three OAS-TL proteins are conformationally different and exhibit distinct substrate specificity. Based on the available evidences we propose the following model: CYSL-1 interacts with EGL-9 and activates HIF-1 that upregulates expression of genes detoxifying sulfide and cyanide, the CYSL-2 acts as a cyanoalanine synthase in the cyanide detoxification pathway and simultaneously produces hydrogen sulfide, while the role of CYSL-3 remains unclear although it exhibits sulfhydrylase activity *in vitro*. All these data indicate that *C. elegans* OAS-TL paralogs have distinct cellular functions and may play different roles in maintaining hydrogen sulfide homeostasis.

1. Introduction

Cysteine is an essential molecule in living organisms due to its highly reactive reduced thiol group. For example, as a component of glutathione, it maintains the redox environment in cells and is a precursor of several key metabolites, including taurine and hydrogen sulfide. *De novo* biosynthesis of cysteine occurs exclusively in bacteria and plants through a sulfur assimilation pathway in which the final key step is mediated by *O*-acetylserine(thiol)lyase (OAS-TL, EC: 2.5.1.47, formerly EC: 4.2.99.8) [1–3]. OAS-TLs are homodimeric enzymes belonging to the β-family of pyridoxal 5-phosphate (PLP)-dependent proteins [4]. The proteins in this family are structurally similar to one another and catalyze various β-replacement reactions [5]. The catalytic activity of an OAS-TL enzyme was first reported by Kredich, et al., who showed that OAS-TL produces cysteine in the sulfur assimilation pathway *via* *O*-acetylserine sulfhydrylase activity [1]. *O*-Acetylserine was shown to be the primary substrate whose binding to the covalently attached PLP cofactor in the active site causes a conformational change in the protein (from an open to a closed state) that allows only small molecules to diffuse out of and into the active site [6]. The external aldimine of α-aminoacrylate – the common intermediate of β-replacement reactions – is formed by releasing acetate, and then sulfide, the secondary substrate, can diffuse into the active site to form cysteine. This reaction opens the enzyme's active site for the next catalytic cycle. However, proteins from the OAS-TL family are known for their ability to utilize various substrates and thus play different biological roles, such as cyanoalanine synthase (CAS) in the cyanide detoxification pathway [7], *S*-sulfocysteine synthase appearing to be important for chloroplast function [8], or cysteine desulfhydrase catabolizing cysteine in the cells [9]. Because OAS-TL enzymes are not present in mammals, they have become targets for the design of antibiotic and antiparasitic drugs. Nevertheless, it has been postulated that OAS-TLs might be ancestral to animal cystathionine beta-synthases (CBSs), which maintain homocysteine homeostasis in the transsulfuration pathway: CBS catalyzes the

Abbreviations: OAS-TL, *O*-acetylserine(thiol)lyase; OASS, *O*-acetylserine sulfhydrylase; CAS, cyanoalanine synthase; CBS, cystathionine beta-synthase; SAT, serine *O*-acetyltransferase; SQRD-1, sulfide-quinon oxidoreductase; PLP, pyridoxal 5-phosphate; MD, molecular dynamics

* Corresponding author at: Charles University in Prague, First Faculty of Medicine, Institute of Inherited Metabolic Disorders, Ke Karlovu 2, 128 08, Praha 2, Czech Republic. Tel.: +420 224967679; fax: +420 224967168.
E-mail address: viktor.kozich@lf1.cuni.cz (V. Kožich).
[1] Present address: Institute of Organic Chemistry and Biochemistry, Academy of Sciences of the Czech Republic, Flemingovo nam. 2, Prague 6, Czech Republic.

1570-9639/$ – see front matter © 2013 Published by Elsevier B.V.
http://dx.doi.org/10.1016/j.bbapap.2013.09.020

β-replacement of serine or cysteine to form cystathionine, utilizing homocysteine as a secondary substrate [10]. CBSs also exhibit *O*-acetylserine sulfhydrylase activity *in vitro* at a low reaction rate, but this function does not appear to be biologically relevant.

Surprisingly, recent studies have shown that the genome of the roundworm *Caenorhabditis elegans* contains several genes predicted to encode proteins from the OAS-TL family, specifically *cysl-1*, *cysl-2*, *cysl-3* and *cysl-4* [11–14]. It was shown that mutations in two of these genes, *cysl-1* and *cysl-2*, decrease *C. elegans* resistance to various stress and toxic conditions, such as hypoxia, hydrogen sulfide or cyanide [11,13]. CYSL-1 physically interacts with EGL-9, a proline dioxygenase that inhibits the transcriptional activity of hypoxia-inducible factor 1 (HIF-1) [13,15]. This interaction, which resembles an ancient interaction between plant OAS-TL and serine *O*-acetyltransferase (SAT), leads to the sequestration of EGL-9 and regulates animal behavior in response to hypoxia; it has been proposed that CYSL-1 serves as a sensor of hypoxic conditions through the hydrogen sulfide that accumulates during hypoxia [13]. CYSL-1 also exhibits *O*-acetylserine sulfhydrylase activity *in vitro*; however, the *in vivo* relevance of such activity is not clear. Whether remaining OAS-TL paralogs have overlapping or distinct functions *in vivo* has not been determined yet, as well as the conservation of these proteins in other nematodes.

In this work, we determined the catalytic activities of the purified recombinant *C. elegans* OAS-TL orthologs that are expressed at the mRNA level, assayed their abilities to interact with the C-terminal peptide of EGL-9, and, through *in silico* analysis, analyzed their phylogeny and the structural features that distinguish them from one other. We show that the biochemical properties of the nematode OAS-TL proteins are highly diverse, suggesting distinct and specific roles for these proteins in *C. elegans* that might be conserved in evolutionarily distant animals.

2. Materials and methods

2.1. Phylogenetic analysis

Multiple amino acid alignment was performed using the Clustal W2 online program [16], and the results were visually inspected. For the phylogenetic analysis, the alignment was bootstrapped 100 times with the Mobyle online software tool using the PHYML 3.0 program [17]. Subsequently, the bootstrapped trees were analyzed using the PHYML 3.67 CONSENSE program. The Dendroscope program was employed to visualize the final tree shape [18]. The proteins included in the multiple alignments and phylogenetic analyses are listed in Supplemental Table 1.

2.2. Protein purification

The *C. elegans* database WormBase contains sequence information on one expressed transcript variant for *cysl-1* and *cysl-2* genes, and on three variants for *cysl-3*. PCR primers were designed to amplify transcripts C17G1.7 (*cysl-1*), K10H10.2 (*cysl-2*) and R08E5.2a (*cysl-3*) which encode full-length nematode proteins. We used a *C. elegans* cDNA library (Invitrogen, Carlsbad, CA, USA) as the template and the following specific cloning primers:

cysl-1 5′-cggtcgactaatggctgatcgcaactctattg-3′ and 5′-atgcggcggctcactcc ataatatcatagttgtgaa-3′
cysl-2 5′-cctgggatccatgtcccgcgaacttatggtc-3′ and 5′-gccgctcgagttaaattc ctaggtattcttt-3′,
cysl-3 5′-cctgggatccatgtctcgtgaattgatggtt-3′ and 5′-gccgctcgagttagagac ccaaatatttctt-3′.

Since there are no reports on posttranslational modifications of other eukaryotic OAS-TL proteins we expressed the nematode orthologs in a bacterial expression system. All recombinant *C. elegans* OAS-TL orthologs were purified using the same procedure. The pGEX-6p-1 vector, carrying the GST coding sequence, was employed for cloning and expressed in *Escherichia coli* BL21 (New England Biolabs, Ipswich, MA, USA—cell C3037H) at 18 °C for 24 h after induction using 100 μM IPTG. The cells were harvested and homogenized *via* sonication (ice/water slush) in lysis buffer containing 150 mM Tris pH 7.5, 1 mM PLP, DTT, 50 mM NaCl, 1 mg/ml lysosyme and a 1× protease inhibitor cocktail (Sigma-Aldrich Corp., St. Louis, MO, USA). After centrifugation (20,000 ×*g* for 1 h), the soluble fraction was loaded onto a GST resin column (GE healthcare, Freiburg, Germany—column 4B). The fusion protein was subsequently cleaved overnight with the PreScission protease (GE healthcare, Freiburg, Germany). The elution fraction containing purified recombinant protein was collected and analyzed for the presence of PLP through UV–visible analysis using a Shimadzu UV-2550 spectrophotometer. The yield was 1–3 mg/l of bacterial culture. The protein was stored at −80 °C in mg/ml concentration in 50 mM Tris–HCl pH 7.0, 150 mM NaCl, EDTA and DTT.

2.3. Enzyme assays

Enzyme assays were carried out at 25 °C in the presence of 150 mM Tris–HCl buffer, pH 7.5, 1 mM PLP, 1 mM DTT, 1 mg/ml BSA, 0–10 mM substrate and 1 μg/ml of purified enzyme (except for reactions with cysteine and *S*-sulfocysteine, which were carried out at pH 8.5, and reactions with *S*-sulfocysteine, which were performed without DTT (DTT reduces *S*-sulfocysteine to cysteine—data not shown). Since we observed decreased enzyme activities at higher than 10 mM concentrations of *O*-acetylserine (data not shown), specific catalytic activities of studied enzymes were measured with 10 mM substrate concentrations. The measurements of specific activity were repeated three times and the results are shown as means with standard deviations. Also, the kinetic analysis of *O*-acetylserine was performed in the presence of 10 mM sulfide, while the kinetics of *S*-sulfocysteine and cysteine were tested in the presence of 10 mM cyanide for all proteins. The kinetics of sulfide were measured in the presence of 10 mM *O*-acetylserine for all proteins, and the kinetics of cyanide were determined in the presence of 10 mM *O*-acetylserine, for CYSL-1 and CYSL-3, or 10 mM cysteine, for CYSL-2. Kinetic measurements were repeated two times. The kinetic constants were evaluated using the Michaelis–Menten and allosteric sigmoidal equations with GraphPad Prism 2 software. The results are shown as means with standard errors. Activities associated with sulfide were detected based on measurement of the cysteine product, as described previously, through HPLC analysis [19]. Activities associated with cyanide and thiosulfate were determined by measuring β-cyanoalanine and *S*-sulfocysteine (products) *via* LC–MS/MS analysis using the EZ:faast kit for amino acid analysis (Phenomenex, Torrance, CA, USA). For the detection of β-cyanoalanine, isotopically labeled L-asparagine-d_8 was employed as an internal standard. The LC–MS/MS analysis was performed in the selected reaction monitoring mode to monitor the transitions (precursor → product) m/z 243.3 → 157.2 and 246.3 → 160.2 for β-cyanoalanine and L-asparagine-d_8, respectively. CBS activities were determined based on measurement of the cystathionine product, as described previously, using LC–MS/MS analysis [20].

2.4. Spectroscopic analysis

The absorption spectra of the purified proteins were recorded with a Shimadzu UV-2550 UV–visible spectrophotometer at 25 °C. The substrate binding affinity was analyzed using 0.5 mg/ml purified enzyme in the presence of 0–20 mM substrate in 50 mM Tris, pH 8.5, because we observed significantly decreased formation of α-aminoacrylate from *S*-sulfocysteine and cysteine at pH 7.5. However, analysis with *O*-acetylserine was carried out in 50 mM Tris, pH 7.5, to prevent *O*-acetylserine conversion to *N*-acetylserine occurring at higher pH. Substrate affinity constants were evaluated *via* one-site-specific binding with the Hill slope using GraphPad Prism 2 software. The fluorescence

Please cite this article as: R. Vozdek, et al., Biochemical properties of nematode O-acetylserine(thiol)lyase paralogs imply their distinct roles in hydrogen sulfide homeostasis, Biochim. Biophys. Acta (2013), http://dx.doi.org/10.1016/j.bbapap.2013.09.020

spectra of the purified proteins (1 μM protein in 50 mM Tris, pH 7.5) were recorded with a PerkinElmer LS55 fluorescence spectrometer. The excitation wavelength was 412 nm (PLP absorption in the form of internal aldimine), and the emission signal (slit width 10 nm) was scanned from 440 to 575 nm, both with and without 10 μM peptides (10 amino acids from the EGL-9 C-terminus—PPSTNPEYYI).

2.5. Quaternary structure analysis

Size exclusion chromatography was performed with the HPLC Shimadzu LC-10A system. We used a Bio-Sil HPLC column (Bio-Rad Lab. 125-0060) equilibrated with 50 mM Tris–HCl, pH 8.0, 1 mM DTT and 100 mM NaCl. We employed the aldolase (158 kDa), ovalbumin (44 kDa), myoglobin (17 kDa), BSA (66 kDa) and 45CBS (90 kDa) proteins as standards. The flow rate was 1 ml/min at 25 °C. Native PAGE was performed using a precast 3–8% gradient polyacrylamide gel (Invitrogen, Carlsbad, CA, USA) in the presence of Laemmli buffer without SDS [21]. Blue-native PAGE was performed as described previously [22] using a precast 3–8% gradient polyacrylamide gel (Invitrogen, Carlsbad, CA, USA) with a high molecular weight calibration kit (GE healthcare, Freiburg, Germany). We loaded 5 μg of purified proteins for both electrophoretic procedures.

2.6. Homology modeling

The structures of the nematode OAS-TL proteins were modeled based on alignments generated through several approaches. First, their amino acid sequences, together with sequences of OAS-TL (PDB ID: 1D6S, 1FCJ, 1O58, 1VE1, 1Y7L, 1Z7W, 2EGU, 2JC3, 2PQM, 2Q3D, 2V03 and 3RR2) and CBS (PDB ID: 1JBQ and 3PC3) were aligned using MUSCLE 3.8.31 [23]. The alignment and structures were then employed to build models. These models showed the best ProSA Z scores. However, visual inspection revealed possible conformational changes in the template structures. Some template structures presented closed conformations of the active sites, whereas others displayed rather open conformations. Therefore, we built a third series of models based on *Drosophila* CBS (3PC3), with corresponding sub-alignments of the Muscle multiple sequence alignment. These structures showed worse ProSA Z scores, but they allowed better comparison of the structures, without induced fit. Using the experimental structure of *Drosophila* cystathionine beta-synthase (3PC2) as a template [24], the structures of the nematode proteins were predicted to be dimers *via* homology modeling with the Modeller package [25].

2.7. Molecular electrostatic visualization

The electrostatic potential was calculated based on the final structures obtained from simulations performed in APBS [26] by solving the Poisson–Boltzmann equation. The relative dielectric constants of the solute and water were set to 2 and 78, respectively, the water radius was set to 1.4 Å and the concentration of NaCl was 0.15 M (Na^+ radius set to 2 Å, Cl^- radius set to 1.8 Å). A smoothed molecular surface was employed as the water–protein boundary. The electrostatic potential was projected onto the molecular surface in PyMOL. Values of pI were calculated using PROPKA 3.1 [27].

2.8. Simulations of molecular dynamics

All simulations were performed in Gromacs 4.5.5 [28]. An Amber 99SB force field [29] was used for proteins, a Generalized Amber Force Field [30] for ligands and the TIP3P model for water. RESP charges calculated at the HF/6-31G* level of theory were used for ligands. Enzymes were simulated with non-covalently bound PLP-aminoacrylate in the active site of one subunit and with PLP covalently bound to a lysine residue in the second subunit. The conjugation of lysine with PLP was performed manually using parameters of similar bonds. Solvent was added to each structure in an octahedral box whose size was chosen so that the shortest distance between the solute and box wall was at least 1.5 nm. Na^+ and Cl^- ions were added to neutralize the box and obtain physiological concentrations.

Initially, only the solvent part of the system was equilibrated by applying very strong position restraints on protein atoms (10,000 kJ/mol/nm^2). The steepest descent algorithm was run in 11,000 steps, followed by 12,000 steps for the conjugate gradient. Subsequently, 2 ps MD simulations of the solvent at a constant volume were performed using a periodic boundary condition, PME treatment of electrostatics, a 1 nm cut-off for non-bonding interactions, the velocity rescaling (v-rescale) temperature coupling method (5 K, 0.8 ps), LINCS constraints on bonds involving hydrogens and a 2 fs step. Thereafter, three cycles of minimization, with gradual diminution of position restraints were performed (1000, 100, 0 kJ/mol/nm^2), with each cycle consisting of the portions corresponding to the steepest descent (5000, 1000 and 3000 steps) and conjugate gradient (10,000, 3000 and 6000 steps). These steps were followed by 2 ps low temperature MD simulations run under the same conditions as in the previous solvent equilibration steps.

The last part of the equilibration process involved heating the system in three steps (up to 150 K, 250 K and 298.15 K), interspersed with constant pressure simulations to ensure equilibration of pressure. Each heating step took 50 ps, and gradual heating was carried out using a temperature annealing algorithm. In contrast to previous steps, the LINCS algorithm was not employed, so the timestep was reduced to 1 fs. Moreover, the time constant for temperature coupling was changed to 1.0 ps. Between these steps, the pressure was equilibrated through a 5 ps simulation using Berendsen barostat, with the pressure coupling time constant set to 1.2 ps. The final equilibration took 50 ps. This was followed by a 10 ns unrestrained MD simulation.

3. Results

3.1. Nematode orthologs constitute a phylogenetically novel class of OAS-TL proteins

Several previous studies have indicated that the roundworm *C. elegans* possesses genes encoding four OAS-TL proteins: CYSL-1, CYSL-2, CYSL-3 and CYSL-4 (Table 1) [11–14]. Using the UniProt database (UniProt release 2013_04), we searched for OAS-TL orthologs in other animals, but we only found these proteins in animals from the nematode phylum. Our phylogenetic analysis of animal CBS proteins and OAS-TL proteins in plants (*Arabidopsis thaliana* and *Glycine max*), bacteria (*E. coli* and *Salmonella typhimurium*), yeasts (*Saccharomyces cerevisiae*), protists (*Trypanosoma cruzi*) and nematodes (*C. elegans*) revealed that the nematode enzymes form a novel, distinct class of OAS-TL proteins (Fig. 1A). The nematode proteins are similar to each other but may be structurally different than other orthologs; nevertheless, the amino acid alignment revealed that the PLP and substrate binding motifs in the active site (see [31]) are conserved in all of the OAS-TL proteins across phyla (Fig. 1B). In contrast to plant OAS-TL enzymes all four nematode orthologs lack the initial signal sequence targeting them to distinct cell compartments such as mitochondria or chloroplasts (Supplemental Fig. 1); this suggests that the nematode OAS-TL enzymes are cytosolic proteins. The fact that the nematode paralogs form a distinct family of OAS-TL proteins lends support for the hypothesis that the *C. elegans* genes encoding the OAS-TL proteins evolved from a common ancestor that was duplicated in the *C. elegans* genome.

To examine the evolutionary development and diversification of these proteins in nematodes, we performed a phylogenetic analysis of OAS-TL protein sequences from the Uniprot database. We found different copy numbers of OAS-TL gene homologs in various worms. Nematodes from the *Caenorhabditis* family present three to four paralogs corresponding to the CYSL-1, CYSL-2 and CYSL-3/CYSL-4 proteins (Supplemental Fig. 2). As CYSL-3 and CYSL-4 are located on the same branch

Table 1
OAS-TL orthologs in *C. elegans*.

Name	ORF	Length (AA)	Calculated MW	Calculated pI (apoprotein)		Expression in tissues	REFs
				folded	unfolded		
CYSL-1	*C17G1.7*	341	35.9	6.60	6.40	Yes	[21]
CYSL-2	*K10H10.2*	337	36.1	8.44	8.09	Yes	[41]
CYSL-3	*R08E5.2*	337	36.2	7.00	7.00	Yes	[42]
CYSL-4	*F59A7.9*	337	36.3	–	–	Not detected	

ORF, open reading frame; AA, amino acids; MW, molecular weight; pI, isoelectric point; REFs, references for expression evidence.

of the phylogenetic tree and share the highest homology at the protein and DNA levels, the *cysl-4* gene likely originated by duplication of *cysl-3*. In contrast, we found that other fully sequenced nematodes possess varying numbers of OAS-TL orthologs: the nematode *Prostionchus pacificus* presents seven OAS-TL orthologs, which predominantly belong to a completely separate branch, while *Ascaris suum* displays only one OAS-TL protein belonging to the CYSL-1 family (Supplemental Fig. 2), and the *Loa loa* and *Brugia malayi* branches did not have any matches.

To verify whether the predicted *C. elegans* genes encoding OAS-TL proteins are transcribed as annotated, we performed PCR amplification

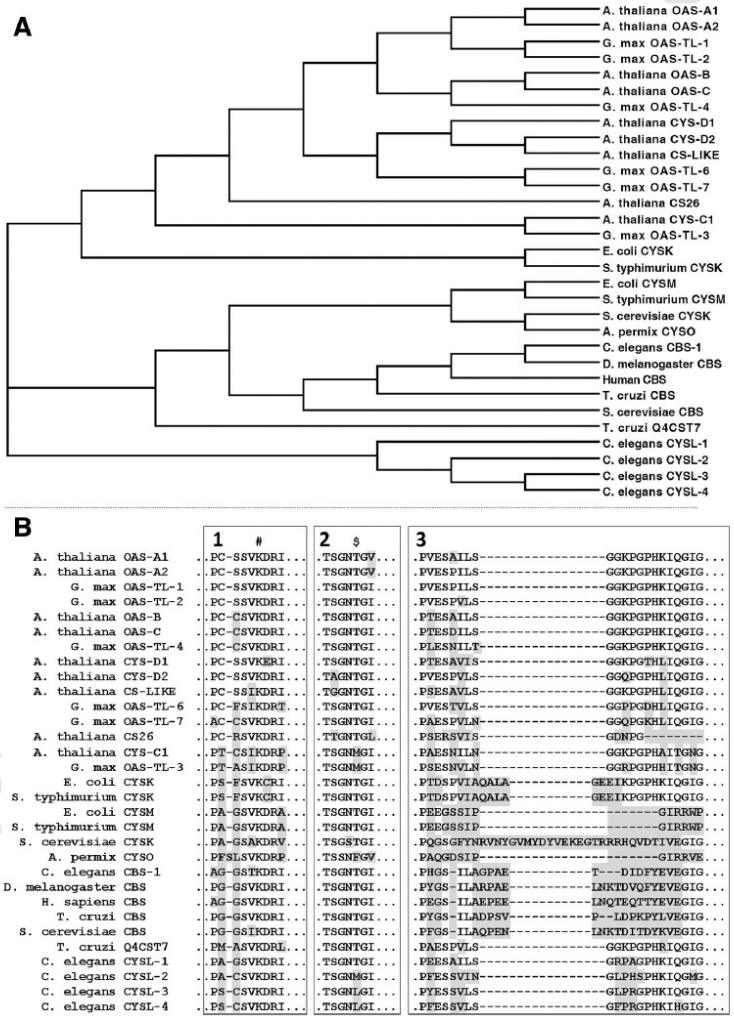

Fig. 1. Phylogenetic analysis of OAS-TL proteins across phyla. A) The rectangular cladogram of aligned amino acid sequences demonstrates that all *C. elegans* orthologs are assigned to a phylogenetically novel OAS-TL branch. B) Amino acid alignment of OAS-TL proteins across phyla. Panel 1 represents the PLP binding motif with a lysine residue that covalently binds the PLP cofactor, indicated by #. Panel 2 represents the substrate binding loop; amino acids indicated by $ are different among worm orthologs. Panel 3 represents the amino acid region that structurally distinguishes specific classes of OAS-TL enzymes; it demonstrates that sequences present in worm proteins resemble sequences in plant OAS-TL enzymes, as indicated by the specific sequence deletions/insertions found in archaea, bacterial CYSK, bacterial CYSM, yeast and animal CBS proteins.

Please cite this article as: R. Vozdek, et al., Biochemical properties of nematode O-acetylserine(thiol)lyase paralogs imply their distinct roles in hydrogen sulfide homeostasis, Biochim. Biophys. Acta (2013), http://dx.doi.org/10.1016/j.bbapap.2013.09.020

of cDNA to detect relevant mRNAs. For the *cysl-3* gene, we only searched for the transcript variant *R08E5.2a*, as this encodes the full-length protein. The *cysl-1*, *cysl-2* and *cysl-3* genes were successfully amplified from cDNA, and sequencing results confirmed their identities based on gene sequences deposited in the *C. elegans* database (www.wormbase.org). In addition, ESTs and peptides for these three genes were found in the online GenBank and Peptide Atlas databases. Moreover, these three genes have been shown to be expressed in previous studies [13,32,33]. This combined evidence shows that the *cysl-1*, *cysl-2* and *cysl-3* genes are expressed and translated into proteins. We were, however, unable to amplify *cysl-4* cDNA or transcripts, and no peptides corresponding to the *cysl-4* sequence were found in the databases, implying that *cysl-4* is a pseudogene in *C. elegans*. Therefore, the *cysl-4* gene was not further studied in this work.

3.2. Catalytic activities and substrate specificities

To examine the possible role of the OAS-TL proteins in *C. elegans* metabolism, we analyzed the catalytic activities of the three purified recombinant proteins. First, we checked for the canonical activity of OAS-TL proteins, *i.e.*, the condensation of *O*-acetylserine with potential secondary substrates, such as sulfide, cyanide and thiosulfate. We determined that all three studied proteins, CYSL-1, CYSL-2 and CYSL-3, can convert *O*-acetylserine and utilize sulfide or cyanide as a secondary substrate to yield cysteine or β-cyanoalanine, respectively, though the CYSL-1 and CYSL-3 proteins exhibited decreased activity with cyanide compared to their activity with sulfide at 10 mM substrate concentrations (Fig. 2). We did not detect *S*-sulfocysteine synthase activity when utilizing thiosulfate as the secondary substrate after *O*-acetylserine. However, it should be noted that the detection limit for *S*-sulfocysteine did not allow us to measure low activities (≤μmol/h/mg, Supplemental Table 2), and thus, we cannot exclude the possibility that the worm orthologs might display residual activities with this secondary substrate.

Second, we examined whether the nematode orthologs can utilize potential primary substrates (other than *O*-acetylserine) that have other functional groups at the β-carbon of the amino acid, such as *S*-sulfocysteine, cysteine, β-cyanoalanine, serine and *O*-phosphoserine. Using a 10 mM substrate concentration, we determined that CYSL-2 can utilize cysteine as the primary substrate to produce β-cyanoalanine (~6900 μmol/h/mg, Fig. 2), which is a canonical activity of cyanoalanine synthase in plants. However, CYSL-1 and CYSL-3 exhibited only residual cyanoalanine synthase activities (18–98 μmol/h/mg, Supplemental Table 2). Moreover, we found that CYSL-2 and CYSL-3 can also utilize *S*-sulfocysteine to produce β-cyanoalanine; to the best of our knowledge, this activity has not been previously reported for any of the OAS-TL proteins across the examined phyla. Based on these observations, we propose that *S*-sulfocysteine might also be used as a substrate to produce cysteine, though unfortunately, we were unable to examine this activity because sulfide acts as a strong reductant of *S*-sulfocysteine, forming cysteine in the absence of an enzyme (Fig. 2). Activities utilizing β-cyanoalanine, serine and *O*-phosphoserine were not detected for any of the studied proteins (Supplemental Table 2). We also demonstrated that none of the OAS-TL proteins in *C. elegans* show cystathionine synthesizing activity when utilizing homocysteine as the secondary substrate, which is in agreement with the notion that CBS-1 is the only enzyme in *C. elegans* with CBS activity [14].

To explore the primary substrate specificity of each *C. elegans* OAS-TL protein, we analyzed their substrate binding affinities *via* UV–visible absorption spectrophotometry. The shift of the PLP absorption peak from 412 nm, corresponding to the internal Schiff base (with PLP bound internally to lysine) to 470 nm, corresponding to α-aminoacrylate, indicates the formation of the common reaction intermediate created by the enzymatic cleavage of the group at the β-carbon of the amino acid. *O*-acetylserine shifted the PLP absorption of all three proteins (Fig. 3A). *S*-sulfocysteine clearly shifted the PLP absorption of CYSL-2 and CYSL-3 to 470 nm, whereas cysteine shifted the PLP absorption maximum only when incubated with the CYSL-2 paralog. In agreement with the determined catalytic activities noted above, neither serine nor *O*-phosphoserine increased PLP absorption at 470 nm (Fig. 3A). Taken together, these data demonstrate that all three CYSL proteins found in *C. elegans* can use *O*-acetylserine to form α-aminoacrylate, while only CYSL-2 can also use cysteine, and CYSL-2 and CYSL-3 can both also utilize *S*-sulfocysteine. On the other hand, neither *O*-phosphoserine nor serine acts as a substrate for any of the OAS-TL enzymes in *C. elegans*.

3.3. Kinetic behavior and substrate binding affinities

To explore the kinetic behavior of nematode OAS-TL enzymes, we determined the kinetic parameters of the reactions. The results were analyzed through two different data fittings, using the Michaelis–Menten and Hill equations. Kinetic analysis revealed that all of the studied proteins exhibit similar Michaelis constants (K_M) for *O*-acetylserine (1–3 mM). However, CYSL-2 displayed a slightly higher affinity for cysteine and *S*-sulfocysteine. On the other hand, CYSL-3 exhibited a lower affinity for *S*-sulfocysteine, presenting a sigmoidal curve (Hill constant of approximately 6.5) and an apparent Michaelis constant of approximately 6.5 mM (Table 2). Next, we determined the Michaelis constants for two secondary substrates—sulfide and cyanide. All three proteins exhibited Michaelis–Menten kinetics for both substrates: the Michaelis constants were similar for sulfide (1.4–1.7 mM), while the Michaelis constants for cyanide differed considerably. While CYSL-1 exhibited the lowest affinity (K_M of 9.3 mM), CYSL-2 exhibited the highest affinity for cyanide, as shown by its Michaelis constant of 0.8 mM (Table 2). These data as well as turnover number and catalytic efficiency

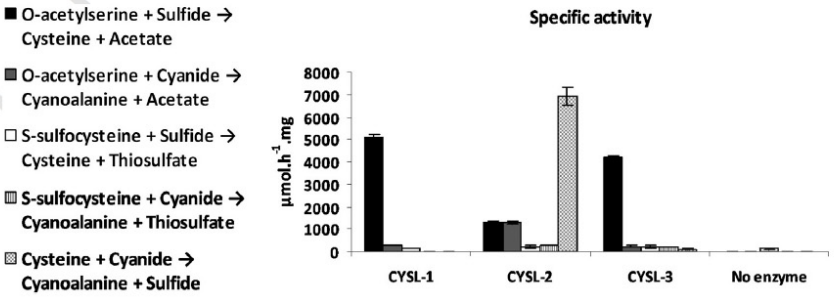

Fig. 2. Specific activities of nematode OAS-TL proteins. Activities were measured in the presence of 10 mM substrate. Reactions with *O*-acetylserine were performed in 150 mM Tris, pH 7.5, preventing the non-enzymatic conversion of *O*-acetylserine to *N*-acetylserine. Reactions with *S*-sulfocysteine and cysteine were performed in 150 mM Tris pH 8.5. All proteins exhibited the ability to convert *O*-acetylserine. CYSL-2 exhibited high cyanoalanine synthase activity when cysteine and cyanide were used as substrates. The activities associated with *S*-sulfocysteine were significantly lower; moreover, the conversion of *S*-sulfocysteine into cysteine was not measurable due to the strong reduction of *S*-sulfocysteine by sulfide (see panel of non-enzymatic conversions).

Please cite this article as: R. Vozdek, et al., Biochemical properties of nematode O-acetylserine(thiol)lyase paralogs imply their distinct roles in hydrogen sulfide homeostasis, Biochim. Biophys. Acta (2013), http://dx.doi.org/10.1016/j.bbapap.2013.09.020

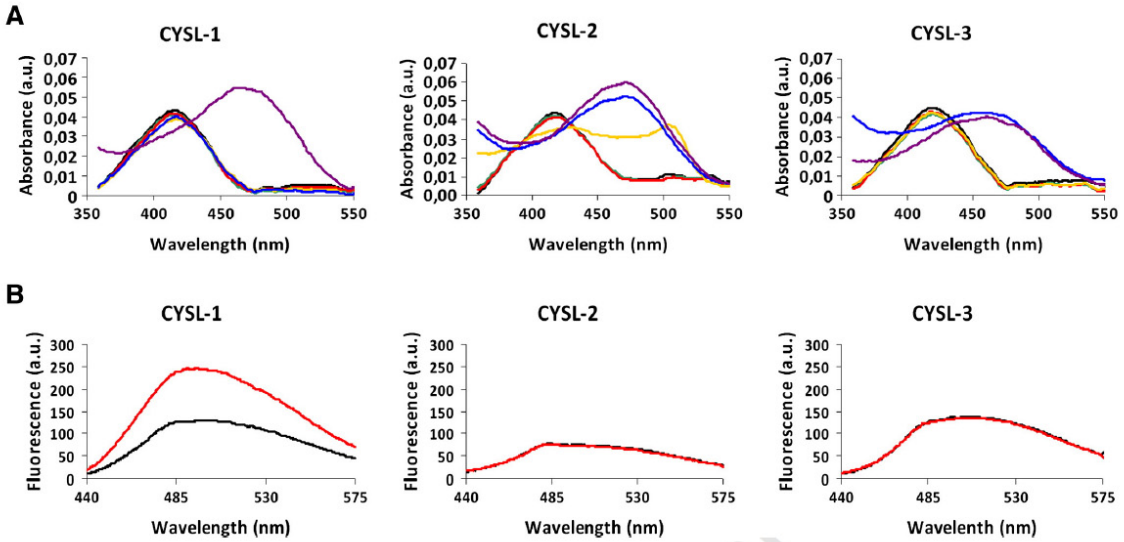

Fig. 3. Spectroscopic analysis of substrate and peptide affinity. A) Substrate binding affinity. Black line—protein without substrate; red—with 10 mM serine; green—with 10 mM *O*-phosphoserine; violet—with 1 mM *O*-acetylserine; blue—with 10 mM *S*-sulfocysteine; yellow—with 10 mM cysteine. The formation of α-aminoacrylate is represented by the maximum absorbance shift from 412 nm to 470 nm; all proteins can bind *O*-acetylserine, while CYSL-2 and CYSL-3 can also utilize *S*-sulfocysteine, and cysteine can be utilized only by CYSL-2. B) Interaction of *C. elegans* OAS-TL proteins with the EGL-9 C-terminus. Black and red lines indicate PLP fluorescence excited at 412 nm in the absence and presence of the peptide (10 amino acids of the C-terminus of the EGL-9 protein), respectively. Fluorescence analysis clearly shows that only CYSL-1 can interact with the EGL-9 C-terminus, as demonstrated by enhanced fluorescence upon the addition of the peptide.

(Table 2), suggest that CYSL-2 may, in fact, function in *C. elegans* to detoxify cyanide by forming *β*-cyanoalanine from cysteine and cyanide.

Next, in order to compare the binding affinities and kinetic constants for primary substrates, we determined the apparent dissociation binding constants (K_D) utilizing detection of the formed α-aminoacrylate by UV–visible spectrometry. We found that the binding affinity constant of *O*-acetylserine was in the micromolar concentration range for all three proteins (45–813 μM), which was much lower than their Michaelis constants (1–3 mM). On the other hand, the K_D of CYSL-2 for cysteine as well as those of CYSL-2 and CYSL-3 for *S*-sulfocysteine were similar to their respective Michaelis constants (Tables 2 and 3, Supplemental Figs. 3 and 4). A sigmoidal trend in both kinetics and substrate binding was apparent only for CYSL-3, suggesting allosteric regulation of CYSL-3 by both *O*-acetylserine and *S*-sulfocysteine. The Hill constants for CYSL-1 and CYSL-2 were close to one, suggesting that these two enzymes are not subject to allosteric modulation. In summary, these data show that nematode orthologs can bind *O*-acetylserine in low concentrations and convert it to stable α-aminoacrylate covalently

Table 2
Kinetic parameters of the enzymes.

		Primary substrate				*Secondary substrate*			
		K_m (mM)	*h*	k_{cat} (s^{-1})	k_{cat}/K_m ($mM^{-1}\,s^{-1}$)	K_m (mM)	*h*	k_{cat} (s^{-1})	k_{cat}/K_m ($mM^{-1}\,s^{-1}$)
OAS + S^{2-} → Cys		*O*-Acetylserine				Sulfide			
	CYSL-1	1.0 ± 0.1	1.6 ± 0.3	51.1 ± 1.0	51.1	1.7 ± 0.2	1.4 ± 0.2	51.1 ± 1.0	30.1
	CYSL-2	1.9 ± 0.3	2.1 ± 0.5	12.8 ± 0.5	6.7	1.4 ± 1.0	0.6 ± 0.2	12.8 ± 0.5	9.1
	CYSL-3	2.7 ± 0.3	1.7 ± 0.3	42.2 ± 0.8	15.6	1.6 ± 0.3	1.0 ± 0.2	42.2 ± 0.8	26.4
OAS + CN^- → CAla		*O*-Acetylserine				Cyanide			
	CYSL-1	1.0 ± 0.1	1.6 ± 0.3	2.5 ± 0.1	2.5	9.3 ± 1.9	1.4 ± 0.3	2.5 ± 0.1	0.3
	CYSL-2	1.9 ± 0.3	2.1 ± 0.5	13.0 ± 0.7	6.8	0.8 ± 0.1	1.1 ± 0.2	13.0 ± 0.7	16.2
	CYSL-3	2.7 ± 0.3	1.7 ± 0.3	2.3 ± 0.1	0.8	2.4 ± 0.4	1.5 ± 0.3	2.3 ± 0.1	1.0
SSC + S^{2-} → Cys		*S*-Sulfocysteine				Sulfide			
	CYSL-1	ND	ND	ND	ND	1.7 ± 0.2	1.4 ± 0.2	ND	ND
	CYSL-2	0.4 ± 0.2	1.0 ± 0.9	ND	ND	1.4 ± 1.0	0.6 ± 0.2	ND	ND
	CYSL-3	6.5 ± 0.3	6.5 ± 1.2	ND	ND	1.6 ± 0.3	1.0 ± 0.2	ND	ND
SSC + CN^- → CAla		*S*-Sulfocysteine				Cyanide			
	CYSL-1	ND	ND	ND	ND	9.3 ± 1.9	1.4 ± 0.3	ND	ND
	CYSL-2	0.4 ± 0.2	1.0 ± 0.9	2.8 ± 0.2	7.0	0.8 ± 0.1	1.1 ± 0.2	2.8 ± 0.2	3.5
	CYSL-3	6.5 ± 0.3	6.5 ± 1.2	1.8 ± 0.0	0.3	2.4 ± 0.4	1.5 ± 0.3	1.8 ± 0.0	0.7
CYS + CN^- → CAla		Cysteine				Cyanide			
	CYSL-1	ND	ND	0.2 ± 0.1	ND	9.3 ± 1.9	1.4 ± 0.3	0.2 ± 0.1	0.0
	CYSL-2	1.2 ± 0.2	1.0 ± 0.2	69.0 ± 4.2	57.5	0.8 ± 0.1	1.1 ± 0.2	69.0 ± 4.2	86.3
	CYSL-3	ND	ND	1.0 ± 0.1	ND	2.4 ± 0.4	1.5 ± 0.3	1.0 ± 0.1	0.4

K_m, Michaelis constant; *h*, Hill constant; k_{cat}, turnover number; k_{cat}/K_M, catalytic efficiency; ND, not determined.

Please cite this article as: R. Vozdek, et al., Biochemical properties of nematode O-acetylserine(thiol)lyase paralogs imply their distinct roles in hydrogen sulfide homeostasis, Biochim. Biophys. Acta (2013), http://dx.doi.org/10.1016/j.bbapap.2013.09.020

Table 3
Substrate binding affinity of the primary substrates.

	O-Acetylserine		Cysteine		*S*-sulfocysteine	
	K_D (mM)		K_D (mM)		K_D (mM)	
CYSL-1	0.045 ± 0.003	1.5 ± 0.1	ND	ND	ND	ND
CYSL-2	0.102 ± 0.019	1.1 ± 0.2	2.9 ± 1.0	0.7 ± 0.1	0.5 ± 0.06	1.9 ± 0.4
CYSL-3	0.813 ± 0.010	4.6 ± 0.2	ND	ND	2.3 ± 0.05	5.2 ± 0.5

K_D, apparent substrate dissociation constant; *h*, Hill constant; ND, not determined.

bound to PLP in the active site; this α-aminoacrylate moiety may thus competitively inhibit binding of other substrates and/or C-terminal peptides of potential interacting partners.

3.4. Specific interaction with the C-terminus of EGL-9

In the next step, we examined whether the CYSL-2 and CYSL-3 proteins could interact with the C-terminus of EGL-9, similar to the CYSL-1 paralog. This type of interaction with the C-terminus of EGL-9 has been previously demonstrated to be necessary for complex formation between CYSL-1 and EGL-9 [13]. Because this interaction is similar to the formation of the cysteine synthase complex involving serine acetyltransferase and *O*-acetylserine sulfhydrylase orthologs in plants, we performed a type of fluorimetric analysis that has previously been employed to study both EGL-9/CYSL-1 and SAT/OASS interactions [13,34]. Using a decapeptide from the EGL-9 C-terminus (PPSTNPEYYI), we observed that the addition of the peptide enhanced the fluorescence of the PLP cofactor only for CYSL-1; no interaction was detectable for CYSL-2 or CYSL-3 (Fig. 3B). These data suggest that only CYSL-1 has the ability to interact with the EGL-9 protein and transduce signals in the EGL-9/HIF-1 cascade.

3.5. Dimeric organization of nematode orthologs and their conformational changes during catalysis

To determine whether the three nematode OAS-TL proteins display the same or different quaternary structure as their orthologs in other species, we subjected the recombinant proteins to analysis *via* gel filtration and Blue-native electrophoresis. Through Blue-native electrophoresis, we observed migration of nematode OAS-TL proteins with a size of approximately 66 kDa (Fig. 4B), which corresponds to a dimeric quaternary structure because the subunit molecular weights are approximately 36 kDa. However, slight differences in migration were observed among paralogs, although all three paralogs show very similar monomeric molecular weights (Table 1) and are highly homologous to each other (see above). Moreover, gel filtration yielded slightly different retention times for these paralogs, and their calculated molecular weights (CYSL-1: 109 kDa, CYSL-2: 72 kDa and CYSL-3: 92 kDa) do not strongly contradict the hypothesis that these proteins are dimers (Fig. 4A). Based on these two analyses, we propose that all three *C. elegans* OAS-TL enzymes exist predominantly as dimers and have the same oligomeric status as their plant and bacterial orthologs.

It should be noted that significant differences in gel migration among paralogs were also observed through native PAGE (Fig. 4C), which simultaneously separates proteins based on their net charge and conformational state. Interestingly, the calculated pIs differed among the nematode OAS-TL proteins (Table 1), although the electrostatic potentials of the modeled protein surfaces (see below) were not significantly different (Fig. 5). Additionally, similar differences in migration were observed through Blue-native PAGE, which diminishes the electrostatic potential of protein surfaces. Therefore, these data suggest that the differences in gel migration observed through native PAGE are caused by subtle conformational changes that are independent of surface electrostatic charge among the nematode paralogs.

It has been reported that bacterial and plant OAS-TL proteins attain a different tertiary structure during catalysis [31,35–37] and upon interaction with SAT peptides [38,39]. Since the nematode paralogs exhibited different kinetic and substrate binding behaviors we hypothesized that also the nematode OAS-TL orthologs may adopt distinct conformations during catalysis. To test this hypothesis we performed simulations of the molecular dynamics (MD) of the modeled nematode OAS-TL proteins. We used a single structural template (fruit fly CBS) to model the nematode OAS-TL structures. All three models were dimeric; there were no significant differences in their electrostatic potentials; and all exhibited open conformation states for both subunits. The MDs were simulated with PLP-aminoacrylate non-covalently bound in the active

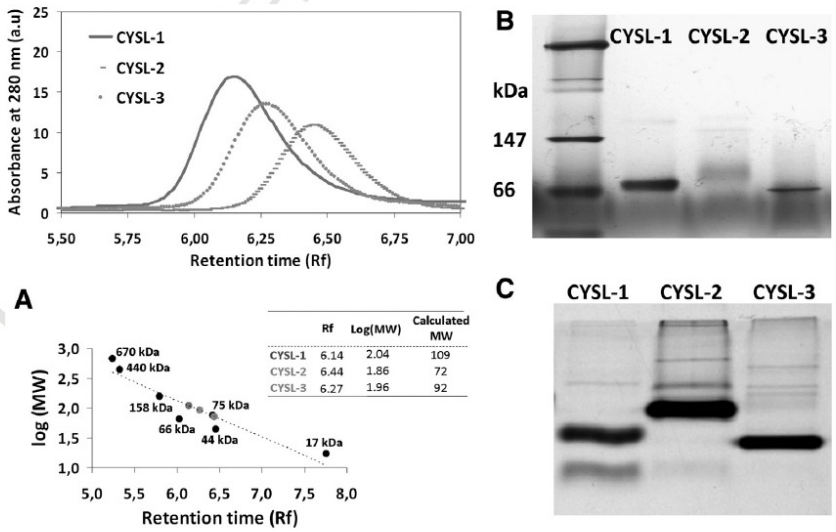

Fig. 4. Quaternary structure of *C. elegans* OAS-TL proteins. A) Size-exclusion chromatography showed that the OAS-TL paralogs in *C. elegans* are eluted with different retention times of between 6.14 and 6.44 min. The calculated molecular weight corresponds to a dimeric status; thyroglobulin (670 kDa), ferritin (440 kDa), aldolase (158 kDa), conalbumin (75 kDa), BSA (66 kDa), ovalbumin (44 kDa) and myoglobin (17 kDa) were used as standards. B) Blue-native PAGE shows the dimeric status of all of the analyzed proteins, as assessed by their migration similar to BSA (66 kDa) in the molecular weight standard. C) Native PAGE shows differences in the migration of these proteins, suggesting their distinct conformation.

Please cite this article as: R. Vozdek, et al., Biochemical properties of nematode O-acetylserine(thiol)lyase paralogs imply their distinct roles in hydrogen sulfide homeostasis, Biochim. Biophys. Acta (2013), http://dx.doi.org/10.1016/j.bbapap.2013.09.020

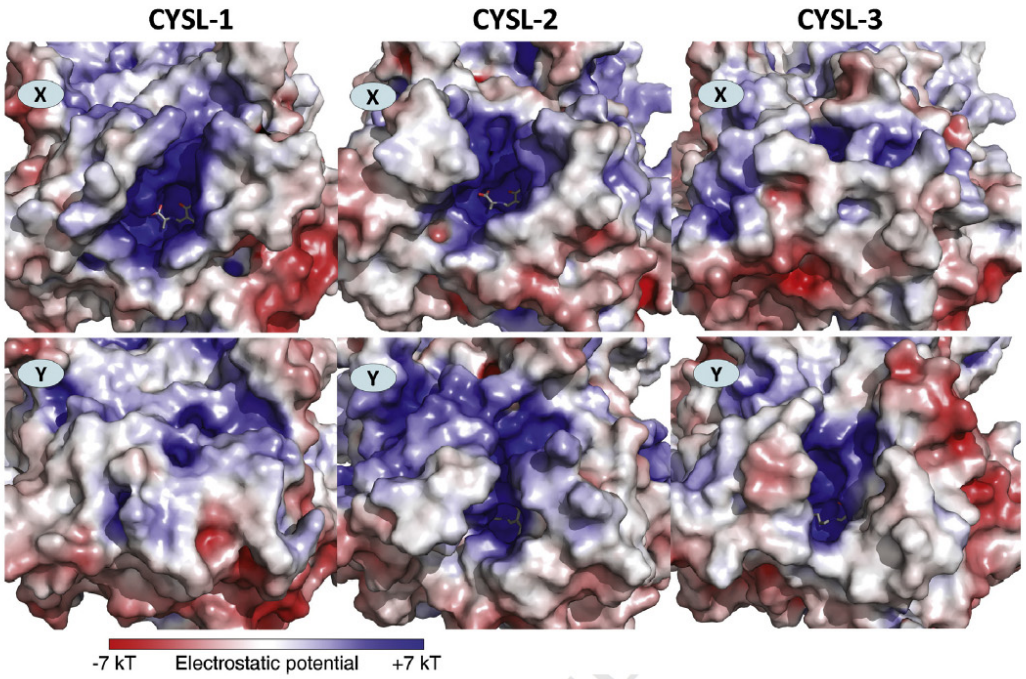

Fig. 5. Molecular dynamics simulation and surface electrostatics of CYSL-1, CYSL-2 and CYSL-3. The top row (subunit X) shows active sites that are occupied with non-covalently bound PLP-aminoacrylate, and the lower row (subunit Y) shows active sites containing PLP covalently bound to a lysine residue. The MD simulation demonstrates that only CYSL-1 closes the unoccupied subunit, while only CYSL-3 closes the occupied subunit.

site of one subunit (subunit X) and with PLP covalently bound in the active site of the second subunit (subunit Y). The resultant structures after a 10 ns MD simulation were compared in terms of the shapes of their active sites (Fig. 5, Supplemental Fig. 5). The active site containing non-covalently bound PLP-aminoacrylate was open and accessible to the secondary substrate in CYSL-1 and CYSL-2, whereas it was closed in CYSL-3. On the other hand, the active site of the second subunit, containing PLP covalently attached to a lysine residue, was generally less accessible; it was closed and inaccessible in CYSL-1 and open in CYSL-2 and CYSL-3. These data suggest that in contrast to CYSL-3, the active site of subunit X of CYSL-1 and CYSL-2 does not close during catalysis. Moreover, the fact that subunit Y of CYSL-3 remained open in the MD simulation might suggest that the enzyme utilizes both subunits, supporting the notion that it could be allosterically regulated by primary substrates. On the other hand, CYSL-1 appears to utilize only one subunit for catalysis. Taken together, the biochemical properties observed through kinetic, substrate binding affinity and structural analyses, together with the molecular dynamic simulations, revealed that the nematode OAS-TL paralogs differ in their conformations and may adopt different conformations during the catalytic cycle. These findings support the notion that *C. elegans* OAS-TL paralogs have adopted distinct functions *in vivo*.

4. Discussion

In this study, we determined the biochemical and structural properties of the recombinant OAS-TL proteins of *C. elegans*, which is the first animal in which OAS-TL proteins have been characterized. Our data show that the nematode paralogs form dimers, similar to their orthologs, and despite their high homology to each other, they differ in their conformations and substrate binding specificities. Interestingly, the calculated level of homology (Supplemental Fig. 6) and visual inspection of the amino acid alignment of the proteins (Fig. 1B) indicated that the worm proteins are most similar to plant enzymes: worm and plant OAS-TL proteins display the same length of the amino acid loop at the protein's surface (this type of loop has been previously proposed to serve as an interface of the CS complex between OASS and SAT [31]), which, in other OAS-TL protein classes, contains specific insertions or deletions (Fig. 1B). Thus, we hypothesize that the nematode and plant genes encoding OAS-TL proteins have evolved from a common ancestor that either was duplicated (*C. elegans*) or disappeared (*L. loa*) within nematode genomes. The existence of genes encoding plant OAS-TL proteins in the *C. elegans* genome is not the sole example of gene adoption. It was previously shown that the *C. elegans* genome contains genes encoding phytochelatin synthases, which are typical plant enzymes that play the same roles in *C. elegans* as in plants [40,41]. All of these facts show that, in contrast to the other animals, some soil roundworms have acquired conserved metabolic machinery from the plant kingdom. A phylogenetic analysis revealed that these animal OAS-TL paralogs constitute a structurally novel class within the OAS-TL protein family, and we propose that these proteins have diverged in nematode species to adopt distinct functions *in vivo*. For example, CYSL-1 was previously shown to have co-opted the mode of interaction observed between plant and bacterial cysteine synthase complexes [13]. What do our *in vitro* data say about the potential cellular functions of nematode orthologs?

The studied worm OAS-TL orthologs exhibit *in vitro O*-acetylserine sulfhydrylase activity, which is, in other species, crucial for the sulfur assimilation pathway (in which reduced sulfur is incorporated into amino acids) [3]. The possibility that *C. elegans* can assimilate inorganic sulfur through *O*-acetylserine sulfhydrylase activity cannot be rejected at this time, but it seems improbable. There is considerable evidence that these worm OAS-TL proteins display functions other than the biosynthesis of cysteine. *C. elegans* possesses genes encoding enzymes involved in the transsulfuration pathway, and thus, *C. elegans* possesses the canonical animal metabolic machinery for cysteine biosynthesis

Please cite this article as: R. Vozdek, et al., Biochemical properties of nematode O-acetylserine(thiol)lyase paralogs imply their distinct roles in hydrogen sulfide homeostasis, Biochim. Biophys. Acta (2013), http://dx.doi.org/10.1016/j.bbapap.2013.09.020

[12,14]. More importantly, a prerequisite for efficient sulfur assimilation in plants and bacteria is the presence of enzymes catalyzing the reduction of sulfate to sulfide and the enzyme serine acetyltransferase, which produces *O*-acetylserine; however, none of these enzymes are predicted to be present in *C. elegans*. Nevertheless, we cannot exclude the possibility that *C. elegans* may receive low amounts of *O*-acetylserine directly from food (bacteria), and we therefore hypothesize that the ability of the nematode OAS-TL proteins to bind *O*-acetylserine has an *in vivo* connection. Similarly, the role of *O*-acetylserine in *S. cerevisiae* is assumed to be something other than serving as an intermediate for cysteine production [42]. We observed that the binding affinities of the nematode OAS-TL proteins to *O*-acetylserine were much higher than their Michaelis constants for *O*-acetylserine. A similar discrepancy between the binding and catalytic constants of *O*-acetylserine has been observed for plant OAS-TL enzymes, and a regulatory role for *O*-acetylserine in the OASS and SAT complexes has been postulated [43]. Thus, we assume that low amounts of *O*-acetylserine can also modulate the CYSL-1/EGL-9 interaction in nematode cells. As noted above, these proteins interact *via* the CYSL-1 active site, and *O*-acetylserine might therefore bind to the CYSL-1 active site to serve as a competitive inhibitor of EGL-9. The MD simulation revealed that CYSL-1 closes its unoccupied active site upon interaction with the substrate, and plant orthologs have been proposed to use only one subunit for the interaction with the SAT C-termini, as previously demonstrated by the MD simulation using SAT peptides [39]. Taking these findings together, it is unlikely that the roundworm *C. elegans* utilizes *O*-acetylserine in the sulfur assimilation pathway to produce cysteine, but it may utilize *O*-acetylserine obtained at low concentrations from food to regulate OAS-TL functions.

The fact that all of the nematode orthologs exhibited sulfhydrylase activities when incubated with sulfide might suggest a role for these proteins in sulfide detoxification. It was previously reported that *cysl-1* mutants are less resistant to sulfide toxicity [11]. In fact, CYSL-1 activates HIF-1 *via* EGL-9 inhibition [13], and HIF-1 subsequently upregulates the sulfide-quinone oxidoreductase SQRD-1, which is the enzyme that reduces sulfide levels in the mitochondria [11]. However, it should be noted that while EGL-9 mutants are resistant to 250 ppm hydrogen sulfide, double egl-9 knockdowns/SQRD-1 mutants are still partially resistant [11]. This suggests that there is likely another mechanism (in addition to sulfide oxidation mediated by the SQRD-1 pathway) epistatic to *egl-9* through which sulfide is detoxified. Interestingly, *cysl-2* is a known *hif-1* target gene that can also be upregulated in the presence of hydrogen sulfide, and thus, CYSL-1 upregulates *cysl-2 via* its EGL-9 interaction [11,32,44]. However, the *cysl-2* gene was shown not to play a role in alleviating sulfide toxicity [11]. The hypothesis that CYSL-3 plays a role in sulfide detoxification has not yet been examined. Nevertheless, the similar affinities for hydrogen sulfide shown by all of the paralogs suggest that none of the nematode OAS-TL proteins can alleviate exposure to toxic levels of hydrogen sulfide *via* sulfhydrylase activity. We hypothesize that these proteins might maintain low sulfide levels in the cells and, thus, regulate hydrogen sulfide signaling.

Our data also show that all of the nematode proteins can utilize *O*-acetylserine to metabolize cyanide. Additionally, we determined that CYSL-2 can utilize cysteine and might therefore represent an

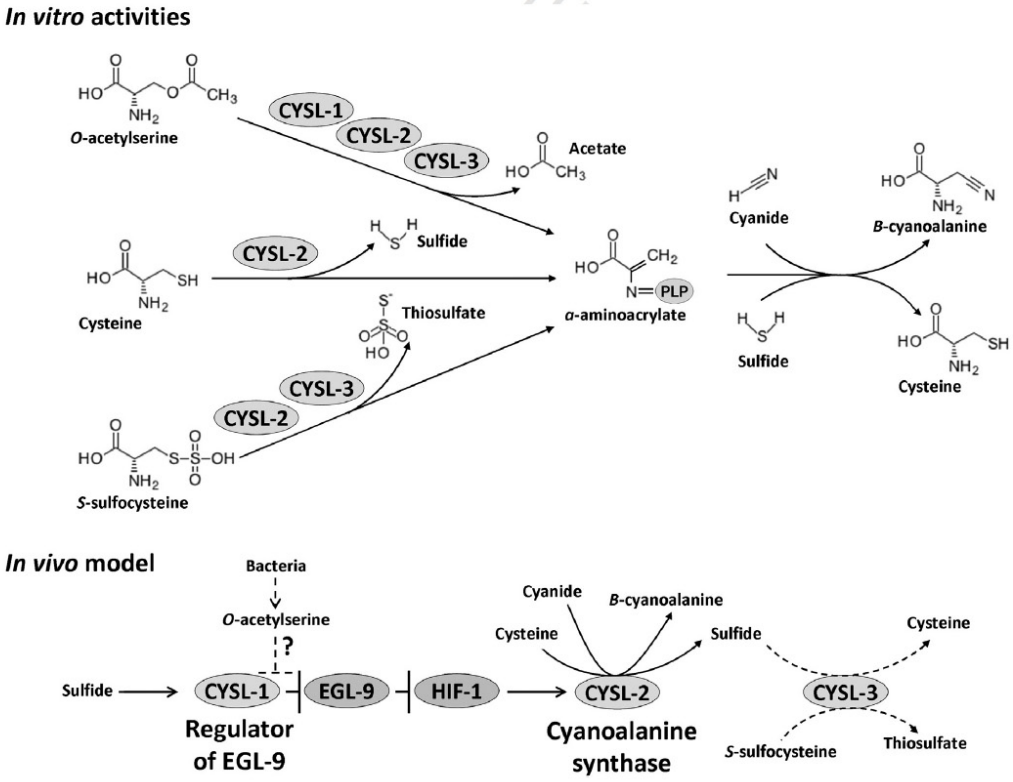

Fig. 6. *In vitro* activities of OAS-TL proteins in *C. elegans* and the proposed *in vivo* model. Only CYSL-1 serves as a regulator of EGL-9; the high binding affinity of *O*-acetylserine to CYSL-1 suggests that *O*-acetylserine might serve as a regulator of the CYSL-1/EGL-9 interaction. CYSL-2 exhibits high cyanoalanine synthase activity when utilizing cysteine, showing that CYSL-2 serves as a cyanoalanine synthase. The role of CYSL-3 remains to be determined; however, biochemical properties suggest that it plays a role in metabolizing *S*-sulfocysteine and/or sulfide.

Please cite this article as: R. Vozdek, et al., Biochemical properties of nematode O-acetylserine(thiol)lyase paralogs imply their distinct roles in hydrogen sulfide homeostasis, Biochim. Biophys. Acta (2013), http://dx.doi.org/10.1016/j.bbapap.2013.09.020

enzyme that both produces and uses hydrogen sulfide (see above). Canonical cyanoalanine synthase activity mediated by CYSL-2 was prominent, which is in line with the observation that *cysl-2* mutants, or animals with decreased expression of *cysl-2*, are less resistant to lethal cyanide concentrations and to paralytic killing by cyanide-producing *Pseudomonas aeruginosa* [11,45,46]. Moreover, expression of *cysl-2* gene is upregulated during cyanide exposure [11]. On the other hand, the catalytic activities of CYSL-1 and CYSL-3 were almost undetectable, and it is therefore unlikely that these two proteins serve as the enzymes responsible for cyanide detoxification. These data clearly show that only CYSL-2 serves as a cyanoalanine synthase in the cyanide detoxification pathway of *C. elegans*.

Interestingly, CYSL-2 and CYSL-3 can utilize a novel endogenous substrate of OAS-TL enzymes, *S*-sulfocysteine, which might suggest that they play a role in reducing high levels of *S*-sulfocysteine, a potent toxic compound [47]. In animals, *S*-sulfocysteine accumulates upon injection of cysteine and when the sulfite concentration is increased [48,49]. CYSL-3 is more highly expressed in well-fed animals compared to Dauer (starving) stage nematodes [33] and might therefore alleviate *S*-sulfocysteine levels as a result of cysteine uptake. However, our data show that the binding affinity of CYSL-3 for this substrate is low compared to that of CYSL-2. Therefore, it is not clear whether the ability of nematode enzymes to bind *S*-sulfocysteine has *in vivo* relevance. It will be interesting to examine whether OAS-TL orthologs in other species in different phyla can bind *S*-sulfocysteine as well.

In summary, the biochemical properties of recombinant proteins determined in this work, together with previous data, suggest a model for the *in vivo* functions of OAS-TL paralogs in *C. elegans*, with implications for hydrogen sulfide metabolism and/or signaling (Fig. 6). First, CYSL-1 is the only OAS-TL protein in *C. elegans* that interacts with EGL-9 and we propose that the uptake of *O*-acetylserine from bacteria might dissociate this interaction. It has been previously shown that the interaction is enhanced by hydrogen sulfide, thus leading to HIF-1 activation and the upregulation of genes involved in sulfide and cyanide detoxification, such as *cysl-2* [13]. We show that CYSL-2 serves as the cyanoalanine synthase in *C. elegans*, releasing hydrogen sulfide. This finding demonstrates that nematodes, unlike mammals, possess four different enzymes that produce hydrogen sulfide *de novo*: cystathionine beta-synthase, cystathionine gamma-lyase, mercaptopyruvate sulfur-transferase and cyanoalanine synthase. The subcellular localization of CYSL-2 in nematodes is unknown; *in silico* predictions suggested that – in contrast to plant CAS [7] – CYSL-2 does not contain the mitochondrial targeting sequence, however, a previous peptide mapping study identified CYSL-2 as a mitochondrial protein [50]. Thus, further studies are needed to determine whether CYSL-2 detoxifies cyanide in the cytosol, mitochondria or in both compartments. Finally, although we demonstrated that CYSL-3 exhibits canonical β-replacement activities, its role in *C. elegans* is unclear and remains to be explored. Our data suggest that CYSL-3 might detoxify sulfide or *S*-sulfocysteine. We also hypothesize that CYSL-3 might have acquired a novel function that has not been assigned to any of the OAS-TL protein to date. The obtained amino acid alignment revealed amino acid variation in the substrate binding loop: CYSL-3 contains leucine at position 79, while CYSL-1, CYSL-2 and other OASS and CAS plant enzymes contain a threonine or methionine (Fig. 1B). The CYSO protein in *Aeropyrum pernix* contains phenylalanine at this position, and CYSO uses *O*-phosphoserine as its substrate [51], supporting the role of this active-site amino acid in the substrate specificity of the OAS-TL enzymes. Because this leucine residue is only present in the nematode CYSL-3/CYSL-4 protein family, we hypothesize that CYSL-3 displays another type of catalytic activity involving a novel primary substrate (instead of *S*-sulfocysteine) in *C. elegans*. We also cannot exclude the possibility that CYSL-3 employs its active site for the interaction with the C-terminus of its hypothetical interacting partner like CYSL-1 does.

As noted above, the genome sequencing of *C. elegans*, the first fully sequenced organism, showed that this animal possesses genes that have previously been found exclusively in bacteria and plants and not in animals. Our data support the hypothesis that nematodes may have adopted OAS-TL genes to protect them from decreased oxygen and increased hydrogen sulfide concentrations in the environment during a Permian–Triassic extinction event around 250 Mya [13,52]. We also hypothesize that additional duplication of the OAS-TL genes in nematodes possibly increased their resistance to cyanogenic bacteria. Interestingly, two other animals have been shown to display cyanoalanine synthase activity similar to that of CYSL-2 in *C. elegans*: the white butterfly *Pieris rapae*, to detoxify cyanogenic glucosides [53], and the grasshopper *Zonocerus variegatus*, to survive feeding on cyanogenic plants [54]. Although the sequences and evolutionary relationships of the enzymes responsible for this activity in these species have not yet been determined, it is possible that these other animals might possess proteins from the OAS-TL family. Therefore, future studies and the sequencing of other animal genomes will provide evidence determining whether these proteins are also conserved in other, evolutionarily distant animals.

Supplementary data to this article can be found online at http://dx.doi.org/10.1016/j.bbapap.2013.09.020.

Acknowledgements

We would like to thank Mrs. Katerina Rakova, Jitka Sokolova Msc. and Ms. Alena Duta for technical assistance, Dr. Vojtech Spiwok for helpful discussion, and Drs. H. Robert Horvitz and Dengke Ma for providing the EGL-9 peptide and discussion.

Funding

This study was supported by the research program of the Charles University in Prague (PRVOUK-P24/LF1/3), and by the research project MH-CZ-DRO (VFN64165). The access to computing and storage facilities owned by parties and projects contributing to the National Grid Infrastructure MetaCentrum "Projects of Large Infrastructure for Research, Development, and Innovations" (LM2010005) and Center CERIT Scientific Cloud, part of the Operational Program Research and Development for Innovations (CZ.1.05/3.2.00/08.0144), and the access to LC–MS/MS that was obtained from project OPPK (CZ.2.16/3.1.00/24012), is highly appreciated.

References

[1] N.M. Kredich, G.M. Tomkins, The enzymic synthesis of L-cysteine in *Escherichia coli* and *Salmonella typhimurium*, J. Biol. Chem. 241 (1966) 4955–4965.
[2] R. Hell, M. Wirtz, Molecular biology, biochemistry and cellular physiology of cysteine metabolism in *Arabidopsis thaliana*, The Arabidopsis book/American Society of Plant Biologists, 9, 2011, p. e0154.
[3] M. Wirtz, M. Droux, Synthesis of the sulfur amino acids: cysteine and methionine, Photosynth. Res. 86 (2005) 345–362.
[4] M.A. Becker, N.M. Kredich, G.M. Tomkins, The purification and characterization of *O*-acetylserine sulfhydrylase-A from *Salmonella typhimurium*, J. Biol. Chem. 244 (1969) 2418–2427.
[5] P.K. Mehta, P. Christen, The molecular evolution of pyridoxal-5′-phosphate-dependent enzymes, Adv. Enzymol. Relat. Areas Mol. Biol. 74 (2000) 129–184.
[6] W.M. Rabeh, P.F. Cook, Structure and mechanism of *O*-acetylserine sulfhydrylase, J. Biol. Chem. 279 (2004) 26803–26806.
[7] Y. Hatzfeld, A. Maruyama, A. Schmidt, M. Noji, K. Ishizawa, K. Saito, beta-Cyanoalanine synthase is a mitochondrial cysteine synthase-like protein in spinach and *Arabidopsis*, Plant Physiol. 123 (2000) 1163–1171.
[8] M.A. Bermudez, M.A. Paez-Ochoa, C. Gotor, L.C. Romero, *Arabidopsis S*-sulfocysteine synthase activity is essential for chloroplast function and long-day light-dependent redox control, Plant Cell 22 (2010) 403–416.
[9] C. Alvarez, L. Calo, L.C. Romero, I. Garcia, C. Gotor, An *O*-acetylserine(thiol)lyase homolog with L-cysteine desulfhydrase activity regulates cysteine homeostasis in *Arabidopsis*, Plant Physiol. 152 (2010) 656–669.
[10] J.P. Kraus, V. Kožich, Cystathionine-β-synthase and its deficiency, in: R. Carmel, D.W. Jacobsen (Eds.), Homocysteine in Health and Disease, Cambridge University Press, Cambridge, U.K., 2001, pp. 223–243.
[11] M.W. Budde, M.B. Roth, The response of *Caenorhabditis elegans* to hydrogen sulfide and hydrogen cyanide, Genetics 189 (2011) 521–532.

Please cite this article as: R. Vozdek, et al., Biochemical properties of nematode O-acetylserine(thiol)lyase paralogs imply their distinct roles in hydrogen sulfide homeostasis, Biochim. Biophys. Acta (2013), http://dx.doi.org/10.1016/j.bbapap.2013.09.020

[12] N.D. Mathew, D.I. Schlipalius, P.R. Ebert, Sulfurous gases as biological messengers and toxins: comparative genetics of their metabolism in model organisms, J. Toxicol. 2011 (2011) 394970.
[13] D.K. Ma, R. Vozdek, N. Bhatla, H.R. Horvitz, CYSL-1 interacts with the O(2)-sensing hydroxylase EGL-9 to promote H(2)S-modulated hypoxia-induced behavioral plasticity in *C. elegans*, Neuron 73 (2012) 925–940.
[14] R. Vozdek, A. Hnizda, J. Krijt, M. Kostrouchova, V. Kozich, Novel structural arrangement of nematode cystathionine beta-synthases: characterization of *Caenorhabditis elegans* CBS-1, Biochem. J. 443 (2012) 535–547.
[15] Z. Shao, Y. Zhang, J.A. Powell-Coffman, Two distinct roles for EGL-9 in the regulation of HIF-1-mediated gene expression in *Caenorhabditis elegans*, Genetics 183 (2009) 821–829.
[16] R. Chenna, H. Sugawara, T. Koike, R. Lopez, T.J. Gibson, D.G. Higgins, J.D. Thompson, Multiple sequence alignment with the Clustal series of programs, Nucleic Acids Res. 31 (2003) 3497–3500.
[17] B. Neron, H. Menager, C. Maufrais, N. Joly, J. Maupetit, S. Letort, S. Carrere, P. Tuffery, C. Letondal, Mobyle: a new full web bioinformatics framework, Bioinformatics 25 (2009) 3005–3011.
[18] D.H. Huson, D.C. Richter, C. Rausch, T. Dezulian, M. Franz, R. Rupp, Dendroscope: an interactive viewer for large phylogenetic trees, BMC Bioinforma. 8 (2007) 460.
[19] K.N. Maclean, J. Sikora, V. Kozich, H. Jiang, L.S. Greiner, E. Kraus, J. Krijt, L.S. Crnic, R.H. Allen, S.P. Stabler, M. Elleder, J.P. Kraus, Cystathionine beta-synthase null homocystinuric mice fail to exhibit altered hemostasis or lowering of plasma homocysteine in response to betaine treatment, Mol. Genet. Metab. 101 (2010) 163–171.
[20] J. Krijt, J. Kopecka, A. Hnizda, S. Moat, L.A. Kluijtmans, P. Mayne, V. Kozich, Determination of cystathionine beta-synthase activity in human plasma by LC–MS/MS: potential use in diagnosis of CBS deficiency, J. Inherit. Metab. Dis. 34 (2011) 49–55.
[21] U.K. Laemmli, Cleavage of structural proteins during the assembly of the head of bacteriophage T4, Nature 227 (1970) 680–685.
[22] I. Wittig, H.P. Braun, H. Schagger, Blue native PAGE, Nat. Protoc. 1 (2006) 418–428.
[23] R.C. Edgar, MUSCLE: multiple sequence alignment with high accuracy and high throughput, Nucleic Acids Res. 32 (2004) 1792–1797.
[24] M. Koutmos, O. Kabil, J.L. Smith, R. Banerjee, Structural basis for substrate activation and regulation by cystathionine beta-synthase (CBS) domains in cystathionine (beta)-synthase, Proc. Natl. Acad. Sci. U. S. A. 107 (2010) 20958–20963.
[25] A. Sali, T.L. Blundell, Comparative protein modelling by satisfaction of spatial restraints, J. Mol. Biol. 234 (1993) 779–815.
[26] N.A. Baker, D. Sept, S. Joseph, M.J. Holst, J.A. McCammon, Electrostatics of nanosystems: application to microtubules and the ribosome, Proc. Natl. Acad. Sci. U. S. A. 98 (2001) 10037–10041.
[27] M.H.M. Olsson, C.R. Sondergard, M. Rostkowski, J.H. Jensen, PROPKA3: consistent treatment of internal and surface residues in empirical pKa predictions, J. Chem. Theory Comput. 7 (2011) 525–537.
[28] S. Pronk, S. Pall, R. Schulz, P. Larsson, P. Bjelkmar, R. Apostolov, M.R. Shirts, J.C. Smith, P.M. Kasson, D. van der Spoel, B. Hess, E. Lindahl, GROMACS 4.5: a high-throughput and highly parallel open source molecular simulation toolkit, Bioinformatics 29 (2013) 845–854.
[29] V. Hornak, R. Abel, A. Okur, B. Strockbine, A. Roitberg, C. Simmerling, Comparison of multiple Amber force fields and development of improved protein backbone parameters, Proteins 65 (2006) 712–725.
[30] J. Wang, R.M. Wolf, J.W. Caldwell, P.A. Kollman, D.A. Case, Development and testing of a general amber force field, J. Comput. Chem. 25 (2004) 1157–1174.
[31] E.R. Bonner, R.E. Cahoon, S.M. Knapke, J.M. Jez, Molecular basis of cysteine biosynthesis in plants: structural and functional analysis of O-acetylserine sulfhydrylase from *Arabidopsis thaliana*, J. Biol. Chem. 280 (2005) 38803–38813.
[32] C. Shen, D. Nettleton, M. Jiang, S.K. Kim, J.A. Powell-Coffman, Roles of the HIF-1 hypoxia-inducible factor during hypoxia response in *Caenorhabditis elegans*, J. Biol. Chem. 280 (2005) 20580–20588.
[33] A. Madi, S. Mikkat, C. Koy, B. Ringel, H.J. Thiesen, M.O. Glocker, Mass spectrometric proteome analysis suggests anaerobic shift in metabolism of Dauer larvae of *Caenorhabditis elegans*, Biochim. Biophys. Acta 1784 (2008) 1763–1770.
[34] B. Campanini, F. Speroni, E. Salsi, P.F. Cook, S.L. Roderick, B. Huang, S. Bettati, A. Mozzarelli, Interaction of serine acetyltransferase with *O*-acetylserine sulfhydrylase active site: evidence from fluorescence spectroscopy, Protein Sci. 14 (2005) 2115–2124.
[35] P. Burkhard, C.H. Tai, C.M. Ristroph, P.F. Cook, J.N. Jansonius, Ligand binding induces a large conformational change in *O*-acetylserine sulfhydrylase from *Salmonella typhimurium*, J. Mol. Biol. 291 (1999) 941–953.
[36] R. Schnell, W. Oehlmann, M. Singh, G. Schneider, Structural insights into catalysis and inhibition of *O*-acetylserine sulfhydrylase from *Mycobacterium tuberculosis*. Crystal structures of the enzyme alpha-aminoacrylate intermediate and an enzyme-inhibitor complex, J. Biol. Chem. 282 (2007) 23473–23481.
[37] H. Yi, M. Juergens, J.M. Jez, Structure of soybean beta-cyanoalanine synthase and the molecular basis for cyanide detoxification in plants, Plant Cell 24 (2012) 2696–2706.
[38] J.A. Francois, S. Kumaran, J.M. Jez, Structural basis for interaction of *O*-acetylserine sulfhydrylase and serine acetyltransferase in the *Arabidopsis* cysteine synthase complex, Plant Cell 18 (2006) 3647–3655.
[39] A. Feldman-Salit, M. Wirtz, E.D. Lenherr, C. Throm, M. Hothorn, K. Scheffzek, R. Hell, R.C. Wade, Allosterically gated enzyme dynamics in the cysteine synthase complex regulate cysteine biosynthesis in *Arabidopsis thaliana*, Structure 20 (2012) 292–302.
[40] O.K. Vatamaniuk, E.A. Bucher, J.T. Ward, P.A. Rea, A new pathway for heavy metal detoxification in animals. Phytochelatin synthase is required for cadmium tolerance in *Caenorhabditis elegans*, J. Biol. Chem. 276 (2001) 20817–20820.
[41] S. Clemens, J.I. Schroeder, T. Degenkolb, *Caenorhabditis elegans* expresses a functional phytochelatin synthase, Eur. J. Biochem. 268 (2001) 3640–3643.
[42] H. Takagi, K. Yoshioka, N. Awano, S. Nakamori, B. Ono, Role of *Saccharomyces cerevisiae* serine *O*-acetyltransferase in cysteine biosynthesis, FEMS Microbiol. Lett. 218 (2003) 291–297.
[43] M. Wirtz, M. Droux, R. Hell, *O*-Acetylserine (thiol) lyase: an enigmatic enzyme of plant cysteine biosynthesis revisited in *Arabidopsis thaliana*, J. Exp. Bot. 55 (2004) 1785–1798.
[44] M.W. Budde, M.B. Roth, Hydrogen sulfide increases hypoxia-inducible factor-1 activity independently of von Hippel–Lindau tumor suppressor-1 in *C. elegans*, Mol. Biol. Cell 21 (2010) 212–217.
[45] J.N. Saldanha, A. Parashar, S. Pandey, J.A. Powell-Coffman, Multiparameter behavioral analyses provide insights to mechanisms of cyanide resistance in *Caenorhabditis elegans*, Toxicol. Sci. (2013).
[46] Z. Shao, Y. Zhang, Q. Ye, J.N. Saldanha, J.A. Powell-Coffman, *C. elegans* SWAN-1 binds to EGL-9 and regulates HIF-1-mediated resistance to the bacterial pathogen *Pseudomonas aeruginosa* PAO1, PloS Pathog. 6 (2010) e1001075.
[47] J.W. Olney, C.H. Misra, T. de Gubareff, Cysteine-*S*-sulfate: brain damaging metabolite in sulfite oxidase deficiency, J. Neuropathol. Exp. Neurol. 34 (1975) 167–177.
[48] A.K. Abbas, W. Xia, M. Tranberg, H. Wigstrom, S.G. Weber, M. Sandberg, *S*-Sulfocysteine is an endogenous amino acid in neonatal rat brain but an unlikely mediator of cysteine neurotoxicity, Neurochem. Res. 33 (2008) 301–307.
[49] S.H. Mudd, F. Irreverre, L. Laster, Sulfite oxidase deficiency in man: demonstration of the enzymatic defect, Science 156 (1967) 1599–1602.
[50] J. Li, T. Cai, P. Wu, Z. Cui, X. Chen, J. Hou, Z. Xie, P. Xue, L. Shi, P. Liu, J.R. Yates 3rd, F. Yang, Proteomic analysis of mitochondria from *Caenorhabditis elegans*, Proteomics 9 (2009) 4539–4553.
[51] K. Mino, K. Ishikawa, A novel *O*-phospho-L-serine sulfhydrylation reaction catalyzed by *O*-acetylserine sulfhydrylase from *Aeropyrum pernix* K1, FEBS Lett. 551 (2003) 133–138.
[52] K. Grice, C. Cao, G.D. Love, M.E. Bottcher, R.J. Twitchett, E. Grosjean, R.E. Summons, S.C. Turgeon, W. Dunning, Y. Jin, Photic zone euxinia during the Permian–triassic superanoxic event, Science 307 (2005) 706–709.
[53] E.J. Stauber, P. Kuczka, M. van Ohlen, B. Vogt, T. Janowitz, M. Piotrowski, T. Beuerle, U. Wittstock, Turning the 'mustard oil bomb' into a 'cyanide bomb': aromatic glucosinolate metabolism in a specialist insect herbivore, PLoS ONE 7 (2012) e35545.
[54] O.O. Ogunlabi, F.K. Agboola, A soluble beta-cyanoalanine synthase from the gut of the variegated grasshopper *Zonocerus variegatus* (L.), Insect Biochem. Mol. Biol. 37 (2007) 72–79.

Please cite this article as: R. Vozdek, et al., Biochemical properties of nematode O-acetylserine(thiol)lyase paralogs imply their distinct roles in hydrogen sulfide homeostasis, Biochim. Biophys. Acta (2013), http://dx.doi.org/10.1016/j.bbapap.2013.09.020

BBA-Proteins and Proteomics, In press

Supplemental Material

Biochemical Properties of Nematode *O*-acetylserine(thiol)lyase Paralogs Imply Their Distinct Roles in Hydrogen Sulfide Homeostasis

Roman Vozdek, Aleš Hnízda, Jakub Krijt, Leona Šerá and Viktor Kožich

Supplemental material contains 2 tables and 6 figures and associated legends.

	Protein	N-terminal sequence	Function	Localization
Arabidopsis thaliana	OAS-A1	----------MASR---IAKDVTEL..	OASS	Cytosol
	OAS-B	----------MAATSSSAFLLNPLTSR-----HRPFKYSPELSSLSLSSRK-AAAFDVSSAAFTLKRQSRSDVVCKAVSIKPEAGVEGLNIADNAAQL..	OASS	Chloroplast
	OAS-C	MVAMIMASRFNREAKLASQILSTLLGNRSCYTSMAATSSSALLLNPLTSSSSSSTLRRFRCSPEISSLSFSSAS-DFSLAMKRQSRSFADGSERDPSVVCEAVKRETGPDGLNIADNVSQL..	OASS	Mitochondria
	CYS-C1	----------MASVSR----------RLLRRETIFCFSHTVRKLFSTVGSPSFAQRLRDLFKDFP----------STNAKRDASLL..	CAS	Mitochondria
	CYS-D1	----------MEEDRCSIKDDATQL..	?	Cytosol
	CYS-D2	----------MEDKCLIKNDITEL..	?	Cytosol
	CS-LIKE	----------MEDRVLIKNDVTEL..	DES	Cytosol
	CS26	---MAFAS-----PSLRLLPQSPLGRITSKLHRFSTAKLSLFSFHHDSSS-------SLAVRTPVSSFVVGAISGKSSTGTKSKSKTKRKPPPPPVTTVAEEQHIAESETVNIAEDVTQL..	SSCS	Chloroplast
C. elegans	CYSL-1	----------MADRNSIGENAAAL..	EGL-9 regulator	
	CYSL-2	----------MSRELMVETGGEL..	CAS	
	CYSL-3	----------MSRELMVQDSGDT..	?	
	CYSL-4	----------MSRELMVHDSGDT..	?	

Supplemental Figure 1: Amino acid alignment of OAS-TL proteins from *Arabidopsis thaliana* and *Caenorhabditis elegans*. Nematode orthologs lack the initial sequence targeting the plant proteins to chloroplasts or mitochondria. OASS, *O*-acetylserine sulfhydrylase; CAS, cyanoalanine synthase; DES, cysteine desulfhydrase; SSCS, *S*-sulfocysteine synthase.

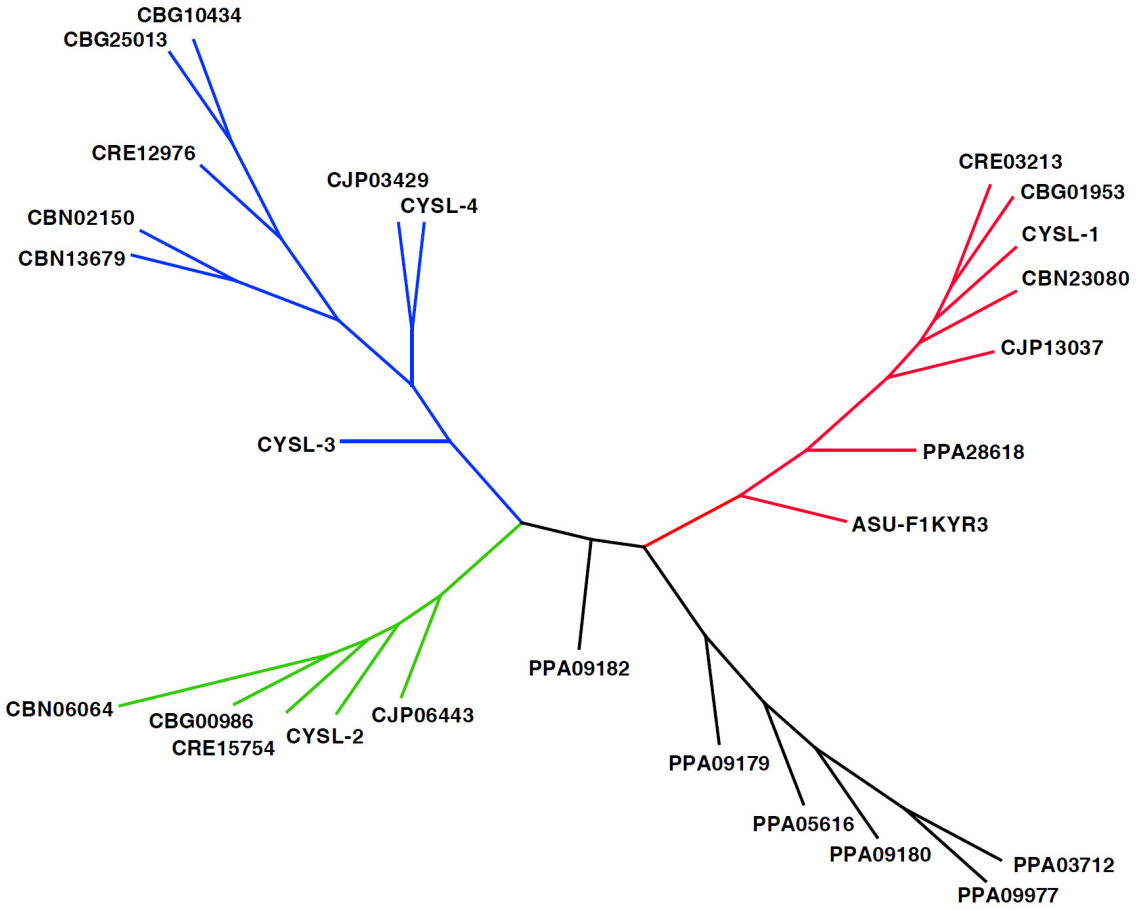

Supplemental Figure 2. Phylogenetic analysis of nematode OAS-TL proteins. Four significant protein branches are evident: the CYSL-1 group is shown in red, CYSL-2 in green, CYSL-3/CYSL-4 in blue and proteins from *P. pacificus* in black. The CYSL-3 and CYSL-4 families are on the same branch. CBG, *C. briggsae*; CRE, *C. remanei*; CBN, *C. brenneri*; CJP, *C. japonica*; PPR, *P. pacificus*; ASU, *A. suum*.

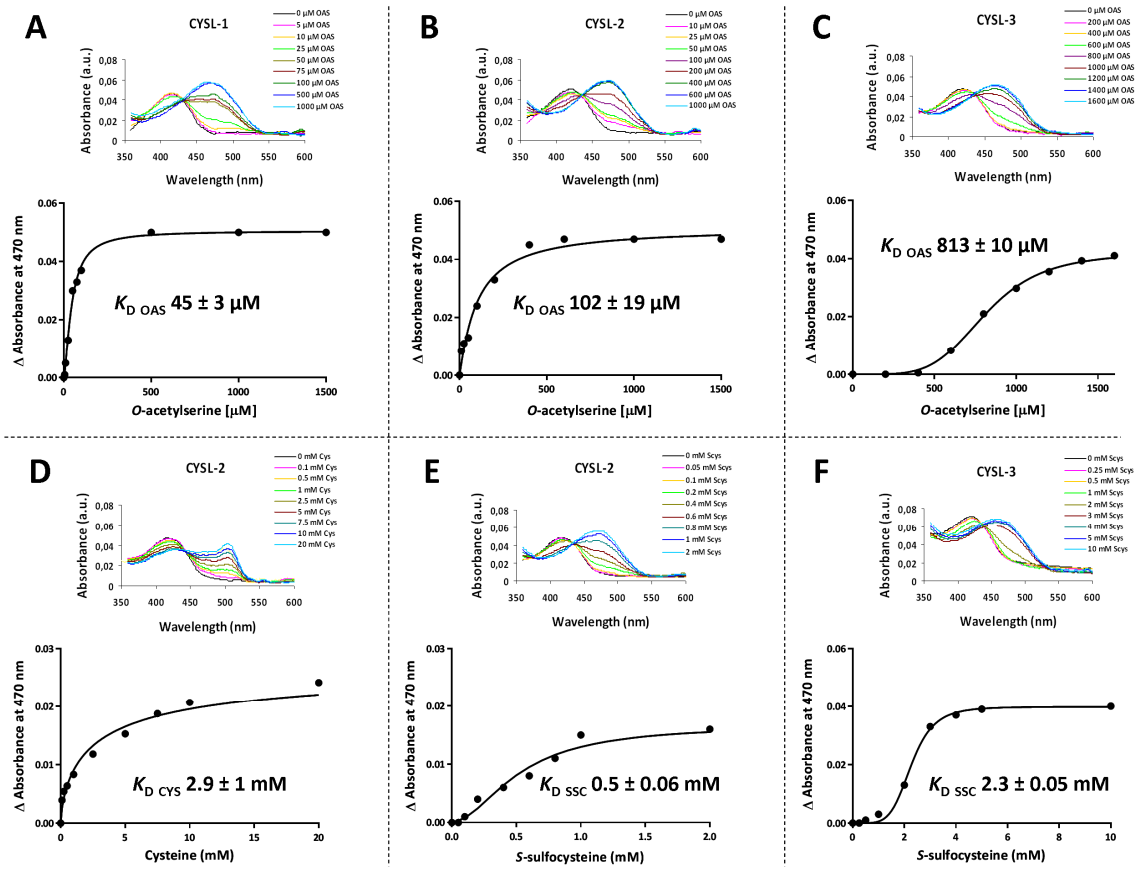

Supplemental Figure 3. Spectroscopic analysis of substrate binding affinities. The absorbance at 470 nm was recorded and subsequently analyzed using the equation for one-site-specific binding with the Hill slope. **A)** CYSL-1 with *O*-acetylserine. **B)** CYSL-2 with *O*-acetylserine. **C)** CYSL-3 with *O*-acetylserine. **D)** CYSL-2 with Cysteine. **E)** CYSL- with *S*-sulfocysteine. **F)** CYSL-3 with *S*-sulfocysteine.

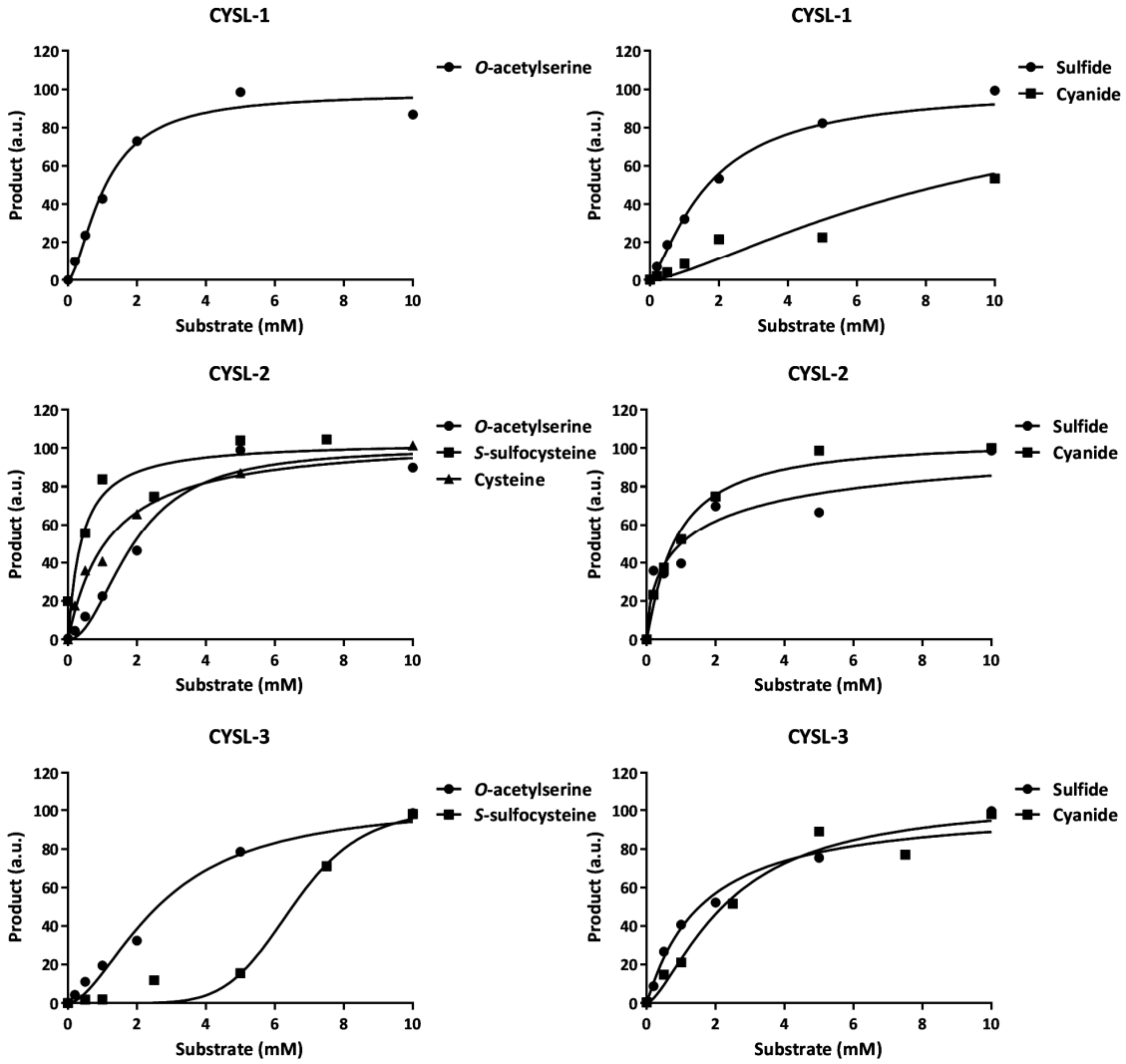

Supplemental Figure 4. Kinetic behavior of nematode OAS-TL proteins. The curves were plotted through allosteric sigmoidal fitting to evaluate Hill constants; to allow better comparison of substrate kinetics, the product values were calculated to be limited to 100 arbitrary units (a.u.). The graphs on the left show the kinetics of the primary substrates, while the graphs on the right show the kinetics of the secondary substrates.

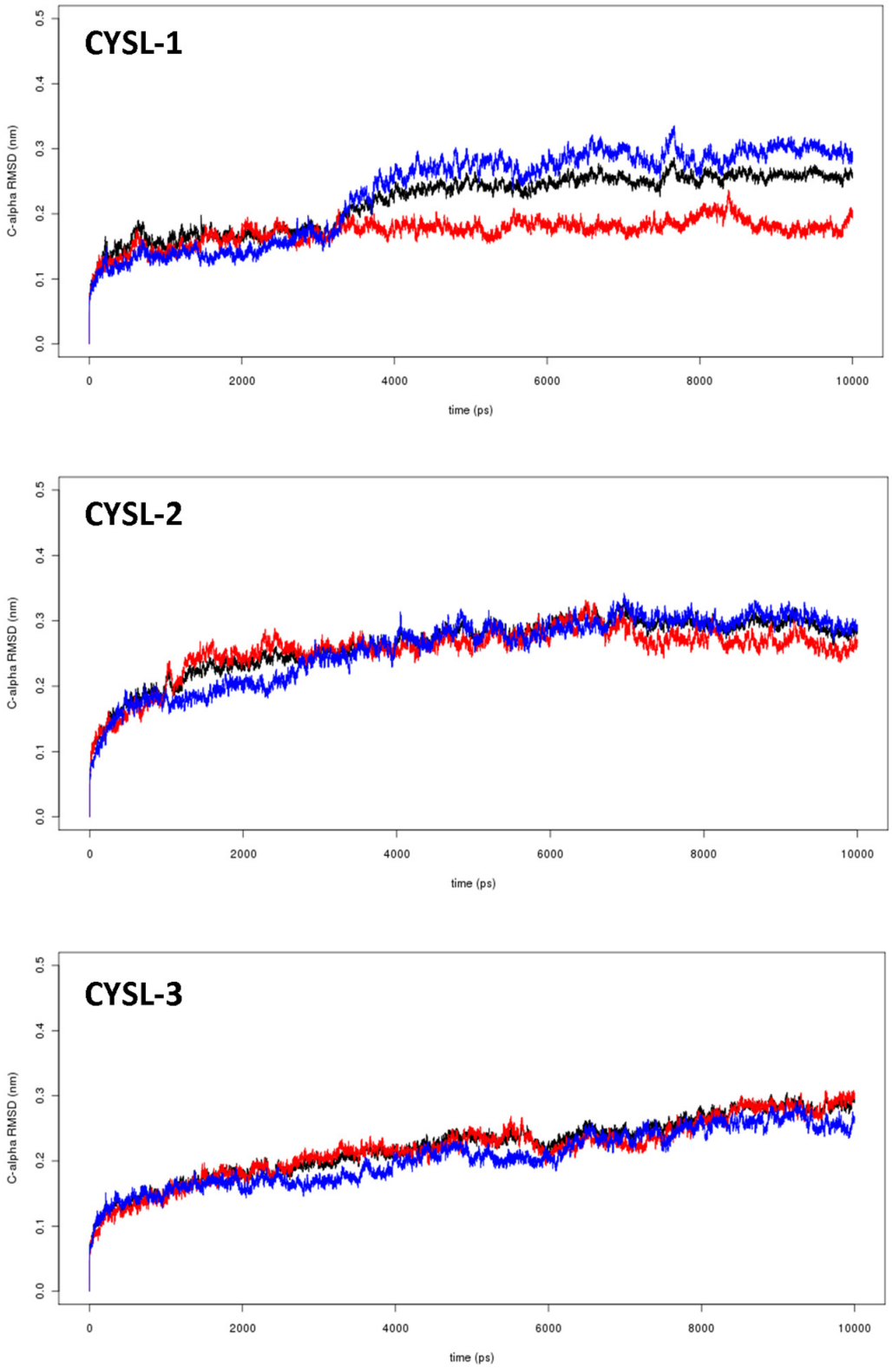

Supplemental Figure 5. **Time development of the root mean square deviation (RMSD) of C-alpha atoms from the initial structure during a molecular dynamics simulation.** All atoms are shown in black, chain A (subunit X) in red and chain B (subunit Y) in blue.

	Plant															Bacteria				Protist	Yeast	Archae	Animal					Nematode			
	OASS							OTHER					CAS			CYSK		CYSM					CBS					CYSL			
	At_OAS-A1	At_OAS-A2	Gm_OAS-TL-1	Gm_OAS-TL-2	At_OAS-B	At_OAS-C	Gm_OAS-TL-4	At_OAS-D1	At_OAS-D2	At_CS_like	Gm_OAS-TL-6	Gm_OAS-TL-7	At_CS26	At_CYS-C1	Gm_OAS-TL-3	Ec_CYSK	St_CYSK	Ec_CYSM	St_CYSM	Tc_Q4CST7	Sc_CYSK	Ap_CYSO	Ce_CBS-1	Dm_CBS	Hs_CBS	Sc_CBS	Tc_CBS	Ce_CYSL-1	Ce_CYSL-2	Ce_CYSL-3	Ce_CYSL-4
At_OAS-A1	100	88	80	79	70	69	68	65	66	63	68	68	59	59	59	54	55	44	43	48	32	19	36	37	37	40	36	57	52	50	49
At_OAS-A2	88	100	82	79	69	69	68	65	67	63	66	67	60	59	60	53	54	40	39	48	30	20	35	37	36	40	36	54	54	50	50
Gm_OAS-TL-1	80	82	100	85	74	73	73	69	70	68	72	72	61	59	60	53	54	42	42	49	30	20	33	36	37	37	35	56	52	49	48
Gm_OAS-TL-2	79	79	85	100	73	71	72	68	69	68	69	70	59	60	59	54	54	42	42	52	31	23	34	35	37	38	38	56	54	52	48
At_OAS-B	70	69	74	73	100	78	71	68	68	66	68	68	53	51	51	56	55	42	42	49	28	16	29	30	30	29	31	53	51	48	46
At_OAS-C	69	69	73	71	78	100	72	67	66	65	67	66	53	52	54	57	56	42	41	51	27	14	30	26	27	28	30	55	52	48	48
Gm_OAS-TL-4	68	68	73	72	71	72	100	66	65	64	65	66	52	51	51	55	54	40	40	47	25	12	28	28	31	31	29	51	51	47	46
At_OAS-D1	65	65	69	68	68	67	66	100	76	78	72	72	56	54	55	52	51	40	41	49	31	19	33	36	36	35	36	53	53	49	51
At_OAS-D2	66	67	70	69	68	66	65	76	100	86	69	67	56	52	54	52	51	39	40	51	32	20	34	37	36	36	37	52	53	52	51
At_CS_like	63	63	68	68	66	65	64	78	86	100	68	67	56	52	54	51	50	40	40	50	33	20	34	35	38	37	35	51	54	51	51
Gm_OAS-TL-6	68	66	72	69	68	67	65	72	69	68	100	79	57	55	56	49	49	39	39	49	32	21	31	32	35	36	34	53	52	50	48
Gm_OAS-TL-7	68	67	72	70	68	66	66	72	67	67	79	100	55	57	55	49	49	40	40	46	29	22	34	33	37	36	32	50	52	51	49
At_CS26	59	60	61	59	53	53	52	56	56	56	57	55	100	47	45	49	49	39	38	43	25	16	26	25	27	26	26	45	45	43	43
At_CYS-C1	59	59	59	60	51	52	51	54	52	52	55	57	47	100	76	45	45	38	38	44	25	16	24	27	29	29	26	48	50	45	46
Gm_OAS-TL-3	59	60	60	59	51	54	51	55	54	54	56	55	45	76	100	45	45	40	40	43	25	18	26	27	27	27	27	47	51	46	45
Ec_CYSK	54	53	53	54	56	57	55	52	52	51	49	49	49	45	45	100	97	41	41	46	31	19	33	33	38	33	34	50	49	46	47
St_CYSK	55	54	54	54	55	56	54	51	51	50	49	49	49	45	45	97	100	41	41	45	31	19	33	33	37	33	34	50	49	47	47
Ec_CYSM	44	40	42	42	42	42	40	40	39	40	39	40	39	38	40	41	41	100	94	41	35	25	35	35	35	33	32	40	43	41	39
St_CYSM	43	39	42	42	42	41	40	41	40	40	39	40	38	38	40	41	41	94	100	41	36	24	35	35	35	34	31	41	43	43	41
Tc_Q4CST7	48	48	49	52	49	51	47	49	51	50	49	46	43	44	43	46	45	41	41	100	29	25	27	29	32	29	30	49	48	47	47
Sc_CYSK	32	30	30	31	28	27	25	31	32	33	32	29	25	25	25	31	31	35	36	29	100	18	25	24	29	28	25	31	30	27	27
Ap_CYSO	19	20	20	23	16	14	12	19	20	20	21	22	16	16	18	19	19	25	24	25	18	100	14	16	17	19	17	17	21	20	21
Ce_CBS-1	36	35	33	34	29	30	28	33	34	34	31	34	26	24	26	33	33	35	35	27	25	14	100	49	46	43	44	34	33	32	32
Dm_CBS	37	37	36	35	30	26	28	36	37	35	32	33	25	27	27	33	33	35	35	29	24	16	49	100	50	39	44	34	32	33	31
Hs_CBS	37	36	37	37	30	27	31	36	36	38	35	37	27	29	27	38	37	35	35	32	29	17	46	50	100	41	45	39	33	32	32
Sc_CBS	40	40	37	38	29	28	31	35	36	37	36	36	26	29	27	33	33	33	34	29	28	19	43	39	41	100	44	34	33	35	36
Tc_CBS	36	36	35	38	31	30	29	36	37	35	34	32	26	26	27	34	34	32	31	30	25	17	44	44	45	44	100	32	32	31	30
Ce_CYSL-1	57	54	56	56	53	55	51	53	52	51	53	50	45	48	47	50	50	40	41	49	31	17	34	34	39	34	32	100	55	51	49
Ce_CYSL-2	52	54	52	54	51	52	51	53	53	54	52	52	45	50	51	49	49	43	43	48	30	21	33	32	33	33	32	55	100	65	63
Ce_CYSL-3	50	50	49	52	48	48	47	49	52	51	50	51	43	45	46	46	47	41	43	47	27	20	32	33	32	35	31	51	65	100	84
Ce_CYSL-4	49	50	48	48	46	48	46	51	51	51	48	49	43	46	45	47	47	39	41	47	27	21	32	31	32	36	30	49	63	84	100

Supplemental Figure 6. Pairwise homologous levels of various OAS-TL proteins across phyla. The numbers represent pairwise scores indicating the percentage of homology. It is evident that the group of nematode orthologs is most homologous to the plant OAS-TL proteins. At, *A. thaliana*; Gm, *G. max*; Ec, *E. coli*; St, *S. typhimurium*; Sc, *S. cerevisiae*; Tc, *T. cruzi*; Ce, *C. elegans*; Dm, *D. melanogaster*; Hs, *H. sapiens*.

Publication 6.1.3

CYSL-1 Interacts with the O_2-Sensing Hydroxylase EGL-9 to Promote H_2S-Modulated Hypoxia-Induced Behavioral Plasticity in *C. elegans*

Neuron (2012)

Neuron
Article

CYSL-1 Interacts with the O_2-Sensing Hydroxylase EGL-9 to Promote H_2S-Modulated Hypoxia-Induced Behavioral Plasticity in *C. elegans*

Dengke K. Ma,[1] Roman Vozdek,[2] Nikhil Bhatla,[1] and H. Robert Horvitz[1,*]
[1]Howard Hughes Medical Institute, Department of Biology, and McGovern Institute for Brain Research, MIT, Cambridge, MA 02139, USA
[2]Institute of Inherited Metabolic Disorders, First Faculty of Medicine, Charles University in Prague and General University Hospital in Prague, Ke Karlovu 2, Prague 2, 128 08 Czech Republic
*Correspondence: horvitz@mit.edu
DOI 10.1016/j.neuron.2011.12.037

SUMMARY

The *C. elegans* HIF-1 proline hydroxylase EGL-9 functions as an O_2 sensor in an evolutionarily conserved pathway for adaptation to hypoxia. H_2S accumulates during hypoxia and promotes HIF-1 activity, but how H_2S signals are perceived and transmitted to modulate HIF-1 and animal behavior is unknown. We report that the experience of hypoxia modifies a *C. elegans* locomotive behavioral response to O_2 through the EGL-9 pathway. From genetic screens to identify novel regulators of EGL-9-mediated behavioral plasticity, we isolated mutations of the gene *cysl-1*, which encodes a *C. elegans* homolog of sulfhydrylases/cysteine synthases. Hypoxia-dependent behavioral modulation and H_2S-induced HIF-1 activation require the direct physical interaction of CYSL-1 with the EGL-9 C terminus. Sequestration of EGL-9 by CYSL-1 and inhibition of EGL-9-mediated hydroxylation by hypoxia together promote neuronal HIF-1 activation to modulate behavior. These findings demonstrate that CYSL-1 acts to transduce signals from H_2S to EGL-9 to regulate O_2-dependent behavioral plasticity in *C. elegans*.

INTRODUCTION

Oxygen (O_2) is essential for most life forms. An abnormally low level of O_2, or hypoxia, affects diverse biological processes, including embryonic development, physiological homeostasis, and behavioral adaptation, as well as many pathological conditions, such as ischemic stroke, neurodegeneration, tumor formation, and metastasis (Kaelin and Ratcliffe, 2008; Semenza, 2010). Evolutionarily conserved proline-4-hydroxylase domain (PHD) enzymes have been identified as intracellular receptors for O_2 (Bruick and McKnight, 2001; Epstein et al., 2001; Ivan et al., 2002). Under normal conditions, PHDs use O_2 as a substrate to hydroxylate the transcription factor hypoxia inducible factor (HIF). Hydroxylated HIF is recognized by the von Hippel-Lindau (VHL) tumor suppressor protein, a component of an E3-ubiquitin ligase complex that targets HIF for proteosomal degradation. Under hypoxic conditions, impaired PHD protein function leads to upregulation of HIF and its target gene expression. Mutations in the human HIF PHD enzyme, EGLN2, can cause congenital erythrocytosis (Percy et al., 2006) and possibly recurrent paragangliomas (Ladroue et al., 2008). With central roles in many human biological processes, HIF PHDs are promising therapeutic targets for treating ischemic stroke, neurodegenerative diseases, and cancer (Mazzone et al., 2009; Quaegebeur and Carmeliet, 2010). The first O_2-sensing PHD enzyme identified was the *C. elegans* EGL-9 protein, the product of a gene defined by mutations that cause an egg-laying behavioral defect (Darby et al., 1999; Epstein et al., 2001; Trent et al., 1983).

C. elegans exhibits diverse genetically tractable behaviors that are regulated by internal physiological states, environmental cues, and behavioral experiences (de Bono and Maricq, 2005; Jorgensen and Rankin, 1997; Sawin et al., 2000). Studies of several *C. elegans* behaviors have significantly increased our understanding of the molecular and neural mechanisms underlying behavioral plasticity, a major problem in neurobiology. *C. elegans* naturally lives in soil or in microbe-rich habitats where O_2 is usually reduced from the ambient level of 21% (Félix and Braendle, 2010) and prefers hypoxic ranges of O_2 concentration when tested in laboratory aerotaxis experiments (Gray et al., 2004). Prior experience of hypoxia can activate HIF-1 and shift the animal's O_2 preference toward lower O_2 levels (Chang and Bargmann, 2008; Cheung et al., 2005). Hypoxia also enhances NaCl chemotaxis through HIF-1-dependent upregulation of TPH-1, a biosynthetic enzyme for the neural modulator serotonin (Pocock and Hobert, 2010). While the EGL-9 pathway chronically monitors O_2 changes to elicit behavioral plasticity through transcriptional regulation, acute sensing of O_2 at levels ranging from 4%–21% is mediated by soluble guanylate cyclase (GCY) family proteins (Cheung et al., 2004; Gray et al., 2004; McGrath et al., 2009; Zimmer et al., 2009).

The evolutionarily conserved EGL-9/HIF-1 pathway is highly regulated to dynamically control the expression of many genes important for hypoxic adaptation (Powell-Coffman, 2010). As 2-oxoglutarate-dependent dioxygenases with Fe^{2+} and ascorbate as cofactors, HIF PHDs are sensitive to ambient O_2 levels as well as to fluctuations in cell metabolic and redox status (Rose et al., 2011). In *C. elegans*, EGL-9 destabilizes HIF-1 via its hydroxylation and subsequent degradation by the VHL-1

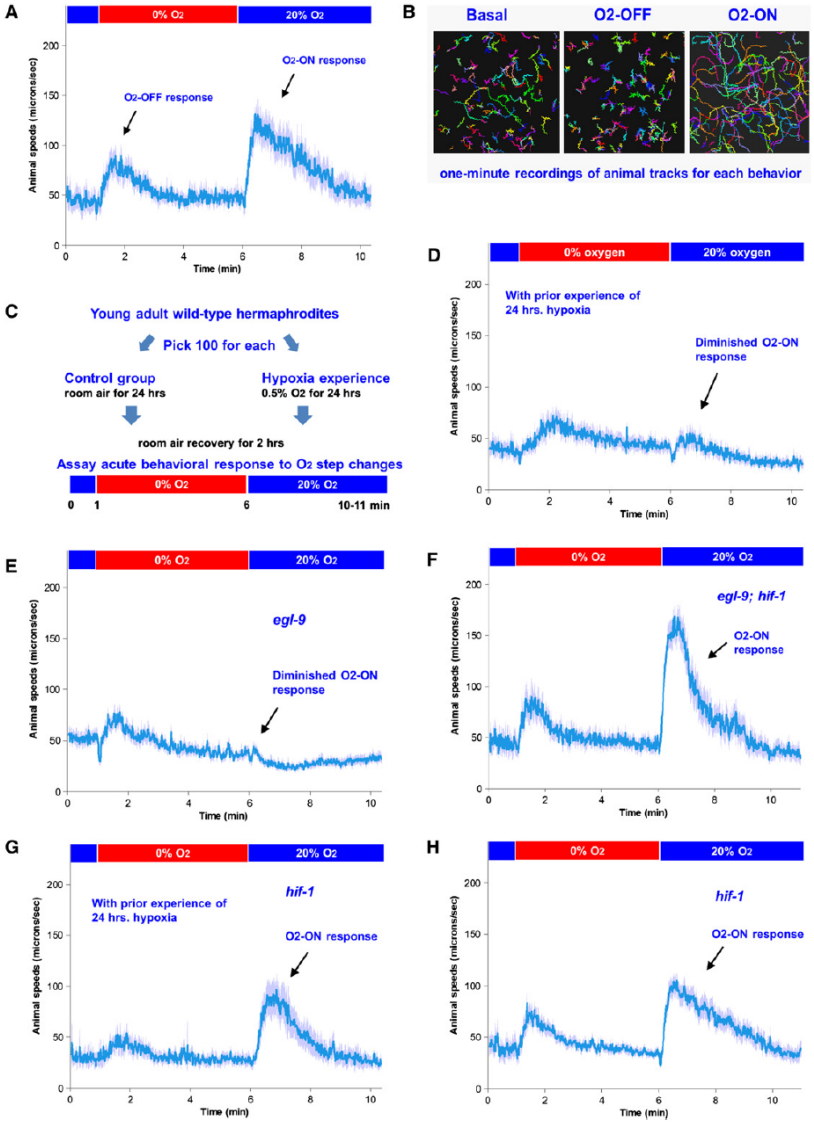

Figure 1. *C. elegans* Displays O_2-Associated Locomotive Behavioral Plasticity

(A) Acute locomotive speed changes during O2-OFF and O2-ON responses. Average speed values with 2 standard errors of the means (indicated by light blue) of a population of animals ($n > 50$) are shown with step changes of O_2 between 20% and 0% at the indicated times. The mean speed differences of all animals within 60 s before or after O_2 restoration are highly significant ($p < 0.001$, one-sided unpaired t test; also see Supplemental Information).

(B) Worm tracks showing locomotive patterns during basal state, O2-OFF, and O2-ON responses. One-minute recordings were made under basal conditions (20% O_2) or immediately following the initiation of O2-OFF or ON responses.

(C) Schematic of behavioral paradigms used to test the effects of prior experience of hypoxia on the O2-ON response.

complex and also inhibits HIF-1 transcriptional activity through unidentified hydroxylation-independent mechanisms (Shao et al., 2009). Similar dual-mode inhibition of HIF has been observed for mammalian HIF PHDs (Ozer et al., 2005; To and Huang, 2005). In addition, the *C. elegans* protein RHY-1 inhibits HIF-1 independently of VHL-1 (Shen et al., 2006), although the relationship between RHY-1 and EGL-9 and the mechanism by which RHY-1 inhibits HIF-1 remain to be established.

Hydrogen sulfide (H_2S), which is endogenously synthesized by many organisms, has recently emerged as a gaseous cell signaling molecule and neuromodulator involved in numerous biological processes. In mammals, H_2S critically affects dilation of blood vessels, hippocampal long-term potentiation, ischemia/reperfusion injury response, cell protection from oxidative stresses and neurodegenerative disorders, including Alzheimer's and Parkinson's disease (Gadalla and Snyder, 2010; Kimura, 2010; Li et al., 2011; Szabó, 2007). H_2S levels increase under hypoxic conditions and can mediate hypoxic effects on vasodilation and ventilatory responses (Olson et al., 2006; Peng et al., 2010). In *C. elegans*, exposure to nonlethal doses of H_2S activates HIF-1 and promotes survival of animals during H_2S exposure (Budde and Roth, 2010). H_2S also activates HIF in mammalian cells (Liu et al., 2010). How H_2S signals are perceived and transmitted to activate HIF and whether H_2S interacts with HIF PHD enzymes to modulate animal behaviors are unknown.

To identify components of the *egl-9/hif-1* pathway, we conducted a series of genetic screens and recovered mutations of *egl-9*, *hif-1*, *rhy-1*, and the gene *cysl-1*. A recent study found that *cysl-1* mutants are sensitized to H_2S toxicity via an unknown mechanism (Budde and Roth, 2011). We demonstrate that CYSL-1 acts upstream of HIF-1 as a signal transduction protein that directly binds to the EGL-9 proline hydroxylase in a H_2S-modulated manner and prevents EGL-9 from inhibiting HIF-1. We show that RHY-1, CYSL-1, and EGL-9 act in a cascade to control HIF-1 activity and modulate locomotive behavioral responses to changes in O_2 levels. *cysl-1* apparently evolved from an ancient metabolic cysteine synthase gene family, and the emergence of *cysl-1* functions in cell signaling exemplifies an intriguing case of gene "co-option" (True and Carroll, 2002) during genome evolution for adaptation to changing environmental conditions.

RESULTS

C. elegans Exhibits Locomotive Behavioral Plasticity in Response to the Experience of Hypoxia

O_2 availability pervasively influences *C. elegans* physiology and behavior, providing rich avenues to dissect fundamental molecular and neural mechanisms for behavioral plasticity. We developed a custom-built multiworm tracker with a computer-controlled gas-flow system (Figure S1A, available online) to seek robust *C. elegans* behaviors. We focused on the locomotion of adult *C. elegans* hermaphrodites (of the laboratory wild-type Bristol strain N2) in response to step changes of O_2 between 20% and 0% (anoxia). We measured the animals' mean locomotion speed and turning angle in the presence of bacterial food after we shifted O_2 concentration between 20% and 0% ("O2-OFF") and between 0% and 20% ("O2-ON"). Reducing O_2 caused a transient increase in locomotion speed and turning angle (Figures 1A, 1B, and S1B). The O2-OFF response resembled the previously reported local search behavior induced by food withdrawal (Gray et al., 2005) and lasted for about one minute after anoxia exposure.

With prolonged exposure to anoxia, animals eventually enter a state of suspended animation (Padilla et al., 2002). To examine the acute behavioral response to O_2 restoration, we returned the environment to 20% O_2 after five minutes of anoxia exposure. Animals responded to the acute elevation of O_2 with a dramatic acceleration of locomotion speed, which we defined as the "O2-ON" response (Figures 1A, 1B, and S1B). The O2-ON response was caused specifically by anoxia/reoxygenation (Figures 1A and S1H) and might reflect an aversive behavior to unfavorable anoxia/reoxygenation signals. The O2-ON response was also observed for animals under conditions without bacterial food, for the Hawaiian strain CB4856, and in response to smaller increases in O_2 levels (from 0% to 5% or 10%) (Figures S1B–S1F). These results identify the O2-ON response as a previously uncharacterized acute locomotive response induced by rapid and large increases in O_2 levels (0% to 5%–20% O_2).

To examine whether prior prolonged exposure to hypoxia would modify the O2-ON response, we cultured adult hermaphrodites at 0.5% O_2 for 24 hr, allowed them to recover for 2 hr in room air, and then tested them in our behavioral assay (Figure 1C). The hypoxia-experienced animals had an essentially normal O2-OFF response, while their O2-ON response was strikingly decreased, with a negligible acceleration in response to O_2 elevation (Figure 1D). To test how long the effects of hypoxia exposure last, we varied the duration of recovery after 24 hr of hypoxia exposure and found significant inhibition of O2-ON response for at least 8 hr after the hypoxia exposure (Figure S1I). To test how long hypoxia exposure is needed for such behavioral modification, we varied the duration of hypoxia experience and found that at least 16 hr of 0.5% O_2 were required to elicit complete inhibition of the O2-ON response (Figure S1J). These data suggest that inhibition of the O2-ON response requires prolonged prior hypoxia experience and can be long-lasting, representing a type of behavioral plasticity.

EGL-9 and HIF-1 Mediate the Hypoxia-Induced Reduction of the O2-ON Response

Since EGL-9 has been identified as the chronic O_2 sensor in *C. elegans* and HIF-1 has been implicated in other types of

(D) Behavior of hypoxia-experienced wild-type animals with suppressed O2-ON response, compared to that of naive animals as shown in (A). Graphs exclusively labeled "With prior experience of 24 hrs. hypoxia" show data for hypoxia-experienced but not naive animals.
(E) Behavior of *egl-9* mutants showing a lack of O2-ON response.
(F) Behavior of *egl-9; hif-1* mutants with a restored O2-ON response compared to that of *egl-9* mutants.
(G) Behavior of hypoxia-experienced *hif-1* mutants with a suppressed O2-ON response, compared to that of hypoxia-experienced wild-type animals.
(H) Behavior of *hif-1* mutants with a normal O2-ON response.

hypoxia-induced behavioral plasticity (Chang and Bargmann, 2008; Epstein et al., 2001; Pocock and Hobert, 2010), we examined *egl-9* and *hif-1* null mutants in our behavioral assays. Strikingly, mutations of *egl-9* caused the animals to be completely defective in the O2-ON response (Figures 1E and S2A). *egl-9* mutants accumulate constitutively active forms of HIF-1 (Epstein et al., 2001; Shao et al., 2009), so we postulated that the *egl-9* phenotype we observed reflect the hypoxia-mimicking effects of *egl-9* mutants that result from constitutive activation of HIF-1. Indeed, we found that *egl-9; hif-1* double mutants displayed a fully restored O2-ON response (Figure 1F). *hif-1* single mutants are severely defective in the hypoxia-induced inhibition of the O2-ON response (Figure 1G), while normal in the acute O2-OFF and O2-ON responses (Figure 1H). We found normal O2-ON responses by *tph-1*, *gcy-31*, *gcy-33*, *gcy-35*, *gcy-36*, *mbk-1*, and *swan-1* mutants and by a strain with apoptotic cell deaths of the URX, AQR, and PQR neurons (*qals2241*); these strains were previously implicated in EGL-9 or O_2-dependent responses (Chang and Bargmann, 2008; Pocock and Hobert, 2010; Shao et al., 2010; Zimmer et al., 2009) (Figures S2B–S2H). Together, these results suggest that the experience of hypoxia inactivates EGL-9, leading to HIF-1 activation and hypoxia-induced inhibition of the O2-ON response.

RHY-1 Is a Positive Regulator of EGL-9 and the O2-ON Response

To determine how EGL-9 is modulated to control the O2-ON behavior, we screened for mutants that resembled *egl-9* mutants. To facilitate this screen, we constructed an integrated transgenic reporter strain (*nIs470*) in which a green fluorescent protein (GFP) variant (Venus) was driven by the promoter of a known HIF-1 target gene, *K10H10.2* (Shen et al., 2006). *egl-9* mutants exhibited bright GFP fluorescence throughout the animal, whereas GFP was essentially absent in *egl-9(+)* and *egl-9; hif-1* double mutants (Figure 2A), indicating that the GFP transgene specifically reports the transcriptional activity of HIF-1.

We used ethyl methansulfonate (EMS) to mutagenize the *egl-9(+)*; $P_{K10H10.2}$*::GFP* (*nIs470*) strain and sought for mutations that activate *K10H10.2::GFP* expression. From a screen of approximately 30,000 haploid genomes, we isolated four mutations that failed to complement *egl-9*, two that failed to complement *vhl-1*, and another two (*n5492* and *n5500*) that identified a third complementation group and were genetically linked to a 900 kb interval on chromosome II (Table S1A, and data not shown). We noticed that this interval contains the gene *rhy-1*, which had been implicated in HIF-1 regulation (Shen et al., 2006). We determined DNA sequences of the *rhy-1* coding region in *n5492* and *n5500* animals and found missense mutations in both (Figures S3A–S3C). The *n5500* and *n5492* alleles caused animals to express ectopic *K10H10.2::GFP* and to be defective in the O2-ON response in a HIF-1-dependent manner (Figures 2B–2D, data not shown). An extrachromosomal array with *rhy-1(+)* genomic DNA rescued the defects in both the O2-ON response and GFP expression (Figures 2E–2F). Furthermore, RNAi against *rhy-1* and a *rhy-1* null deletion allele *ok1402* conferred the same phenotype as that of *n5500* mutants (Figures 2G and S3D). We conclude that *n5492* and *n5500* are alleles of *rhy-1* and that *rhy-1* is necessary for the O2-ON response.

To define the genetic relationship of *rhy-1* to *egl-9* and *hif-1*, we performed epistasis analysis by constructing double loss-of-function (LOF) or gain-of-function (GOF) mutants. *hif-1* is epistatic to *rhy-1*, since *hif-1* LOF suppressed *rhy-1* LOF phenotypes (Figures 2B and 2D). *egl-9* overexpression by an integrated transgene suppressed the *rhy-1* LOF phenotype of *K10H10.2::GFP* expression and the impaired O2-ON response, whereas *rhy-1* overexpression failed to suppress the corresponding *egl-9* LOF phenotype (Figure S3F and Table 1C). These data suggest a genetic pathway in which RHY-1 positively regulates EGL-9, which inhibits HIF-1 to regulate HIF-1 targets and behavior.

A *rhy-1(n5500)* Suppressor Screen Identified *cysl-1* as a Key Regulator of EGL-9 and Behavior

To identify the mechanism by which RHY-1 regulates EGL-9 and HIF-1, we performed a screen for suppressors of the ectopic expression of *K10H10.2::GFP* by *rhy-1(n5500)* mutants. From a screen of approximately 50,000 haploid genomes, we isolated 17 independent *n5500* suppressors that defined at least four genes (Table 1A). Two mutations failed to complement *hif-1* and restored the O2-ON response defects of *rhy-1(n5500)* animals. Mutations from the second complementation group caused reduced expression both of *K10H10.2::GFP* and of coinjection markers and are alleles of *tam-1*, which is known to be required for repetitive transgene expression (Hsieh et al., 1999). The third complementation group of seven alleles, including *n5515*, appeared to define a different gene involved in HIF-1 regulation. We also isolated three *egl-9* alleles (*n5535*, *n5539*, and *n5552*) that dominantly suppressed *rhy-1(n5500)*.

Three-factor mapping placed *n5515* between *dpy-6* and *egl-15* on chromosome X. Single-nucleotide polymorphism (SNP) mapping using the Hawaiian strain further positioned *n5515* within a 0.28 map unit region. We used RNAi against candidate genes in this region and found that RNAi against a single gene, *C17G1.7 (cysl-1)*, fully recapitulated the *n5515* phenotype. Sequence determination revealed that all seven mutants contained mutations in the *cysl-1* coding region, including five missense transition mutations, one nonsense transversion mutation, and a 330 bp deletion (*n5536*) (Figures 3A and S5C, Table 1B). Both *n5536* and another deletion allele of *cysl-1*, *ok762*, conferred the same phenotype as that of *n5515* mutants. Like *hif-1* alleles but unlike *tam-1* alleles, the *cysl-1* null alleles restored the O2-ON response defect of *rhy-1(n5500)* mutants (Table 1C, Figures 3B–3E, and data not shown).

To define the relationship of *cysl-1* with *egl-9*, *hif-1*, and *rhy-1*, we performed epistasis analysis by constructing double mutants for individual pairs of *rhy-1*, *cysl-1*, *egl-9*, and *hif-1* mutations (Table 1C). *hif-1* was epistatic to all three other genes. *egl-9* was epistatic to *cysl-1*, which was epistatic to *rhy-1* (Figures 3D–3G and Table 1C). Semiquantitative measurements by western blots of GFP protein in various single or multiple mutants were consistent with phenotypic analyses of *K10H10.2::GFP* fluorescence levels and O2-ON responses, e.g., *cysl-1* completely suppressed *rhy-1* in GFP levels (Figure 3H). Furthermore, the endogenous expression of *K10H10.2* exhibited patterns of regulation similar to that of GFP driven by the *K10H10.2* promoter (Figure 3I). These results led us to suggest

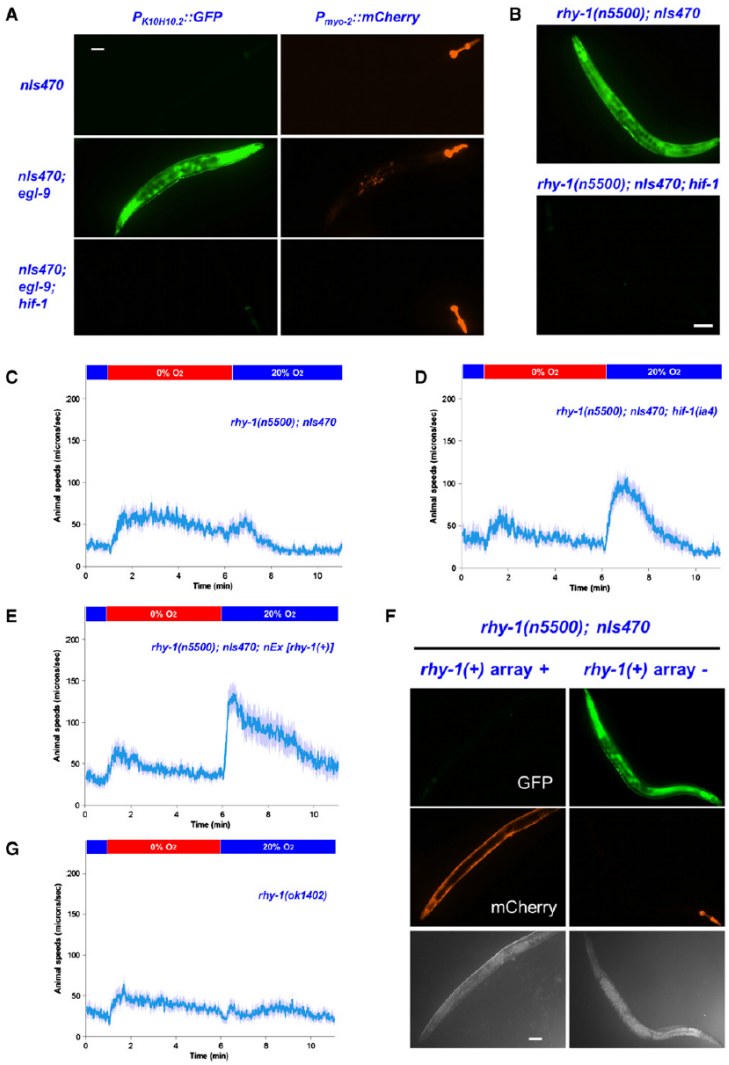

Figure 2. RHY-1 Modulates HIF-1 and the O2-ON Behavioral Response through EGL-9

(A) Fluorescence micrographs showing constitutive GFP signals in *egl-9(-)* mutants with the transgenic reporter $P_{K10H10.2}$::*GFP* (*nls470*), indicating high HIF-1 transcriptional activity. GFP signals are absent in the wild-type and in *egl-9(sa307); hif-1(ia4)* double mutants, except for weak GFP fluorescence in the pharynx. *myo-2::mCherry* expressed in pharyngeal muscles was used as the co-injection marker. Scale bar: 25 μm.

(B) *rhy-1(n5500)* mutants with strong constitutive GFP expression that is suppressed by *hif-1* mutations.

(C) *rhy-1(n5500)* mutants show a defective O2-ON response.

(D) *rhy-1(n5500); hif-1(ia4)* double mutants show a restored O2-ON response.

(E) An extrachromasomal array containing *rhy-1(+)* genomic fragments rescues the behavioral defect in the O2-ON response of *rhy-1(n5500)* mutants.

(F) Rescued *K10H10.2::GFP* ectopic expression of *rhy-1(n5500)* mutants by *rhy-1(+)* arrays. *myo-3::mCherry* expressed in body wall muscles was the coinjection marker.

(G) *rhy-1(ok1402)* null mutants show a defective O2-ON response.

Table 1. Genetic Screens Identify *cysl-1* as a Regulatory Component of the *egl-9* Pathway

(A) *rhy-1(n5500)* Suppressors

Chr.	Alleles	Phenotype	Genes
V	*n5513, n5527*	Recessive	*hif-1*
V	*n5512, n5514, n5516, n5538, n5541*	Recessive	*tam-1*
V	*n5535, n5539, n5552*	Dominant	*egl-9*
X	*n5515, n5518, n5519, n5521, n5522, n5536, n5537*	Recessive	*cysl-1 (C17G1.7)*

(B) *cysl-1* Alleles from *rhy-1(n5500)* Suppressor Screen

Genotype	GFP	O2-ON Response	Mutation	A.A. Change
nIs470 IV	0%	Normal		
n5500 II; nIs470 IV	100%	Defective		
n5500 II; nIs470 IV; n5515 X	0%	Normal	GGA- > AGA	G183R
n5500 II; nIs470 IV; n5518 X	0%	Normal	TAT- > TAA	Y93Ochre
n5500 II; nIs470 IV; n5519 X	0%	Normal	AGA- > AAA	R259K
n5500 II; nIs470 IV; n5522 X	0%	Normal	GCT- > GTT	A88V
n5500 II; nIs470 IV; n5521 X	0%	Normal	GGG- > GAG	G181E
n5500 II; nIs470 IV; n5537 X	0%	Normal	CCA- > CTA	P75L
n5500 II; nIs470 IV; n5536 X	0%	Normal	deletion	

(C) Epistatic Analysis of the RHY-1/CYSL-1/EGL-9/HIF-1 Pathway

Genotype	GFP	O2-ON Response
nIs470; egl-9(n586)	100%	Defective
nIs470; rhy-1(n5500)	100%	Defective
nIs470; hif-1(ia4)	0%	Normal
nIs470; cysl-1(ok762)	0%	Normal
nIs470; egl-9(n586); hif-1(ia4)	0%	Normal
nIs470; rhy-1(ok1402); hif-1(ia4)	0%	Normal
nIs470; rhy-1(ok1402); cysl-1(ok762)	0%	Normal
nIs470; egl-9(sa307); cysl-1(ok762)	100%	Defective
nIs470; rhy-1(n5500); nIs [egl-9(+)]	0%	Normal
nIs470; egl-9(n586); nEx [rhy-1(+)]	100%	Defective

a genetic pathway in which *rhy-1* inhibits *cysl-1*, which inhibits *egl-9*, which inhibits *hif-1*, which promotes *K10H10.2* expression and inhibits the O2-ON response.

cysl-1 Is Expressed in and Functions in Neurons

To explore the function of CYSL-1 in HIF-1 regulation and behavioral modulation, we determined the expression pattern of *cysl-1* using an integrated transcriptional GFP reporter and an extrachromosomal translational GFP reporter. A 2.8 kb promoter of *cysl-1* drove GFP expression mainly in the nervous system of adult hermaphrodites (Figure 4A). The *cysl-1::GFP* expression pattern was similar for the transcriptional and translational reporters (Figures 4A–4E and S4A). GFP was observed in subsets of pharyngeal neurons, amphid sensory neurons and tail neurons, starting from late embryonic stages and persisting into adults. We identified GFP-positive cells as the AVM sensory neuron, the BDU interneurons (Figure 4B), and the pharyngeal I1 interneurons and M2 motor neurons (Figure 4C), based on their characteristic processes and nuclear positions. GFP in body wall muscles, hypoderm, and intestine was present in larvae but only weakly detectable in adult animals.

The neuronal expression pattern of *cysl-1* is consistent with its role in O2-ON behavioral modulation. However, *cysl-1* mutations suppressed ectopic *K10H10.2::GFP* expression in the hypoderm of *rhy-1* mutants (Figures 3C and S3B, Table 1B). To further examine the site-of-function of *cysl-1*, we generated transgenic strains harboring a wild-type *cysl-1* cDNA driven by the *ric-19* neural-specific promoter (Ruvinsky et al., 2007). *ric-19* promoter-driven neuronal expression of *cysl-1*, but not *dpy-7* promoter-driven hypodermal expression of *cysl-1*, rescued the O2-ON behavior of *rhy-1; cysl-1* double mutants (Figures 4F, 4G, and S4B). Hypodermal expression of *cysl-1* rescued the *K10H10.2::GFP* expression of *rhy-1; cysl-1* mutants (Figure S4C). These data support the hypothesis that *cysl-1* functions in neurons to control HIF-1 activity for O2-ON behavioral modulation. We suggest that hypodermal *K10H10.2* expression reflects HIF-1 activation but is not functionally important for O2-ON behavioral modulation. In support of this notion, we found that *egl-9(-); K10H10.2 (-)* double mutants were defective in the O2-ON response, just as are *egl-9(-)* single mutants (Figure S4D). As an independent test of the importance of neuronal regulation of HIF-1 for O2-ON behavioral modulation, we introduced

a stabilized form of the HIF-1 protein (P621A) into various tissues in the *egl-9; hif-1* double mutant background. Proline 621 of HIF-1 is the hydroxylation target of EGL-9, and the P621 mutant HIF-1 protein is enhanced in stability (Epstein et al., 2001; Pocock and Hobert, 2010). Stabilization of HIF-1 protein was not sufficient to cause a defect in the O2-ON response (Figure S4E), suggesting that additional P621 hydroxylation-independent activation of HIF-1 is required for suppressing the O2-ON response. This hypothesis is also consistent with the partially defective O2-ON response of *vhl-1(-)* mutants (Figure S2F). In the *egl-9; hif-1* background, neuronal expression of *hif-1*(P621A) driven by an *unc-14* promoter resulted in a defective O2-ON response (Figure 4H). By contrast, hypodermal expression of *hif-1*(P621A) driven by the *dpy-7* promoter or muscle-specific expression of *hif-1*(P621A) driven by the *unc-120* promoter did not cause a defective O2-ON response (Figures 4I and S4F). These results indicate a neuronal site-of-function of *cysl-1* in regulating the *egl-9*/*hif-1* pathway to modulate the O2-ON response.

cysl-1 Encodes a Member of an Evolutionarily Ancient Cysteine Synthase/Sulfhydrylase Gene Family

We used BLASP to search the NCBI protein database and found many CYSL-1 homologs belonging to the cystathionine-beta synthase/cysteine synthase (CBS/CS) family of the fold type-II pyridoxal-5′-phosphate (PLP)-dependent proteins in diverse species ranging from bacteria to humans (Figures 5A and S5A). The *cysl-1(n5515)* allele we isolated from the *rhy-1(n5500)* suppressor screen converted glycine 183 to arginine (Figure 5A, Table 1B). Strikingly, this glycine is 100% conserved among the *cysl-1* homologs of all species examined (bacteria, yeast, flies, zebrafish, mice, and humans) and is positioned at the core of a motif sequence crucial for binding to the obligate cofactor PLP (Aitken et al., 2011) (Figures 5A and S6C). Interestingly, one of the CYSL-1 paralogs is the HIF-1 target gene *K10H10.2*, indicating a possible feedback regulation of this gene family. We raised a polyclonal CYSL-1 antibody and found reduced levels of steady-state CYSL-1(*n5515*) proteins in soluble fractions of *C. elegans* and bacterial homogenates compared to those of wild-type CYSL-1 (Figures 5B and S5B). The introduction at residue 183 of arginine, which has a long protruding hydrophilic side chain (Figure S6E), could disrupt binding to PLP and render the protein improperly folded and unstable. *n5521*, *n5522*, and *n5537* mutants similarly showed reduced levels of CYSL-1 (Figures 5B and S5B, S6C–S6F).

We studied recombinant CYSL-1 proteins purified from *E. coli* and found that CYSL-1 exhibited properties typical of type-II PLP-dependent proteins (Figures S5D–S5G). We tested several biochemical reactions that had previously been associated with other PLP-dependent CBS enzymes and cysteine synthases (Aitken et al., 2011; Mozzarelli et al., 2011). While assays for O-phosphoserine sulfhydrylase, cyanoalanine synthase, and cystathionine beta-synthase failed to yield significant enzymatic activities, CYSL-1 exhibited activity as an O-acetylserine sulfhydrylase (OASS), converting OAS and sulfide into L-cysteine and acetate (Figures 5C and 5D). However, the Michaelis constant K_M for sulfide (4.2 mM) of purified CYSL-1 was at least an order of magnitude higher than those of bona fide cysteine synthases, CYSL-1 homologs from bacteria and plants (Figure 5E), suggesting that the cysteine synthase activity of CYSL-1 might be insignificant physiologically in vivo and dispensable for regulating the *egl-9*/*hif-1* pathway. *cysl-1(n5519)* mutations suppressed HIF-1 target expression and restored the O2-ON response of *rhy-1(n5500)* mutants, yet the CYSL-1(*n5519)* mutant protein, with the abnormal lysine (R259K) residue on its surface far from the active site (Figure S6F) exhibited levels of OAS sulfhydrylase activity similar to that of wild-type CYSL-1 (Figures S6A and S6B, Table 1B). Notably, the CYSL-1(*n5519*) mutant protein exhibited steady-state levels comparable to that of wild-type CYSL-1 (Figures 5B and S5B). We obtained four additional lines of evidence supporting the notion that CYSL-1 regulates the EGL-9 pathway as a cell-signaling mediator independently of its cysteine synthase activity. First, the *C. elegans* genome does not appear to encode any homologs of O-serine acetyltransferase (SAT), which is an obligate component of the cysteine synthase pathway in bacteria and plants (Mozzarelli et al., 2011; Wirtz and Droux, 2005). BLASTP searches of animal protein databases against bacterial or plant SAT protein queries yielded only three significant hits (E value < 1e-30), in honey bees, *Xenopus*, and *Caenorhabditis remanei*, respectively. However, all three lack the invariant C-terminal isoleucine essential for binding to OASS (Campanini et al., 2005; Francois et al., 2006; Mozzarelli et al., 2011), and no other *Caenorhabditis* species appeared in the search. Second, a potential bacterial source of OAS as a cysteine synthase substrate for CYSL-1 is unlikely, since feeding *rhy-1(n5500)* mutants on a *cysE*-deleted *E. coli* strain deficient in OAS synthesis did not rescue the *rhy-1(n5500)* phenotype (Figure S6H). Third, we found that a lysine in an otherwise highly conserved motif crucial both for binding SATs and for functional CS activity (Bonner et al., 2005) is a proline in CYSL-1 (Figure S6G). Fourth, we found that CYSL-1 directly interacts with the C terminus of EGL-9 instead of forming a cysteine synthase complex via its active site, as shown and discussed below.

CYSL-1 Interacts with EGL-9 to Mediate H_2S-Induced HIF-1 Activation and Behavioral Plasticity

In our *rhy-1(n5500)* suppressor screen, we isolated three mutations (*n5535*, *n5539*, and *n5552*) that strongly suppressed *K10H10.2::GFP* expression and the defective O2-ON response (Table 1A and Figure 6A). Linkage mapping placed *n5535* on the right arm of chromosome V close to *egl-9*, which prompted us to determine the sequence of the *egl-9* coding region of these mutants. We found that *n5535* animals carry a missense mutation that converts the EGL-9 C-terminal sequence EYYI to KYYI, while the *n5539* and *n5552* alleles alter a splicing donor and a splicing acceptor site, respectively, causing EGL-9 to be prematurely truncated near the EGL-9 C terminus without affecting the O_2-sensing proline-hydroxylase domain (Figure 6B). We noticed that the EYYI sequence of EGL-9 resembles the C-terminal SAT sequence DYVI, which penetrates into the active site of OASS, the CYSL-1 homolog in *Arabidopsis* (Francois et al., 2006). These observations, together with the dominant nature of the *n5535* phenotype and our epistasis analysis indicating that CYSL-1 inhibits EGL-9, suggested that *n5535* might disrupt an EGL-9-interacting interface with CYSL-1 and in that way dominantly suppress *rhy-1* LOF phenotypes.

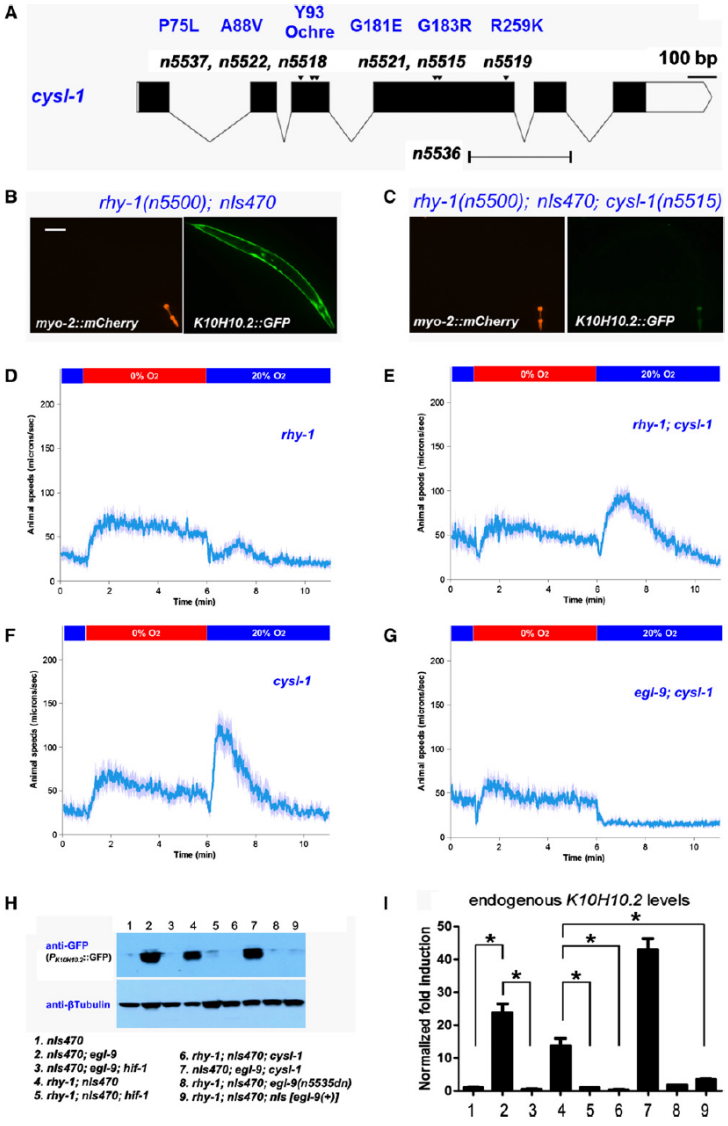

Figure 3. A Modifier Screen Identified *cysl-1* as a Regulator of HIF-1 and Behavior

(A) A schematic of the *cysl-1* gene, indicating the seven alleles isolated from the *rhy-1(n5500)* suppressor screen. This drawing was generated by the Exon-Intron Graphic Maker (WormWeb.org).

(B) *K10H10.2::GFP* expression in *rhy-1(n5500); nls470* mutants with *myo-2::mCherry* as the coinjection marker. Scale bar: 25 μm.

(C) *K10H10.2::GFP* expression is absent in *rhy-1(n5500); nls470; cysl-1(n5515)* mutants.

(D and E) A defective O2-ON response of *rhy-1(n5500)* mutants is suppressed by the *cysl-1(5515)* mutation.

(F) *cysl-1(ok762)* null mutants show a normal O2-ON response.

To test directly whether CYSL-1 binds to the EGL-9 C terminus, we generated a series of *egl-9* mutant constructs and analyzed them in a yeast two-hydrid assay. In this assay, EGL-9 proteins without the N-terminal zinc-finger domain specifically associated with CYSL-1, while the C terminus alone or the full-length protein exhibited nonspecific activation of the assay reporter without CYSL-1 (Figure 6C and data not shown). A five-amino-acid deletion of the EGL-9 C terminus (*egl-9* ΔPEYYI) abolished the specific interaction between EGL-9 and CYSL-1. Furthermore, EGL-9(*n5535*) mutant proteins harboring an E720K substitution near the C terminus, or C-terminally truncated proteins caused by *n5539*, completely failed to interact with CYSL-1. We also probed the CYSL-1 interaction with EGL-9 using an independent fluorometric assay previously used to demonstrate direct peptide interactions between OASS and SAT proteins (Campanini et al., 2005; Francois et al., 2006). Wild-type EGL-9 C-terminal peptides with the last four, ten, or 14 amino acid residues significantly enhanced the intrinsic fluorometric emission of CYSL-1 in a dose-dependent manner (Figures S7A–S7D). Such enhancements were completely abolished for mutant peptides in which either the terminal isoleucine residue was substituted with alanine or the glutamic acid residue was substituted with lysine, as in *egl-9(n5535)* mutants (Figures S7E and S7F). These results demonstrated direct association between CYSL-1 and EGL-9 specifically mediated by the C-terminal residues of EGL-9.

Because CYSL-1, with its presumptive evolutionary origin from sulfide metabolism pathways, is associated with the EGL-9 C terminus and our genetic analysis identified CYSL-1 as a negative regulator of EGL-9, we wondered whether CYSL-1 might transduce signals from H_2S to the HIF-1 transcriptional pathway through EGL-9 inhibition. To test this hypothesis, we first confirmed previous findings that low nonlethal exposure of H_2S can activate HIF-1 as assayed by *K10H10.2::GFP* expression and by real-time RT-PCR analysis of two different HIF-1 target genes, *K10H10.2* and *nhr-57* (Figures 6D–6F). We found that the strong induction of *K10H10.2* and *nhr-57* in response to H_2S exposure was strikingly absent in *cysl-1* mutants and also in *egl-9(n5535)* mutants containing the E720K mutation, which selectively disrupts the interaction between CYSL-1 and EGL-9 (Figures 6D–6F). Although H_2S exposure can activate the HIF-1 target genes *K10H10.2* and *nhr-57*, it was not sufficient to inhibit the O2-ON response (Figures S7G). H_2S was previously shown to upregulate HIF-1 activity independently of VHL-1 (Budde and Roth, 2010), indicating that HIF-1 protein stabilization acts in parallel with H_2S exposure for enhanced HIF-1 activation. Supporting this notion, we found that H_2S elicited inhibition of the O2-ON response in animals (*otIs197 [P_{unc-14}::hif-1P621A]*) harboring the stabilized mutant P651A HIF-1 protein in neurons (Figures S7G–S7I). Furthermore, exposure to H_2S markedly enhanced the interaction between CYSL-1 and EGL-9 in vivo (Figure 6G). These data indicate that CYSL-1 and its interaction with the EGL-9 C terminus are crucial for activation of HIF-1 targets in response to H_2S exposure and that this mechanism acts together with EGL-9-mediated HIF-1 hydroxylation to regulate HIF-1 and modulate the O2-ON response.

Because hypoxia promotes H_2S accumulation (Olson, 2011; Olson et al., 2006; Peng et al., 2010), we directly tested whether the experience of hypoxia requires CYSL-1 to modulate the *egl-9/hif-1* pathway and the O2-ON behavioral response. Unlike wild-type animals, which exhibited robust hypoxia experience-induced inhibition of the O2-ON response, *cysl-1* mutants were defective in such behavioral plasticity (Figure 6H). Naive wild-type animals and *cysl-1* mutants without prior hypoxia experience were both normal in the O2-ON response (Figures 1A and 3F). Furthermore, *egl-9(n5535)* mutants, in which the E720K mutation disrupts interaction with CYSL-1, were defective in the hypoxia-induced inhibition of the O2-ON response (Figure 6I). These results demonstrate that CYSL-1 and its interaction with EGL-9 are essential for hypoxia experience-dependent inhibition of the O2-ON response.

DISCUSSION

Our studies have identified a hypoxia-induced behavioral plasticity of *C. elegans*, delineated a genetic pathway for its regulation (Figure 7A), discovered CYSL-1 from a genetic screen as a key component of this pathway, and elucidated essential roles of the interaction between CYSL-1 and EGL-9 in mediating H_2S signaling to HIF-1 and for hypoxia experience-dependent behavioral modulation (Figures 7B and 7C). Our combined genetic, biochemical, and behavioral data support the following model. Under conditions of no prior experience of hypoxia, EGL-9 inhibits both the stability (via hydroxylation) and the transcriptional activity of HIF-1 to allow a robust O2-ON locomotive behavioral response; RHY-1 negatively regulates CYSL-1 to prevent it from inhibiting EGL-9 (Figure 7B). Under hypoxic conditions, decreased O_2 levels cause impaired EGL-9 hydroxylase activity and consequent stabilization of the HIF-1 protein; H_2S, endogenously and/or from local environments accumulates during prolonged hypoxia and promotes the interaction of EGL-9 and CYSL-1, which sequesters EGL-9 and thus prevents EGL-9 from inhibiting the transcriptional activity of HIF-1; together, EGL-9 sequestration by CYSL-1 and hypoxia-induced impairment of the hydroxylase activity of EGL-9 drive activation of neuronal HIF-1 target genes to coordinate a transcriptional program that culminates in inhibition of the O2-ON response (Figure 7C).

The O2-ON response occurs within a brief window (<30 s), which might reflect a rapid aversive behavioral response to unfavorable anoxia/reoxygenation signals, whereas the EGL-9-mediated O_2-sensing mechanism operates during a much longer period (24 hr) of hypoxia exposure (Figures 1A–1H). Several neurons (URX, AQR, PQR, BAG) and specific guanylate cyclases have been identified as O_2 sensors for hyperoxia avoidance

(G) *egl-9(sa307); cysl-1(ok762)* double mutants with a defective O2-ON response.
(H) Western blots of reporter GFP expression driven by the *K10H10.2* promoter from single or multiple LOF or GOF mutants of *rhy-1*, *cysl-1*, *egl-9*, and *hif-1*.
(I) Real-time PCR quantification of endogenous K10H10.2 mRNA levels (normalized to the control group of *nls470* animals) in various mutants as indicated in (H).
*$p < 0.01$, one-way ANOVA, Bonferroni posttest.

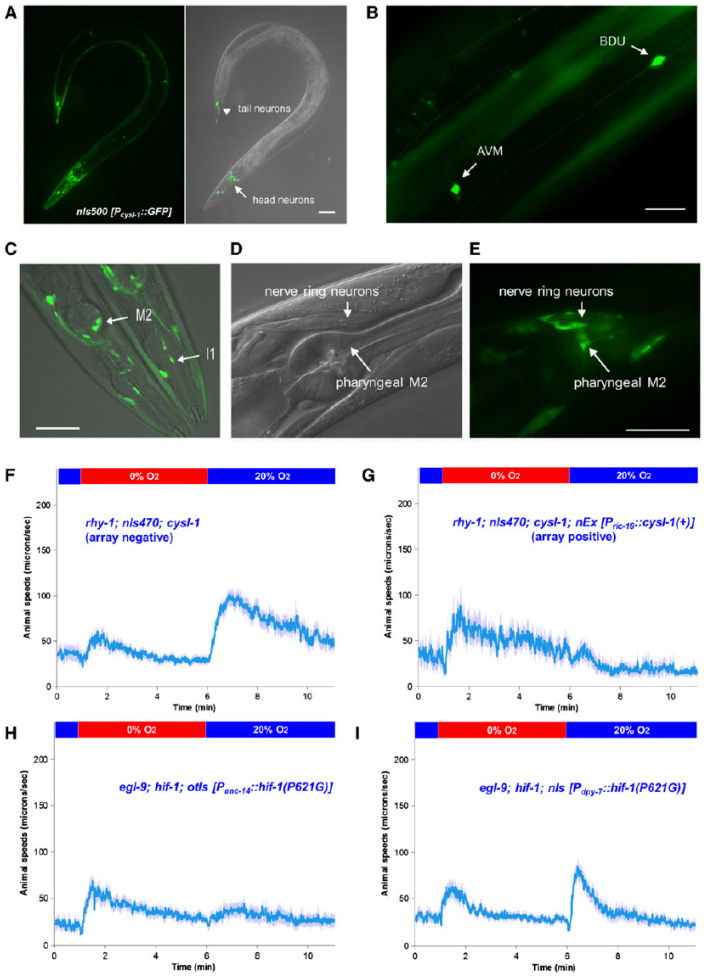

Figure 4. Expression Pattern and Site-of-Function of CYSL-1

(A) Fluorescence and Nomarski images showing the expression pattern of *cysl-1* as visualized by the integrated transcriptional GFP reporter *nls500*, which harbors a 2.8 kb promoter of *cysl-1* fused to GFP. Head neurons are indicated by the arrow, and tail neurons are indicated by the arrowhead.

(B) Enlarged view of fluorescence micrograph showing AVM and BDU neurons. Scale bars: 25 μm.

(C) Confocal microscopic view of pharyngeal (I1 and M2 indicated by arrows) and head neurons.

(D and E) Expression patterns of *cysl-1* as visualized by the extrachromasomal array *nEx1838* with a translational GFP reporter harboring the promoter and genomic coding regions of *cysl-1* fused in-frame to GFP.

(F and G) Rescue of *cysl-1(n5515)* phenotypes by neuronal expression of *cysl-1(+)* cDNA driven by the *ric-19* promoter.

(H) The *unc-14* promoter-driven neuronal activation of HIF-1 causes defects in the O2-ON response of *egl-9(sa307); hif-1(ia4)* double mutants.

(I) The *dpy-7* promoter-driven hypodermal activation of HIF-1 does not cause defects in the O2-ON response of *egl-9; hif-1* double mutants.

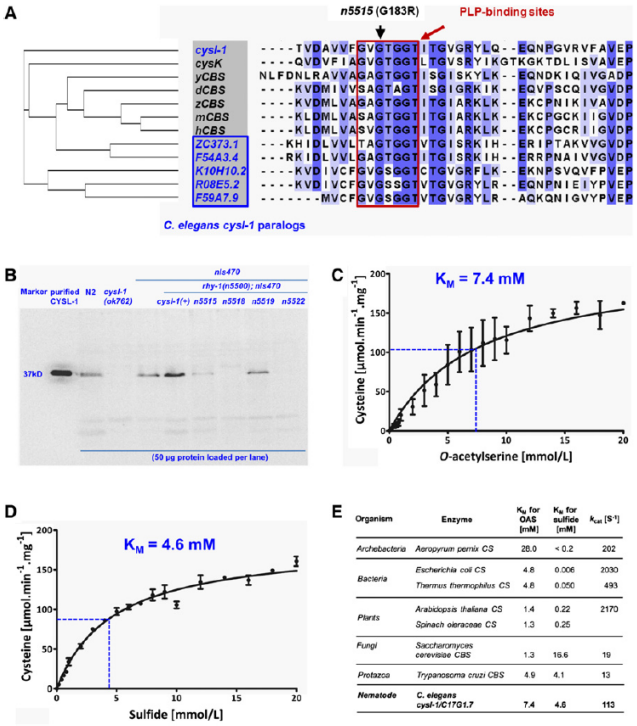

Figure 5. Evolutionary and Enzymatic Characteristics of CYSL-1

(A) Alignment of CYSL-1 homologs identifies a highly conserved glycine disrupted by *cysl-1(n5515)*. This phylogenetic tree was generated using ClusterW2 and is displayed in a cladogram. The PLP-binding site is highlighted by the red box (Aitken et al., 2011). *C. elegans cysl-1* paralogs are indicated in the blue box.

(B) Endogenous CYSL-1 protein levels as determined by SDS-PAGE and western blots and a polyclonal antibody against CYSL-1. *C. elegans* protein lysates from various genetic backgrounds were analyzed. Protein samples of 50 µg were loaded per lane.

(C and D) Purified recombinant CYSL-1 exhibits intrinsic cysteine synthase activity. Dependence of cysteine generation on varying OAS concentration with 20 mM sulfide and varying sulfide concentration with 20 mM OAS, respectively. Means of three measurements are shown and the Michaelis-Menten equation was used for curve fitting. Error bars represent SD (E) K_M and k_{cat} values of CYSL-1 (determined from Figures 5C and 5D) and OAS sulfhydrylases of other species as established from previous studies (Bonner et al., 2005; Mino et al., 2000; Mozzarelli et al., 2011; Ono et al., 1994). K_M: Michaelis value, k_{cat}: turnover number.

(5%–10% to 21% O_2) in *C. elegans* (Cheung et al., 2004; Gray et al., 2004; Zimmer et al., 2009), but the O2-ON behavior appears to depend on distinct O_2 sensors (0% to 5%–20% O_2) and neural mechanisms (Figures S1G and S2B–S2G). In contrast to naive animals, hypoxia-experienced animals suppress the subsequent O2-ON response and do so in a manner that depends on HIF-1 activation of target genes in neurons (Figures 4F–4I), and the behavioral effect can last for up to 8 hr after the initial trigger stimulus of 24 hr of hypoxia (Figures S1I and S1J). Such experience-dependent persistent neural modification might represent a behavioral plasticity that acts as a gain-control mechanism to dampen neural responses to strong environmental stimuli (Demb, 2008). The experience of hypoxia might also produce preconditioning effects and reduce the O2-ON response to anoxia/reoxygenation-induced cellular signals.

Our studies and those of others (Chang and Bargmann, 2008; Cheung et al., 2005; Pocock and Hobert, 2010) demonstrate that HIF-1 plays crucial roles in hypoxia experience-dependent *C. elegans* behavioral modifications. We identified a genetic pathway that regulates HIF-1 and hypoxia-induced behavioral plasticity (Figure 7A). What are the underlying molecular mechanisms? RHY-1 is an endoplasmic reticulum acyltransferase-like protein (Figure S3C) and appears to downregulate the abundance of CYSL-1 protein (Figure 5B). One possibility is that RHY-1 promotes CYSL-1 N-terminal acetylation, a modification known to alter plant CYSL-1-like sulfhydrylases (Wirtz et al., 2010), and in this way also promotes CYSL-1 degradation (Hwang et al., 2010). All three *egl-9* alleles isolated from our *rhy-1(n5500)* suppressor screen disrupt the EGL-9 C terminus without affecting the O_2-sensing PHD domain, suggesting that CYSL-1 sequestration of EGL-9 operates in parallel to EGL-9 hydroxylation of HIF-1 and that EGL-9 regulates HIF-1 at two different levels. Specifically, hypoxia might activate HIF-1 both by causing CYSL-1-mediated sequestration of EGL-9 and by preventing O_2-stimulated HIF-1 degradation. Under normoxic conditions, EGL-9 might act in part through SWAN-1 and MBK-1 (Shao et al., 2010) independently of RHY-1 and CYSL-1 to inhibit HIF-1 transcriptional activity. Such dual-mode EGL-9 inhibition of HIF-1 is consistent with previous studies of *C. elegans* and mammalian cells indicating that EGL-9-like HIF proline hydroxylases inhibit HIF proteins through both enzymatic hydroxylation to decrease HIF protein stability and nonenzymatic suppression of HIF transcriptional activities (Ozer et al., 2005; Shao et al., 2009; To and Huang, 2005). However, in previous studies (Budde and Roth, 2010; Shen et al., 2005) hypoxia has not fully mimicked the effects of EGL-9 inactivation and it has been unclear whether or not the second EGL-9 pathway mediates a response to hypoxia. Importantly, we found that sufficient hypoxia can fully mimic the suppressed O2-ON

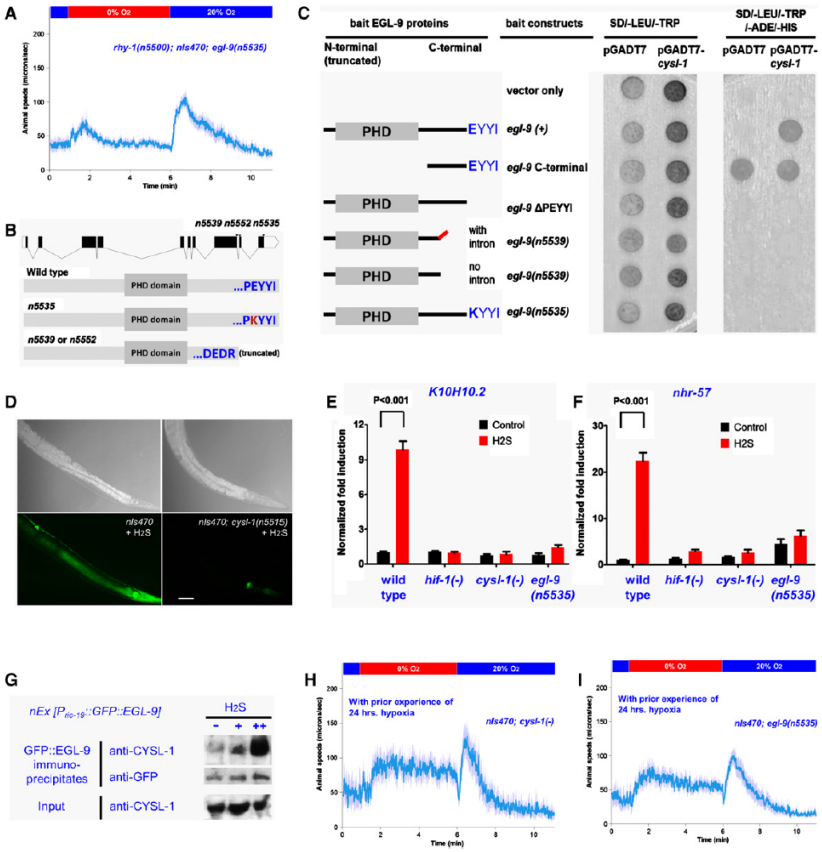

Figure 6. CYSL-1 Interaction with EGL-9 Mediates H_2S Signaling to HIF-1 and Behavioral Plasticity

(A) The gain-of-function mutation *egl-9(n5535)* fully suppresses the O2-ON defect of *rhy-1(n5500)* mutants.

(B) Two dominant suppressors of *rhy-1(n5500)* alter the C terminus of EGL-9. *n5535* converts glutamic acid 720 to lysine, while *n5539* and *n5552* are splice-donor and acceptor mutations, respectively, that result in a C-terminally truncated EGL-9 protein.

(C) Yeast two-hybrid assays with colony growth on selective plates (SD/-LEU/-TRP, or SD/-LEU/-TRP/-HIS3/-ADE) after cotransformation of *cysl-1* prey constructs and various *egl-9* bait constructs. The growth with vector-only control group, i.e., pGADT7 with *egl-9*-C-terminal, indicates non-specific reporter activation. All *egl-9* constructs lack the N-terminal domain, which conferred moderate non-specific reporter activation. Note the specific association of CYSL-1 with EGL-9 with an intact C terminus but not with *n5535* or *n5539* mutant EGL-9.

(D) Exposure to low H_2S induced GFP fluorescence from the *K10H10.2::GFP* reporter in wild-type but not *cysl-1* mutant animals. Scale bars: 25 μm.

(E) QPCR measurements of the endogenous HIF-1 target *K10H10.2* mRNA in the wild-type and in *hif-1(ia4)*, *cysl-1(ok762)*, or *egl-9(n5535)* mutant backgrounds. $p < 0.001$, two-way ANOVA, Bonferroni posttest.

(F) QPCR measurements of the endogenous HIF-1 target *nhr-57* in the wild-type and in *hif-1(ia4)*, *cysl-1(ok762)*, or *egl-9(n5535)* mutant backgrounds.

(G) Protein Co-IP experiments showing that the interaction between endogenous CYSL-1 and the GFP::EGL-9 fusion protein in vivo is markedly enhanced by H_2S exposure. GFP-bound protein complexes isolated from lysates of the strain *nEx [P_{nlc-19}::egl-9::gfp]* using anti-GFP affinity beads were analyzed by SDS-PAGE and western blots. GFP levels served as internal loading controls.

(H) Behavior of *cysl-1* null mutants with decreased inhibition of the O2-ON response after 24 hr hypoxia experience as compared to hypoxia-experienced wild-type animals.

(I) Behavior of *egl-9(n5535)* mutants with decreased inhibition of the O2-ON response after 24 hr hypoxia experience.

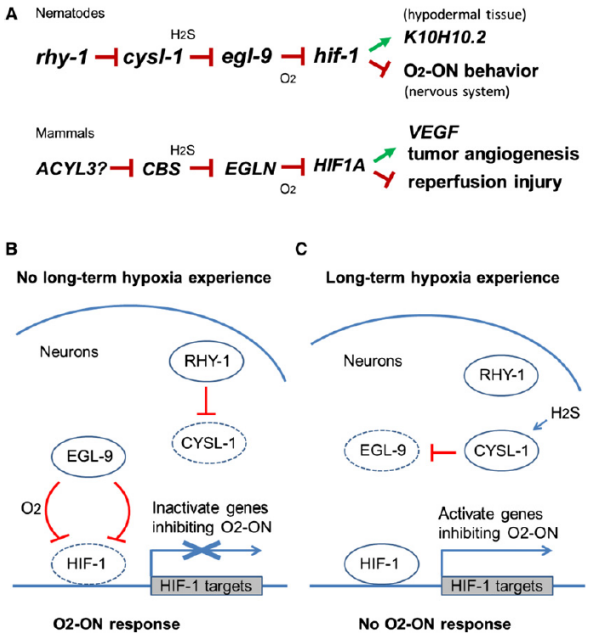

Figure 7. Models for Behavioral Plasticity Mediated by the RHY-1/CYSL-1/EGL-9/HIF-1 Pathway

(A) The genetic pathway in which *rhy-1*, *cysl-1*, and *egl-9* act in a negative-regulatory cascade to control the activity of HIF-1, which functions in neurons to modulate the O2-ON response and in the hypoderm to regulate *K10H10.2* expression.

(B) Model depicting the major molecular interactions in neurons of naive animals without experience of hypoxia, enabling the normal O2-ON response. EGL-9 promotes HIF-1 degradation (indicated by HIF-1 with dotted line) by O_2-dependent hydroxylation and also inhibits HIF-1 transcriptional activity.

(C) Model depicting the major molecular interactions in neurons of animals with experience of hypoxia leading to their suppressed O2-ON response. Decreased O_2 during hypoxia impairs HIF-1 hydroxylation, which stabilizes HIF-1 but alone is not sufficient to activate HIF-1 targets. Hypoxia also increases H_2S levels to promote CYSL-1 sequestration of EGL-9, thus alleviating inhibition of HIF-1 transcriptional activity. EGL-9 inactivation (indicated with dotted line) by the dual regulatory mechanisms drives HIF-1 activation. See text for details.

response in *egl-9* mutants (Figures 1D and 1E), indicating that hypoxia indeed not only stabilizes HIF-1 but also acts via CYSL-1 and H_2S to facilitate HIF-1 transactivation for modulation of the O2-ON response.

In vertebrates, H_2S drastically increases under hypoxic conditions to levels that are inversely correlated with tissue O_2 levels (Olson, 2011; Olson et al., 2006; Peng et al., 2010). H_2S is endogenously produced by multiple types of enzymes in animals and is constantly oxidized, so its increase might be directly regulated by local O_2 levels to mediate effects of hypoxia (Chen et al., 2004; Kimura, 2010; Olson, 2011; Peng et al., 2010; Singh et al., 2009). In both *C. elegans* and mammalian cells, H_2S has been shown to promote HIF-1 activity and upregulate HIF-1 target genes (Budde and Roth, 2010; Liu et al., 2010). However, the mechanism by which H_2S elicits its effects on HIF-1 has been unknown. Our findings demonstrate an essential role of CYSL-1 in mediating H_2S upregulation of HIF-1 target genes through CYSL-1 interaction with the EGL-9 C terminus. A recent study found that *cysl-1* mutants are sensitive to H_2S and hypothesized that CYSL-1 might act in a pathway downstream of HIF-1 to enzymatically assimilate H_2S (Budde and Roth, 2011). Unexpectedly, our studies show that CYSL-1 acts upstream of HIF-1 by directly inhibiting EGL-9 in a manner that is modulated by H_2S accumulation. Interestingly, both H_2S and RHY-1 appear to regulate HIF-1 activity in a VHL-1-independent manner (Budde and Roth, 2010; Shen et al., 2006), consistent with the notion that CYSL-1 inhibits EGL-9 and mediates H_2S activation of HIF-1 independently of EGL-9 hydroxylase activity. Bisulfide is known to bind to an allosteric regulatory site of *Salmonella* OASS proteins, which are highly similar to CYSL-1 in *C. elegans*, and can stabilize the interaction between OASS and the SAT C terminus (Salsi et al., 2010). H_2S inhibits mitochondrial cytochrome-C oxidase and can also directly modify target proteins via sulfhydration (Mustafa et al., 2009). Although CYSL-1 has only weak intrinsic sulfhydrylase activity in vitro, it remains possible that H_2S might modify EGL-9 via CYSL-1-modulated sulfhydration to facilitate sequestration of EGL-9 by CYSL-1. The detailed mechanism by which H_2S and its in vivo derivatives modulate CYSL-1 and EGL-9 to regulate HIF-1 remains to be investigated.

CYSL-1-homologous CBS proteins in mammals are known to be major H_2S-biosynthetic enzymes (Chen et al., 2004; Singh et al., 2009), and we suggest that the pathway we identified is fundamentally similar in nematodes and mammals (Figure 7A). In nematodes, H_2S and CYSL-1 regulate HIF-1 through EGL-9. In mammals, H_2S also regulates HIF proteins (Li et al., 2011; Liu et al., 2010), and we propose that CYSL-1-like CBS proteins generate endogenous H_2S to modulate HIF. In mammals, HIF activation protects tissues from reperfusion injury (Loor and Schumacker, 2008); we propose that the *C. elegans* O2-ON behavior reflects an aversive response to unfavorable reoxygenation signals and is analogous to reperfusion injury in mammals. Just as *C. elegans* HIF-1 activates a set of target genes, mammalian HIF can activate *VEGF* to promote tumor angiogenesis (Kaelin and Ratcliffe, 2008; Semenza, 2010). Given that HIF proline hydroxylases and H_2S are emerging as promising pharmaceutical targets for a wide spectrum of human diseases—including reperfusion injury, ischemia, neurodegenerative diseases, and malignant cancer (Kimura, 2010; Li et al., 2011; Olson, 2011; Quaegebeur and Carmeliet, 2010; Szabó, 2007)—the link we have established

from H_2S and CYSL-1 to the inhibition of EGL-9 might lead to novel therapeutic strategies to treat these disorders.

Our analyses of the physiological function and evolution of CYSL-1 also provide surprising insights into how an ancient metabolic enzyme might have been co-opted during evolution to perform a novel function in intracellular signal transduction. CYSL-1 is more closely related to bacterial and plant cysteine synthases than to animal type-II PLP-dependent enzymes. Instead of forming a CS complex with an OAS acetyltransferase, *C. elegans* CYSL-1 apparently binds the EGL-9 C terminus via an interface derived from an ancient interaction module between OASS and SAT in plants and bacteria. Such a shift in or acquisition of a new gene function, termed "gene co-option," is a salient feature of genome evolution and can drive formation of novel biological traits that are selected (True and Carroll, 2002). Of CYSL-1 and its five *C. elegans* paralogs, ZC373.1 is more similar to eukaryotic CBS proteins, whereas CYSL-1, R08E5.2, and F59A7.9 form another homologous group related only distantly to their pro- and eukaryotic counterparts (Figure 5A). Thus, the *cysl-1* gene family might have divergently evolved and hence accommodated newly acquired functions beyond its metabolic roles in bacteria and plants. Interestingly, the expansion of the CBS protein family in nematodes and acquisition of CYSL-1-binding motifs in EGL-9 homologs appear to have coevolved (Figure S7J) and occurred in a period approximately coincidental with anoxic H_2S release on Earth during the Permian-Triassic mass extinction (Grice et al., 2005). Co-option of CYSL-1 from an ancient sulfide-related metabolic enzyme into a cell-signaling mediator might have had adaptive value, enabling animals to efficiently couple decreased O_2 and increased H_2S levels under hypoxia or other adverse environmental conditions with enhanced cellular protection and behavioral flexibility for better survival and reproduction.

EXPERIMENTAL PROCEDURES

EMS Mutagenesis and Genetic Mapping

To screen for mutations that activate the HIF-1 target gene reporter *nIs470*, we mutagenized otherwise wild-type animals carrying the *K10H10.2::GFP* transgene with EMS and observed the F2 progeny using a fluorescence dissecting microscope. Animals with constitutively bright GFP fluorescence under conditions of normoxia (21% O_2) were isolated. Such mutants defined alleles of *egl-9*, *vhl-1* and *rhy-1*. To screen for suppressors of *rhy-1(n5500)*, *rhy-1(n5500) II; nIs470 IV* animals were backcrossed six times to eliminate background mutations and then mutagenized with EMS. The F2 progeny were scored to identify animals that lacked GFP expression under normoxic conditions.

To map *n5500*, the polymorphic Hawaiian CB4856 strain was crossed with *n5500; nIs470* animals to obtain F2 progeny for SNP mapping (Davis et al., 2005). To map the *n5500* suppressor *n5515* using genetic markers, *n5500 II; nIs470 IV; n5515* males were crossed with *n5500 II; nIs470 IV; dpy-6(e14) egl-15(n484) X* hermaphrodites. Seven out of fifteen Egl non-Dpy F2 progeny segregated GFP-negative *n5500*-suppressed animals. Refined mapping using SNP analysis further positioned *n5515* between *dpy-6* and *egl-15* in an interval between the SNPs pk6127 and pk6138. To map the dominant suppressor *n5535*, *n5500; nIs470; n5535* hermaphrodites were crossed with *n5500; nIs470* males, and GFP-positive F2 animals were isolated for SNP mapping.

Behavioral Analysis and H_2S Exposure

Locomotive responses to step changes of O_2 were measured using a custom-built multiworm tracker and a gas-flow system controlled in real-time by MATLAB (see Figure S1). The gas flow consisted of pre-mixed 20%, 10%, 5%, or 0% O_2 balanced by N_2. Well-fed young adult hermaphrodites (50–100 per assay) were transferred to a Petri plate freshly seeded with the bacterium OP50 and allowed to stabilize for 1 hr before the assay at 20°C. Worm-tracking videos were analyzed later using MATLAB to calculate instantaneous locomotion speeds and other behavioral parameters. A hypoxia chamber (Coy Laboratory) that contained 0.5% O_2 balanced by N_2 was used for experiments involving hypoxia experience. After 24 hr of hypoxia exposure, animals were allowed to recover in room air at 20°C for 2 hr preceding the acute behavioral assay. For experiments involving H_2S exposure, 1 μl of 0.1M NaHS, an established H_2S donor that releases H_2S from solution, was dropped on the edge of agar-containing Petri plates and immediately sealed with tape to ensure airtight conditions. To obtain optimal effects, 24 hr duration of H_2S exposure was used for behavioral experiments; 12 hr duration was used for GFP induction; and 1 hr duration was used for biochemical interaction experiments and quantitative real-time PCR.

SUPPLEMENTAL INFORMATION

Supplemental Information includes seven figures, one table, and Supplemental Experimental Procedures and can be found with this article online at doi:10.1016/j.neuron.2011.12.037.

ACKNOWLEDGMENTS

We thank Jo Anne Powell-Coffman, Yuichi Iino, Rene Garcia, Michael Hengartner, Mark Roth, Andy Fire, and Erik Jorgensen for reagents; the *Caenorhabditis* Genetics Center for strains; Na An, Rita Droste, and Tove Ljungars for technical assistance; Ales Hnizda, Jakub Krijt, and Milan Kodicek for help with characterization of purified CYSL-1; Viktor Kozich for helpful discussion; and Shunji Nakano, Takashi Hirose, Nick Paquin, Howard Chang, and Shuo Luo for comments. This work was supported by grant GM24663 to H.R.H from the NIH. R.V. was supported by grant No. 21709 from Grant Agency of Charles University, Prague, Czech Republic and by the Research Project of Charles University No. MSM0021620806. H.R.H. is an Investigator of the Howard Hughes Medical Institute and the David H. Koch Professor of Biology at MIT. N.B is supported by a National Science Foundation Graduate Research Fellowship. D.K.M. is supported by a Helen Hay Whitney Foundation postdoctoral fellowship.

Accepted: December 22, 2011
Published: March 7, 2012

REFERENCES

Aitken, S.M., Lodha, P.H., and Morneau, D.J. (2011). The enzymes of the transsulfuration pathways: active-site characterizations. Biochim. Biophys. Acta *1814*, 1511–1517.

Bonner, E.R., Cahoon, R.E., Knapke, S.M., and Jez, J.M. (2005). Molecular basis of cysteine biosynthesis in plants: structural and functional analysis of O-acetylserine sulfhydrylase from *Arabidopsis thaliana*. J. Biol. Chem. *280*, 38803–38813.

Bruick, R.K., and McKnight, S.L. (2001). A conserved family of prolyl-4-hydroxylases that modify HIF. Science *294*, 1337–1340.

Budde, M.W., and Roth, M.B. (2010). Hydrogen sulfide increases hypoxia-inducible factor-1 activity independently of von Hippel-Lindau tumor suppressor-1 in *C. elegans*. Mol. Biol. Cell *21*, 212–217.

Budde, M.W., and Roth, M.B. (2011). The response of *Caenorhabditis elegans* to hydrogen sulfide and hydrogen cyanide. Genetics *189*, 521–532.

Campanini, B., Speroni, F., Salsi, E., Cook, P.F., Roderick, S.L., Huang, B., Bettati, S., and Mozzarelli, A. (2005). Interaction of serine acetyltransferase with O-acetylserine sulfhydrylase active site: evidence from fluorescence spectroscopy. Protein Sci. *14*, 2115–2124.

Chang, A.J., and Bargmann, C.I. (2008). Hypoxia and the HIF-1 transcriptional pathway reorganize a neuronal circuit for oxygen-dependent behavior in *Caenorhabditis elegans*. Proc. Natl. Acad. Sci. USA *105*, 7321–7326.

Chen, X., Jhee, K.H., and Kruger, W.D. (2004). Production of the neuromodulator H2S by cystathionine beta-synthase via the condensation of cysteine and homocysteine. J. Biol. Chem. *279*, 52082–52086.

Cheung, B.H., Arellano-Carbajal, F., Rybicki, I., and de Bono, M. (2004). Soluble guanylate cyclases act in neurons exposed to the body fluid to promote *C. elegans* aggregation behavior. Curr. Biol. *14*, 1105–1111.

Cheung, B.H., Cohen, M., Rogers, C., Albayram, O., and de Bono, M. (2005). Experience-dependent modulation of *C. elegans* behavior by ambient oxygen. Curr. Biol. *15*, 905–917.

Darby, C., Cosma, C.L., Thomas, J.H., and Manoil, C. (1999). Lethal paralysis of *Caenorhabditis elegans* by *Pseudomonas aeruginosa*. Proc. Natl. Acad. Sci. USA *96*, 15202–15207.

Davis, M.W., Hammarlund, M., Harrach, T., Hullett, P., Olsen, S., and Jorgensen, E.M. (2005). Rapid single nucleotide polymorphism mapping in *C. elegans*. BMC Genomics *6*, 118.

de Bono, M., and Maricq, A.V. (2005). Neuronal substrates of complex behaviors in *C. elegans*. Annu. Rev. Neurosci. *28*, 451–501.

Demb, J.B. (2008). Functional circuitry of visual adaptation in the retina. J. Physiol. *586*, 4377–4384.

Epstein, A.C., Gleadle, J.M., McNeill, L.A., Hewitson, K.S., O'Rourke, J., Mole, D.R., Mukherji, M., Metzen, E., Wilson, M.I., Dhanda, A., et al. (2001). *C. elegans* EGL-9 and mammalian homologs define a family of dioxygenases that regulate HIF by prolyl hydroxylation. Cell *107*, 43–54.

Félix, M.A., and Braendle, C. (2010). The natural history of *Caenorhabditis elegans*. Curr. Biol. *20*, R965–R969.

Francois, J.A., Kumaran, S., and Jez, J.M. (2006). Structural basis for interaction of O-acetylserine sulfhydrylase and serine acetyltransferase in the *Arabidopsis* cysteine synthase complex. Plant Cell *18*, 3647–3655.

Gadalla, M.M., and Snyder, S.H. (2010). Hydrogen sulfide as a gasotransmitter. J. Neurochem. *113*, 14–26.

Gray, J.M., Karow, D.S., Lu, H., Chang, A.J., Chang, J.S., Ellis, R.E., Marletta, M.A., and Bargmann, C.I. (2004). Oxygen sensation and social feeding mediated by a *C. elegans* guanylate cyclase homologue. Nature *430*, 317–322.

Gray, J.M., Hill, J.J., and Bargmann, C.I. (2005). A circuit for navigation in *Caenorhabditis elegans*. Proc. Natl. Acad. Sci. USA *102*, 3184–3191.

Grice, K., Cao, C., Love, G.D., Böttcher, M.E., Twitchett, R.J., Grosjean, E., Summons, R.E., Turgeon, S.C., Dunning, W., and Jin, Y. (2005). Photic zone euxinia during the Permian-triassic superanoxic event. Science *307*, 706–709.

Hsieh, J., Liu, J., Kostas, S.A., Chang, C., Sternberg, P.W., and Fire, A. (1999). The RING finger/B-box factor TAM-1 and a retinoblastoma-like protein LIN-35 modulate context-dependent gene silencing in *Caenorhabditis elegans*. Genes Dev. *13*, 2958–2970.

Hwang, C.S., Shemorry, A., and Varshavsky, A. (2010). N-terminal acetylation of cellular proteins creates specific degradation signals. Science *327*, 973–977.

Ivan, M., Haberberger, T., Gervasi, D.C., Michelson, K.S., Günzler, V., Kondo, K., Yang, H., Sorokina, I., Conaway, R.C., Conaway, J.W., and Kaelin, W.G., Jr. (2002). Biochemical purification and pharmacological inhibition of a mammalian prolyl hydroxylase acting on hypoxia-inducible factor. Proc. Natl. Acad. Sci. USA *99*, 13459–13464.

Jorgensen, E.M., and Rankin, C. (1997). Neural Plasticity. In *C. ELEGANS* II, Second Edition, D.L. Riddle, T. Blumenthal, B.J. Meyer, and J.R. Priess, eds. (Cold Spring Harbor, NY: Cold Spring Harbor Laboratory Press), pp. 769–790.

Kaelin, W.G., Jr., and Ratcliffe, P.J. (2008). Oxygen sensing by metazoans: the central role of the HIF hydroxylase pathway. Mol. Cell *30*, 393–402.

Kimura, H. (2010). Hydrogen sulfide: from brain to gut. Antioxid. Redox Signal. *12*, 1111–1123.

Ladroue, C., Carcenac, R., Leporrier, M., Gad, S., Le Hello, C., Galateau-Salle, F., Feunteun, J., Pouysségur, J., Richard, S., and Gardie, B. (2008). PHD2 mutation and congenital erythrocytosis with paraganglioma. N. Engl. J. Med. *359*, 2685–2692.

Li, L., Rose, P., and Moore, P.K. (2011). Hydrogen sulfide and cell signaling. Annu. Rev. Pharmacol. Toxicol. *51*, 169–187.

Liu, X., Pan, L., Zhuo, Y., Gong, Q., Rose, P., and Zhu, Y. (2010). Hypoxia-inducible factor-1α is involved in the pro-angiogenic effect of hydrogen sulfide under hypoxic stress. Biol. Pharm. Bull. *33*, 1550–1554.

Loor, G., and Schumacker, P.T. (2008). Role of hypoxia-inducible factor in cell survival during myocardial ischemia-reperfusion. Cell Death Differ. *15*, 686–690.

Mazzone, M., Dettori, D., Leite de Oliveira, R., Loges, S., Schmidt, T., Jonckx, B., Tian, Y.M., Lanahan, A.A., Pollard, P., Ruiz de Almodovar, C., et al. (2009). Heterozygous deficiency of PHD2 restores tumor oxygenation and inhibits metastasis via endothelial normalization. Cell *136*, 839–851.

McGrath, P.T., Rockman, M.V., Zimmer, M., Jang, H., Macosko, E.Z., Kruglyak, L., and Bargmann, C.I. (2009). Quantitative mapping of a digenic behavioral trait implicates globin variation in *C. elegans* sensory behaviors. Neuron *61*, 692–699.

Mino, K., Yamanoue, T., Sakiyama, T., Eisaki, N., Matsuyama, A., and Nakanishi, K. (2000). Effects of bienzyme complex formation of cysteine synthetase from *escherichia coli* on some properties and kinetics. Biosci. Biotechnol. Biochem. *64*, 1628–1640.

Mozzarelli, A., Bettati, S., Campanini, B., Salsi, E., Raboni, S., Singh, R., Spyrakis, F., Kumar, V.P., and Cook, P.F. (2011). The multifaceted pyridoxal 5′-phosphate-dependent O-acetylserine sulfhydrylase. Biochim. Biophys. Acta *1814*, 1497–1510.

Mustafa, A.K., Gadalla, M.M., Sen, N., Kim, S., Mu, W., Gazi, S.K., Barrow, R.K., Yang, G., Wang, R., and Snyder, S.H. (2009). H2S signals through protein S-sulfhydration. Sci. Signal. *2*, ra72.

Olson, K.R. (2011). The therapeutic potential of hydrogen sulfide: separating hype from hope. Am. J. Physiol. Regul. Integr. Comp. Physiol. *301*, R297–R312.

Olson, K.R., Dombkowski, R.A., Russell, M.J., Doellman, M.M., Head, S.K., Whitfield, N.L., and Madden, J.A. (2006). Hydrogen sulfide as an oxygen sensor/transducer in vertebrate hypoxic vasoconstriction and hypoxic vasodilation. J. Exp. Biol. *209*, 4011–4023.

Ono, B., Kijima, K., Inoue, T., Miyoshi, S., Matsuda, A., and Shinoda, S. (1994). Purification and properties of *Saccharomyces cerevisiae* cystathionine beta-synthase. Yeast *10*, 333–339.

Ozer, A., Wu, L.C., and Bruick, R.K. (2005). The candidate tumor suppressor ING4 represses activation of the hypoxia inducible factor (HIF). Proc. Natl. Acad. Sci. USA *102*, 7481–7486.

Padilla, P.A., Nystul, T.G., Zager, R.A., Johnson, A.C., and Roth, M.B. (2002). Dephosphorylation of cell cycle-regulated proteins correlates with anoxia-induced suspended animation in *Caenorhabditis elegans*. Mol. Biol. Cell *13*, 1473–1483.

Peng, Y.J., Nanduri, J., Raghuraman, G., Souvannakitti, D., Gadalla, M.M., Kumar, G.K., Snyder, S.H., and Prabhakar, N.R. (2010). H2S mediates O2 sensing in the carotid body. Proc. Natl. Acad. Sci. USA *107*, 10719–10724.

Percy, M.J., Zhao, Q., Flores, A., Harrison, C., Lappin, T.R., Maxwell, P.H., McMullin, M.F., and Lee, F.S. (2006). A family with erythrocytosis establishes a role for prolyl hydroxylase domain protein 2 in oxygen homeostasis. Proc. Natl. Acad. Sci. USA *103*, 654–659.

Pocock, R., and Hobert, O. (2010). Hypoxia activates a latent circuit for processing gustatory information in *C. elegans*. Nat. Neurosci. *13*, 610–614.

Powell-Coffman, J.A. (2010). Hypoxia signaling and resistance in *C. elegans*. Trends Endocrinol. Metab. *21*, 435–440.

Quaegebeur, A., and Carmeliet, P. (2010). Oxygen sensing: a common crossroad in cancer and neurodegeneration. Curr. Top. Microbiol. Immunol. *345*, 71–103.

Rose, N.R., McDonough, M.A., King, O.N., Kawamura, A., and Schofield, C.J. (2011). Inhibition of 2-oxoglutarate dependent oxygenases. Chem. Soc. Rev. *40*, 4364–4397.

Ruvinsky, I., Ohler, U., Burge, C.B., and Ruvkun, G. (2007). Detection of broadly expressed neuronal genes in *C. elegans*. Dev. Biol. *302*, 617–626.

Salsi, E., Campanini, B., Bettati, S., Raboni, S., Roderick, S.L., Cook, P.F., and Mozzarelli, A. (2010). A two-step process controls the formation of the bienzyme cysteine synthase complex. J. Biol. Chem. *285*, 12813–12822.

Sawin, E.R., Ranganathan, R., and Horvitz, H.R. (2000). *C. elegans* locomotory rate is modulated by the environment through a dopaminergic pathway and by experience through a serotonergic pathway. Neuron *26*, 619–631.

Semenza, G.L. (2010). Defining the role of hypoxia-inducible factor 1 in cancer biology and therapeutics. Oncogene *29*, 625–634.

Shao, Z., Zhang, Y., and Powell-Coffman, J.A. (2009). Two distinct roles for EGL-9 in the regulation of HIF-1-mediated gene expression in *Caenorhabditis elegans*. Genetics *183*, 821–829.

Shao, Z., Zhang, Y., Ye, Q., Saldanha, J.N., and Powell-Coffman, J.A. (2010). *C. elegans* SWAN-1 Binds to EGL-9 and regulates HIF-1-mediated resistance to the bacterial pathogen *Pseudomonas aeruginosa* PAO1. PLoS Pathog. *6*, e1001075.

Shen, C., Nettleton, D., Jiang, M., Kim, S.K., and Powell-Coffman, J.A. (2005). Roles of the HIF-1 hypoxia-inducible factor during hypoxia response in *Caenorhabditis elegans*. J. Biol. Chem. *280*, 20580–20588.

Shen, C., Shao, Z., and Powell-Coffman, J.A. (2006). The *Caenorhabditis elegans rhy-1* gene inhibits HIF-1 hypoxia-inducible factor activity in a negative feedback loop that does not include *vhl-1*. Genetics *174*, 1205–1214.

Singh, S., Padovani, D., Leslie, R.A., Chiku, T., and Banerjee, R. (2009). Relative contributions of cystathionine beta-synthase and gamma-cystathionase to H2S biogenesis via alternative trans-sulfuration reactions. J. Biol. Chem. *284*, 22457–22466.

Szabó, C. (2007). Hydrogen sulphide and its therapeutic potential. Nat. Rev. Drug Discov. *6*, 917–935.

To, K.K., and Huang, L.E. (2005). Suppression of hypoxia-inducible factor 1alpha (HIF-1alpha) transcriptional activity by the HIF prolyl hydroxylase EGLN1. J. Biol. Chem. *280*, 38102–38107.

Trent, C., Tsung, N., and Horvitz, H.R. (1983). Egg-laying defective mutants of the nematode *Caenorhabditis elegans*. Genetics *104*, 619–647.

True, J.R., and Carroll, S.B. (2002). Gene co-option in physiological and morphological evolution. Annu. Rev. Cell Dev. Biol. *18*, 53–80.

Wirtz, M., and Droux, M. (2005). Synthesis of the sulfur amino acids: cysteine and methionine. Photosynth. Res. *86*, 345–362.

Wirtz, M., Heeg, C., Samami, A.A., Ruppert, T., and Hell, R. (2010). Enzymes of cysteine synthesis show extensive and conserved modifications patterns that include N(α)-terminal acetylation. Amino Acids *39*, 1077–1086.

Zimmer, M., Gray, J.M., Pokala, N., Chang, A.J., Karow, D.S., Marletta, M.A., Hudson, M.L., Morton, D.B., Chronis, N., and Bargmann, C.I. (2009). Neurons detect increases and decreases in oxygen levels using distinct guanylate cyclases. Neuron *61*, 865–879.

Neuron, Volume *73*

Supplemental Information

CYSL-1 Interacts with the O_2-Sensing Hydroxylase EGL-9 to Promote H_2S-Modulated Hypoxia-Induced Behavioral Plasticity in *C. elegans*

Dengke K. Ma, Roman Vozdek, Nikhil Bhatla, and H. Robert Horvitz

Supplemental Information includes seven supplemental figures and associated legends, one supplemental table, Supplemental Experimental Procedures, and references.

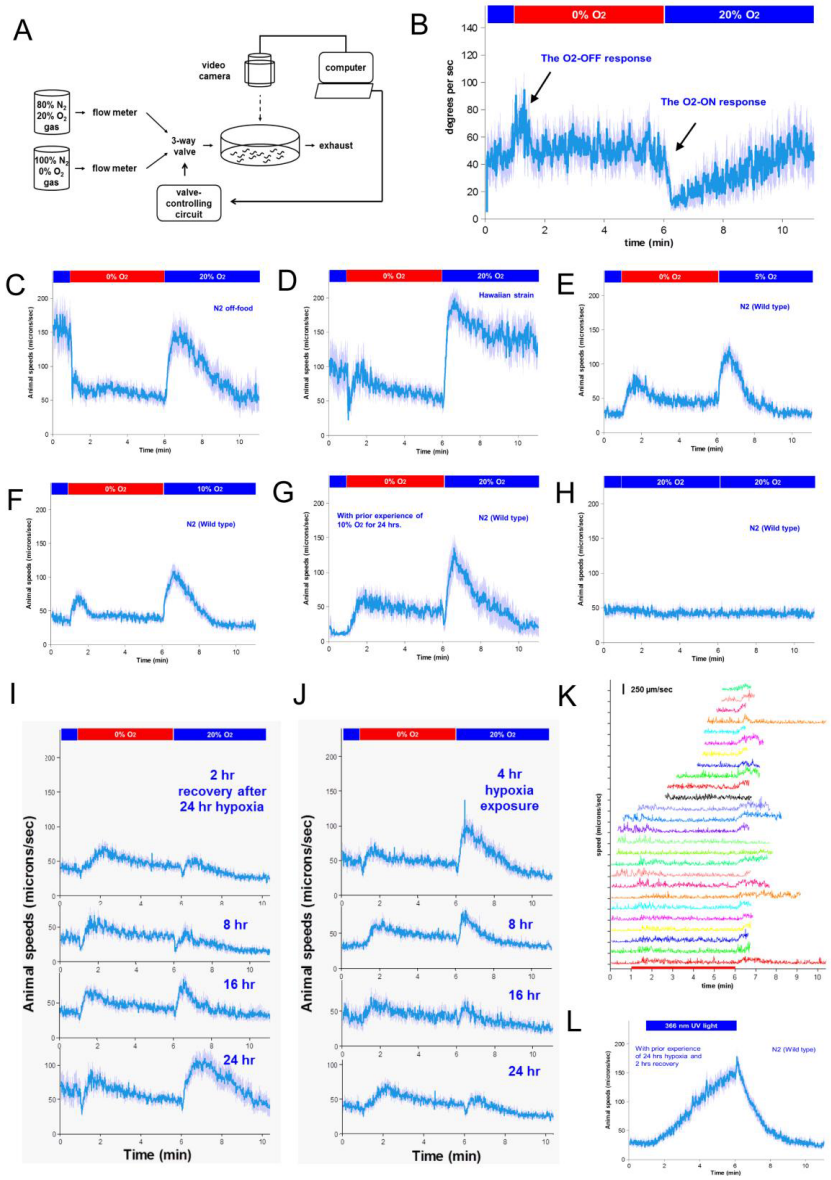

Figure S1. *C. elegans* locomotive behavioral response to O_2 and associated behavioral plasticity, Related to Figure 1

(A) schematic illustration of the experimental set-up for measurements of *C. elegans* locomotive behavioral responses to changes in O_2 levels. (B) Measurements of turning angle changes during the behavioral session, showing the increased frequency of turning (local radial search) during the O2-OFF response and the decreased frequency of turning (forward acceleration) during the O2-ON response. (C) Behavior of wild-type hermaphrodites on Petri plates without bacteria. (D) Behavior of Hawaiian strain CB4856 animals. (E) Behavior of wild-type hermaphrodites in response to 5% O_2 restoration after anoxia. (F) Behavior of wild-type hermaphrodites in response to 10% O_2 restoration after anoxia. (G) Behavior of wild-type hermaphrodites after grown under 10% O_2 for 24 hrs followed by 2 hrs recovery in room air, to control for potential effects of CO_2 deprivation or for dehydrating effects of the hypoxic chamber. (H) Behavior of wild-type hermaphrodites in response to mock gas transitions, i.e. with 20% O_2 instead of 0% O_2 from the minute-2 to the minute-6 of the behavioral session, to control for potential effects of CO_2 deprivation or for dehydrating effects of the continuous gas flow. (I) Behaviors of animals with different recovery durations after 24 hr hypoxia experience. (J) Behaviors of animals with different durations of hypoxia exposure. (K) Individual traces for 26 animals with continuous uninterrupted paths during the 30 second intervals before and after the return of O_2 from Figure 1A. (A worm's path can be truncated if it moves out of the field-of-view or collides with another worm.) Of these 26 traces, 23 show an apparent increase in speed after O_2 was restored. The instantaneous speed of each animal over time is plotted as a different color, and traces are stacked for clarity. (L) Behavior of wild-type animals showing locomotive acceleration in response to 366 nm UV stimuli after being cultured under 0.5% O_2 for 24 hrs followed by 2 hrs recovery in room air. Unlike the O2-ON response, the acceleration in response to UV stimuli is not suppressed by experience of hypoxia.

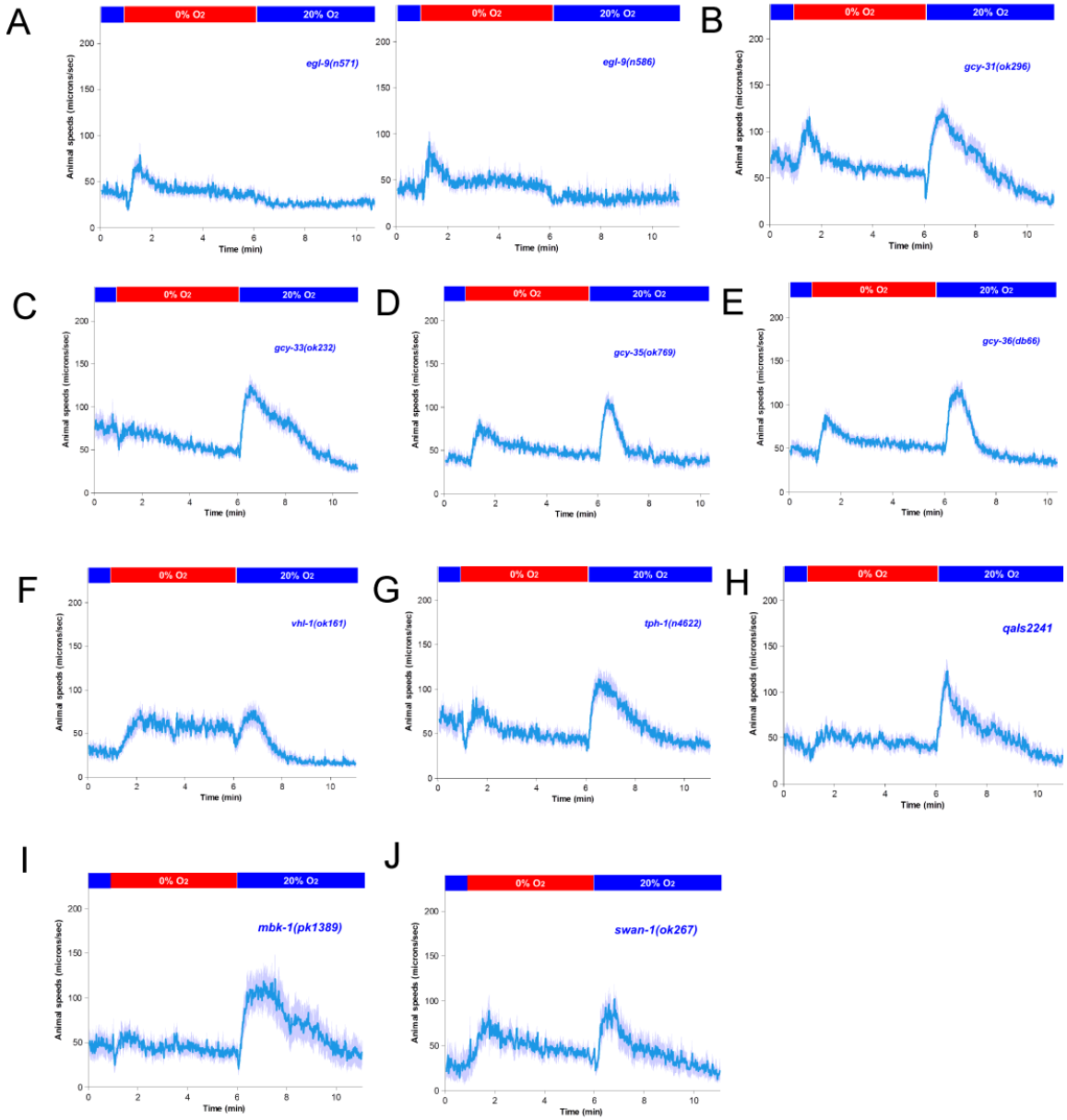

Figure S2. Genes and cells potentially involved in the O2-ON response, Related to Figure 1
(A) Behavior of animals with *egl-9* alleles *n571* and *n586*, showing defective O2-ON responses. (B-E) Behavior of *gcy-31, gcy-33, gcy-35,* and *gcy-36* null mutants, showing normal O2-ON responses. (F) Behavior of *vhl-1* null mutants, showing partially defective O2-ON response. (G) Behavior of *tph-1* null 5 mutants, showing a normal O2-ON response. (H) Behavior of *qaIs2241 [Pgcy-36::egl-1(+), Pgcy-35::GFP, lin-15(+)]* animals with apoptotic cell deaths of AQR, PQR and URX neurons, in which the *gcy-36* promoter is activated, showing a normal O2-ON response. (I) Behavior of *mbk-1* null mutants, showing normal O2-ON response. (J) Behavior of *swan-1* null mutants, showing normal O2-ON response.

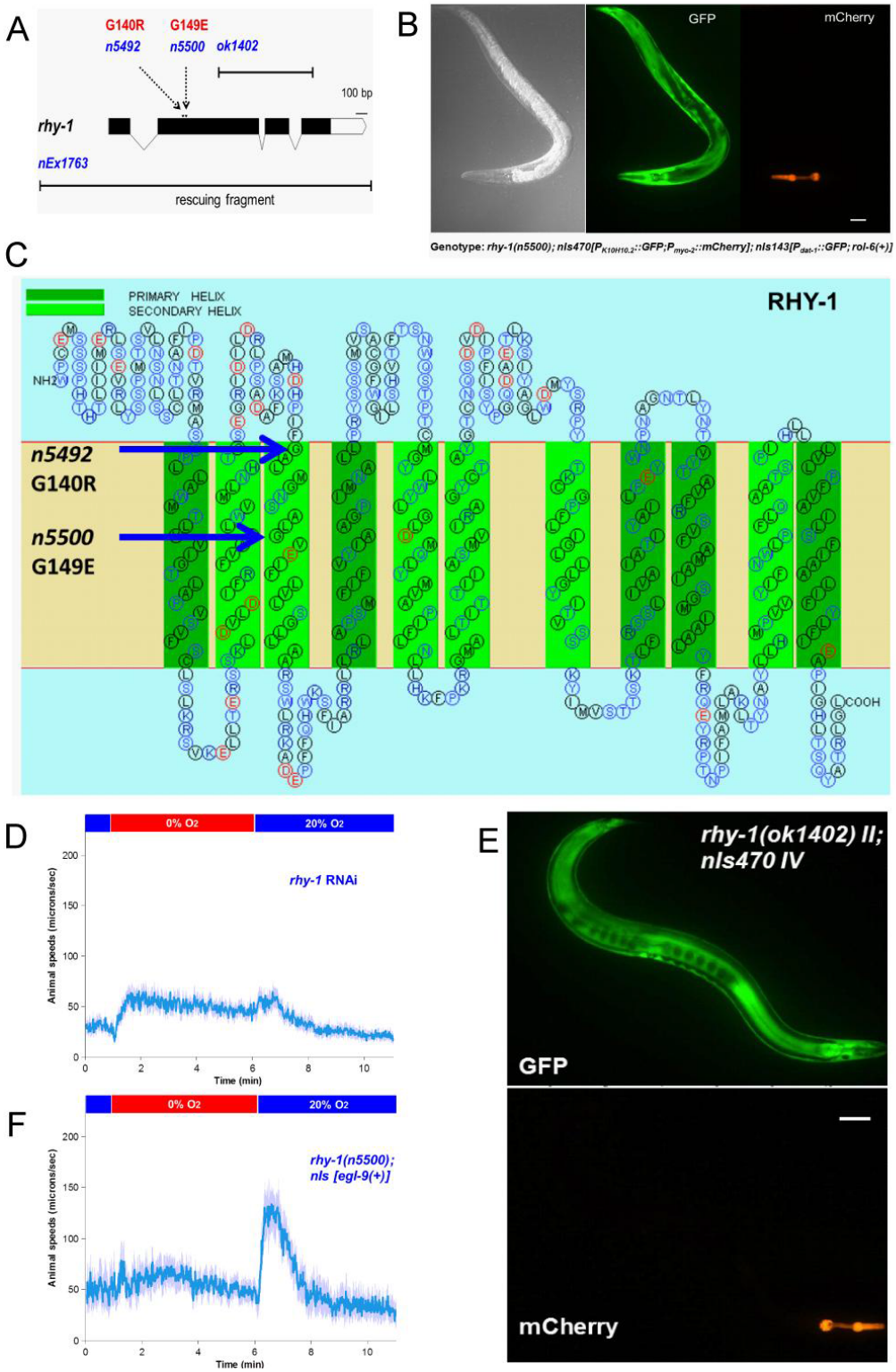

Figure S3. RHY-1 is essential for HIF-1 regulation of *K10H10.2* and the O2-ON response, Related to Figure 2.

(A) schematic of the *rhy-1* gene, showing mutations and a rescuing genomic fragment. (B) Fluorescence micrograph and Nomarski image showing reporter GFP expression driven by the *K10H10.2* promoter in *rhy-1(n5500)* mutants. *myo-2::mCherry* was used as the co-injection marker. The *rol-6* dominant marker was used to better reveal GFP expression in hypodermal tissues. (C) Predicted secondary structure of RHY-1 with ER membrane-spanning regions. (D) RNAi against *rhy-1* phenocopied the *n5500* allele in inhibiting the O2-ON response. (E) Fluorescence micrograph showing *K10H10.2::GFP* expression of mutants with a *rhy-1* deletion allele. *myo-2::mCherry* was used as the co-injection marker. (F) Behavior of *rhy-1* mutants with an integrated transgene overexpressing wild-type *egl-9,* indicating a suppressed O2-ON response.

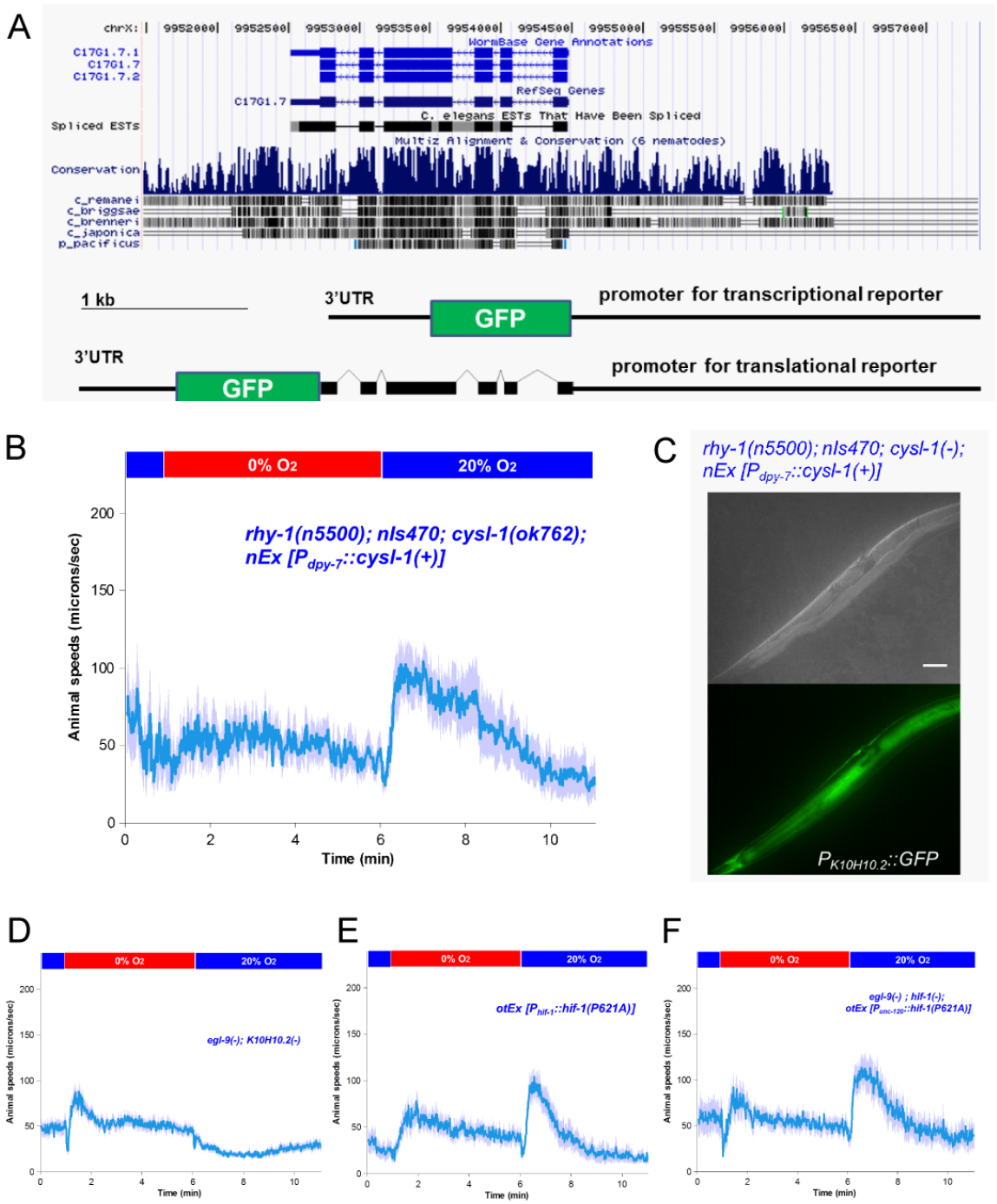

Figure S4. *cysl-1* expression patterns and site-of-function analysis, Related to Figure 4 9

(A) Genome browser view of *cysl-1* gene structure, showing the promoter region that was used to construct transcriptional and translational GFP reporters. (B) Behavior of *rhy-1; cysl-1* mutants with *cysl-1* cDNA expressed in hypodermal tissues, showing the O2-ON response not suppressed. (C) The *dpy-7*-driven hypodermal expression of *cysl-1* cDNA rescued the *K10H10.2::GFP* expression in *rhy-1; cysl-1* double mutants. (D) Behavior of *egl-9(-); K10H10.2(-)* mutants with a defective O2-ON response. (E) Behavior of *otEx [Phif-1::hif-1(P621A)]* animals, indicating that stabilization of HIF-1 was not sufficient to cause an O2-ON defect. (F) Behavior of *egl-9(-); hif-1(-); otEx [Punc-120::hif-1(P621A)]* animals, indicating that stabilization of HIF-1 specifically in muscles was not sufficient to rescue the *egl-9(-); hif-1(-)* double mutant behavioral phenotype in the O2-ON response.

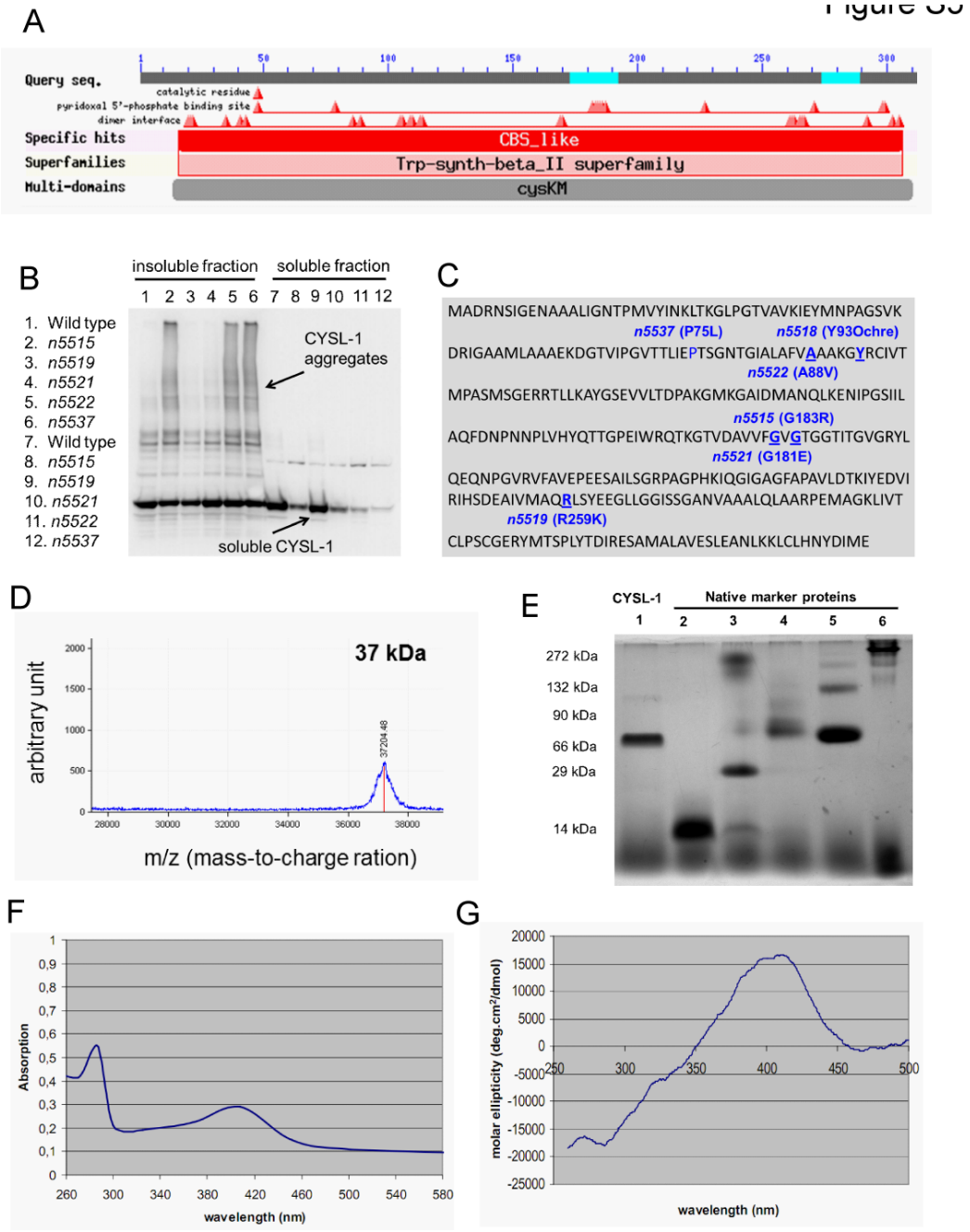

Figure S5. Properties of recombinant and endogenous CYSL-1 wild-type and mutant proteins, Related to Figure 5

(A) BLASTP searches of NCBI databases against the CYSL-1 protein query revealed a CBS-like domain in CYSL-1 belonging to type-II PLP-dependent enzyme family and cysteine synthase (cysKM) family proteins. Predicted catalytic residues, PLP-binding sites and dimer interfaces are indicated. (B) Western blots using antibodies against GST to detect wild-type GST-CYSL-1 or *n5515, n5521, n5522,* and *n5537* mutant GST-CYSL-1 from soluble or insoluble fractions of bacterial lysates, showing that these missense mutations caused CYSL-1 to reside in the inclusion bodies during purification. (C) Coding amino acid residues affected by six *cysl-1* missense or nonsense mutations highlighted in CYSL-1. (D) Purified CYSL-1 was analyzed by peptide mass fingerprinting using MALDI-TOF. The molecular weight was determined to be 37.2 kD. (E) Native electrophoresis of purified CYSL-1, revealing a molecular weight of about 70 kDa and indicating that CYSL-1 forms homodimers. Lane 1: CYSL-1, 2: α-Lactalbumin (14.2 kDa), 3: Carbonic Anhydrase (29 kDa), 4: Ovalbumin (90 kDa), 5: BSA (66 and 132 kDa), 6: Urease (272 and 545 kDa). (F) Recombinant CYSL-1 purified from *E. coli* was analyzed by UV/visible absorption spectrometer, showing a spectrum characteristic for type-II PLP-dependent enzymes (Mozzarelli et al., 2011). (G) Purified recombinant CYSL-1 proteins from *E. coli* were analyzed by circular dichroism, showing a absorption spectrum characteristic for type-II PLP-dependent enzymes (Mozzarelli et al., 2011).

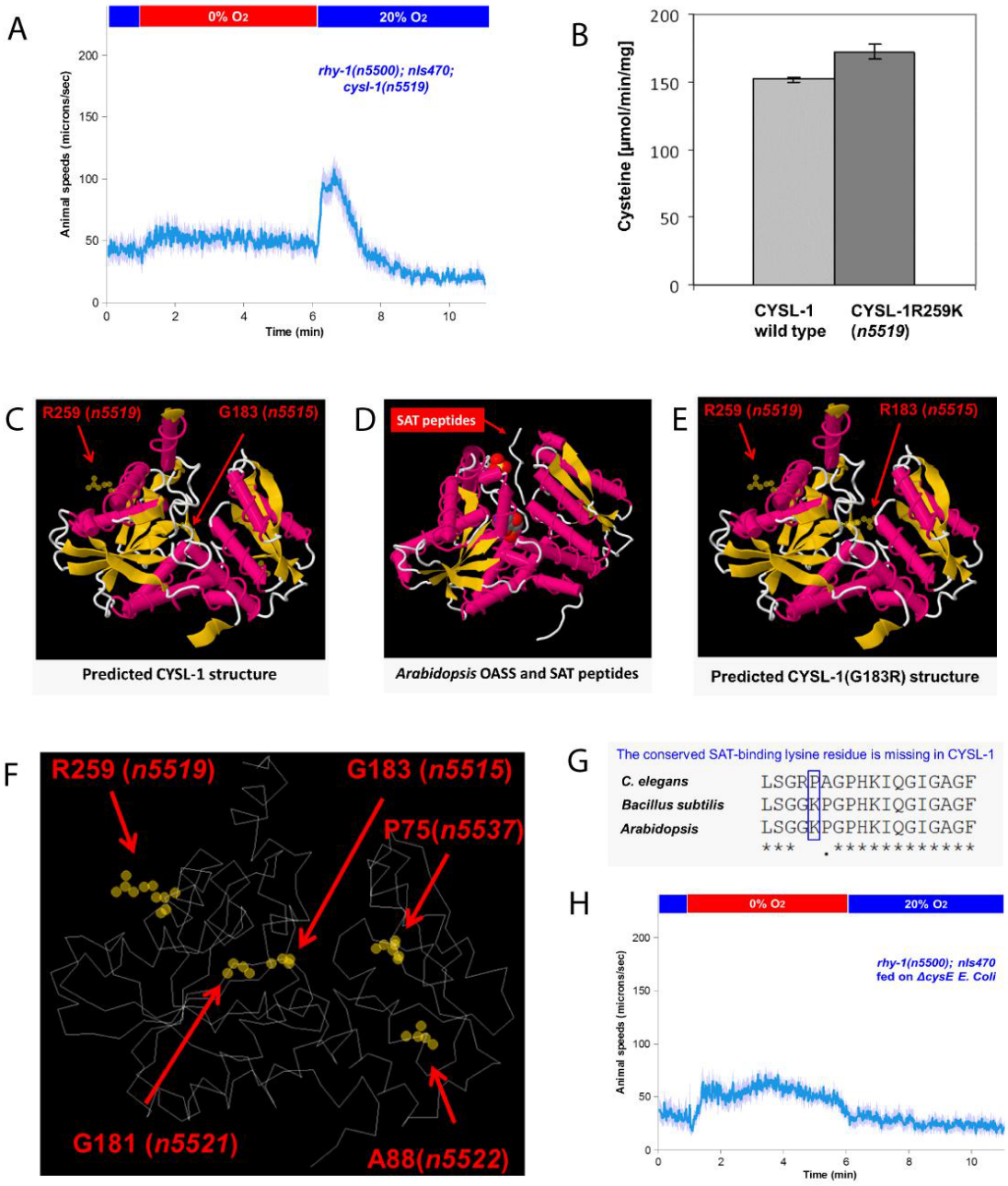

Figure S6. CYSL-1 regulates the O2-ON response independently of cysteine synthase activity, Related to Figure 5 13

(A) Behavior of *rhy-1(n5500); nIs470; cysl-1(n5519)* mutants with restored O2-ON response. (B) Measured cysteine levels indicating cysteine synthase activities of recombinant wild-type CYSL-1 and CYSL-1(*n5519*) mutant proteins purified from *E. coli*. CYSL-1(*n5519*) mutant proteins exhibited normal activity levels. (C) A sequence homology model of the three-dimensional structure of CYSL-1, using the SWISS-MODEL platform, compared with *Arabidopsis* OASS, which shares 58% a.a. identity with CYSL-1. (D) The *Arabidopsis* OASS protein (PDB ID: 2isq) with the active site occupied by SAT C-terminal peptides. (E) A homology-model structure of CYSL-1 G183R mutants with the substituted arginine blocking the PLP active site. (F) Predicted locations of the residues affected by *cysl-1* mutations. Note that *n5515, n5521, n5522,* and *n5537* residues all reside internally within the CYSL-1 protein, whereas the *n5519*-affected arginine residue sits on the surface of the protein far away from the active site. (G) Multiple sequence alignment of *C. elegans* CYSL-1, bacterial and plant OASS proteins, showing that the lysine (K) residue important for binding SATs in bacteria and plants is missing in *C. elegans* CYSL-1. (H) Behavior of *rhy-1(n5500); nIs470* mutants fed on an OAS-deficient bacterial strain (*ΔcysE*). Note that the O2-ON response defect of *rhy-1(n5500)* mutants is not restored.

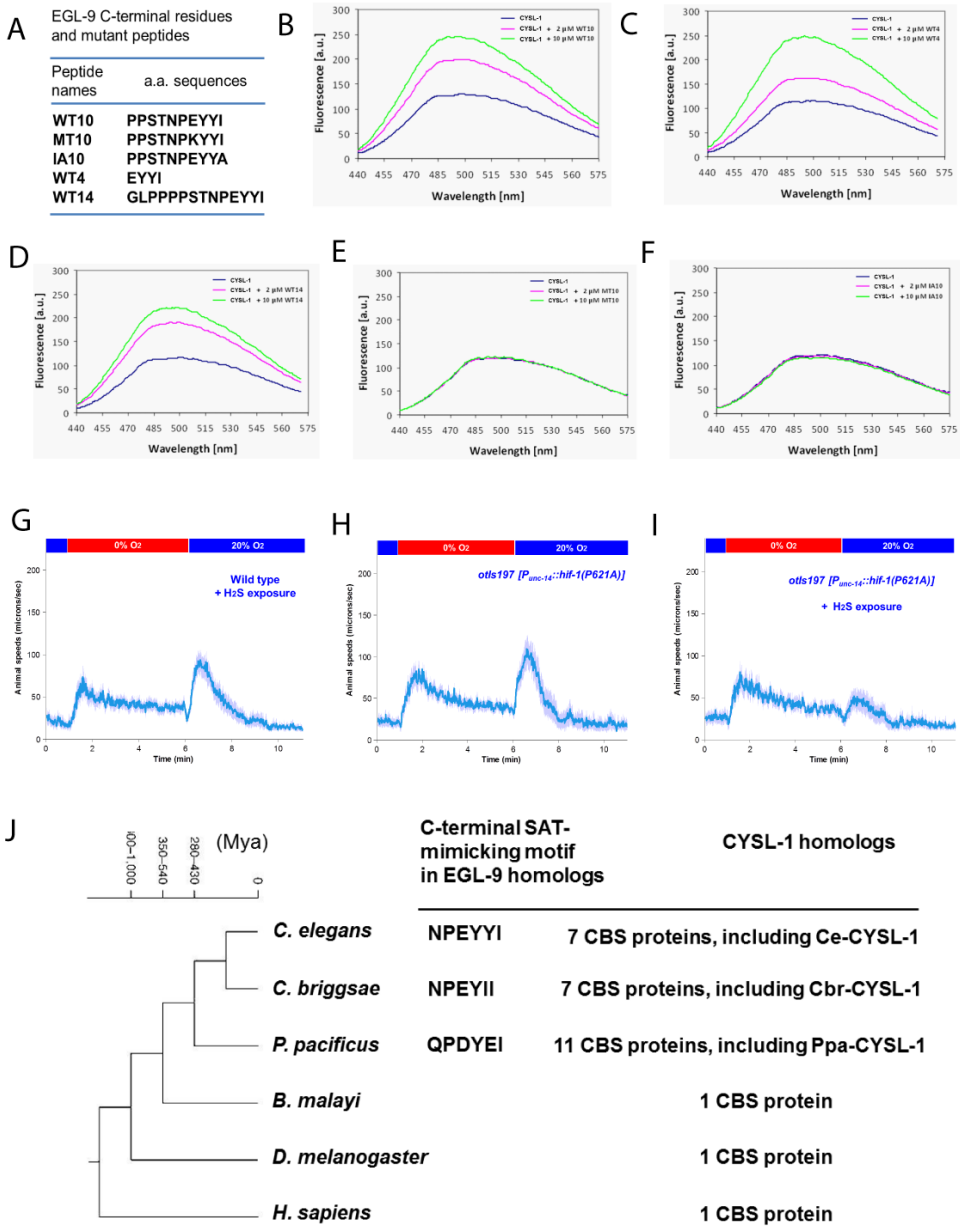

Figure S7. EGL-9 interaction with CYSL-1 and the behavioral effects of H_2S, Related to Figure 6
(A) EGL-9 C-terminal peptide sequences used to measure peptide binding-induced enhancements of intrinsic CYSL-1 fluorometric emission upon 412 nm excitation. (B) Peptides of the wild-type EGL-9 with 10 C-terminal amino acid residues at 2 μM or 10 μM concentrations enhanced the fluorometric emission of CYSL-1 in a dose-dependent manner. (C) Peptides of the wild-type EGL-9 with 14 C-terminal animo acid residues at 2 μM or 10 μM concentrations enhanced the fluorometric emission of CYSL-1 in a dose-dependent manner. (D) Peptides of the wild-type EGL-9 with four C-terminal animo acid residues at 2 μM or 10 μM concentrations enhanced the fluorometric emission of CYSL-1 in a dose-dependent manner. (E) Mutant EGL-9 peptide (E720K caused by *n5535*) with 10 C-terminal amino acid residues at 2 μM or 10 μM concentrations failed to enhance the fluorometric emission of CYSL-1. (F) The mutant EGL-9 peptides with the terminal isoleucine substituted with alanine at 2 μM or 10 μM concentrations failed to enhance the fluorometric emission of CYSL-1. (G) Behavior of wild-type animals after H2S exposure for 24 hrs, showing a normal O2-ON response. (H) Behavior of *otIs197* animals with HIF-1 stabilized in neurons, showing a normal O2-ON response. (I) Behavior of *otIs197* animals after H2S exposure for 24 hrs, showing a defective O2-ON response. (J) Co-evolution of CYSL-1 and the C-terminus of EGL-9. C-terminal SAT-mimicking motifs were found in EGL-9 homologs of *C. elegans, C. briggsae*, and *P. pacificus* but not in *Drosophila* and *H. sapiens*. Expansion of CBS gene family and acquisition of CYSL-1 homologs follow the same phylogenic distribution. Evolutionary relationships and divergence times (Dieterich et al., 2008) of these species were indicated on the left. Mya: Million years ago.

Supplemental Table 1

(A) Mutants with activation of *nIs470* under normoxic conditions

LG	Alleles	Phenotype	Genes	Penetrance
V	*n5496, n5484, n5480, n5482*	Recessive	***egl-9***	100%
X	*n5495, n5498*	Recessive	***vhl-1***	100%
II	*n5492, n5500*	Recessive	***rhy-1***	100%

(B) Primers used for QPCR and molecular cloning

Primer name	**Primer sequence**
DM15_act-3 Q5p	tccatcatgaagtgcgacat
DM16_act-3 Q3p	tagatcctccgatccagacg
DM25_K10H10.2 Q5p	tccacatagcccacacaaaa
DM26_K10H10.2 Q3p	gttggctccagacgagattc
DM97_K10H10.2 pro Clone5p	cacgtcgaccacattttgtaagtttcagacgtttc
DM98_K10H10.2 pro Clone3p	cacccgggcggccgctatgatgagttgattggcagagga
DM173_K10H 2transps c5p	caccagatagggattccatttaggcttt
DM174_K10H 1transps c5p	caccaaaggtttgtattacgggaaca
DM179_C17G1.7 Q5p	cgcaactctattggcgaaa
DM180_C17G1.7 Q3p	cgctccaatacgatctttgac
DM217_nhr-57 Q5p	gtatgccggaaaaagaacga
DM218_nhr-57 Q3p	atgcaggggaagatgaacag
DM264_ric-19 pro c5p	caccggccttctgaagttatca
DM265_ric-19 pro c3p	gttcaaagtgaagagctctctcg
DM327_hsp-16.2 Pro c5p	caccaagagcatttgaatcagaatatg
DM328_hsp-16.2 Pro c5p	atgattatagtttgaagatttctaatttcac
DM365_hif-1PA cDNA c5p	caccgctagcatggaagacaatcggaaaag
DM366_hif-1PA cDNA c3p	ccgagctctcaagagagcattggaaatggg
DM685_rhy-1 genomic c5p	caccgcggccgcccgggcaagcaccaatgggaaatctg
DM686_rhy-1 genomic c3p	tcaatggcattagcaactcg
DM764_dpy-7 promoter c5p	cacctgtctctgacgcctgtgagt
DM765_dpy-7 promoter c3p	tttgttttcacagagcggtaga
DM869_C17G1.7 cDNA c5p	caccgctagccggcttaccgccatggctgatcgcaactctattgg
DM870_C17G1.7 cDNA c3p	ccgagctcactccataatatcatagttgtgaaga
DM871_C17G1.7 promoter c3p	tctgaaacatcgactatgagttaaatg
DM872_C17G1.7 codutr c3p	ccactagtcttagtgtctgcgggttca
DM907_C17G1.7 procod if5p	tggctagcgtcgacggtaccaaatcccgagtgttctgcat
DM908_C17G1.7 procod if3p	tcatttttttctaccggtaccccctccataatatcatagttgtgaaga
DM930_csi-1 cDNA to pGADT7 if5p	ggaggccagtgaattcatggctgatcgcaactctattgg
DM931_csi-1 cDNA to pGADT7 if3p	cacccgggtggaattctcactccataatatcatagttgtgaaga
DM932_egl-9 cDNA to pGBKT7 if5p	catggaggccgaattcatgagcagtgccccaaat
DM933_egl-9 cDNA to pGBKT7 if3p	ggatccccgggaattctcagatgtaatactctgggtttgtgg
DM934_egl-9nc cDNA to pGBKT7 if3p	ggatccccgggaattctcagtttgtggaaggaggtggtg
DM941_egl-9(n5535) cDNA to pGBKT7 if3p	ggatccccgggaattctcagatgtaatactttgggtttgtgg
DM952_hif-1 cDNA to pGADT7 if5p	ggaggccagtgaattcatggaagacaatcggaaaag
DM953_hif-1 cDNA to pGADT7 if3p	cacccgggtggaattctcaagagagcattggaaatggg
DM955_myc-egl-9a to pRSET if3p	cagccggatcaagctttcagatgtaatactctgggtttgtgg
DM956_egl-9ct to pGBKT7 if5p	catggaggccgaattcatggctttggcaaaaggaaaaga
DM958_egl-9NC2 to pGBKT7 if3p	ggatccccgggaattcttaaaaattatctctatcttcatctgctgcagatacc
DM959_egl-9NC3 to pGBKT7 if3p	ggatccccgggaattctcatctatcttcatctgctgcagatacc

(C) Statistics of the O2-ON response in various strains under different conditions

Strain	**Mean speed during 1 min before O2-ON**	**N**	**SE**	**Mean speed during 1 min after O2-ON**	**N**	**SE**	**p-value of the speed difference before and after O2-ON response**	**p-value of the difference in the O2-ON response between strains**
Wild type	48.3	90	1.4	100.7	125	3.4	<0.01	<0.01, vs *egl-9(sa307)*
egl-9(sa307)	39.1	304	0.9	35.3	288	1.2	N.S.	<0.01, vs wild type
egl-9(sa307); hif-1(ia4)	43.3	148	0.7	128.3	185	3.4	<0.01	<0.01, vs *egl-9(sa307)*
hif-1(ia4)	35.3	426	0.6	81.5	492	1.9	<0.01	N.S., vs wild type
wild type [after 24 hrs hypoxia experience]	42.6	119	1	47	125	1.7	N.S.	<0.01, vs naïve wild type
hif-1(ia4) [after 24 hrs hypoxia experience]	28.4	50	0.8	68.6	61	4.7	<0.01	<0.01, vs wild type with hypoxia
cysl-1(ok762) [after 24 hrs hypoxia experience]	79.6	48	3.3	96.1	47	6.9	<0.01	<0.01, vs wild type with hypoxia
rhy-1(n5500)	42.9	74	1.4	45.7	83	3	N.S.	<0.01, vs wild
rhy-1(n5500); hif-1(ia4)	29.7	54	1.4	73.5	72	4.1	<0.01	<0.01, vs *rhy-1(n5500)*
rhy-1(n5500); nEx[rhy-1(+)]	38.3	89	1.2	102.3	96	4.6	<0.01	<0.01, vs *rhy-1(n5500)*
rhy-1(n5500); cysl-1(n5515)	44.8	91	1.1	70.8	102	2.9	<0.01	<0.01, vs *rhy-1(n5500)*
rhy-1(n5500); egl-9(n5535d)	35.6	110	1.1	80.2	148	2.5	<0.01	<0.01, vs *rhy-1(n5500)*
egl-9(sa307); cysl-1(ok762)	43.2	97	1.4	21.8	85	1.4	N.S.	<0.01, vs *cysl-1(ok762)*
cysl-1(ok762)	46.1	65	2.5	97.7	88	5.5	<0.01	<0.01, vs *egl-9(sa307); cysl-1(ok762)*
rhy-1; cysl-1; nEx[Pric-19::cysl-1]	42.1	46	1.9	33.8	37	2.8	N.S.	<0.01, vs *rhy-1(n5500); cysl-1(ok762)*
rhy-1; cysl-1; nEx[Pdpy-7::cysl-1]	41.4	35	2.6	76.2	45	5	<0.01	N.S., vs *rhy-1; cysl-1;*
egl-9; hif-1; otIs[Punc-14::hif-1(P621G)]	30.2	63	1.4	30.8	61	1.9	N.S.	<0.01, vs *egl-9(sa307); hif-1(ia4)*
egl-9; hif-1; nIs[Pdpy-7::hif-1(P621G)]	28.2	90	0.8	58.4	115	2.1	<0.01	N.S., vs *egl-9; hif-1;*

Supplemental Experimental Procedures

Mutations and Strains

C. elegans strains were cultured as described (Brenner, 1974). The N2 Bristol strain (Brenner, 1974) was used as the reference wild-type strain, and the polymorphic Hawaiian strain CB4856 (Wicks et al., 2001) was used for some genetic mapping. Mutations used were as follows: LG I, *gcy-35(ok769)* ; LG II, *rhy-1(n5487, n5492, n5497, n5500, ok1402), K10H10.2(ok3516), tph-1(n4622)*; LG IV, *him-8(e1489)*; LG V, *egl-9(sa307, n586, n587, n5480, n5482, n5496, n5484, n5535, n5539)* (Darby et al., 1999; Trent et al., 1983)*, tam-1(n5512, n5514, n5516, n5538, n5541, cc567)* (Hsieh et al., 1999)*, hif-1(ia4, n5513, n5527)* (Shen et al., 2005)*, gcy-33(ok232)*; LG X, *dpy-6(e14), cysl-1(n5515, n5518, n5519, n5521, n5522, n5536, n5537, ok762), egl-15(n484), vhl-1(n5495, n5488, ok161), gcy-36(db66)* (Cheung et al., 2004)*, gcy-31(ok296)*. Transgenic strains were generated by germline transformation (Mello et al., 1991). Transgenic constructs (at 20–50 ng/µl) were co-injected with mCherry reporters, and lines of mCherry-positive animals were established. Gamma irradiation was used for generating integrated transgenes.

Molecular biology, QPCR and protein characterization

Constructs were generated mostly using the Gateway system (Invitrogen) and Infusion cloning (Clontech) techniques (Hartley et al., 2000). Promoters of *K10H10.2, ric-19, dpy-7, hsp-16.2*, and *cysl-1* were amplified using PCR and cloned into entry vectors. cDNA fragments of *GFP, mCherry, hif-1, egl-9, rhy-1* and *cysl-1* were cloned into destination vectors that can recombine with corresponding entry vectors to yield final desired constructs. GFP translational fusion and yeast two-hybrid constructs were generated using PCR and Infusion cloning. Primer sequences are shown in Table S1. QPCR was performed with reverse-transcribed mRNA samples and SYBR green dyes in a Realplex thermal cycler, and results were analyzed using the ddT method in GraphPad Prism. GST-tagged CYSL-1 was purified from IPTG-induced bacterial strain BL21 using glutathione sepharose resins. GST-CYSL-1 was studied using fluorescence spectrophotometry after being cleaved using PreScission proteases. The intrinsic fluorescence emission of CYSL-1 in 50 mM Tris pH 7 in the absence or presence of peptide was monitored using a fluorescence spectrometer (Perkin Elmer LS55). The excitation wavelength was 412 nm (slit width of 5 nm) with an emission signal scanned from 440 to 575 nm (slit width of 10 nm). The absorption and CD spectra of C17G1.7 were recorded using a UV-VIS spectrophotometer (Shimadzu UV2550) and a chiroptic spectrometer (Jasco J-810). To measure OASS activity, we determined cysteine levels by HPLC as described previously (Maclean et al., 2010). To test if H2S modulates the interaction between CYSL-1 and EGL-9 *in vivo*, a GFP::EGL-9 translational reporter strain *nEx*[P*ric-19::egl-9::gfp*] was cultured with or without exposure to H2S for 1 hr, and GFP::EGL-9 complexes from homogenized cell lysates (TissueRupter, Qiagen) were isolated using anti-GFP-conjugated agarose beads (GFP-Trap from ChromoTech). For western blots, samples were separated by SDS-PAGE, and immuno-blotting was performed using polyclonal GFP antibodies (Invitrogen) or polyclonal CYSL-1 antibodies prepared against purified recombinant CYSL-1 (Exbio Praha, a.s., Vestec, Czech Republic).

Bioinformatics

The BLASTP program from NCBI was used to search for proteins homologous to CYSL-1 (Altschul et al., 1990). Multiple sequence alignments for *C. elegans* full-length CYSL-1 and its homologs from other species were generated and analyzed using ClusterW2 (Larkin et al., 2007), and the results were displayed and annotated on JalView (Waterhouse et al., 2009). Secondary structure and membrane-spanning segment predictions for RHY-1 were generated using SOSUI (Hirokawa et al., 1998), and the IPR002656 Acyltransferase 3 motif was annotated using InterPro from EMBO-EBI (http://www.ebi.ac.uk/interpro/). Structural homology modeling for CYSL-1 wild-type and CYSL-1 G183R mutant proteins was performed using SWISS-MODEL (Arnold et al., 2006), and the pdb files were displayed and annotated using FirstGlance in Jmol (http://molvis.sdsc.edu/fgij/index.htm).

Statistical analyses

One-sided unpaired t-tests were used to compare the mean speeds of all animals within 60 seconds before or after O2 restoration. Speed differences are highly significant ($p<0.001$) for the graphs in Figure 1A, 1F, 1G, 1H, 2D, 2E, 3E, 3F, 4F, 4I, 6A, 6H, 6I but not for the graphs in Figure 1D, 1E, 2C, 2G, 3D, 4G, 4H (e.g., Figure 1A datasets yield a p-value of 7.4 x 10^-28). Two-way ANOVA was used to calculate the P values to test for significant interaction of genotypes or between different conditions. The numbers and the comparisons made are summarized in Table S1C. One-way or two-way ANOVA followed by Bonferroni post-tests were used to compare normalized steady-state transcript levels as measured in gene expression by quantitative real-time PCR.

Supplemental References

Altschul, S.F., Gish, W., Miller, W., Myers, E.W., and Lipman, D.J. (1990). Basic local alignment search tool. J Mol Biol *215*, 403-410.

Arnold, K., Bordoli, L., Kopp, J., and Schwede, T. (2006). The SWISS-MODEL workspace: a web-based environment for protein structure homology modelling. Bioinformatics *22*, 195-201.

Brenner, S. (1974). The genetics of *Caenorhabditis elegans*. Genetics *77*, 71-94.

Cheung, B.H., Arellano-Carbajal, F., Rybicki, I., and de Bono, M. (2004). Soluble guanylate cyclases act in neurons exposed to the body fluid to promote *C. elegans* aggregation behavior. Curr Biol *14*, 1105-1111.

Darby, C., Cosma, C.L., Thomas, J.H., and Manoil, C. (1999). Lethal paralysis of *Caenorhabditis elegans* by *Pseudomonas aeruginosa*. Proc Natl Acad Sci U S A *96*, 15202-15207.

Dieterich, C., Clifton, S.W., Schuster, L.N., Chinwalla, A., Delehaunty, K., Dinkelacker, I., Fulton, L., Fulton, R., Godfrey, J., Minx, P*., et al.* (2008). The *Pristionchus pacificus* genome provides a unique perspective on nematode lifestyle and parasitism. Nat Genet *40*, 1193-1198.

Hartley, J.L., Temple, G.F., and Brasch, M.A. (2000). DNA cloning using in vitro site-specific recombination. Genome Res *10*, 1788-1795.

Hirokawa, T., Boon-Chieng, S., and Mitaku, S. (1998). SOSUI: classification and secondary structure prediction system for membrane proteins. Bioinformatics *14*, 378-379.

Hsieh, J., Liu, J., Kostas, S.A., Chang, C., Sternberg, P.W., and Fire, A. (1999). The RING finger/B-box factor TAM-1 and a retinoblastoma-like protein LIN-35 modulate context-dependent gene silencing in *Caenorhabditis elegans*. Genes Dev *13*, 2958-2970.

Larkin, M.A., Blackshields, G., Brown, N.P., Chenna, R., McGettigan, P.A., McWilliam, H., Valentin, F., Wallace, I.M., Wilm, A., Lopez, R*., et al.* (2007). Clustal W and Clustal X version 2.0. Bioinformatics *23*, 2947-2948.

Maclean, K.N., Sikora, J., Kozich, V., Jiang, H., Greiner, L.S., Kraus, E., Krijt, J., Crnic, L.S., Allen, R.H., Stabler, S.P*., et al.* (2010). Cystathionine beta-synthase null homocystinuric mice fail to exhibit altered hemostasis or lowering of plasma homocysteine in response to betaine treatment. Mol Genet Metab *101*, 163-171.

Mello, C.C., Kramer, J.M., Stinchcomb, D., and Ambros, V. (1991). Efficient gene transfer in *C. elegans*: extrachromosomal maintenance and integration of transforming sequences. EMBO J *10*, 3959-3970.

Mozzarelli, A., Bettati, S., Campanini, B., Salsi, E., Raboni, S., Singh, R., Spyrakis, F., Kumar, V.P., and Cook, P.F. (2011). The multifaceted pyridoxal 5'-phosphate-dependent O-acetylserine sulfhydrylase. Biochim Biophys Acta, 10.1016/j.physletb.2003.1010.1071.

Shen, C., Nettleton, D., Jiang, M., Kim, S.K., and Powell-Coffman, J.A. (2005). Roles of the HIF-1 hypoxia-inducible factor during hypoxia response in *Caenorhabditis elegans*. J Biol Chem *280*, 20580-20588.

Trent, C., Tsung, N., and Horvitz, H.R. (1983). Egg-laying defective mutants of the nematode *Caenorhabditis elegans*. Genetics *104*, 619-647.

Publication 6.1.4

Hydrogen Sulfide in Cell Signaling: Signal Transduction, Cellular Bioenergetics and Physiology in *C. elegans*

General Physiology and Biophysics (2013)

doi: 10.4149/gpb_2013001

Review

Hydrogen sulfide in cell signaling, signal transduction, cellular bioenergetics and physiology in *C. elegans*

Katalin Módis[1], Katarzyna Wolanska[2] and Roman Vozdek[3]

[1] *Department of Anesthesiology, University of Texas Medical Branch, Galveston TX, USA*
[2] *University of Exeter Medical School, Exeter, United Kingdom*
[3] *Institute of Inherited Metabolic Disorders, First Faculty of Medicine, Charles University in Prague and General University Hospital in Prague, Prague, Czech Republic*

Abstract. Hydrogen sulfide (H_2S), long viewed as a toxic gas and environmental hazard, is emerging as a biological mediator with remarkable physiological and pathophysiological relevance. H_2S is now viewed as the third main gasotransmitter in the mammalian body. Its pharmacological characteristic possesses similarities to the other two gasotransmitters – nitric oxide (NO) and carbon monoxide (CO). Many of the biological effects of H_2S follow a bell-shaped concentration-response; at low concentration or at lower release rates it has beneficial and cytoprotective effects, while at higher concentrations or fast release rates toxicity becomes apparent. Cellular bioenergetics is a prime example for this bell-shaped dose-response, where H_2S, at lower concentrations/rates serves as an inorganic substrate and electron donor for mitochondrial ATP generation, while at high concentration it inhibits mitochondrial respiration by blocking the Complex IV in the mitochondrial electron transport chain. The current review is aimed to focus on the following aspects of H_2S biology: 1) a general overview of the general pharmacological characteristics of H_2S, 2) a summary of the key H_2S-mediated signal transduction pathways, 3) an overview of role of H_2S in regulation of cellular bioenergetics, 4) key aspects of H_2S physiology in *C. elegans* (a model system) and, finally 5) the therapeutic potential of H_2S donating molecules in various disease states.

Key words: Signal transduction — Bioenergetics — Oxygen sensing — Nematodes — H_2S donors

Abbreviations: CAT, cysteine aminotransferase; CBS, cystathionine β-synthase; CSE, cystathioneine γ-lyase; ETHE1, surfur dioxygenase/dioxygenase ethylmalonic encephalopathy; GAPDH, glyceraldehyde 3-phosphate dehydrogenase; GSH, glutathione; HIF-1, hypoxia inducible factor; HO-1, heme oxygenase; 3-MP, 3-mercaptopyruvate; 3-MST, 3-mercaptopyruvate sulfurtransferase; Nrf2, nuclear factor E2 related factor 2; PDE, phosphodiesterase; SQR, sulfide:quinone oxidoreductase; Trx1, thioredoxin reductase; TST, thiosulfate sulfure transferase/rhodanese.

Introduction

In addition to nitric oxide (NO) and carbon monoxide (CO), hydrogen sulfide (H_2S) is now considered the third gasotransmitter and cellular signaling molecule (Szabo 2007; Wagner et al. 2009; Whiteman et al. 2011; Wang 2012). All these three small molecules freely diffuse through cell membranes to exert their cellular signaling actions.

H_2S is a colorless, flammable, water-soluble gas with the characteristic smell of rotten eggs. Most of the earlier literature focused on its toxicological effects considering as an environmental hazard and as a mitochondrial broad-spectrum poison, affecting the nervous, respiratory, and cardiovascular system (Beauchamp et al. 1984; Reiffenstein et al. 1992). The toxicological effects of H_2S are mainly attributed to the inhi-

Correspondence to: Katalin Módis, Department of Anesthesiology, University of Texas Medical Branch, 601 Harborside dr., Bldg. 21, Rm. 4.202E, Galveston, TX 77555, USA
E-mail: katalin.modis@gmail.com

bition of cytochrome *c* oxidize in the mitochondrial electron transport chain (Cooper et al. 2008). This enzyme catalyzes the oxidation of cytochrome *c* molecules and transfers the electrons to the molecular oxygen to produce water. Inhibition of cytochrome *c* oxidase by H_2S results in uncoupling of mitochondria, during which the oxidative phosphorylation is no longer linked to further ATP production and the cell dies by energy depletion. The toxicological effect of H_2S on mitochondrial respiration is manifested at higher concentrations; *in vivo*, *via* the inhaled route, H_2S above 500 ppm can cause rapid unconsciousness and respiratory arrest (Turner et al. 1980). Utilization of nitrite and hyperbaric O_2 therapy have been used as antidotes to H_2S toxicity (Reiffenstein et al. 1992).

In sharp contrast to the toxicological effects of H_2S, over the last decade, H_2S has attracted increasing attention in cell signaling in physiological and pathophysiological conditions. Emerging findings indicate that physiological amounts of H_2S can stimulate the mitochondrial oxygen consumption and ATP production. The oxidation of H_2S by mitochondria, coupled to the ATP synthesis capability of mammalian cells, has been retained by modern-day organisms from a long-gone oxic and asulfidic world. The first sections of the current review will focus on the signaling and bioenergetic aspects of H_2S biology. Then, we will discuss the role of H_2S in the biology of the nematode *Caenorhabditis elegans* (*C. elegans*), as this model system has been instrumental in recent years in unveiling various H_2S-mediated cellular pathways. Finally, since H_2S donation/supplementation may be relevant for future therapeutic approaches, in the last section of our review we will cover the therapeutic potential of novel H_2S-releasing donor molecules.

H_2S, the third gasotransmitter

H_2S biosynthesis in mammalian cells

H_2S is generated in mammalian cells *via* enzymatic and, to a lesser degree, non-enzymatic pathways (Figure 1). Among the three key H_2S-generating enzymes, cystathionine β-synthase (CBS; EC 4.2.1.22) and cystathionine γ-lyase (CSE; EC 4.4.1.1) have been investigated extensively. Both enzymes use pyridoxal-5'-phosphate (vitamin B6) as a cofactor and metabolize L-cysteine to produce H_2S. For this, L-cysteine, can either be derived from alimentary sources and liberated from endogenous proteins or synthesized endogenously from L-methionine through the reverse transsulfuration pathway using homocysteine as an intermediate in the process (Wang 2002; Fiorucci et al. 2006). The role of a third enzyme, 3-mercaptopyruvate sulfurtransferase (3-MST; EC 2.8.1.2), along with cysteine aminotransferase (CAT; CAT 2.6.1.3) in the process of H_2S biosynthesis has recently been demonstrated as well. Cysteine, along with alpha-ketoglutarate (alpha-KG), is converted into 3-mercaptopyruvate (3-MP) by CAT. 3-MP is then converted by 3-MST to form H_2S and pyruvate. Both CBS and CSE are localized to cytoplasm, while 3-MST is mainly localized to the mitochondria and partly to the cytoplasm (Kuo et al. 1983; Kimura 2011).

Free and bound sulfide in the mammalian cells

The definition of what constitutes "free sulfide", as opposed to "bound sulfide" deserves a brief discussion. Free sulfide is a dissolved H_2S gas, which is a weak acid (pH ~ 4) and in solution exists in the equilibrium $H_2S \leftrightarrow HS^- \leftrightarrow S^{2-}$. Nearly equal amounts of H_2S and HS^- exist within the cell, and approximately a 20% H_2S/80% HS^- ratio in extracellular fluid and plasma at 37°C and pH 7.4. Moreover, the bound sulfide pool, (bound sulfane sulfur pool), is localized to the cytoplasm and generates H_2S under reducing conditions. Glutathione and cysteine are the major cellular reducing compounds. The size of bound sulfane sulfur pool also depends on the H_2S-producing activity of the cells (Szabo 2007; Predmore et al. 2012; Wang 2012).

The concentration of H_2S in plasma and tissue homogenates

The plasma concentration of sulfide is regulated at the level of its generation and its consumption. There is no consensus on the actual extracellular (circulating) levels of H_2S: various reports describe it in mammalian blood mainly in the micromolar concentration range. In healthy animals and humans the physiological range of H_2S in circulation has been estimated at 10–100 μM (Richardson et al. 2000; Zhao et al. 2001; Hyspler et al. 2002; Hongfang et al. 2006; Whiteman et al. 2009; Wang 2012). Aging appears to have no effect on circulating H_2S. A study revealed no change in serum H_2S concentration among three age groups of humans spanning 50–80 years (34–36 μM) (Chen et al. 2005). Rat serum contains 46 μM H_2S (Zhao et al. 2001), and it is 34 μM in mouse serum (Li et al. 2005). In New Zealand rabbits, a quantitative assay detects a plasma H_2S level around 16.5 μM (Srilatha et al. 2009). Plasma H_2S at micromolar ranges has also been reported in many other vertebrates (Olson 2012; Olson et al. 2012). Endogenous levels of H_2S in rat brain homogenates are 50–160 μM (Abe et al. 1996; Hosoki et al. 1997). Similarly, significant degree of H_2S biosynthesis has been documented in the liver, kidney, and pancreas (Goodwin et al. 1989; Warenycia et al. 1989; Yusuf et al. 2005). H_2S production was clearly measured in the cardiovascular system (Hosoki et al. 1997; Zhao et al. 2001; Yang et al. 2008; Coletta et al. 2012). This discrepancy relates to the differences in the various methods to measure the free sulfide concentration: many methods are likely to liberate sulfide from its bound forms, thereby producing concentrations that are likely to

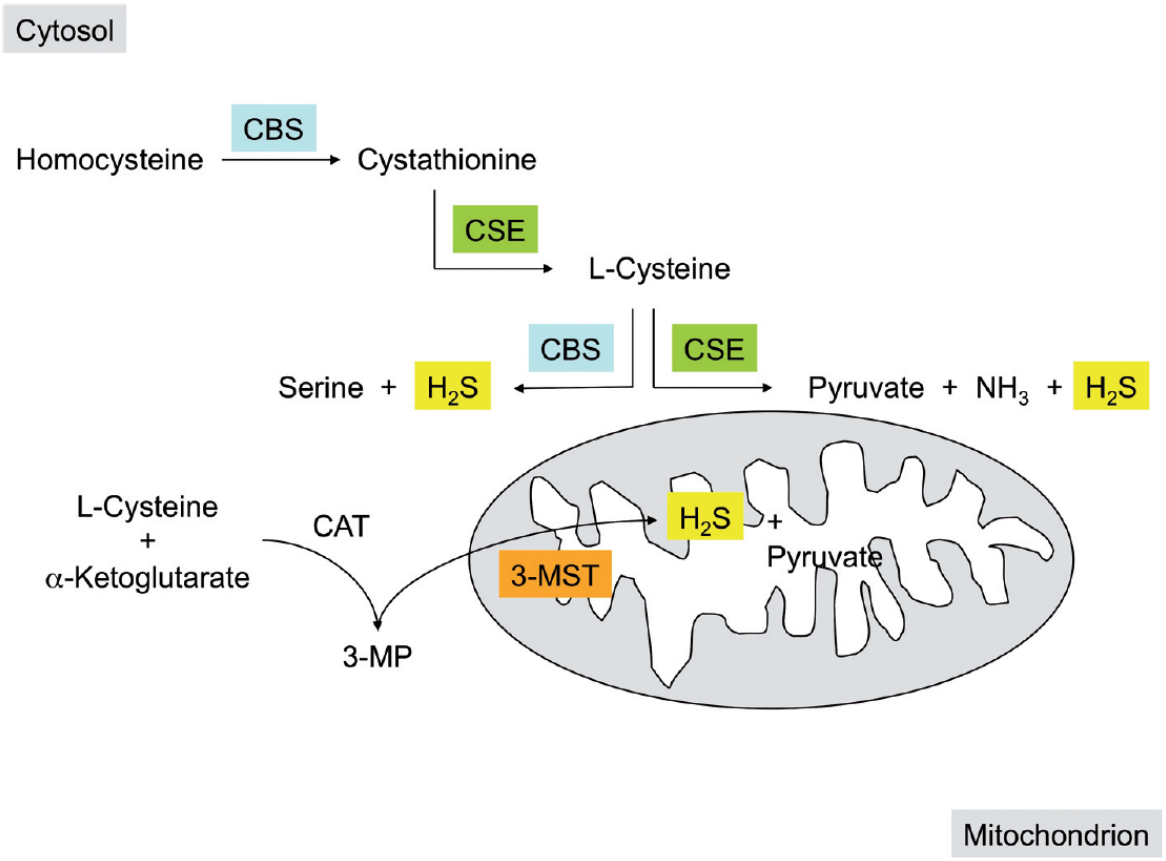

Figure 1. Enzymatic pathways of H_2S production in mammalian cells. Cystathionine β-synthase (CBS) catalyses the production of cystathionine from homocysteine. Cystathionine γ-lyase (CSE), subsequently converts cystathionine to L-cysteine. Then CBS and CSE enzymes, utilizing the same substrate, convert L-cysteine to form hydrogen sulphide (H_2S). The above reactions predominantly take place in the cytosol. In the mitochondria, L-cysteine in the presents of α-ketoglutarate can be converted to 3-mercaptopyruvate (3-MP) by cysteine aminotransferase (CAT), which can then be converted to H_2S by 3-mercaptopyruvate sulfurtransferase (3-MST). 3-MST is localized both in the mitochondria and in the cytosol.

represent a mixture of free and bound sulfide (Hannestad et al. 1989; Togawa et al. 1992; Ogasawara et al. 1993; Hughes et al. 2009; Wintner et al. 2010).

There are also several reports describing significant changes in the plasma levels of H_2S in various disease states. In many animal models of disease, the plasma/tissue levels of endogenous sulfide/sulfane sulfur and/or H_2S-generating enzymes level are reduced; for example in cardiac ischemia (Elrod et al. 2007; Predmore et al. 2011), hypertension (Yang et al. 2008), hyperhomocysteinemia (Gupta et al. 2009), erectile dysfunction (Qiu et al. 2012), chronic kidney disease (Perna et al. 2012), diabetes (Brancaleone et al. 2008; Whiteman et al. 2010; Suzuki et al. 2011) gastrointestinal tract inflammation (Fiorucci et al. 2005), asthma (Tian et al. 2012), wound healing (Coletta et al. 2012). On the other hand, there are certain conditions, including circulatory shock (Hui et al. 2003; Collin et al. 2005; Zhang et al. 2006) or certain forms of cancer (Guo et al. 2012; Lai et al. 2012), in which increased circulating/tissue sulfide levels were reported.

Taken together, an abundance of recent experimental evidence suggests that H_2S plays a prominent role in normal physiology as well as in various pathophysiological conditions.

H_2S-mediated signal transduction pathways

The biological actions of H_2S are mediated by a wide array of molecular mechanisms (Figure 2). It is likely that this list

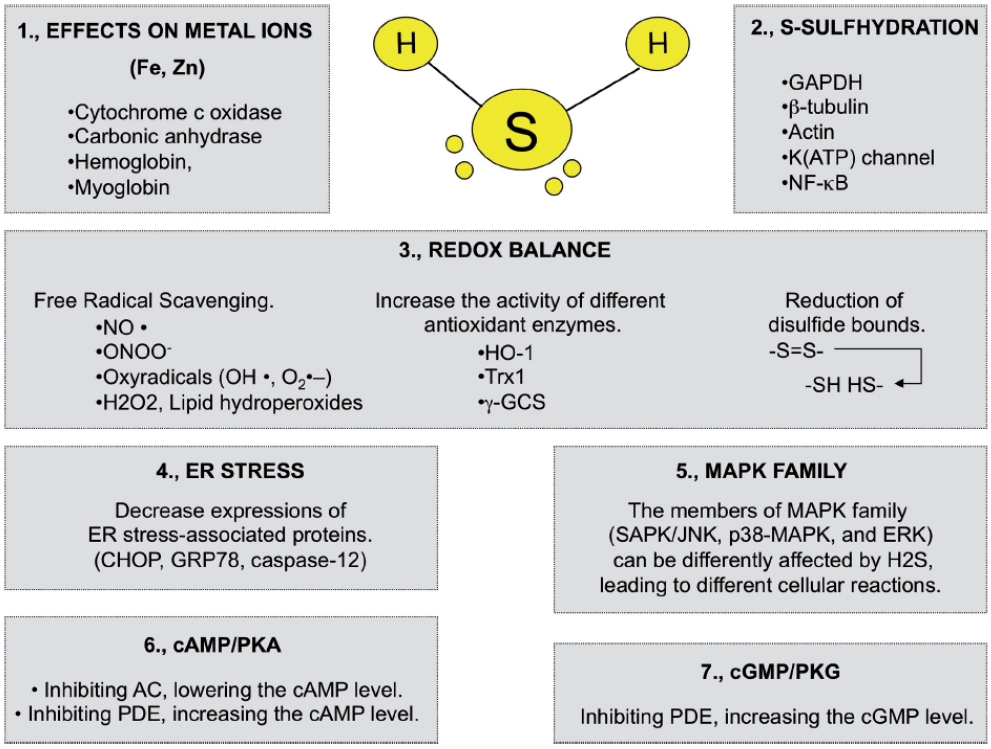

Figure 2. Possible biological effects of H_2S in mammalian cells. (**1**) H_2S can target metalloproteins such as cytochrome c oxidase, carbonic anhydrase, hemoglobin and myoglobin. (**2**) H_2S also participates in reactions yielding protein persulfides, protein polysulfides and protein associated sulfur (GAPDH, β-tubulin, K_{ATP} channels, actin, NF-κB). This mode of action is called S-sulphydration and occurs on the cysteine residue of proteins. (**3**) H_2S has a role in regulation of the redox balance. It can reduce disulfide bonds in proteins involved in oxidant sensing; regulate expression of antioxidant genes e.g. heme oxygenase 1 (HO-1), thioredoxin reductase (TrxR), γ-glutamylcysteine synthetase (γ-GCS) and reacts with various reactive oxygen and nitrogen species, resulting in free-radical scavenging. H_2S is involved in the regulation of ER stress (**4**) and the regulation of MAPK superfamily enzymes (**5**). H_2S is also responsible in the alteration of cellular cAMP/cGMP levels *via* the inhibition of phosphodiesterases enzymes (PDEs) (**6**, **7**). CHOP, C/EBP homologous protein; GRP78, glucose-regulated protein 78; SAPK/JNK, stress-activated protein kinase/c-JunNH2-terminal kinase; AC, adenylyl cyclase.

is incomplete and will grow further as H_2S biology expands. It is also likely that the relative importance of each of these pathways is different in different cell types, organs, species and in health or disease (for further details, see Szabo 2007; Paul et al. 2012; Wang 2012. H_2S signaling has been shown to involve the following pathways:

1) H_2S is known to interact with metalloproteins such as cytochrome *c* oxidase and carbonic anhydrase interacting with heme moiety and metal ions (Zn, Fe). Such interactions usually results in inhibition of the protein function, as determined for cytochrome *c* oxidase (Hill et al. 1984). The binding of sulfide to hemoglobin or myoglobin results in formation of sulfhemoglobin or sulfmyoglobin that decreases affinity to oxygen and thus diminishes oxygen transport in the body (Pietri et al. 2011).

2) H_2S can induce covalent modification of cysteine residues in proteins through S-sulfhydration (protein persulfides, protein-Cys-S-SH) that is considered to increase and stabilize the protein activity, respectively (GAPDH, β-tubulin, actin, K_{ATP} channel, p65 subunit of the nuclear factor NF-κB). This process may occur at cysteines exposed to surface of proteins or localized in their active sites, and form either disulfide bonds (protein-Cys-S-S-R), or sulfenic acid (protein-Cys-S-OH) (Finkel 2012), or even from cyclic sulfonamide conformation (Krishnan et al. 2012). *S*-sulfhydration is term for persulfide bond Cys-S-SH and commonly is compared with *S*-nitrosation Cys-S-NO, a mechanism of the other signaling molecule and gasotransmitter NO. While S-sulfhydration is considered to increase and stabilize the protein activity, *S*-nitrosation leads to inhibition of the

protein function, as determined for glyceraldehyde 3-phosphate dehydrogenase (GAPDH) (Mustafa et al. 2009), or the transcription factor NF-κB (Sen et al. 2012). In these cases, H_2S and NO may act sequentially by posttranslational modification of the proteins and thus activate and subsequently inactivate protein activity, respectively.

H_2S is an endogenous activator of the ATP-dependent potassium channel (K_{ATP} channel) *via* sulfhydration. This mechanism modulates cell metabolism and vasorelaxation (Zhao et al. 2001; Mustafa et al. 2011). In addition to the activation of K_{ATP} channel other types of potassium, calcium, chloride channels and ion exchangers are regulated by H_2S *via* mechanism, which are different from protein S-sulfhydration (Li et al. 2011; Wang 2012).

3) H_2S, as an antioxidant and a reducing agent, participates in regulation of the redox balance: Some of its redox actions are the consequence of the reduction of disulfide bonds, while others may relate to direct reactions with various reactive oxygen and nitrogen species, resulting in free-radical scavenging (e.g. peroxynitrite, superoxide anion, hydroxyl radical, nitric oxide, lipid hydroperoxide), although the rate constants of these reactions appear to be low (Carballal et al. 2011). *Via* these mechanisms, H_2S provides a reducing/antioxidant environment to intracellular compartments, including the mitochondria; loss of this environment – in conditions such as hyperglycemia – can facilitate mitochondrial ROS production and mitochondrial dysfunction (Suzuki et al. 2011; Szabo 2012).

Sulfide can also indirectly upregulate several antioxidant enzymes (e.g. heme oxygenase 1 (HO-1, it produces CO), thioredoxin reductase (Trx1) through increasing the nuclear accumulation of nuclear factor E2-related factor 2 (Nrf2), a key transcription factor that regulates antioxidant genes by its increased accumulation in the nucleus (Calvert et al. 2009). *Via* induction of Nrf2, H_2S may also regulate the levels of Trx and Trx reductase. In conjunction with this finding that Trx enhances the H_2S-producing activity of 3MST (as the reduced form of Trx helps 3-MST enzyme release the produced H_2S from its active site) Trx may induce positive feedback that promotes H_2S production through Nrf2 induction (Mikami et al. 2011).

Another indirect effect of H_2S on antioxidant defense involves upregulation of cellular glutathione levels via enhancing the activity of gamma-glutamyl-cysteine synthetase and up-regulating cystine transport. Cystine (cysteine) is the rate-limiting substrate of glutathione synthesis (Kimura et al. 2004). Besides the thioredoxin system the glutathione (GSH) is the other major factor generally responsible for the low redox potential and high free SH level inside the cells.

4) The endoplasmic reticulum (ER) is responsible for lipid synthesis and the maturation and folding of membrane proteins, secretory proteins etc. It also plays an important role in regulating intracellular signaling process, including calcium homeostasis. ER stress refers to altered ER function in general, to liberation of a large amount of calcium, and to accumulation of unfolded protein aggregates or excessive protein traffic specifically. Different research groups have demonstrated that homocysteine provokes ER stress in cardiomyocytes and this is related to reduced CSE expression and H_2S production. Also the expression of different ER stress-associated proteins, including C/EBP homologous protein (CHOP), caspase-12 and glucose-regulated proteins 78 (GRP78) were decreased after the administration of H_2S *in vivo* and/or *in vitro* (Chang et al. 2008; Wei et al. 2010).

5) The MAPK superfamily contains three main members: stress-activated protein kinase/c-JunNH2-terminal kinase (SAPK/JNK), p38-MAPK, and ERK. The activities of MAPK are very important in regulating cell proliferation, apoptosis, differentiation, inflammation, and cycle progression (Wang 2012). The activation of the same MAPK family member can be differently affected by H_2S, leading to different cellular reactions. Furthermore, a MAPK family member in different cells may be responsible for the opposite functional consequences. For example, H_2S increased endothelial cell proliferation *via* stimulating a sustained phosphorylation of ERK (Papapetropoulos et al. 2009). ERK activation has also been implicated in the H_2S-mediated myocardial protection pathways (Osipov et al. 2009). The same increase in ERK phosphorylation by the H_2S donor NaHS leads to inhibited proliferation of smooth muscle cells (Yang et al. 2004; Yang et al. 2010).

6) H_2S also plays a role in regulation of cAMP/PKA and cGMP/PKG pathways. cAMP and cGMP are signaling molecules playing roles in many cellular functions by activating protein kinase A (PKA) or protein kinase G (PKG), respectively. PKA and PKG phosphorylate various proteins serving as regulators of different cellular signaling pathways. Both metabolites, cAMP and cGMP, are usually hydrolyzed by the enzymatic activity of phosphodiesterase (PDE) to 5'GMP or 5'AMP. H_2S also plays a role in regulation of endogenous levels of these metabolites, because it functions as an endogenous PDE inhibitor such in vasorelaxation and angiogenesis (Papapetropoulos et al. 2009; Coletta et al. 2012; Fusco et al. 2012).

Coletta and colleagues recently have demonstrated that the H_2S donor NaHS concentration-dependently decreases the activity of purified PDE5A. This finding suggests that the H_2S-induced increase in endothelial cell cGMP levels and subsequent endothelial proliferation is due to reduced cGMP degradation (Coletta et al. 2012).

In the context of cAMP/PKA signaling, other studies have shown that H_2S can also decrease cAMP production by inhibiting adenylyl cyclase (AC). The decreased cAMP in vascular smooth muscle cells (Lim et al. 2008) and in juxtaglomerular cells (Lu et al. 2010) was observed

and a similar suppression of cAMP levels by H_2S has also been demonstrated in cardiomyocytes (Yong et al. 2008). Whether NaHS directly inhibits AC was not tested in these studies. In the context of these studies it is interesting to mention that a complete cAMP-PKA system is localized in the mitochondrial matrix and the protein kinase A (PKA) regulates ATP production by phosphorylation of mitochondrial proteins, including subunits of cytochrome *c* oxidase (Acin-Perez et al. 2009). Whether H_2S regulates this system remains a subject of further investigations.

The role of H_2S in cellular bioenergetics

It was well known for several decades that organisms in sulfide-rich environments (in certain swamps and hydrothermal vents) can synthesize ATP from sulfide (Grieshaber et al. 1998; Yong et al. 2001; Searcy 2003; Hildebrandt et al. 2008). Only within the last 6 years did it become apparent that these pathways are also conserved in mammalian cells (Goubern et al. 2007).

To understand the bioenergetic role of H_2S we have to retrace the evolution of eukaryotes. Mitochondria arose from endosymbiosis (a single evolutionary event). This union was highly advantageous to the host cell because it (i) prevents oxygen toxicity, (ii) utilizes a mechanism of hydrogen transfer and /or (iii) enable sulfur cycling (sulfur syntrophy) (Searcy 2003; Olson 2012). Sulfur is a versatile molecule with oxidation states ranging from –2 to +6. Hydrogen sulfide or some sulfur moiety is omnipresent; delivering from extraterrestrial sources, such as meteorites, producing in a pre-biotic atmosphere or generating underwater in the effluent of hydrothermal vents on the deep ocean floor. Sulfide and sulfur species must have been an integral component of early life, irrespective of life's origin. These compounds exist in a variety of oxidation states and because of this ability they can transfer energy and may have had a key role in the great endosymbiotic event. According to this symbiotic relationship a host, sulfur-reducing Archea ($S^0 \rightarrow H_2S$) incorporated a sulfide (H_2S, the oxidation state of -2) oxidizing α-protobacteria resulting the eukaryotic cell. Eukaryotes slowly adapted from a sulfidic and anoxic world to one that was highly oxic and asulfidic. It has also become evident that, even in the present-day oxic environment, mammalian cells can utilize the redox chemistry of sulfide as a "source of energy" (Goubern et al. 2007; Lagoutte et al. 2010; Bouillaud et al. 2011; Mimoun et al. 2012; Módis et al. 2012) or a "metabolism as an O_2 sensor" (Olson et al. 2010; Olson 2012) to show that these ancient biochemical pathways are still employed by modern-day eukaryotes.

In mammals there are different cellular pathways to eliminate the endogenously produced H_2S as well as H_2S introduced into the body from the environment. H_2S can be exhaled or mainly excreted in urine primarily as sulfate or thiosulfate and in feces as free sulfide. Methylation (CH_3SH) is another catabolic pathway for H_2S, mainly takes place in the cytosol. The half-life of free H_2S in blood is relatively short as it is being scavenged by methemoglobin to form sulfhemoglobin. Notably, besides its excretion by urine the second most important pathway in the catabolism of H_2S is its inactivation through mitochondrial oxidation (reviewed in Wang 2012).

H_2S is produced by the three enzymes CBS, CSE and 3-MST intracellularly (see above). During normoxia, H_2S is continuously oxidized by mitochondria generating sulfate and thiosulfate (Figure 3.), thereby maintaining low intracellular H_2S levels while being eliminated as sulfate and thiosulfate. This represents a form of detoxification process for H_2S.

A mitochondrial membrane-bound enzyme, termed sulfide:quinone oxidoreductase (SQR), oxidizes sulfide to the level of elemental sulfur, simultaneously reducing a cysteine disulfide such that a persulfide group is formed at one of the cysteines (SQR-SSH). The electrons are donated into the respiratory chain *via* the coenzyme Q (Q oxidized = Q reduced), and finally transferred to oxygen by cytochrome oxidase (complex IV). The dioxygenase ethylmalonic encephalopathy (ETHE1, which has a sulfur dioxygenase activity) in the mitochondrial matrix oxidizes persulfides to sulfite (SO_3^{2-}), consuming molecular oxygen and water (Tiranti et al. 2009). Subsequently, sulfite is further oxidized to sulfate (SO_4^{2-}) by sulfite oxidase (SOX). Thiosulfate sulfur transferase (TST) (also known as one isoenzyme of the rhodanese) produces thiosulfate ($S_2O_3^{2-}$) by transferring the second persulfide from the SQR to sulfite. Taken together, this sulfide oxidizing unit (SOU) acts independently constituting of the sulfide quinone reductase (SQR) and of two other enzymes the sulfur dioxygenase (ETHE1) and TST, acts independently to ensure the final oxidation of the two disulfides (-SSH) bound to SQR into oxidized cysteine linked by a disulfide bond (Bouillaud et al. 2011).

Sulfide and mitochondria

The O_2 sensor theory

Oxidative phosphorylation is the major ATP-producing pathway in most mammalian cells. Molecular oxygen (O_2) is the terminal electron acceptor in oxidative phosphorylation, and essential for the ATP generation. Insufficient oxygen supply induces hypoxic conditions that can be serious if it accompanies reduced nutrition supply and accumulation of harmful metabolic waste. A fall in oxygen availability (hypoxia) decreases mitochondrial H_2S oxidation resulting in an increase in biologically active H_2S level and initiation of hypoxic responses.

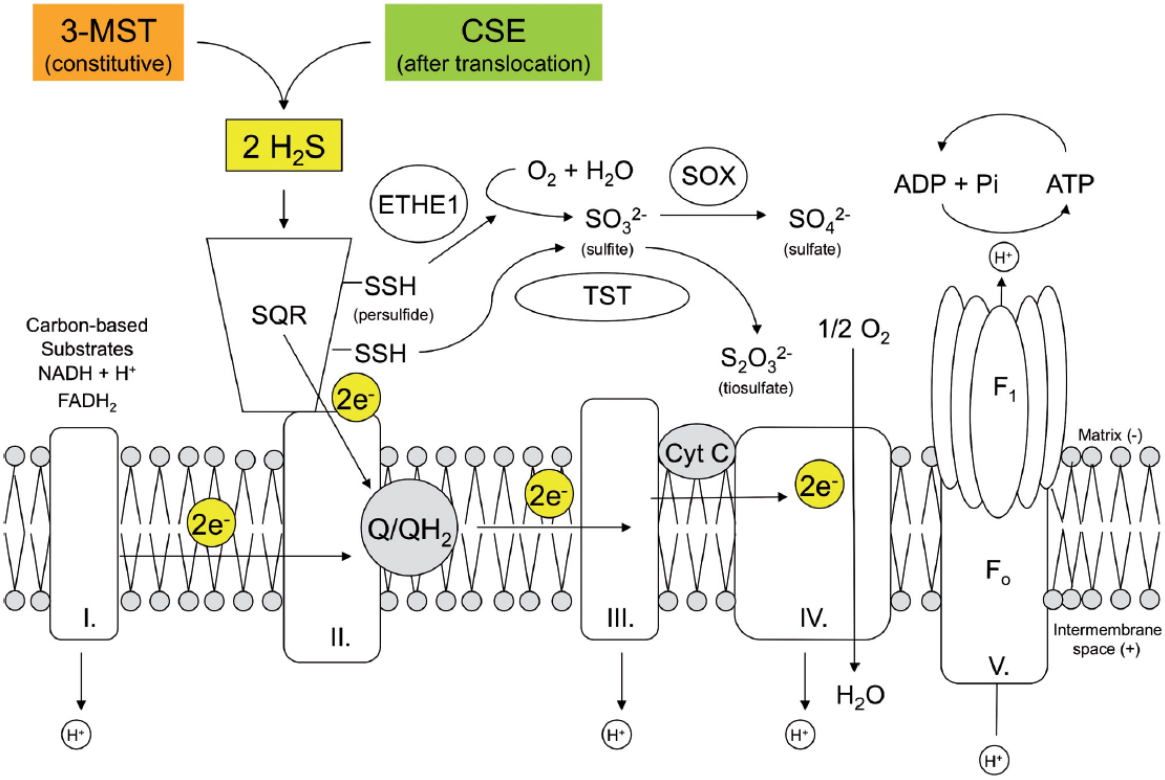

Figure 3. H_2S oxidation and consequent bioenergetic effects in the mitochondria of mammalian cells. Oxidation of carbon-based substrates leads to the reduction of the NAD or FAD coenzymes. The reduced forms of these coenzymes (NADH + H, $FADH_2$) yield electrons to coenzyme Q of the mitochondrial respiratory chain. NADH + H is oxidized by mitochondrial complex I. $FADH_2$ coenzymes yield electrons through the function of complex II (succinate dehydrogenase). Both complexes (I and II) donate electrons *via* coenzyme Q of the mitochondrial electron transport chain. The sulfide-oxidizing unit acts independently. It is constituted of the mitochondrial membrane-bound sulfide quinone reductase (SQR) and of two other enzymes the sulfur dioxygenase (ETHE1, also called dioxygenase ethylmalonic encephalopathy) and the thiosulfate sulfur transferase (TST, also known as one isoenzyme of the rhodanese), ensuring the final oxidation of the two disulfides (-SSH) bound to SQR into oxidized cysteine linked by a disulfide bond. The sulfur dioxygenase in the mitochondrial matrix oxidizes persulfides to sulfite (SO_3^{2-}), consuming molecular oxygen and water. Sulfite, then, is further oxidized to sulfate (SO_4^{2-}) by sulfite oxidase (SOX). The thiosulfate sulfur transferase (TST) produces thiosulfate ($S_2O_3^{2-}$) by transferring the second persulfide from the SQR to sulfite. Taken together, SQR is responsible for the oxidation of H_2S in the mitochondria. While from two H_2S molecules, two disulfides (-SSH) bounds are created on the SQR, two electrons derived from 2 H_2S also enter the mitochondrial electron transport chain, promoting mitochondrial ATP generation. These actions are considered beneficial and physiological, and tend to occur at lower H_2S concentrations/rates. On the other hand, higher concentrations of H_2S can inhibit complex IV, thereby inhibiting mitochondrial respiration. Finally, the utilized H2S in the mitochondria can be produced by the constitutively present 3-mercaptopyruvate sulfurtransferase (3-MST) or by the translocated cystathionine γ -lyase (CSE) enzyme.

In the body there are different oxygen-sensing tissues, like glomus cells of the carotid vasculature, or neuroendocrine cells as chromaffin cells. The glomus cells of the carotid body express both CSE and CBS and produce H_2S (Peng et al. 2010). CSE is also expressed in neonatal adrenal medullary chromaffin cells of rats and mice. The concept that H_2S acts an "O_2 sensor" was first demonstrated by Olson and his colleagues in 2006 (Olson et al. 2006). According to their hypothesis the following mechanism exists in oxygen-sensing cells: Blood vessels and chemoreceptors can detect oxygen levels and initiate appropriate physiological responses. In addition, hypoxia stimulates H_2S production from these oxygen-sensing cells while the lack of oxygen also induces a reduced H_2S oxidation by mitochondria. Finally, the resulting H_2S has a role in responding to hypoxia with cardiovascular and respiratory reflexes; H_2S closes calcium-sensitive

potassium (BKCa) channels to depolarize chemoreceptor cells (Telezhkin et al. 2009), triggering catecholamine secretion and hypoxia-induced hyperventilation (Olson et al. 2010). Initially, this mechanism was based on the constitutive sulfide production in the cytoplasm by CSE and CBS enzyme and its reduced oxidization in the mitochondria, although it now appears that sulfide may also be generated within the mitochondria *via* the function of 3-MST (Shibuya et al. 2009).

Many details of the above mechanisms need to be further elucidated in future studies. How does H_2S "sense" the oxygen levels in the carotid body? Does the oxygen level (PO_2), *per se*, have a direct effect on the activity of CBS or CSE enzymes? CBS itself may not bind oxygen, but it can be quickly oxidized from the ferrous (Fe^{2+}) to the ferric state (Fe^{3+}) *via* an outer sphere electron transfer (Banerjee et al. 2005). Furthermore, which one is the real oxygen sensor(s)? CSE/CBS, H_2S (*per se*) or the products during H_2S oxidation, such as sulfite (SO_3^{2})? Addressing these questions will provide further important insights into the basic physiological regulation of O_2 sensing.

H_2S as a source of energy in mammalian cells

Based on the pioneering work of Krebs and Szent-Györgyi over half a century ago, the standard model of mammalian cellular bioenergetics was formulated. Krebs cycle products such as NADH and succinate are the obligatory factors that drive mitochondrial electron transport and maintain oxidative phosphorylation and ATP production. The electron transport chain proteins (Complexes I-IV) in the inner mitochondria membrane pass electrons along the chain, and oxygen serves as the terminal electron acceptor at Complex IV (cytochrome *c* oxidase). Mitchell has subsequently recognized that the purpose of this process is to pump protons from the mitochondrial matrix into the intermembrane space, in order to build a chemiosmotic gradient across the membrane. This electrochemical gradient is harnessed by Complex V, thereby generating ATP (Nelson et al. 2008; Voet et al. 2008) (Figure 3).

Data emerging over the last decade has suggested that in bacteria and archaea living in oxygen-deprived environments the electron transport utilizes alternative electron donors (such as nitrate, nitrite, or hydrogen sulfide) (Grieshaber et al. 1998; Searcy 2003; Hildebrandt et al. 2008). However, the generally held view was that these processes are obscure, inefficient, and exclusively reserved to non-mammalian cells. Sulfide has been shown to donate electrons to the mitochondrial respiratory chain in clams, worms, or fishes adapted to environments showing a comparable concentration of sulfide with that measured inside the mammalian gut (Grieshaber et al. 1998). This characteristic is likely to be inherited from the prokaryotic ancestor of mitochondria. These existing evidences show that electrons from sulfide could be given to the mitochondrial respiratory chain at the level of coenzyme Q (Ouml et al. 1997) or cytochrome *c* (Powell et al. 1986).

Hydrogen sulfide has a biphasic effect on mitochondrial function. At lower concentrations (under 5 μM) H_2S has a stimulatory effect on respiration, donating electrons to the electron transport chain while generating ATP. At higher concentration (above 10 μM) has an inhibitory effect on mitochondrial respiration blocking the cytochrome *c* oxidase (Complex IV) and inducing a complete shutdown of the mitochondrial electron transport chain. Taken together, the biological significance of the two opposing effects of H_2S on mitochondrial respiration, i.e. stimulation of ATP generation (Yong et al. 2001; Goubern et al. 2007; Lagoutte et al. 2010; Bouillaud et al. 2011) *vs.* inhibition of mitochondrial electron transport at Complex IV (Nicholls 1975; Khan et al. 1990; Collman et al. 2009) remained to be resolved.

In 2001, Yong and Searcy published a very surprising report: they demonstrated that low concentrations of H_2S (under 5 μM concentration) increased O_2 consumption in isolated chicken liver mitochondria. In addition, they reported that the oxidation of H_2S is coupled with measurable ATP production and increased mitochondrial membrane potential (Yong et al. 2001). The same report also considered that higher concentration of H_2S may serve as an uncoupler, however, the mechanism of uncoupling was not explored thoroughly. One possibility is that H_2S might be able to shuttle H^+ across the inner mitochondrial membrane in a manner similar to protonophore uncouplers. However, the results of Yong and Searcy showed that the membrane potential varies during constant sulfide input, suggesting that this coupling phenomenon of H_2S may be switched off and on. Thus, uncoupling may involve an actively regulated metabolic switch, such as a gated H^+ leakage channel, but the existence of this explanation still needs to be directly confirmed in future studies. Taken together, Yong and Searcy were the first who demonstrated that mitochondria, which are not adapted to sulfidic environments, but nevertheless can oxidize sulfide with coupled ATP synthesis. This type of biochemistry has not been observed previously in non-sulfide-adapted species. Therefore, Searcy and Lee suggested first that coupled respiration on sulfide is a widespread and primitive trait of mitochondria.

In 2007, Goubern and his colleagues suggested that exogenously administered H_2S can act as an electron donor and a potential inorganic source of energy in mammalian cells (Goubern et al. 2007). They used two different human colon adenocarcinoma cell lines (CaCo2 and HT-29 $Glc^{-/+}$). In these permeabilized cells subjected to H_2S an elevated O_2 consumption and increase mitochondrial membrane potential were detected. This was the first report

that indicated sulfide can lead to mitochondrial energizing in mammalian cells, and also the first report to conclude that when sulfide is oxidized by mitochondria in colonocytes there are two sites for oxygen consumption: 1) the formation of water at the level of mitochondrial complex IV (cytochrome *c* oxidase), and 2) the formation of sulfur containing oxygenated products (thiosulfate, sulfite, sulfate). In addition, when sulfide reaches a threshold of concentration sufficient to inhibit cytochrome *c* oxidase (complex IV), according to their data electrons are redirected toward mitochondrial complex II (succinate dehydrogenase). In these conditions it acts in reverse mode and reduces fumarate into succinate. This would allow an anaerobic oxidation of sulfide. This group, however, concluded that – in contrast to Yong's and Searcy's assumptions – sulfide *per se* does not lead to increased permeability of the mitochondrial inner membrane for protons, and therefore does not cause "uncoupling" studied in permeabilized cells (Goubern et al. 2007).

In a follow-up study in 2010, Lagoutte and colleagues found that exposure of CHO cells overexpressing human SQR to chemical H_2S donors resulted in an increase in cellular oxygen consumption and ATP production (Goubern et al. 2007; Lagoutte et al. 2010; Bouillaud et al. 2011). This group also demonstrated that the appropriate H_2S concentration, which stimulates the mitochondrial respiration depended on different cell types and related to the various expression levels of SQR protein. In further studies Mimoun and his colleagues have showed that sulfide oxidizing capacity is increased with their level of differentiation in colonocytes (Mimoun et al. 2012). In this study, however, it was concluded that sulfide is not primarily oxidized for increasing the cellular level of ATP but rather for allowing its detoxification. These findings are best conceptualized in the context that in mammals the indigenous sulfate-reducing bacteria in the large intestine represents another source of H_2S, which is frequently considered an endogenous "environmental insult" to the colonic epithelium (Magee et al. 2000; Attene-Ramos et al. 2007; Attene-Ramos et al. 2010). Accordingly, the mitochondrial sulfide oxidation in colonocytes proved to be indispensable for maintaining physiological conditions of large intestine.

Although there are now several studies, in a variety of cell types demonstrating the biphasic effect of H_2S on cellular bioenergetics (stimulation at lower concentration, inhibition at higher) (Goubern et al. 2007; Lagoutte et al. 2010; Bouillaud et al. 2011; Groeger et al. 2012). From the above studies it remains unclear whether endogenously produced H_2S plays a role as an inorganic substrate in the physiological regulation of mitochondrial function. However, it has very recently been demonstrated that H_2S produced by 3-MST, rather than CSE or CBS, has a prominent role in the regulation of mitochondrial function in isolated liver mitochondria and in the cultured murine hepatoma cell line Hepa1c1c7 (Módis et al. 2012). According to this finding the endogenous intramitochondrial H_2S-producing pathway governed by 3-MST, complements and balances the bioenergetic role of Krebs cycle-derived electron donors. This pathway may serve a physiological role in the maintenance of mitochondrial electron transport and cellular bioenergetics. CSE could play a role since, recent studies by Wang and colleagues showed that under conditions of hypoxia, CSE may translocate to the mitochondria, thereby exerting positive bioenergetic effects (Fu et al. 2012). The possible role of the three H_2S producing enzymes (CSE, CBS, 3-MST) in the regulation of mitochondrial function needs to be thoroughly clarified as H_2S is a gaseous molecule and it can be easily diffusing to the mitochondria. In this case determining whether which H_2S producing enzyme has the main role in the regulation of mitochondrial function is likely to be highly complex.

H_2S physiology in model systems

Over the last decade, many of the studies aimed to explore the physiology or pathophysiology of H_2S relied on invertebrate model organisms. Using *C. elegans* models, it has been demonstrated by several studies that exposure to H_2S increases the viability and survival of animals protecting them from otherwise lethal conditions. It was also shown in rodents the exogenous H_2S leads to a hibernation-like state (suspended animation), with a decreased metabolic rate and core body temperature (Blackstone et al. 2005). Further studies showed that these regulatory effects induced by H_2S inhalation protect animals from hypoxia, hemorrhage and also diminish ischemia-reperfusion injuries (Blackstone et al. 2007; Ganster et al. 2010). In *Drosophila melanogaster*, also known as the common fruit fly (another common model system), the administration of H_2S was shown to result in elevated desiccation tolerance (Zhong et al. 2010). In *C. elegans* nematode model, as a multicellular organism – that is utilized as a model system to address fundamental questions in developmental biology – H_2S was found to promote thermotolerance and to prolong longevity (Miller et al. 2007).

Studies utilizing roundworm *C. elegans* can be highly useful to explore the molecular alterations mediated by H_2S. One of the focus of these studies was hypoxia tolerance; another one was signal transduction during hypoxia. Using such systems, it has been demonstrated that exogenous H_2S leads to translocation of the hypoxia inducible factor HIF-1, worm ortholog of the mammalian HIF-1α subunit (HIF-1) to the nucleus and promotes HIF-1 transcriptional activity in the hypodermis (Budde et al. 2010). Activated HIF-1 and its target genes such as sulfide:quinone oxidore-

ductase (SQRD-1; the mammalian equivalent being SQR) are essential for worm survival in sulfide-rich environment (Budde et al. 2010; Budde et al. 2011). (As discussed above, SQR is known to have a prominent role in oxidizing H_2S in mitochondria in mammals as well).

Exposure to H_2S also elicits a transcriptional response mediated by SKN-1 (Miller et al. 2011), a conserved transcription factor that is encoded by the *Nrf2* gene in humans; both SKN-1 and Nrf2 are indispensable for the resistance of oxidative and xenobiotic stress (An et al. 2003). According to other studies, worms live longer in non-lethal H_2S containing conditions (Miller et al. 2007), and HIF-1 and SKN-1 play a key role in prolonging their lifespan (Kell et al. 2007; Tullet et al. 2008; Hwang et al. 2011). In line of these findings, other studies showed that the garlic constituents, such as diallyl trisulfide (organic H_2S donors) increased the lifespan of *C. elegans via* a mechanism, which included SKN-1 activation (Powolny et al. 2011).

In a separate line of studies it was demonstrated that H_2S exposure induces an elevated activity of SIR-2.1, a homolog of NAD^+-dependent deacetylase, that also has a role in prolonged lifespan in *C. elegans* (Miller et al. 2007). Since the mechanism in which H_2S increases the lifespan of *C. elegans* is independent of other common mechanisms related to increase lifespan of *C. elegans*, like the insulin/IGF signaling (IIS) pathway (Miller et al. 2007), or attenuated mitochondrial function or dietary restriction (Miller et al. 2007), it is possible that there are two distinct mechanisms regulating lifespan of *C. elegans* during the H_2S induction – increased activity of SIR2.1 and transcriptional activation of HIF-1 and/or SKN-1.

HIF-1 and SKN-1/Nrf2 activation by the administration of H_2S may be conserved among other animal models; it was shown that cultured rat cells treated with H_2S exhibit HIF-1 activation (Liu et al. 2010), and also the Nrf2 translocation to the nucleus occurs in murine cardiomyocytes (Calvert et al. 2009). These data imply that the regulation of two important transcription factors mediated by H_2S is evolutionarily conserved in distinct organisms. However, the exact signaling pathways mediated by HIF-1 and SKN-1/Nrf2 remains to be clarified thoroughly in future studies.

In *C. elegans*, under normoxic conditions, a conserved proline residue in the worm ortholog of the mammalian HIF-1α subunit (HIF-1) is hydroxylated by EGL-9 (Epstein et al. 2001), a conserved dioxygenase in the mammalian EGLN protein family (Taylor 2001). The hydroxylation of the proline residue permits the binding of VHL-1 (protein von Hipple Lindau) to HIF-1 and thus targets HIF-1 for proteasomal degradation by the ubiquitination pathway (Epstein et al. 2001). Further studies demonstrated that EGL-9 also negatively regulates HIF-1 transcriptional activity through a VHL-1-independent pathway (Shao et al. 2009); negative HIF-1 transcriptional regulation *via* the VHL-1-independent mechanism has also been observed in mammalian cells (To et al. 2005).

What then is the exact mechanism of H_2S-mediated HIF-1 activation? Since the levels of H_2S dramatically increase during hypoxia (see above), it is probable that hypoxia and H_2S interact in modulating HIF-1 activity. It is also conceivable that impaired mitochondrial function by H_2S (which will accumulate during hypoxia) will trigger HIF-1 activation; hypoxia or inhibited transport of electrons in the inner mitochondrial membrane results in the generation of reactive oxygen species that *per se* together with hypoxia activate HIF-1 by impairing the hydroxylase activity of EGL-9 in the VHL-1-dependent pathway (Hwang et al. 2011).

Nevertheless, it was demonstrated that H_2S activates HIF-1 by VHL-1-independent signaling (Budde et al. 2010). It was shown that CYSL-1, ortholog of plant/bacterial *O*-acetylserine sulfhydrylase, inhibits EGL-9 in VHL-1-independent manner. Intriguingly, the mechanism of such regulation has evolved from the regulation of cysteine biosynthesis in bacteria and plants: similarly to formation of cysteine synthase complex in these species, the nematode CYSL-1 interacts with the C-terminal peptide of EGL-9 that leads to the sequestration of EGL-9 and the subsequent activation of HIF-1. Such CYSL-1/EGL-9 association is enhanced by the exposure to H_2S in a dose-dependent manner (Ma et al. 2012). However, the exact mechanism by which H_2S enhances CYSL-1/EGL-9 interaction to activate HIF-1 remains to be determined in future studies.

The effects of endogenously produced H_2S on *C. elegans* physiology need to be elucidated thoroughly. It should be noted that these animals possess several genes coding the enzymes of H_2S metabolism, however, only one has been experimentally characterized; CBS-1 (nematode cystathionine beta synthase encoded by ZC373.1 gene. It has been shown that in contrast to mammalian CBS enzymes, CBS-1, does not possess the heme-binding and Bateman domains that are essential for inhibition and activation of CBS activity by carbon monoxide and S-adenosylmethionine, respectively (Vozdek et al. 2012). These data and also the fact that *C. elegans* genome possesses genes coding for the H_2S metabolic enzymes conserved in plants and bacteria, and not in mammals, strongly suggests that some molecular mechanisms of H_2S action may be different in *C. elegans* compared to mammals. Further experimental studies can address this matter directly.

H_2S-releasing molecules and their therapeutic applications

Given the beneficial signaling and bioenergetic effects of H_2S, it has been repeatedly postulated that administration (supplementation) of appropriate amounts of H_2S can be of therapeutic potential (Szabo 2007, 2010). However, such efforts must be well-controlled in order to avoid the potential

Table 1. Applications of various H_2S donors in different disease models

Compound	Disease/*in vitro* or animal model	Main effects of the drug and signaling pathways involved	Reference
Classical (fast releasing) H_2S donors			
Na_2S IK-1001	**Dermal wound healing** Rat wound healing model; chicken chorioallantoic membranes	IK-1001 increased vascular length of chicken chorioallantoic membranes and improved wound re-epithelialization compared to saline.	(Papapetropoulos et al. 2009)
Sodium hydrosulfide NaHS	**Type 1 and type 2 diabetes** Renal epithelial cells OVE26 mice T1D model; C57BL/KsJ lepr $^{-}/^{-}$ (db/db mice) T2D model	NaHS inhibited high glucose-induced activation of mammalian target of rapamycin (mTOR) complex 1 (mTORC1). NaHS attenuated high glucose-induced matrix protein synthesis via activating AMP-activated protein kinase.	(Lee et al. 2012)
NaHS, Na_2S, Lawesson's reagent, N-acetylcysteine (NAC)	**Leukocyte-mediated inflammation** Aspirin-induced inflammation in rat; rat air pouch model; carrageenan-induced hindpaw edema in rat	NaHS and Na_2S inhibited aspirin-induced leukocyte adhesion in mesenteric venules likely via activation of K_{ATP} channels. NaHS, Lawesson's reagent, and NAC inhibited leukocyte infiltration in a rat air pouch model. NaHS and Na_2S significantly reduced carrageenan-induced paw edema most likely via K_{ATP} channel activation, as similar effect was observed with pinacidil (K_{ATP} channel agonist) and opposite with glibenclamide (K_{ATP} channel antagonist).	(Zanardo et al. 2006)
Slow-releasing H_2S donors (comparison with fast releasing donor if stated)			
GYY4137 NaHS	**Sepsis** mouse RAW 264.7 macrophage cell line	GYY4137 inhibited LPS-induced synthesis of the pro-inflammatory mediators (TNF-α, IL-1β, IL-6, NO, PGE2), and stimulated the synthesis of the anti-inflammatory cytokine IL-10. GYY4137 significantly inhibited LPS-induced phosphorylation of HSP27 and ATF-2 and caused inhibition of the activation of NF-κB. Conversely, NaHS had no effect on IL-10 production and was not effective as GYY4137 in reducing LPS-induced synthesis of pro-inflammatory mediators.	(Whiteman et al. 2010)
GYY4137	**Sepsis** LPS-induced endotoxic shock in rats	GYY4137 inhibited neutrophil infiltration and activity, and decreased tissue damage via inhibition of LPS-induced activation of NF-κB and STAT-3, reduction of the synthesis of the pro-inflammatory mediators (TNF-α, IL-1β, IL-6, CRP, L-selectin, NO, PGE2), and induction of the synthesis of the anti-inflammatory cytokine IL-10. GYY4137 decreased development of hypotension in rats.	(Li et al. 2009)
GYY4137	**Hypertension** Isolated rat aortic rings; perfused kidney; spontaneously hypertensive rats (SHR) and L-NAME-induced hypertension	GYY4137 induced relaxation of rat aortic rings and renal vasculature of perfused kidneys via opening of K_{ATP} channels. It also reduced systemic blood pressure in SHR and mitigated vasoconstrictor response to angiotensin II and noradrenaline in perfused kidney.	(Li et al. 2008)
GYY4137 NaHS	**COPD, asthma and pulmonary hypertension** Human primary pulmonary smooth muscle cells	Both GYY4137 and NaHS inhibited serum-induced proliferation of pulmonary smooth muscle cells. NaHS decreased IL-8 release, via reduction of phosphorylation of ERK-1/2 and p38.	(Perry et al. 2011)
GYY4137 NaHS	**Cancer** Human cancer cell lines: cervical cancer (HeLa); colon cancer (HCT-116); hepatic cancer (Hep G2), osteosarcoma (U2OS) breast cancer MCF-7; promyelocytic leukemia (HL-60); acute myelocytic leukemia (MV4-11) and normal human lung fibroblasts (IMR90, WI-38). HL-60 and MV4-11 xenografts in SCID mice	GYY4137, but not NaHS, significantly inhibited cell viability of all cancer cells tested. Viability of normal human lung fibroblasts was not affected by GYY4137 treatment. In MCF7 cells GYY4137 induced cleavage of PARP and pro-caspase 9 and partially arrested cell cycle in G2/M phase. HL-60 and MV4-11 xenografts in SCID mice were significantly inhibited with GYY4137 treatment.	(Lee et al. 2011)
S-allylcysteine (SAC)	**Myocardial infarction** Acute myocardial infarction in rat	Pretreatment with SAC significantly reduced mortality and infarct size without affecting BP. SAC increased left ventricular CSE expression, activity and plasma H_2S levels in AMI rats compared to control, PAG or SAC+PAG groups.	(Chuah et al. 2007)

Table 1. Continued

Compound	Disease/*in vitro* or animal model	Main effects of the drug and signaling pathways involved	Reference
S-allylcysteine (SAC) S-propyl-l-cysteine (SPC) S-propargyl-cysteine (SPRC)	**Myocardial infarction** Acute myocardial infarction in rat, primary rat cardiomyocytes	SPRC protected effects both adult rat hearts and neonatal cardiomyocytes through upregulation of CSE expression. SAC, SPC and SPRC reduced oxidative stress in rat acute myocardial infarction via preservation of SOD and GPx activities and tissue GSH levels. They also reduced MDA formation.	(Wang et al. 2009; Wang et al. 2010)
S-propargyl-cysteine (SPRC), a structural analogue of S-allylcysteine (SAC).	**Cancer** Human gastric carcinoma (SGC-7901) cell line. Gastric cancer xenografts in nude mice	SPRC reduced cell viability, proliferation and migration of SPRC-7901 cells. SPRC induced apoptosis and cell cycle arrest in the G1/S phase. In nude mice SPRC significantly reduced tumor volume and stimulated apoptosis via of p53 and Bax. SPRC treatment up-regulated the expression of CSE in tumors and elevated plasma H_2S levels.	(Ma et al. 2011)
S-propargyl-cysteine (SPRC),	**Pancreatitis** Caerulein-induced acute pancreatitis (AP) in mice.	SPRC administered 3h, but not 12 h before AP induction, significantly reduced inflammation in pancreas and lungs. SPRC treatment was associated with increase of anti-inflammatory cytokine (IL-10) and decrease of pro-inflammatory cytokines (IL-6, IL-1β).	(Sidhapuriwala et al. 2012)
Dithiolethione-modified drugs of known structure			
S-Latanoprost (ACS-67)	**Retinal ischaemia** Rat retina and retinal ganglion cells (RGC-5)	Intravitreal injection of ACS67 decreased ischemia-mediated damage to the retina and optic nerve, and increased intracellular GSH levels. ACS67, but not latanoprost, ameliorated H_2O_2-induced toxicity in RGC-5 cells.	(Osborne et al. 2010)
S-Naproxen (ATB-346)	**Gastric ulcers** Healthy rats and rats with compromised gastric mucosal defence; mouse airpouch model	ATB-346 showed improved gastric and intestinal safety compared to parent drug and accelerated healing of preexisting gastric ulcers. ATB-346 was more effective than naproxen in suppressing COX-2 activity and leukocyte infiltration.	(Wallace et al. 2010)
S-Mesalamine (ATB-429)	**Ulcerative Colitis** TNBS induced colitis in mice	ATB-429 modulated nociception to colorectal distension (CRD) via reduction of colonic COX-2 and IL-1β mRNA and spinal c-Fos mRNA expression. This effect was mediated by activation of K_{ATP} channels, as ATB-429-induced antinociception was abolished by glibenclamide. ATB-429 significantly reduced the severity of colitis in mice, colonic granulocyte infiltration and levels of inflammatory cytokines (TNF-α, IFN-γ, IL-1, IL-2, IL-12 and RANTES).	(Distrutti et al. 2006; Fiorucci et al. 2007)
H_2S-releasing L-DOPA hybrids *ACS83, ACS84, ACS85, ACS86*	**Parkinson's disease** Human monocyte THP-1; human astrocytoma U373 cell line; human neuroblastoma SH-SY5Y cell line; primary human microglial and astrocyte cells	H_2S releasing L-DOPA hybrids decreased the release of TNFα, NO and IL-6 from stimulated microglia, astrocytes and from THP-1 and U373 cell lines. They also showed a neuroprotective effect to SH-SY5Y cells via reduction of the toxicity of supernatants from these stimulated cells. S-DOPAs increased intracellular H_2S and GSH levels.	(Lee et al. 2010)
S-Diclofenac (ATB-337/ACS-5)	**NSAID - induced gastrointestinal injury in rats** Carrageenan-induced hindpaw edema in rats; carrageenan-induced hindpaw edema in rats	S –diclofenac significantly decreased gastrointestinal toxicity compared with parent counterpart. S-diclofenac had no effect on hematocrit, whereas diclofenac caused 50% reduction. Compared to diclofenac S –diclofenac did not increase gastric granulocyte infiltration, expression of TNF-α, lymphocyte function associated antigen-1 and ICAM-1. S-diclofenac –mediated inhibition of COX-1 and COX-2 was equally effective as for parent drug. S –diclofenac did not induce leukocyte adhesion and significantly reduced paw edema. S –diclofenac was more potent than parent drug at reducing both hindpaw edema and neutrophil infiltration measured with myeloperoxidase activity. S-diclofenac was also more effective in reduced hindpaw nitrite/nitrate concentration. Both drugs were similar in terms of reduction of carrageenan-induced rise in PGE_2 and H_2S levels.	(Wallace et al. 2010) (Sidhapuriwala et al. 2007)
S-Diclofenac (ATB-337/ACS-5)	**Atherosclerosis and restenosis after angioplasty** Normal rat aortic smooth muscle cells (A-10) and SV40 immortalized smooth muscle cells (CRL-2018)	S –Diclofenac induced smooth muscle cell apoptosis via stabilization of p53 along with induction of downstream proteins (p21, p53AIP1 and Bax).	(Baskar et al. 2008)

Table 1. Continued

Compound	Disease/*in vitro* or animal model	Main effects of the drug and signaling pathways involved	Reference
S-Diclofenac (ACS-5) S-sulindac (ACS-18)	**Cancer** Hydrocarbon receptor signaling pathway mediated carcinogenesis; human hepatoma cell line-HepG2, human colorectal adenocarcinoma cell line - LS180	S –NSAIDs inhibited both expression and activity of the carcinogen activating enzymes cytochromes P-450 (CYP) CYP1A1, CYP1B1, and CYP1A2 via down-regulation of the aryl hydrocarbon receptor (AhR) pathway. S-sulindac stimulated expression of carcinogen detoxification enzymes e.g., glutathione reductase, glutathione S-transferase A2, glutamate cysteine ligase.	(Bass et al. 2009)
S-diclofenac (ACS-5), S-sulindac (ACS-18) S-valproate NaHS	**Cancer angiogenesis** HUVECs; human adenocarcinoma HT-29 cell line; Wt C57B16 mice, athymic nude mice [Cr:(NCr)-nu fBR] and EGFP transgenic zebrafish embryos	S-NSAIDs, S-valproate and dithiolethiones inhibited HUVECs proliferation, angiogenesis in muscle and HT29 tumor explants independently of COX inhibition. NaHS at similar concentrations had no inhibitory effect on cell proliferation, suggesting that the observed results for S-NSAIDs were due to ADT-OH moiety not H_2S per se. S-NSAIDs and S-valproate induced HSP27 phosphorylation. Developmental angiogenesis in zebrafish embryos was inhibited by valproic acid and dithiolethiones, but S-NSAIDs failed to show the same effect.	(Isenberg et al. 2007)
S-valproate S-diclofenac S-sulindac	**Cancer** Human non-small cell lung cancer cell lines A549 and NCI-H1299. A549 or NCI-H1299 xenografts in nude mice	S –valproate, S-sulindac and S -diclofenac decreased PGE(2) levels (reduction of COX-2 activity) and inhibited cancer cell proliferation in vitro. Xenograft proliferation in nude mice was inhibited only by S-valproate and S-diclofenac which was associated with increased expression of E-cadherin and decreased expression of vimentin and ZEB1 (a transcriptional E-cadhedrin suppressor).	(Moody et al. 2010)
S-sildenafil (ACS-6) NaHS	**Acute respiratory distress syndrome** Porcine pulmonary arterial endothelial cells	Both S-sildenafil and NaHS ameliorated TNF-α - induced superoxide formation with IC(50) ~10 nM and <1 nM, respectively. Both NaHS and S-sildenafil inhibited TNFα - induced gp91(phox) expression (a catalytic subunit of NADPH oxidase) via PKA or PKG and PKA dependent pathways, respectively.	(Muzaffar et al. 2008)
Hydrogen sulfide-releasing aspirin (HS-ASA), ADT-OH	**Cancer** Human breast cancer MDA-MB-231 (ER^-, PR^-, not over expressing Her2 receptor) cell line; normal human mammary epithelial (HMEpC) cell line; tumor xenografts in athymic SCID mice	HS-ASA inhibited the growth of triple negative MDA-MB-231 cells via induction of apoptosis and G0/G1 cell cycle arrest, increased production of ROS, reduction of thioredoxin reductase activity and inhibition of NF-κB signaling due to decreased translocation of p65 into the nucleus. HS-ASA treatment significantly reduced growth of tumor xenografts via down-regulation of NF-κB, inhibition of cell proliferation and induction of apoptosis.	(Chattopadhyay et al. 2012; Chattopadhyay et al. 2012)
Hydrogen sulfide-releasing aspirin ACS14 and its deacetylated metabolite ACS21	**Metabolic syndrome/ hypertension** Buthionine sulfoximine (BSO) – induced metabolic syndrome in rat (associated with GSH depletion); isolated heart and aortic rings	Both ACS14 and ACS21 did not cause gastric lesions; sustained the GSH levels, ameliorated BSO-induced hypertension, lowered plasma TXB_2 levels, 8-isoprostane and insulin. ACS14 and ACS21 protected the heart from ischemia/reperfusion, limited vascular endothelial dysfunction and hypertension. ACS14 decreased plasma TXB_2 levels comparable to aspirin, but lacked adverse effects to gastric mucosa. ACS14 increased H_2S and GSH production and increased HO-1 promoter activity.	(Rossoni et al. 2010) (Sparatore et al. 2009)
S-ASA S-sulindac, S-iburofen, S-naproxen	**Cancer** Human cancer cell lines: colon adenocarcinoma (HT-29, SW-480 and HCT-15); pancreatic cancer (MIA PaCa-2 and BxPC-3), prostate cancer (LNCAP) lung cancer (A549) breast cancer (MCF-7, MDA-MB-231 and SK-BR-3), T cell leukemia (Jurkat)	HS-NSAIDs were 28 to 3000-fold more potent than their conventional counterparts in inhibiting growth of all cancer cell lines studied. The most potent HS-ASA decreased cancer cell proliferation, stimulated apoptosis and induced G0/G1 cell cycle arrest. The effects were most likely due to additive effects of both ASA and ADT-OH as a mixture of the two components gave similar, however, 95-fold decreased growth inhibition comparing to intact HS-ASA. ASA and ADT-OH alone were less active than the intact HS-ASA.	(Chattopadhyay et al. 2012; Chattopadhyay et al. 2012)

ASA, acetylsalicylic acid (aspirin); BP, blood pressure; COPD, chronic obstructive pulmonary disease; COX-1, cyclooxygenase-1; COX-2, cyclooxygenase-2; GPx, glutathione peroxidase; GSH, glutathione; HO-1, heme oxygenase-1; HSP, heat shock protein; HUVECs, human umbilical vein endothelial cells; IL, Interleukin; K_{ATP} channels, ATP-sensitive potassium channels; MDA, malon dialdehyde; NF-κB, nuclear factor-kappa B; NSAIDs, non-steroidal anti-inflammatory drugs; PGE_2, prostaglandin E_2; SCID,severe combined immunodeficiency; SHR, spontaneously hypertensive rat; SOD, superoxide dismutase; T2D, type 2 diabetes; TBX_2, thromboxane B X_2.

of cytotoxicity that is associated with high concentrations or high release rates of this mediator. Currently, several classes of slow-releasing H_2S pro-drugs are in various stages of research and development. The biological effects of several classes of such donors are summarized in Table 1.

Many H_2S donors have been used over the years by many research groups to examine the potential role of H_2S in physiological and pathophysiological conditions, utilizing most of the time the sodium salts (Na_2S and NaHS). However, the problem with these donors is that they deliver an instantaneous bolus of H_2S in seconds once added into solution (Li et al. 2008; Whiteman et al. 2010). It is highly unlikely that cells, tissues or organs will ever be exposed to such a high concentrations of H_2S under physiological conditions, since CSE CBS and 3-MST all produce H_2S in a slow and sustained manner (Singh et al. 2009; Huang et al. 2010; Whiteman et al. 2010, 2011; Le Trionairre et al. 2012). Although there are multiple lines of data generated with fast-releasing H_2S donors, showing benefits in various pathophysiological conditions, the therapeutic index of these compounds is rather narrow (Elrod et al. 2007; Esechie et al. 2008; Simon et al. 2008, 2011; Baumgart et al. 2009; Esechie et al. 2009; Osipov et al. 2009; Szabo et al. 2011; Wagner et al. 2011; Bracht et al. 2012). Given the physiological concentrations of H_2S detected in humans (from nanomolar to micromolar, depending on the method used), this raises more questions about the role of physiological H_2S levels and highlights the need for any therapeutically relevant H_2S donor to deliver the "right amount" of H_2S, in order to mimic the effects of endogenously synthesized H_2S (or to substitute for it in H_2S-deficient states).

From the various H_2S donors, it is worth mentioning the H_2S releasing derivatives of anti-inflammatory drugs (S-diclofenac) (Li et al. 2007), the ophthalmic solution used to control intraocular pressure (S-Latanoprost) (Osborne et al. 2010), as well as certain garlic compounds (diallyl sulfide, diallyl disulfide) (Benavides et al. 2007) and GYY4137 (Whiteman et al. 2010) which are characterized by moderate and slow release of H_2S compared to sulfide salts. The *in vivo* H_2S releasing ability of diallyl disulfide has subsequently been demonstrated in rodents (Insko et al. 2009). L-thioglycine and L-thiovaline represent another novel examples of H_2S donors (Zhou et al. 2012). In addition, other methods have also been proposed to increase biological H_2S levels, such as approaches attempting to increase endogenous H_2S level by providing substrates of H_2S-generating enzymes. Selected examples include L-cysteine and N-acetylcysteine.

Conclusions and future directions

H_2S, since its 'rebirth' as a biological mediator and the third gasotransmitter, attracts considerable attention both in physiological and pathophysiological contexts. Clearly, one area of active inquiry and considerable future exploration will be its biosynthesis. Although much is known about the biochemistry of its two PLP-dependent enzymes CSE and CBS, as well as the third enzyme system, 3-MST/CAT, further studies are needed to explore the exact molecular mechanisms of H_2S biosynthesis in health and disease. Up- or downregulation of this enzyme may occur in various pathophysiological conditions; there may be post-translational modifications in these enzymes, as well as processes affecting its substrate or co-factor availability. Much future work is needed to explore them. These enzymes also likely to contribute to the regulation of mitochondrial function, which remains to be studied in the future. As mentioned above, during the last 6 years inquiring reports have demonstrated that H_2S is not only an inhibitor of mitochondrial function, but mitochondria can also use it as an inorganic electron donor, that supports electrons to the mitochondrial respiratory chain. It remains to be determined in future studies whether these finding is a biochemical curiosity, or whether it also has (patho)physiological relevance; can it act as a source of energy in conditions when cellular energy supply are limited (such as in hypoxic and stress conditions)?

Similarly, the absolute levels of endogenous H_2S and distinguishing the different sulfur pools (Wintner et al. 2010) in health and disease remain to be elucidated; as mentioned above, there is a considerable debate even with respect to the actual basal/physiological levels of H_2S. One of the tools that needs to be improved/refined is the selective targeting of each of the H_2S-producing enzymes. Investigators working in the field would do much better if the specificity and selectivity of the currently available inhibitors would be improved (Whiteman et al. 2011).

Due to utilizing the nematode *Caenorhabditis elegans* as an experimental model system, many possibilities have opened that will help us elucidate certain key regulating mechanisms in H_2S biology. We have no doubt that further utilization of *C. elegans* model system in the field of H_2S biology will yield new insights in many areas, including the regulation of HIF-1, in the regulation of signal transduction pathways and possibly in cellular bioenergetics as well.

Finally, the intensive research of H_2S-releasing donors is expected to produce tangible benefits in the near future. As overviewed in the current article, several classes of slow-releasing H_2S pro-drugs are under various stages of research and development. Further chemical modifications should yield compounds with improved specificity and potency; hopefully well fine-tailored to their respective clinical applications. The administration routes of H_2S donor molecules could include compounds delivered *via* inhalation, injection, skin patch, or oral administration, in order to maximize their potency and safety and to decrease side effects. It may also be possible in the future to design

tissue-type or cell-type targeted strategies and approaches to alter local H_2S levels. Toxicological evaluation and early-stage clinical trials with some of the new H_2S donors is expected to take some of these compounds to the "next level", which is the clinical stage (safety and efficacy studies). Short-term H_2S infusion has been demonstrated to be safe in healthy human volunteers (Toombs et al. 2010), providing a yardstick for future human studies as far as dosing, as well as identifying exhaled H_2S as a potential human H_2S biomarker.

The current short review only highlighted a few, selected, rapidly developing areas of H_2S biology. Although it is clear that H_2S does not work in isolation, but, rather, it works in cooperation and interaction with other gasotransmitters (Szabo 2010; Szabo et al. 2011; Coletta et al. 2012) in the current review we did not have space to explore this aspect of H_2S biology in detail. Similarly, we did not review any of the results obtained with pharmacological inhibitors of H_2S biosynthesis or studies using genetic models such as animals lacking CSE. We also did not mention several other novel areas of H_2S biology, such as its role in the regulation of immune functions, or its role in various pathophysiological conditions. Clearly, there are a great number of emerging areas of H_2S biology, and we are certain that continuing research will continue to unveil many additional novel roles of this fascinating biological mediator.

Acknowledgments: The authors are the winners of Young Investigator Award among PhD students and postdoctoral fellows at the First European Conference on the Biology of Hydrogen Sulfide, Smolenice, Slovakia, June 2012. This work was supported by the James W. McLaughlin Fellowship Fund at University of Texas Medical Branch to M. K. K. W. was founded by a fellowship from The Peninsula College of Medicine and Dentistry (PCMD). R. V. was supported by the research programs of the Charles University in Prague (PRVOUK-P24/LF1/3 and SVV 264502). The authors wish to thank Dr. Csaba Szabo, Dr. Matt Whiteman and Dr. Ciro Coletta for their helpful comments and reviewing our manuscript.

References

Abe K., Kimura H. (1996): The possible role of hydrogen sulfide as an endogenous neuromodulator. J. Neurosci. **16,** 1066–1071

Acin-Perez R., Salazar E., Kamenetsky M., Buck J., Levin L. R., Manfredi G. (2009): Cyclic AMP produced inside mitochondria regulates oxidative phosphorylation. Cell. Metab. **9,** 265–276 http://dx.doi.org/10.1016/j.cmet.2009.01.012

An J. H., Blackwell T. K. (2003): SKN-1 links C. elegans mesendodermal specification to a conserved oxidative stress response. Genes. Dev. **17,** 1882–1893 http://dx.doi.org/10.1101/gad.1107803

Attene-Ramos M. S., Nava G. M., Muellner M. G., Wagner E. D., Plewa M. J., Gaskins H. R. (2010): DNA damage and toxicogenomic analyses of hydrogen sulfide in human intestinal epithelial FHs 74 Int cells. Environ. Mol. Mutagen. **51,** 304–314

Attene-Ramos M. S., Wagner E. D., Gaskins H. R., Plewa M. J. (2007): Hydrogen sulfide induces direct radical-associated DNA damage. Mol. Cancer. Res. **5,** 455–459 http://dx.doi.org/10.1158/1541-7786.MCR-06-0439

Banerjee R., Zou C. G. (2005): Redox regulation and reaction mechanism of human cystathionine-beta-synthase: a PLP-dependent hemesensor protein. Arch. Biochem. Biophys. **433,** 144–156 http://dx.doi.org/10.1016/j.abb.2004.08.037

Baskar R., Sparatore A., Del Soldato P., Moore P. K. (2008): Effect of S-diclofenac, a novel hydrogen sulfide releasing derivative inhibit rat vascular smooth muscle cell proliferation. Eur. J. Pharmacol. **594,** 1–8 http://dx.doi.org/10.1016/j.ejphar.2008.07.029

Bass S. E., Sienkiewicz P., Macdonald C. J., Cheng R. Y., Sparatore A., Del Soldato P., Roberts D. D., Moody T. W., Wink D. A., Yeh G. C. (2009): Novel dithiolethione-modified nonsteroidal anti-inflammatory drugs in human hepatoma HepG2 and colon LS180 cells. Clin. Cancer. Res. **15,** 1964–1972 http://dx.doi.org/10.1158/1078-0432.CCR-08-1870

Baumgart K., Radermacher P., Wagner F. (2009): Applying gases for microcirculatory and cellular oxygenation in sepsis: effects of nitric oxide, carbon monoxide, and hydrogen sulfide. Curr. Opin. Anaesthesiol. **22,** 168–176 http://dx.doi.org/10.1097/ACO.0b013e328328d22f

Beauchamp R. O., Jr., Bus J. S., Popp J. A., Boreiko C. J., Andjelkovich D. A. (1984): A critical review of the literature on hydrogen sulfide toxicity. Crit. Rev. Toxicol.13, 25–97 http://dx.doi.org/10.3109/10408448409029321

Benavides G. A., Squadrito G. L., Mills R. W., Patel H. D., Isbell T. S., Patel R. P., Darley-Usmar V. M., Doeller J. E., Kraus D. W. (2007): Hydrogen sulfide mediates the vasoactivity of garlic. Proc. Natl. Acad. Sci. U.S.A. **104,** 17977–17982 http://dx.doi.org/10.1073/pnas.0705710104

Blackstone E., Morrison M., Roth M. B. (2005): H2S induces a suspended animation-like state in mice. Science **308,** 518 http://dx.doi.org/10.1126/science.1108581

Blackstone E., Roth M. B. (2007): Suspended animation-like state protects mice from lethal hypoxia. Shock **27,** 370–372 http://dx.doi.org/10.1097/SHK.0b013e31802e27a0

Bouillaud F., Blachier F. (2011): Mitochondria and sulfide: a very old story of poisoning, feeding, and signaling? Antioxid. Redox. Signal. **15,** 379–391 http://dx.doi.org/10.1089/ars.2010.3678

Bracht H., Scheuerle A., Groger M., Hauser B., Matallo J., McCook O., Seifritz A., Wachter U., Vogt J. A., Asfar P., Matejovic M., Moller P., Calzia E., Szabo C., Stahl W., Hoppe K., Stahl B., Lampl L., Georgieff M., Wagner F., Radermacher P., Simon F. (2012): Effects of intravenous sulfide during resuscitated porcine hemorrhagic shock. Crit. Care. Med. **40,** 2157–2167 http://dx.doi.org/10.1097/CCM.0b013e31824e6b30

Brancaleone V., Roviezzo F., Vellecco V., De Gruttola L., Bucci M., Cirino G. (2008): Biosynthesis of H2S is impaired in non-obese diabetic (NOD) mice. Br. J. Pharmacol. **155,** 673–680 http://dx.doi.org/10.1038/bjp.2008.296

Budde M. W., Roth M. B. (2010): Hydrogen sulfide increases hypoxia-inducible factor-1 activity independently of von Hippel-Lindau tumor suppressor-1 in C. elegans. Mol. Biol. Cell. **21,** 212–217
http://dx.doi.org/10.1091/mbc.E09-03-0199

Budde M. W., Roth M. B. (2011): The Response of Caenorhabditis elegans to Hydrogen Sulfide and Hydrogen Cyanide. Genetics. **189,** 521–532
http://dx.doi.org/10.1534/genetics.111.129841

Calvert J. W., Jha S., Gundewar S., Elrod J. W., Ramachandran A., Pattillo C. B., Kevil C. G., Lefer D. J. (2009): Hydrogen sulfide mediates cardioprotection through Nrf2 signaling. Circ. Res. **105,** 365–374
http://dx.doi.org/10.1161/CIRCRESAHA.109.199919

Carballal S., Trujillo M., Cuevasanta E., Bartesaghi S., Möller M. N., Folkes L. K., García Bereguiaín M. A., Gutiérrez-Merino C., Wardman P., Denicola A., Radi R., Alvarez B. (2011): Reactivity of hydrogen sulfide with peroxynitrite and other oxidants of biological interest. Free. Radic. Biol. Med. **50,** 196–205
http://dx.doi.org/10.1016/j.freeradbiomed.2010.10.705

Chang L., Geng B., Yu F., Zhao J., Jiang H., Du J., Tang C. (2008): Hydrogen sulfide inhibits myocardial injury induced by homocysteine in rats. Amino Acids **34,** 573–585
http://dx.doi.org/10.1007/s00726-007-0011-8

Chattopadhyay M., Kodela R., Nath N., Barsegian A., Boring D., Kashfi K. (2012): Hydrogen sulfide-releasing aspirin suppresses NF-kappaB signaling in estrogen receptor negative breast cancer cells in vitro and in vivo. Biochem. Pharmacol. **83,** 723–732
http://dx.doi.org/10.1016/j.bcp.2011.12.019

Chattopadhyay M., Kodela R., Nath N., Dastagirzada Y. M., Velazquez-Martinez C. A., Boring D., Kashfi K. (2012): Hydrogen sulfide-releasing NSAIDs inhibit the growth of human cancer cells: a general property and evidence of a tissue type-independent effect. Biochem. Pharmacol. **83,** 715–722
http://dx.doi.org/10.1016/j.bcp.2011.12.018

Chen Y. H., Yao W. Z., Geng B., Ding Y. L., Lu M., Zhao M. W., Tang C. S. (2005): Endogenous hydrogen sulfide in patients with COPD. Chest **128,** 3205–3211
http://dx.doi.org/10.1378/chest.128.5.3205

Chuah S. C., Moore P. K., Zhu Y. Z. (2007): S-allylcysteine mediates cardioprotection in an acute myocardial infarction rat model via a hydrogen sulfide-mediated pathway. Am. J. Physiol. Heart. Circ. Physiol. **293,** H2693–2701
http://dx.doi.org/10.1152/ajpheart.00853.2007

Coletta C., Papapetropoulos A., Erdelyi K., Olah G., Modis K., Panopoulos P., Asimakopoulou A., Gero D., Sharina I., Martin E., Szabo C. (2012): Hydrogen sulfide and nitric oxide are mutually dependent in the regulation of angiogenesis and endothelium-dependent vasorelaxation. Proc. Natl. Acad. Sci. U.S.A. **109,** 9161–9166
http://dx.doi.org/10.1073/pnas.1202916109

Collin M., Anuar F. B., Murch O., Bhatia M., Moore P. K., Thiemermann C. (2005): Inhibition of endogenous hydrogen sulfide formation reduces the organ injury caused by endotoxemia. Br. J. Pharmacol. **146,** 498–505
http://dx.doi.org/10.1038/sj.bjp.0706367

Collman J. P., Ghosh S., Dey A., Decreau R. A. (2009): Using a functional enzyme model to understand the chemistry behind hydrogen sulfide induced hibernation. Proc. Natl. Acad. Sci. U.S.A. **106,** 22090–22095
http://dx.doi.org/10.1073/pnas.0904082106

Cooper C. E., Brown G. C. (2008): The inhibition of mitochondrial cytochrome oxidase by the gases carbon monoxide, nitric oxide, hydrogen cyanide and hydrogen sulfide: chemical mechanism and physiological significance. J. Bioenerg. Biomembr. **40,** 533–539
http://dx.doi.org/10.1007/s10863-008-9166-6

Distrutti E., Sediari L., Mencarelli A., Renga B., Orlandi S., Russo G., Caliendo G., Santagada V., Cirino G., Wallace J. L., Fiorucci S. (2006): 5-Amino-2-hydroxybenzoic acid 4-(5-thioxo-5H-[1,2]dithiol-3yl)-phenyl ester (ATB-429), a hydrogen sulfide-releasing derivative of mesalamine, exerts antinociceptive effects in a model of postinflammatory hypersensitivity. J. Pharmacol. Exp. Ther. **319,** 447–458
http://dx.doi.org/10.1124/jpet.106.106435

Elrod J. W., Calvert J. W., Morrison J., Doeller J. E., Kraus D. W., Tao L., Jiao X., Scalia R., Kiss L., Szabo C., Kimura H., Chow C. W., Lefer D. J. (2007): Hydrogen sulfide attenuates myocardial ischemia-reperfusion injury by preservation of mitochondrial function. Proc. Natl. Acad. Sci. U.S.A. **104,** 15560–15565
http://dx.doi.org/10.1073/pnas.0705891104

Epstein A. C., Gleadle J. M., McNeill L. A., Hewitson K. S., O'Rourke J., Mole D. R., Mukherji M., Metzen E., Wilson M. I., Dhanda A., Tian Y. M., Masson N., Hamilton D. L., Jaakkola P., Barstead R., Hodgkin J., Maxwell P. H., Pugh C. W., Schofield C. J., Ratcliffe P. J. (2001): C. elegans EGL-9 and mammalian homologs define a family of dioxygenases that regulate HIF by prolyl hydroxylation. Cell **107,** 43–54
http://dx.doi.org/10.1016/S0092-8674(01)00507-4

Esechie A., Enkhbaatar P., Traber D. L., Jonkam C., Lange M., Hamahata A., Djukom C., Whorton E. B., Hawkins H. K., Traber L. D., Szabo C. (2009): Beneficial effect of a hydrogen sulphide donor (sodium sulphide) in an ovine model of burn- and smoke-induced acute lung injury. Br. J. Pharmacol. **158,** 1442–1453
http://dx.doi.org/10.1111/j.1476-5381.2009.00411.x

Esechie A., Kiss L., Olah G., Horvath E. M., Hawkins H., Szabo C., Traber D. L. (2008): Protective effect of hydrogen sulfide in a murine model of acute lung injury induced by combined burn and smoke inhalation. Clin. Sci. (Lond.) **115,** 91–97
http://dx.doi.org/10.1042/CS20080021

Finkel T. (2012): From sulfenylation to sulfhydration: what a thiolate needs to tolerate. Sci. Signal. **5,** pe10.
http://dx.doi.org/10.1126/scisignal.2002943

Fiorucci S., Antonelli E., Distrutti E., Rizzo G., Mencarelli A., Orlandi S., Zanardo R., Renga B., Di Sante M., Morelli A., Cirino G., Wallace J. L. (2005): Inhibition of hydrogen sulfide generation contributes to gastric injury caused by anti-inflammatory nonsteroidal drugs. Gastroenterology **129,** 1210–1224
http://dx.doi.org/10.1053/j.gastro.2005.07.060

Fiorucci S., Distrutti E., Cirino G., Wallace J. L. (2006): The emerging roles of hydrogen sulfide in the gastrointestinal tract and liver. Gastroenterology **131,** 259–271
http://dx.doi.org/10.1053/j.gastro.2006.02.033

Fiorucci S., Orlandi S., Mencarelli A., Caliendo G., Santagada V., Distrutti E., Santucci L., Cirino G., Wallace J. L. (2007): Enhanced activity of a hydrogen sulphide-releasing derivative of mesalamine (ATB-429) in a mouse model of colitis. Br. J. Pharmacol. **150,** 996–1002
http://dx.doi.org/10.1038/sj.bjp.0707193

Fu M., Zhang W., Wu L., Yang G., Li H., Wang R. (2012): Hydrogen sulfide (H2S) metabolism in mitochondria and its regulatory role in energy production. Proc. Natl. Acad. Sci. U.S.A. **109,** 2943–2948
http://dx.doi.org/10.1073/pnas.1115634109

Fusco F., d'Emmanuele di Villa Bianca R., Mitidieri E., Cirino G., Sorrentino R., Mirone V. (2012): Sildenafil Effect on the Human Bladder Involves the L-cysteine/Hydrogen Sulfide Pathway: A Novel Mechanism of Action of Phosphodiesterase Type 5 Inhibitors. Eur. Urol. **62,** 1174–1180
http://dx.doi.org/10.1016/j.eururo.2012.07.025

Ganster F., Burban M., de la Bourdonnaye M., Fizanne L., Douay O., Loufrani L., Mercat A., Cales P., Radermacher P., Henrion D., Asfar P., Meziani F. (2010): Effects of hydrogen sulfide on hemodynamics, inflammatory response and oxidative stress during resuscitated hemorrhagic shock in rats. Crit. Care **14,** R165

Goodwin L. R., Francom D., Dieken F. P., Taylor J. D., Warenycia M. W., Reiffenstein R. J., Dowling G. (1989): Determination of sulfide in brain tissue by gas dialysis/ion chromatography: postmortem studies and two case reports. J. Anal. Toxicol. **13,** 105–109

Goubern M., Andriamihaja M., Nubel T., Blachier F., Bouillaud F. (2007): Sulfide, the first inorganic substrate for human cells. FASEB J. **21,** 1699–1706
http://dx.doi.org/10.1096/fj.06-7407com

Grieshaber M. K., Volkel S. (1998): Animal adaptations for tolerance and exploitation of poisonous sulfide. Annu. Rev. Physiol. **60,** 33–53
http://dx.doi.org/10.1146/annurev.physiol.60.1.33

Groeger M., Matallo J., McCook O., Wagner F., Wachter U., Bastian O., Gierer S., Reich V., Stahl B., M H. L., Szabo C., Georgieff M., Radermacher P., Calzia E., Wagner K. (2012): Temperature and Cell-type Dependency of Sulfide-Effects on Mitochondrial Respiration. Shock **38,** 367–374
http://dx.doi.org/10.1097/SHK.0b013e3182651fe6

Guo H., Gai J. W., Wang Y., Jin H. F., Du J. B., Jin J. (2012): Characterization of hydrogen sulfide and its synthases, cystathionine beta-synthase and cystathionine gamma-lyase, in human prostatic tissue and cells. Urology **79,** 483.e1–5

Gupta S., Kuhnisch J., Mustafa A., Lhotak S., Schlachterman A., Slifker M. J., Klein-Szanto A., High K. A., Austin R. C., Kruger W. D. (2009): Mouse models of cystathionine beta-synthase deficiency reveal significant threshold effects of hyperhomocysteinemia. FASEB J. **23,** 883–893
http://dx.doi.org/10.1096/fj.08-120584

Hannestad U., Margheri S., Sorbo B. (1989): A sensitive gas chromatographic method for determination of protein-associated sulfur. Anal. Biochem. **178,** 394–398
http://dx.doi.org/10.1016/0003-2697(89)90659-3

Hildebrandt T. M., Grieshaber M. K. (2008): Redox regulation of mitochondrial sulfide oxidation in the lugworm, Arenicola marina. J. Exp. Biol. **211,** 2617–2623
http://dx.doi.org/10.1242/jeb.019729

Hill B. C., Woon T. C., Nicholls P., Peterson J., Greenwood C., Thomson A. J. (1984): Interactions of sulphide and other ligands with cytochrome c oxidase. An electron-paramagnetic-resonance study. Biochem. J. **224,** 591–600

Hongfang J., Cong B., Zhao B., Zhang C., Liu X., Zhou W., Shi Y., Tang C., Junbao D. (2006): Effects of hydrogen sulfide on hypoxic pulmonary vascular structural remodeling. Life Sci. **78,** 1299–1309
http://dx.doi.org/10.1016/j.lfs.2005.07.009

Hosoki R., Matsuki N., Kimura H. (1997): The possible role of hydrogen sulfide as an endogenous smooth muscle relaxant in synergy with nitric oxide. Biochem. Biophys. Res. Commun. **237,** 527–531
http://dx.doi.org/10.1006/bbrc.1997.6878

Huang S., Chua J. H., Yew W. S., Sivaraman J., Moore P. K., Tan C. H., Deng L. W. (2010): Site-directed mutagenesis on human cystathionine-gamma-lyase reveals insights into the modulation of H2S production. J. Mol. Biol. **396,** 708–718
http://dx.doi.org/10.1016/j.jmb.2009.11.058

Hughes M. N., Centelles M. N., Moore K. P. (2009): Making and working with hydrogen sulfide: The chemistry and generation of hydrogen sulfide in vitro and its measurement in vivo: a review. Free. Radic. Biol. Med. **47,** 1346–1353
http://dx.doi.org/10.1016/j.freeradbiomed.2009.09.018

Hui Y., Du J., Tang C., Bin G., Jiang H. (2003): Changes in arterial hydrogen sulfide (H(2)S) content during septic shock and endotoxin shock in rats. J. Infect. **47,** 155–160
http://dx.doi.org/10.1016/S0163-4453(03)00043-4

Hwang A. B., Lee S. J. (2011): Regulation of life span by mitochondrial respiration: the HIF-1 and ROS connection. Aging (Albany NY) **3,** 304–310

Hyspler R., Ticha A., Indrova M., Zadak Z., Hysplerova L., Gasparic J., Churacek J. (2002): A simple, optimized method for the determination of sulphide in whole blood by GC-mS as a marker of bowel fermentation processes. J. Chromatogr. B. Analyt. Technol. Biomed. Life. Sci. **770,** 255–259
http://dx.doi.org/10.1016/S1570-0232(01)00632-8

Insko M. A., Deckwerth T. L., Hill P., Toombs C. F., Szabo C. (2009): Detection of exhaled hydrogen sulphide gas in rats exposed to intravenous sodium sulphide. Br. J. Pharmacol. **157,** 944–951
http://dx.doi.org/10.1111/j.1476-5381.2009.00248.x

Isenberg J. S., Jia Y., Field L., Ridnour L. A., Sparatore A., Del Soldato P., Sowers A. L., Yeh G. C., Moody T. W., Wink D. A., Ramchandran R., Roberts D. D. (2007): Modulation of angiogenesis by dithiolethione-modified NSAIDs and valproic acid. Br. J. Pharmacol. **151,** 63–72
http://dx.doi.org/10.1038/sj.bjp.0707198

Kell A., Ventura N., Kahn N., Johnson T. E. (2007): Activation of SKN-1 by novel kinases in Caenorhabditis elegans. Free. Radic. Biol. Med. **43,** 1560–1566
http://dx.doi.org/10.1016/j.freeradbiomed.2007.08.025

Khan A. A., Schuler M. M., Prior M. G., Yong S., Coppock R. W., Florence L. Z., Lillie L. E. (1990): Effects of hydrogen sulfide exposure on lung mitochondrial respiratory chain enzymes in rats. Toxicol. Appl. Pharmacol. **103,** 482–490
http://dx.doi.org/10.1016/0041-008X(90)90321-K

Kimura H. (2011): Hydrogen sulfide: its production and functions. Exp. Physiol. **96,** 833–835

Kimura Y., Kimura H. (2004): Hydrogen sulfide protects neurons from oxidative stress. FASEB J. **18,** 1165–1167

Krishnan N., Fu C., Pappin D. J., Tonks N. K. (2012): H2S-Induced sulfhydration of the phosphatase PTP1B and its role in the endoplasmic reticulum stress response. Sci. Signal. **4,** ra86
http://dx.doi.org/10.1126/scisignal.2002329

Kuo S. M., Lea T. C., Stipanuk M. H. (1983): Developmental pattern, tissue distribution, and subcellular distribution of cysteine: alpha-ketoglutarate aminotransferase and 3-mercaptopyruvate sulfurtransferase activities in the rat. Biol. Neonate. **43,** 23–32
http://dx.doi.org/10.1159/000241634

Lagoutte E., Mimoun S., Andriamihaja M., Chaumontet C., Blachier F., Bouillaud F. (2010): Oxidation of hydrogen sulfide remains a priority in mammalian cells and causes reverse electron transfer in colonocytes. Biochim. Biophys. Acta. **1797,** 1500–1511
http://dx.doi.org/10.1016/j.bbabio.2010.04.004

Lai K. C., Kuo C. L., Ho H. C., Yang J. S., Ma C. Y., Lu H. F., Huang H. Y., Chueh F. S., Yu C. C., Chung J. G. (2012): Diallyl sulfide, diallyl disulfide and diallyl trisulfide affect drug resistant gene expression in colo 205 human colon cancer cells in vitro and in vivo. Phytomedicine **19,** 625–630
http://dx.doi.org/10.1016/j.phymed.2012.02.004

Lee H. J., Mariappan M. M., Feliers D., Cavaglieri R. C., Sataranatarajan K., Abboud H. E., Choudhury G. G., Kasinath B. S. (2012): Hydrogen sulfide inhibits high glucose-induced matrix protein synthesis by activating AMP-activated protein kinase in renal epithelial cells. J. Biol. Chem. **287,** 4451–4461
http://dx.doi.org/10.1074/jbc.M111.278325

Lee M., Tazzari V., Giustarini D., Rossi R., Sparatore A., Del Soldato P., McGeer E., McGeer P. L. (2010): Effects of hydrogen sulfide-releasing L-DOPA derivatives on glial activation: potential for treating Parkinson disease. J. Biol. Chem. **285,** 17318–17328
http://dx.doi.org/10.1074/jbc.M110.115261

Lee Z. W., Zhou J., Chen C. S., Zhao Y., Tan C. H., Li L., Moore P. K., Deng L. W. (2011): The slow-releasing hydrogen sulfide donor, GYY4137, exhibits novel anti-cancer effects in vitro and in vivo. PLoS One **6,** e21077
http://dx.doi.org/10.1371/journal.pone.0021077

Li L., Bhatia M., Zhu Y. Z., Zhu Y. C., Ramnath R. D., Wang Z. J., Anuar F. B., Whiteman M., Salto-Tellez M., Moore P. K. (2005): Hydrogen sulfide is a novel mediator of lipopolysaccharide-induced inflammation in the mouse. FASEB J. **19,** 1196–1198

Li L., Rose P., Moore P. K. (2011): Hydrogen sulfide and cell signaling. Annu. Rev. Pharmacol. Toxicol. **51,** 169–187
http://dx.doi.org/10.1146/annurev-pharmtox-010510-100505

Li L., Rossoni G., Sparatore A., Lee L. C., Del Soldato P., Moore P. K. (2007): Anti-inflammatory and gastrointestinal effects of a novel diclofenac derivative. Free. Radic. Biol. Med. **42,** 706–719
http://dx.doi.org/10.1016/j.freeradbiomed.2006.12.011

Li L., Salto-Tellez M., Tan C. H., Whiteman M., Moore P. K. (2009): GYY4137, a novel hydrogen sulfide-releasing molecule, protects against endotoxic shock in the rat. Free. Radic. Biol. Med. **47,** 103–113
http://dx.doi.org/10.1016/j.freeradbiomed.2009.04.014

Li L., Whiteman M., Guan Y. Y., Neo K. L., Cheng Y., Lee S. W., Zhao Y., Baskar R., Tan C. H., Moore P. K. (2008): Characterization of a novel, water-soluble hydrogen sulfide-releasing molecule (GYY4137): new insights into the biology of hydrogen sulfide. Circulation **117,** 2351–2360
http://dx.doi.org/10.1161/CIRCULATIONAHA.107.753467

Lim J. J., Liu Y. H., Khin E. S., Bian J. S. (2008): Vasoconstrictive effect of hydrogen sulfide involves downregulation of cAMP in vascular smooth muscle cells. Am. J. Physiol. Cell. Physiol. **295,** C1261–1270
http://dx.doi.org/10.1152/ajpcell.00195.2008

Liu X., Pan L., Zhuo Y., Gong Q., Rose P., Zhu Y. (2010): Hypoxia-inducible factor-1alpha is involved in the pro-angiogenic effect of hydrogen sulfide under hypoxic stress. Biol. Pharm. Bull. **33,** 1550–1554
http://dx.doi.org/10.1248/bpb.33.1550

Lu M., Liu Y. H., Goh H. S., Wang J. J., Yong Q. C., Wang R., Bian J. S. (2010): Hydrogen sulfide inhibits plasma renin activity. J. Am. Soc. Nephrol. **21,** 993–1002
http://dx.doi.org/10.1681/ASN.2009090949

Ma D. K., Vozdek R., Bhatla N., Horvitz H. R. (2012): CYSL-1 interacts with the O2-sensing hydroxylase EGL-9 to promote H2S-modulated hypoxia-induced behavioral plasticity in C. elegans. Neuron **73,** 925–940
http://dx.doi.org/10.1016/j.neuron.2011.12.037

Ma K., Liu Y., Zhu Q., Liu C. H., Duan J. L., Tan B. K., Zhu Y. Z. (2011): H2S donor, S-propargyl-cysteine, increases CSE in SGC-7901 and cancer-induced mice: evidence for a novel anti-cancer effect of endogenous H2S? PLoS One **6,** e20525
http://dx.doi.org/10.1371/journal.pone.0020525

Magee E. A., Richardson C. J., Hughes R., Cummings J. H. (2000): Contribution of dietary protein to sulfide production in the large intestine: an in vitro and a controlled feeding study in humans. Am. J. Clin. Nutr. **72,** 1488–1494

Mikami Y., Shibuya N., Kimura Y., Nagahara N., Ogasawara Y., Kimura H. (2011): Thioredoxin and dihydrolipoic acid are required for 3-mercaptopyruvate sulfurtransferase to produce hydrogen sulfide. Biochem. J. **439,** 479–485
http://dx.doi.org/10.1042/BJ20110841

Miller D. L., Budde M. W., Roth M. B. (2011): HIF-1 and SKN-1 coordinate the transcriptional response to hydrogen sulfide in Caenorhabditis elegans. PLoS One **6,** e25476
http://dx.doi.org/10.1371/journal.pone.0025476

Miller D. L., Roth M. B. (2007): Hydrogen sulfide increases thermotolerance and lifespan in Caenorhabditis elegans. Proc. Natl. Acad. Sci. U.S.A. **104,** 20618–20622
http://dx.doi.org/10.1073/pnas.0710191104

Mimoun S., Andriamihaja M., Chaumontet C., Atanasiu C., Benamouzig R., Blouin J. M., Tome D., Bouillaud F., Blachier F. (2012): Detoxification of H(2)S by differentiated colonic epithelial cells: implication of the sulfide oxidizing unit and of the cell respiratory capacity. Antioxid. Redox. Signal. **17,** 1–10
http://dx.doi.org/10.1089/ars.2011.4186

Módis K., Coletta C., Erdélyi K., Papapetropoulos A., Szabo C. (2013): Intramitochondrial hydrogen sulfide production by

3-mercaptopyruvate sulfurtransferase maintains mitochondrial electron flow and supports cellular bioenergetics. FASEB J. **27**, 601–611
http://dx.doi.org/10.1096/fj.12-216507

Moody T. W., Switzer C., Santana-Flores W., Ridnour L. A., Berna M., Thill M., Jensen R. T., Sparatore A., Del Soldato P., Yeh G. C., Roberts D. D., Giaccone G., Wink D. A. (2010): Dithiolethione modified valproate and diclofenac increase E-cadherin expression and decrease proliferation of non-small cell lung cancer cells. Lung Cancer **68**, 154–160
http://dx.doi.org/10.1016/j.lungcan.2009.06.012

Mustafa A. K., Gadalla M. M., Sen N., Kim S., Mu W., Gazi S. K., Barrow R. K., Yang G., Wang R., Snyder S. H. (2009): H2S signals through protein S-sulfhydration. Sci. Signal. **2**, ra72
http://dx.doi.org/10.1126/scisignal.2000464

Mustafa A. K., Sikka G., Gazi S. K., Steppan J., Jung S. M., Bhunia A. K., Barodka V. M., Gazi F. K., Barrow R. K., Wang R., Amzel L. M., Berkowitz D. E., Snyder S. H. (2011): Hydrogen sulfide as endothelium-derived hyperpolarizing factor sulfhydrates potassium channels. Circ. Res. **109**, 1259–1268
http://dx.doi.org/10.1161/CIRCRESAHA.111.240242

Muzaffar S., Jeremy J. Y., Sparatore A., Del Soldato P., Angelini G. D., Shukla N. (2008): H2S-donating sildenafil (ACS6) inhibits superoxide formation and gp91phox expression in arterial endothelial cells: role of protein kinases A and G. Br. J. Pharmacol. **155**, 984–994
http://dx.doi.org/10.1038/bjp.2008.326

Nelson D., Cox M. E. (2008): Lehninger Principles of Biochemistry.

Nicholls P. (1975): Inhibition of cytochrome c oxidase by sulphide. Biochem. Soc. Trans. **3**, 316–319

Ogasawara Y., Ishii K., Togawa T., Tanabe S. (1993): Determination of bound sulfur in serum by gas dialysis/high-performance liquid chromatography. Anal. Biochem. **215**, 73–81
http://dx.doi.org/10.1006/abio.1993.1556

Olson K. R. (2012): Mitochondrial adaptations to utilize hydrogen sulfide for energy and signaling. J. Comp. Physiol. B. **182**, 881–897
http://dx.doi.org/10.1007/s00360-012-0654-y

Olson K. R., Donald J. A., Dombkowski R. A., Perry S. F. (2012): Evolutionary and comparative aspects of nitric oxide, carbon monoxide and hydrogen sulfide. Respir. Physiol. Neurobiol. **184**, 117–129
http://dx.doi.org/10.1016/j.resp.2012.04.004

Olson K. R., Dombkowski R. A., Russell M. J., Doellman M. M., Head S. K., Whitfield N. L., Madden J. A. (2006): Hydrogen sulfide as an oxygen sensor/transducer in vertebrate hypoxic vasoconstriction and hypoxic vasodilation. J. Exp. Biol. **209**, 4011–4023
http://dx.doi.org/10.1242/jeb.02480

Olson K. R., Whitfield N. L. (2010): Hydrogen sulfide and oxygen sensing in the cardiovascular system. Antioxid. Redox. Signal. **12**, 1219–1234
http://dx.doi.org/10.1089/ars.2009.2921

Osborne N. N., Ji D., Abdul Majid A. S., Fawcett R. J., Sparatore A., Del Soldato P. (2010): ACS67, a hydrogen sulfide-releasing derivative of latanoprost acid, attenuates retinal ischemia and oxidative stress to RGC-5 cells in culture. Invest. Ophthalmol. Vis. Sci. **51**, 284–294
http://dx.doi.org/10.1167/iovs.09-3999

Osipov R. M., Robich M. P., Feng J., Liu Y., Clements R. T., Glazer H. P., Sodha N. R., Szabo C., Bianchi C., Sellke F. W. (2009): Effect of hydrogen sulfide in a porcine model of myocardial ischemia-reperfusion: comparison of different administration regimens and characterization of the cellular mechanisms of protection. J. Cardiovasc. Pharmacol. **54**, 287–297
http://dx.doi.org/10.1097/FJC.0b013e3181b2b72b

Ouml, Lkel S., Grieshaber M. (1997): Sulphide oxidation and oxidative phosphorylation in the mitochondria of the lugworm. J. Exp. Biol. **200**, 83–92

Papapetropoulos A., Pyriochou A., Altaany Z., Yang G., Marazioti A., Zhou Z., Jeschke M. G., Branski L. K., Herndon D. N., Wang R., Szabo C. (2009): Hydrogen sulfide is an endogenous stimulator of angiogenesis. Proc. Natl. Acad. Sci. U.S.A. **106**, 21972–21977
http://dx.doi.org/10.1073/pnas.0908047106

Paul B. D., Snyder S. H. (2012): H(2)S signalling through protein sulfhydration and beyond. Nat. Rev. Mol. Cell. Biol. **13**, 499–507
http://dx.doi.org/10.1038/nrm3391

Peng Y. J., Nanduri J., Raghuraman G., Souvannakitti D., Gadalla M. M., Kumar G. K., Snyder S. H., Prabhakar N. R. (2010): H2S mediates O2 sensing in the carotid body. Proc. Natl. Acad. Sci. U.S.A. **107**, 10719–10724
http://dx.doi.org/10.1073/pnas.1005866107

Perna A. F., Ingrosso D. (2012): Low hydrogen sulphide and chronic kidney disease: a dangerous liaison. Nephrol. Dial. Transplant. **27**, 486–493
http://dx.doi.org/10.1093/ndt/gfr737

Perry M. M., Hui C. K., Whiteman M., Wood M. E., Adcock I., Kirkham P., Michaeloudes C., Chung K. F. (2011): Hydrogen sulfide inhibits proliferation and release of IL-8 from human airway smooth muscle cells. Am. J. Respir. Cell. Mol. Biol. **45**, 746–752
http://dx.doi.org/10.1165/rcmb.2010-0304OC

Pietri R., Roman-Morales E., Lopez-Garriga J. (2011): Hydrogen sulfide and hemeproteins: knowledge and mysteries. Antioxid. Redox. Signal. **15**, 393–404
http://dx.doi.org/10.1089/ars.2010.3698

Powell M. A., Somero G. N. (1986): Hydrogen sulfide oxidation is coupled to oxidative phosphorylation in mitochondria of solemya reidi. Science **233**, 563–566
http://dx.doi.org/10.1126/science.233.4763.563

Powolny A. A., Singh S. V., Melov S., Hubbard A., Fisher A. L. (2011): The garlic constituent diallyl trisulfide increases the lifespan of C. elegans via skn-1 activation. Exp. Gerontol. **46**, 441–452
http://dx.doi.org/10.1016/j.exger.2011.01.005

Predmore B. L., Lefer D. J. (2011): Hydrogen sulfide-mediated myocardial pre- and post-conditioning. Expert. Rev. Clin. Pharmacol. **4**, 83–96
http://dx.doi.org/10.1586/ecp.10.56

Predmore B. L., Lefer D. J., Gojon G. (2012): Hydrogen sulfide in biochemistry and medicine. Antioxid. Redox. Signal. **17**, 119–140
http://dx.doi.org/10.1089/ars.2012.4612

Qiu X., Villalta J., Lin G., Lue T. F. (2012): Role of hydrogen sulfide in the physiology of penile erection. J. Androl. **33**, 529–535

http://dx.doi.org/10.2164/jandrol.111.014936
Reiffenstein R. J., Hulbert W. C., Roth S. H. (1992): Toxicology of hydrogen sulfide. Annu. Rev. Pharmacol. Toxicol. **32,** 109–134
http://dx.doi.org/10.1146/annurev.pa.32.040192.000545
Richardson C. J., Magee E. A., Cummings J. H. (2000): A new method for the determination of sulphide in gastrointestinal contents and whole blood by microdistillation and ion chromatography. Clin. Chim. Acta. **293,** 115–125
http://dx.doi.org/10.1016/S0009-8981(99)00245-4
Rossoni G., Manfredi B., Tazzari V., Sparatore A., Trivulzio S., Del Soldato P., Berti F. (2010): Activity of a new hydrogen sulfide-releasing aspirin (ACS14) on pathological cardiovascular alterations induced by glutathione depletion in rats. Eur. J. Pharmacol. **648,** 139–145
http://dx.doi.org/10.1016/j.ejphar.2010.08.039
Searcy D. G. (2003): Metabolic integration during the evolutionary origin of mitochondria. Cell. Res. **13,** 229–238
http://dx.doi.org/10.1038/sj.cr.7290168
Sen N., Paul B. D., Gadalla M. M., Mustafa A. K., Sen T., Xu R., Kim S., Snyder S. H. (2012): Hydrogen sulfide-linked sulfhydration of NF-kappaB mediates its antiapoptotic actions. Mol. Cell. **45,** 13–24
http://dx.doi.org/10.1016/j.molcel.2011.10.021
Shao Z., Zhang Y., Powell-Coffman J. A. (2009): Two distinct roles for EGL-9 in the regulation of HIF-1-mediated gene expression in Caenorhabditis elegans. Genetics **183,** 821–829
http://dx.doi.org/10.1534/genetics.109.107284
Shibuya N., Tanaka M., Yoshida M., Ogasawara Y., Togawa T., Ishii K., Kimura H. (2009): 3-Mercaptopyruvate sulfurtransferase produces hydrogen sulfide and bound sulfane sulfur in the brain. Antioxid. Redox. Signal. **11,** 703-714
http://dx.doi.org/10.1089/ars.2008.2253
Sidhapuriwala J., Li L., Sparatore A., Bhatia M., Moore P. K. (2007): Effect of S-diclofenac, a novel hydrogen sulfide releasing derivative, on carrageenan-induced hindpaw oedema formation in the rat. Eur. J. Pharmacol. **569,** 149–154
http://dx.doi.org/10.1016/j.ejphar.2007.05.003
Sidhapuriwala J. N., Hegde A., Ang A. D., Zhu Y. Z., Bhatia M. (2012): Effects of S-propargyl-cysteine (SPRC) in caerulein-induced acute pancreatitis in mice. PLoS One **7,** e32574
http://dx.doi.org/10.1371/journal.pone.0032574
Simon F., Giudici R., Duy C. N., Schelzig H., Oter S., Groger M., Wachter U., Vogt J., Speit G., Szabo C., Radermacher P., Calzia E. (2008): Hemodynamic and metabolic effects of hydrogen sulfide during porcine ischemia/reperfusion injury. Shock **30,** 359–364
http://dx.doi.org/10.1097/SHK.0b013e3181674185
Simon F., Scheuerle A., Groger M., Stahl B., Wachter U., Vogt J., Speit G., Hauser B., Moller P., Calzia E., Szabo C., Schelzig H., Georgieff M., Radermacher P., Wagner F. (2011): Effects of intravenous sulfide during porcine aortic occlusion-induced kidney ischemia/reperfusion injury. Shock **35,** 156–163
http://dx.doi.org/10.1097/SHK.0b013e3181f0dc91
Singh S., Padovani D., Leslie R. A., Chiku T., Banerjee R. (2009): Relative contributions of cystathionine beta-synthase and gamma-cystathionase to H2S biogenesis via alternative trans-sulfuration reactions. J. Biol. Chem. **284,** 22457–22466
http://dx.doi.org/10.1074/jbc.M109.010868
Sparatore A., Perrino E., Tazzari V., Giustarini D., Rossi R., Rossoni G., Erdmann K., Schroder H., Del Soldato P. (2009): Pharmacological profile of a novel H(2)S-releasing aspirin. Free. Radic. Biol. Med. **46,** 586–592
http://dx.doi.org/10.1016/j.freeradbiomed.2008.11.013
Srilatha B., Hu L., Adaikan G. P., Moore P. K. (2009): Initial characterization of hydrogen sulfide effects in female sexual function. J. Sex. Med. **6,** 1875–1884
http://dx.doi.org/10.1111/j.1743-6109.2009.01291.x
Suzuki K., Olah G., Modis K., Coletta C., Kulp G., Gero D., Szoleczky P., Chang T., Zhou Z., Wu L., Wang R., Papapetropoulos A., Szabo C. (2011): Hydrogen sulfide replacement therapy protects the vascular endothelium in hyperglycemia by preserving mitochondrial function. Proc. Natl. Acad. Sci. U.S.A. **108,** 13829–13834
http://dx.doi.org/10.1073/pnas.1105121108
Szabo C. (2007): Hydrogen sulphide and its therapeutic potential. Nat. Rev. Drug. Discov. **6,** 917–935
http://dx.doi.org/10.1038/nrd2425
Szabo C. (2010): Gaseotransmitters: new frontiers for translational science. Sci. Transl. Med. **2,** 59ps54
http://dx.doi.org/10.1126/scitranslmed.3000721
Szabo C. (2010): Medicinal Chemistry and Therapeutic Applications of the Gasotransmitters NO, CO, and H2S and their Prodrugs. Burger's Medicinal Chemistry, Drug Discovery and Development **5,** 265–367
Szabo C. (2012): Roles of hydrogen sulfide in the pathogenesis of diabetes mellitus and its complications. Antioxid. Redox. Signal. **17,** 68–80
http://dx.doi.org/10.1089/ars.2011.4451
Szabo C., Papapetropoulos A. (2011): Hydrogen sulphide and angiogenesis: mechanisms and applications. Br. J. Pharmacol. **164,** 853–865
http://dx.doi.org/10.1111/j.1476-5381.2010.01191.x
Szabo G., Veres G., Radovits T., Gero D., Modis K., Miesel-Groschel C., Horkay F., Karck M., Szabo C. (2011): Cardioprotective effects of hydrogen sulfide. Nitric Oxide **25,** 201–210
http://dx.doi.org/10.1016/j.niox.2010.11.001
Taylor M. S. (2001): Characterization and comparative analysis of the EGLN gene family. Gene **275,** 125–132
http://dx.doi.org/10.1016/S0378-1119(01)00633-3
Telezhkin V., Brazier S. P., Cayzac S., Muller C. T., Riccardi D., Kemp P. J. (2009): Hydrogen sulfide inhibits human BK(Ca) channels. Adv. Exp. Med. Biol. **648,** 65–72
http://dx.doi.org/10.1007/978-90-481-2259-2_7
Tian M., Wang Y., Lu Y. Q., Yan M., Jiang Y. H., Zhao D. Y. (2012): Correlation between serum H2S and pulmonary function in children with bronchial asthma. Mol. Med. Report. **6,** 335–338
Tiranti V., Viscomi C., Hildebrandt T., Di Meo I., Mineri R., Tiveron C., Levitt M. D., Prelle A., Fagiolari G., Rimoldi M., Zeviani M. (2009): Loss of ETHE1, a mitochondrial dioxygenase, causes fatal sulfide toxicity in ethylmalonic encephalopathy. Nat. Med. **15,** 200–205
http://dx.doi.org/10.1038/nm.1907
To K. K., Huang L. E. (2005): Suppression of hypoxia-inducible factor 1alpha (HIF-1alpha) transcriptional activity by

the HIF prolyl hydroxylase EGLN1. J. Biol. Chem. **280,** 38102–38107
http://dx.doi.org/10.1074/jbc.M504342200

Togawa T., Ogawa M., Nawata M., Ogasawara Y., Kawanabe K., Tanabe S. (1992): High performance liquid chromatographic determination of bound sulfide and sulfite and thiosulfate at their low levels in human serum by pre-column fluorescence derivatization with monobromobimane. Chem. Pharm. Bull. (Tokyo). **40,** 3000–3004
http://dx.doi.org/10.1248/cpb.40.3000

Toombs C. F., Insko M. A., Wintner E. A., Deckwerth T. L., Usansky H., Jamil K., Goldstein B., Cooreman M., Szabo C. (2010): Detection of exhaled hydrogen sulphide gas in healthy human volunteers during intravenous administration of sodium sulphide. Br. J. Clin. Pharmacol. **69,** 626–636
http://dx.doi.org/10.1111/j.1365-2125.2010.03636.x

Tullet J. M., Hertweck M., An J. H., Baker J., Hwang J. Y., Liu S., Oliveira R. P., Baumeister R., Blackwell T. K. (2008): Direct inhibition of the longevity-promoting factor SKN-1 by insulin-like signaling in C. elegans. Cell **132,** 1025–1038
http://dx.doi.org/10.1016/j.cell.2008.01.030

Turner R., Fairhurst S. (1980): Toxicology of Substances in Relation to Major Hazards: Hydrogen Sulphide. London: HSE Books.

Voet D., Viet J., Pratt C., Eds. (2008): Fundamentals of Biochemistry.

Vozdek R., Hnizda A., Krijt J., Kostrouchova M., Kozich V. (2012): Novel structural arrangement of nematode cystathionine beta-synthases: characterization of Caenorhabditis elegans CBS-1. Biochem. J. **443,** 535–547
http://dx.doi.org/10.1042/BJ20111478

Wagner F., Asfar P., Calzia E., Radermacher P., Szabo C. (2009): Bench-to-bedside review: Hydrogen sulfide--the third gaseous transmitter: applications for critical care. Crit. Care. **13,** 213
http://dx.doi.org/10.1186/cc7700

Wagner F., Scheuerle A., Weber S., Stahl B., McCook O., Knoferl M. W., Huber-Lang M., Seitz D. H., Thomas J., Asfar P., Szabo C., Moller P., Gebhard F., Georgieff M., Calzia E., Radermacher P., Wagner K. (2011): Cardiopulmonary, histologic, and inflammatory effects of intravenous Na2S after blunt chest trauma-induced lung contusion in mice. J. Trauma. **71,** 1659–1667
http://dx.doi.org/10.1097/TA.0b013e318228842e

Wallace J. L., Caliendo G., Santagada V., Cirino G. (2010): Markedly reduced toxicity of a hydrogen sulphide-releasing derivative of naproxen (ATB-346). Br. J. Pharmacol. **159,** 1236–1246
http://dx.doi.org/10.1111/j.1476-5381.2009.00611.x

Wang Q., Liu H. R., Mu Q., Rose P., Zhu Y. Z. (2009): S-propargyl-cysteine protects both adult rat hearts and neonatal cardiomyocytes from ischemia/hypoxia injury: the contribution of the hydrogen sulfide-mediated pathway. J. Cardiovasc. Pharmacol. **54,** 139–146
http://dx.doi.org/10.1097/FJC.0b013e3181ac8e12

Wang Q., Wang X. L., Liu H. R., Rose P., Zhu Y. Z. (2010): Protective effects of cysteine analogues on acute myocardial ischemia: novel modulators of endogenous H(2)S production. Antioxid. Redox. Signal. **12,** 1155–1165
http://dx.doi.org/10.1089/ars.2009.2947

Wang R. (2002): Two's company, three's a crowd: can H2S be the third endogenous gaseous transmitter? FASEB J. **16,** 1792–1798
http://dx.doi.org/10.1096/fj.02-0211hyp

Wang R. (2012): Physiological implications of hydrogen sulfide: a whiff exploration that blossomed. Physiol. Rev. **92,** 791–896
http://dx.doi.org/10.1152/physrev.00017.2011

Warenycia M. W., Goodwin L. R., Benishin C. G., Reiffenstein R. J., Francom D. M., Taylor J. D., Dieken F. P. (1989): Acute hydrogen sulfide poisoning. Demonstration of selective uptake of sulfide by the brainstem by measurement of brain sulfide levels. Biochem. Pharmacol. **38,** 973–981
http://dx.doi.org/10.1016/0006-2952(89)90288-8

Wei H., Zhang R., Jin H., Liu D., Tang X., Tang C., Du J. (2010): Hydrogen sulfide attenuates hyperhomocysteinemia-induced cardiomyocytic endoplasmic reticulum stress in rats. Antioxid. Redox. Signal. **12,** 1079–1091
http://dx.doi.org/10.1089/ars.2009.2898

Whiteman M., Le Trionnaire S., Chopra M., Fox B., Whatmore J. (2011): Emerging role of hydrogen sulfide in health and disease: critical appraisal of biomarkers and pharmacological tools. Clin. Sci. (Lond.) **121,** 459–488
http://dx.doi.org/10.1042/CS20110267

Whiteman M., Li L., Rose P., Tan C. H., Parkinson D. B., Moore P. K. (2010): The effect of hydrogen sulfide donors on lipopolysaccharide-induced formation of inflammatory mediators in macrophages. Antioxid. Redox. Signal. **12,** 1147–1154
http://dx.doi.org/10.1089/ars.2009.2899

Whiteman M., Gooding K. M., Whatmore J. L., Ball C. I., Mawson D., Skinner K., Tooke J. E., Shore A. C. (2010): Adiposity is a major determinant of plasma levels of the novel vasodilator hydrogen sulphide. Diabetologia **53,** 1722–1726
http://dx.doi.org/10.1007/s00125-010-1761-5

Whiteman M., Moore P. K. (2009): Hydrogen sulfide and the vasculature: a novel vasculoprotective entity and regulator of nitric oxide bioavailability? J. Cell. Mol. Med. **13,** 488–507
http://dx.doi.org/10.1111/j.1582-4934.2009.00645.x

Wintner E. A., Deckwerth T. L., Langston W., Bengtsson A., Leviten D., Hill P., Insko M. A., Dumpit R., VandenEkart E., Toombs C. F., Szabo C. (2010): A monobromobimane-based assay to measure the pharmacokinetic profile of reactive sulphide species in blood. Br. J. Pharmacol. **160,** 941–957
http://dx.doi.org/10.1111/j.1476-5381.2010.00704.x

Yang G., Sun X., Wang R. (2004): Hydrogen sulfide-induced apoptosis of human aorta smooth muscle cells via the activation of mitogen-activated protein kinases and caspase-3. FASEB J. **18,** 1782–1784

Yang G., Wu L., Bryan S., Khaper N., Mani S., Wang R. (2010): Cystathionine gamma-lyase deficiency and overproliferation of smooth muscle cells. Cardiovasc. Res. **86,** 487–495
http://dx.doi.org/10.1093/cvr/cvp420

Yang G., Wu L., Jiang B., Yang W., Qi J., Cao K., Meng Q., Mustafa A. K., Mu W., Zhang S., Snyder S. H., Wang R. (2008): H2S as a physiologic vasorelaxant: hypertension in mice with deletion of cystathionine gamma-lyase. Science **322,** 587–590
http://dx.doi.org/10.1126/science.1162667

Yong Q. C., Pan T. T., Hu L. F., Bian J. S. (2008): Negative regulation of beta-adrenergic function by hydrogen sulphide in the rat hearts. J. Mol. Cell. Cardiol. **44,** 701–710 http://dx.doi.org/10.1016/j.yjmcc.2008.01.007

Yong R., Searcy D. G. (2001): Sulfide oxidation coupled to ATP synthesis in chicken liver mitochondria. Comp. Biochem. Physiol. B. Biochem. Mol. Biol. **129,** 129–137 http://dx.doi.org/10.1016/S1096-4959(01)00309-8

Yusuf M., Kwong Huat B. T., Hsu A., Whiteman M., Bhatia M., Moore P. K. (2005): Streptozotocin-induced diabetes in the rat is associated with enhanced tissue hydrogen sulfide biosynthesis. Biochem. Biophys. Res. Commun. **333,** 1146–1152 http://dx.doi.org/10.1016/j.bbrc.2005.06.021

Zanardo R. C., Brancaleone V., Distrutti E., Fiorucci S., Cirino G., Wallace J. L. (2006): Hydrogen sulfide is an endogenous modulator of leukocyte-mediated inflammation. FASEB J. **20,** 2118–2120 http://dx.doi.org/10.1096/fj.06-6270fje

Zhang H., Zhi L., Moore P. K., Bhatia M. (2006): Role of hydrogen sulfide in cecal ligation and puncture-induced sepsis in the mouse. Am. J. Physiol. Lung. Cell. Mol. Physiol. **290,** L1193–1201 http://dx.doi.org/10.1152/ajplung.00489.2005

Zhao W., Zhang J., Lu Y., Wang R. (2001): The vasorelaxant effect of H(2)S as a novel endogenous gaseous K(ATP) channel opener. EMBO J. **20,** 6008–6016 http://dx.doi.org/10.1093/emboj/20.21.6008

Zhong J. F., Wang S. P., Shi X. Q., Mu L. L., Li G. Q. (2010): Hydrogen sulfide exposure increases desiccation tolerance in Drosophila melanogaster. J. Insect. Physiol. **56,** 1777–1782 http://dx.doi.org/10.1016/j.jinsphys.2010.07.009

Zhou Z., von Wantoch Rekowski M., Coletta C., Szabo C., Bucci M., Cirino G., Topouzis S., Papapetropoulos A., Giannis A. (2012): Thioglycine and L-thiovaline: biologically active H(2)S-donors. Bioorg. Med. Chem. **20,** 2675–2678 http://dx.doi.org/10.1016/j.bmc.2012.02.028

Received: September 5, 2012
Final version accepted: October 24, 2012